THE

LONDON, EDINBURGH, AND DUBLIN

PHILOSOPHICAL MAGAZINE

AND

JOURNAL OF SCIENCE.

[SEVENTH SERIES.]

OCTOBER 1935.

XXXIX. *The Use of Electron Lenses for β-rays.*

By OTTO KLEMPERER *.

(1) *Introduction.*

BUSCH † has shown that the magnetic field of a short coil is able to concentrate electron beams quite analogously to the focussing of light beams by an optical lens. Such "electron lenses" are in common use for concentrating electron beams in cathode-ray oscillographs and for producing enlarged images of electron-emitting objects in electron microscopes. Recently the so-called "geometric electron optics" applying merely optical conceptions to electron beams has developed as a great and important section in electron physics ‡.

According to a suggestion of C. D. Ellis the author tried here to make use of the well elaborated principles of electron optics for β-ray spectrography. In the following paper experiments are described on the peculiarities of single electron lenses producing a series of electron images from a β-ray source which could be detected by a Geiger-Müller counter. The single lens acts in this way as a β-ray spectrograph with very high

* Communicated by C. D. Ellis.

† H. Busch, *Arch. Elektrotechn.* vol. xviii. p. 583 (1927).

‡ O. Klemperer, 'Einführung in die Elektronik,' Berlin (1933); E. Brüche and O. Scherzer, 'Geometrische Elektronenoptik,' Berlin (1934).

intensity. Furthermore there is described the construction and the peculiarities of a β-ray spectrograph, consisting of two "lenses" and a deflecting magnetic "prism" between them. This spectrograph is constructed somewhat analogously to the ordinary light spectrographs; it seems likely to have higher dispersion, higher intensity and resolving power than the usual semicircular type that has been used nearly exclusively in β-ray-spectrography till now.

(2) *Single Lens Spectrograph.*

The method used here for obtaining β ray-spectra by a single electron lens is shown in fig. 1. L represents the cross-section of a big flat cylindrical coil containing

Fig. 1.

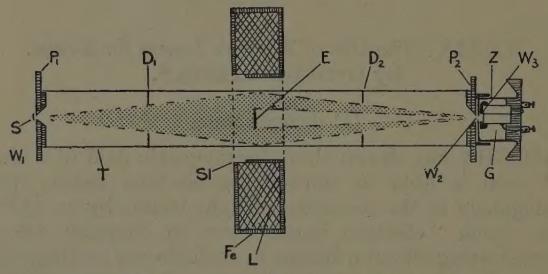

Single lens spectrograph (schematic diagram).

1550 turns of copper wire. The coil is 5 cm. thick, its inner and outer radii are 5 and 12 cm. respectively. On the axis of the coil lies the evacuated brass tube T, about 120 cm. long with 7 cm. diameter. At the ends of the tube are the lids P_1 and P_2, containing small circular windows W_1 and W_2, of 3 and 5 mm. diameter, covered by cellophane sheets. The radioactive source S, fastened in front of the window W_1, emits the β-rays, which are focussed in the direction of W_2. In a cylindrical ring soldered on the lid P_2 one can slip in the brass vessel Z, containing a small Geiger-Müller counter G. Z is closed by the cellophane window W_3. The focussed β-rays are transmitted through the windows W_2 and W_3 and registered in the counter G. In the middle of the tube T there is suspended a brass disk E, of 2·2 cm. diameter,

which stops the α-rays from the source and helps to prevent β-rays from penetrating straight through to the counter. Two diaphragms, D_1 and D_2, consisting of circular holes of 3 cm. diameter, are arranged to stop β-rays from being reflected from the walls of the tube.

The focal length of an electron lens is given by

$$f=\frac{4(\mathrm{H}\rho)^2}{\int \mathrm{H}^2(x)\,dx}, \quad \ldots\ldots\ldots \quad (1)$$

or for a given coil

$$cf\mathrm{I}^2=(\mathrm{H}\rho)^2, \quad \ldots\ldots\ldots \quad (2)$$

where

f=focus length in cm.;

$\mathrm{H}\rho$=Gauss × cm., measuring the velocity of the focussed electrons;

$\mathrm{H}(x)$=the magnetic field strength along the x-axis, that is, the axis of the coil;

c=a constant for a given coil;

I=coil current here measured in amps.

In the spectrograph of fig. 1 object and image distance are fixed. Therefore, as one can see from eq. (2), every β-ray velocity is focussed at the tube counter window W_3 by a corresponding coil current I. For testing the spectrograph the active deposit of the thor um was very convenient, as it emits one very strong β-line—that is, the F-line of ThB, which has a $\mathrm{H}\rho=1385$, corresponding to an energy of 150 electron kilovolts. The other β-lines which this deposit emits are at least ten times weaker than the F-line. In addition to the line spectrum there is emitted a continuous β-ray spectrum with an upper limit of $\mathrm{H}\rho=9000$. Fig 2 shows the spectrum obtained with a thin activated wire. Its activity was only 1 microcurie. The solid line represents the number of kicks in the Geiger-Müller counter plotted against the coil current. For no coil current one has a very small effect of about 8 kicks/min. in the counter consisting of the natural effect=4 kicks/min. (cosmic rays etc.) and additional 4 kicks due partly to γ-rays but mainly to scattered β-rays emitted from the source. For a coil current of 1·35 amps. a very distinct maximum of 120 kicks/min. belonging to the electrons of the F-line

is reached. Afterwards the curve falls steeply, but rises later on again owing to the increasing abundance of faster electrons in the continuous spectrum. Curves like this were obtained only after a careful adjustment of the coil, which was hung in a universal suspension and could be rotated both around its horizontal and vertical axes. Furthermore, the coil could be translated in either direction perpendicular to the coil axis. To find the right adjustment a stronger source was used (say 5 microcuries), the coil current kept at about 3 amps.,

Fig. 2.

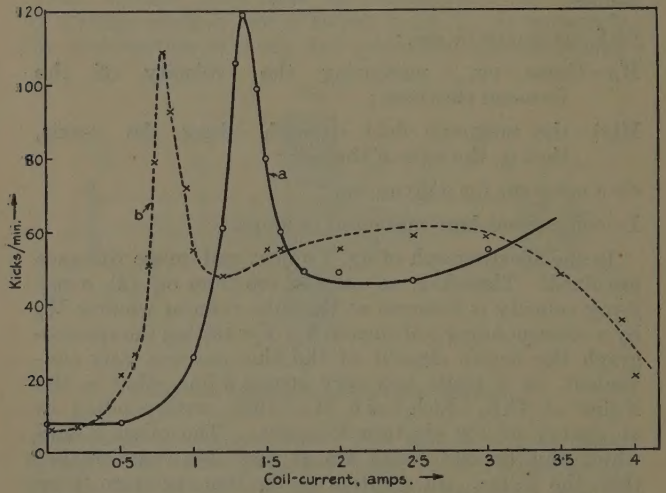

β-ray spectra of 1 microcurie Th(B+C) taken with the single lens spectrograph: (a) with air coil, (b) with iron coil.

and the position of the coil then adjusted by listening to the number of kicks in the Geiger-Müller counter. When these reached a maximum it was an indication that the coil was approximately adjusted. Then the coil current was gradually diminished until the peak belonging to the F-line appeared. With the coil current found in this way the sharp focal point due to the F-line was near the counter window, and the final geometric adjustment of the coil was achieved by noting the number of kicks for the different positions of the coil.

A change of the position of the coil along its axis was avoided, as it has been found by special experiments that a position halfway between source and counter was the best. If the coil is brought nearer to the source a greater solid angle of the β-rays is subtended, but as the image area is increased one cannot get the whole image through the counter window. Probably this is the reason why the peak in the curves in that case becomes much smaller in comparison with the background. Experiments were also made to find the optimum size of the central disk E. The best diameter was found to be 2–3 cm. Smaller diameters caused a larger background intensity in comparison with the peak—too large a diameter diminished the overall intensity. Outer magnetic fields must be avoided as much as possible, as they distort the paths of the β-rays. In principle therefore the axis of the tube should be orientated as nearly parallel as possible to the earth's magnetic field. However, the effect of a given angle between this axis and the earth's field may easily be compensated by turning the coil through a small angle, and it proved more convenient to have the whole apparatus in a horizontal plane.

A comparison of the yield of electrons in the spectrograph with the number of F-line electrons emitted per disintegration is useful in ascertaining the quality of the adjustment. From Gurney's * results one can calculate that the number of F-line electrons emitted per microcurie per minute is equal to 5×10^5. In this β-ray spectrograph the solid angle of the β-rays which are concentrated into the Geiger-counter is $\omega = 8 \times 10^{-4}$. It is limited by the first diaphragm D (diameter = 3 cm., distance from the source = 28 cm.) as well as by the tube diameter (= 7 cm.), the disk E, and the distance of the lens from the source (= 60 cm.). The β-rays have to traverse in their path three windows, W_1, W_2, W_3, each of about 2 cm. air equivalent stopping power. In estimating the effect of the windows one must consider scattering and in the first window the straggling produced. The correction factors are difficult to determine with any accuracy, but a total transmission factor for the three windows of between 35 and 50 per cent. seems reasonable †. One would therefore expect from 1 microcurie a count

* R. W. Gurney, Proc. Roy. Soc. cxii. p. 380 (1926).
† O. Klemperer, *l. c.* p. 226.

at the maximum of between 140 and 200 electrons/min. With a source of 1 microcurie, the experimental count, after discarding 20 kicks/min. of the background, was about 100 electrons/min. This is in fair agreement with the above estimation when it is remembered that the radioactive material was on a 0·3 mm. nickel wire, so that the material on the back of the wire was scarcely effective at all. In addition the strength of the source could only be determined approximately. It was measured by a β-ray electroscope calibrated by means of a Th(B+C) source, allowed to decay for some days, and measured originally in a γ-ray electroscope by comparison with a radium standard.

To attain higher intensities one ought to use lenses with larger apertures—that means either larger diameters or shorter focal lengths. The focal length of the lens is inversely proportional to the number of ampere turns. For a given number of ampere turns one can decrease the focal length very much by surrounding the coil with sheet-iron, leaving a small annular gap on the inside of the coil. An iron shield of this type is shown in fig. 1 and designated by Fe. Using a shield of 5 mm. thick sheet-iron with a 2 cm. wide gap and the coil described above one obtains with the unchanged arrangement of fig. 1 a β-ray spectrum shown by the broken curve in fig. 2. The peak belonging to the F-line now appears at 0·8 amp. The relative position of the peaks of the solid and of the broken curve is given by the ratio of the currents 1·35 : 0·8. According to equation (2) the focal lengths are proportional to the squares of the currents. Therefore it follows that the focal length of the same coil has become shorter by a factor 3 when surrounded with the iron shield. As the coil could easily stand a current of 4 amps. one could therefore focus an electron velocity of about 7000 Hρ within the focal length of 30 cm. fixed by the geometry of the apparatus. Curve *b* drops sharply for currents larger than 3 amps., due to the decrease of the β-ray intensity of the continuous spectrum.

(3) *Suitability of Different Types of Electron Lenses for β-ray Spectrography.*

The advantage of the "iron coil" over the "air coil" is its shorter focal length. Furthermore the axial magnetic field of an iron coil falls off much more sharply.

This is important if one uses either several lenses or lenses in conjunction with magnets (see § 4), where it would be troublesome if the different fields were to overlap and disturb each other. To get a good working spectrograph it was necessary to investigate the exact magnetic field distribution for the different types of electron lenses. The field strength along the axis, obtained by means of a small search coil (1 cm. diameter) and a ballistic galvanometer, is shown for different

Fig. 3.

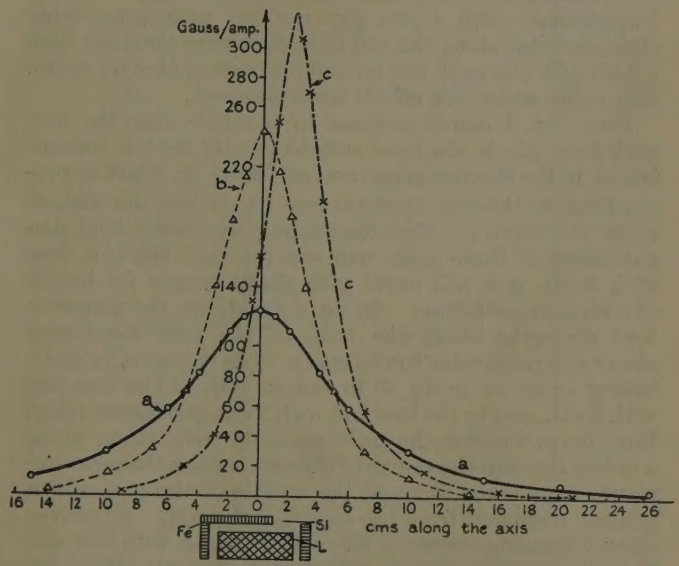

Field distribution of magnetic electron lenses along their axes : (*a*) air coil ; (*b*) iron coil with 6 cm. gap ; (*c*) iron coil with 2 cm. gap.

electron lenses in fig. 3. In all cases the same coil, already described in the beginning of § 2, was used. Curve "*a*" shows the field distribution for the simple uncovered coil, which does not contain any iron. Curve "*b*" refers to this coil if its ends and the outer cylindrical surface is covered by plates made of 5 mm. thick soft iron. Only the inner cylindrical surface is left uncovered as magnetic gap. Curve "*c*" finally shows the same field distribution if also the inner cylindrical surface is covered

by iron plate leaving a gap " Sl " of only 2 cm., as is to be seen from the cross-section drawn in the bottom of fig 3. The centre of the coil was chosen in each case as the zero point of the axis. The maximum field-strength of curve *a* and *b* lies, of course, at this zero point, but the maximum of curve *c* is somewhat shifted, as the magnetic gap was arranged at the end of the coil. All the curves were taken with a coil current of 1 amp., up to 4 amps. ; the field strengths, even of the iron coils, were proportional to the coil current within the limit of accuracy of the measurement (about 1 per cent.). Experiments with 1 cm. gap did not give appreciably stronger fields along the coil axis than were obtained with a 2 cm. gap (curve *c*), but for coil currents of above 2 amps. noticeable saturation effects were observed.

From fig. 3 one is inclined to conclude that the lens with 2 cm. gap is the most suitable, as its field is concentrated in the shortest range and as $\int H^2(x)\,dx$, which is proportional to the lens aperture (see eq. 1), has the highest value for curve *c*. But considering the radial field distributions of these coils one can see that the iron lens with 2 cm. gap will never give sharp images for beams of a large cross-section. In fig. 4 are shown the magnetic field strengths along the radii of the coils mentioned above (perpendicular to the axis). The curves *a*, *b*, and *c* belong again (as in fig. 3) to the air coil, to the iron coil with 6 cm., and to the iron coil with 2 cm. gap respectively. For curves *a* and *b* the measurements were taken along a radius through the centre of the coil. For *c* the measurements were taken through the middle of the gap, which is 2 cm. displaced from the centre of the coil. All curves show increasing values of the field strength with increase in radius. That means, referring to eq. (1), that for peripheral rays this lens will have a shorter focal length than for rays of the same velocity travelling near the coil axis. For the focussing of beams diverging originally through a wide angle this " spherical aberration " of the electron lens becomes still worse as our formula (1) holds for small divergence angles only. To be more accurate the right-hand side ought to be multiplied by $\cos\alpha$, if α is the initial angle between the ray being considered and the axis of the lens. In the spectrograph shown in fig. 2 $\alpha \leqslant 3{\cdot}3°$, so that $\cos\alpha \leqslant 0{\cdot}998$ is almost negligible. Furthermore, as one moves along the axis of the coil

the change of field strength with increasing radius, $\frac{\partial H}{\partial r}$, becomes gradually less and less, and eventually changes sign. For instance, curve *d* in fig. 4 shows the radial field distribution of the iron coil with 6 cm. gap measured at a distance of 6 cm. from the coil centre (=3 cm. from the iron shield of the coil). The curve

Fig. 4.

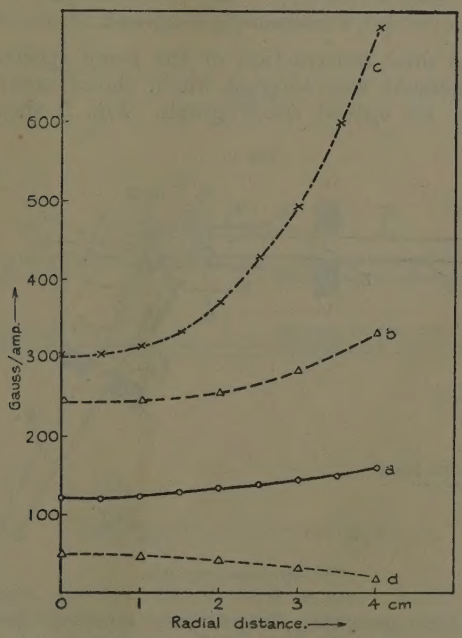

Radial field distribution in magnetic lenses : (*a*) through the centre of the air coil ; (*b*) through the middle of the 6 cm. gap of the iron coil ; (*c*) through the middle of the 2 cm. gap of the iron coil ; (*d*) 6 cm. from the centre of the iron coil with 6 cm. gap.

shows already a noticeable slope as one approaches the peripheral regions. The very inconvenient distribution of the field strength inside the coil is therefore somewhat compensated by the distribution of the external field strength. For accurate spectrographic measurements

the aberration of the iron lens with a 2 cm. gap would have been too great, but the iron lens with a 6 cm. gap seemed suitable enough and was chosen for use in the spectrograph described in the next section. For a possible later construction of a spectrograph with a very large aperture perhaps special coils should be made, the field of which over the whole space would be adapted to the cosine of the angles of divergence of the beams starting from the source.

(4) *Two-Lens Spectrograph.*

For the final construction of the β-ray spectrograph an arrangement was adopted which shows many similarities to an optical spectrograph. Fig. 5 shows the

Fig. 5.

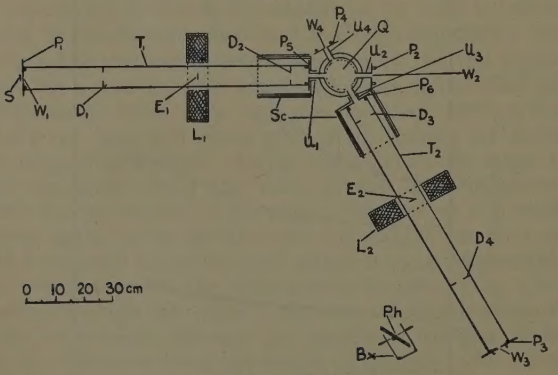

Two-lens spectrograph.

general arrangement. β-rays were emitted from the source S into the tube T_1, and they were concentrated by the electron lens L_1 in the direction of the window W_2 rather similar to the one-lens spectrograph of fig. 1. By listening to the kicks of a tube counter, which could be slipped into the ring of the plate P_2, the first arm of the spectrograph could be adjusted in the same manner as was described for the one-lens spectrograph in § 2. The electron lens L_2, concentrating the β-rays in the tube T_2 of the second arm of the spectrograph, could be adjusted in a similar way if a tube counter was

attached at the lid P_4 on the window W_4, and if a β-ray source was fastened on the window W_3 of a lid P_3. After such an adjustment of each arm separately, the β-rays could be bent from the one arm into the other by means of a magnetic " prism," box Q, which was arranged between the pole pieces of a large Dubois magnet. For the adjustment of the single arms this magnet had to be, of course, quite demagnetized ; that was done by repeatedly reversing a direct current, which was diminished step by step down to zero. The last traces of residual magnetism had to be compensated by a current of some

Fig. 6.

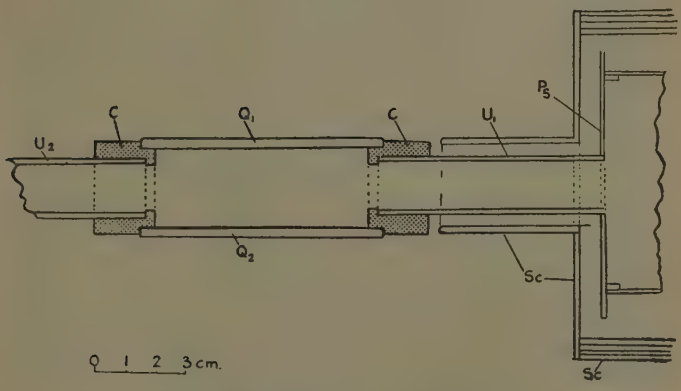

Magnetic deflexion box (cross-section).

milliamps. through the Dubois magnet until a search coil (sensitivity 0·03 Gauss/mm. galvanometer deflexion) pulled out of the stray field of the Dubois produced no longer any appreciable deflexion of the ballistic galvanometer. The magnetic deflexion box Q is shown in larger scale in fig. 6. The circular parallel plates Q_1 and Q_2 were made of 5 mm. thick iron sheet with a diameter of 8 cm. They fitted closely inside the pole-pieces of the Dubois magnet, and left between them a magnetic gap of 2·5 cm. They were soldered into the brass ring C. Four large holes were drilled through this ring C, to hold the four iron tubes U_1, U_2, U_3, and U_4. The tubes U_1

and U_3 included an angle of 60°, through which the β-rays were deflected. The magnetic deflexion box could easily be disconnected from the other parts of the apparatus, as the lids P_5 and P_6, soldered on the iron tubes U_1 and U_3, merely fitted tightly over the ends of the big brass tubes T_1 and T_2, and were sealed with plasticene. The ends of the tubes T_1 and T_2 were carefully shielded from the stray field of the Dubois magnet by the surrounding iron screens Sc. These screens were very essential, as without them the spectrograph refused to allow any β-rays to pass from one arm into the other. The β-ray beam was defined again by the diaphragms D_1, D_2, D_3, D_4, and the central disks E_1 and E_2, with almost the same dimensions as used in the one-lens spectrograph of § 2.

During the adjustment of the single arms a current through the magnetic lenses of 0·88 amps. was sufficient to focus the F-line electrons from the window W_1 to the window W_2. For guiding the β-rays through the whole spectrograph it was necessary that they should be concentrated first near the centre of the magnetic box, to form there a first image. From the distance between W_1 and W_2 (=120 cm.) one calculates the focal length to be 30 cm. To shorten the focal length in order to form the image in the centre of the deflexion box, which was 10 cm. from W_2, the focal length of the electron lens had to be reduced to 27·4 cm. For this the coil current was calculated, according to eq. (2), to be $I_L = 0{\cdot}92$ amps. From this focal point in the centre of the box, the β-rays spread out again, and after being bent through the field of the Dubois magnet they were focussed by the lens L_2 at the window W_3. As the two arms of the apparatus were quite symmetrical and the two lenses were quite equivalent the same current in L_2 as in L_1 could be used.

Electron lenses are different from optical lenses in so far as their images are always rotated through a given angle referred to the object (this angle may not be 180°, as for optical lenses). In order to eliminate this rotation effect the current through both coils, which were connected in series, ran in opposite directions. Therefore the rotation of the first image was cancelled by the second lens and the second image had exactly the same direction as the object.

The electron beam where it passed through the magnetic deflexion box was very narrow; it entered and left

the magnetic field boundaries almost normally. This fact was very essential to avoid distortions of the image *.

Using the fixed lens current $I_L = 0{\cdot}92$ (calculated above), the current through the Dubois magnet I_{Db} was varied until a sharp maximum, belonging to the F-line electrons, was obtained in the tube counter at the window W_3. Of this maximum about 80 per cent. of the β-rays detected previously at the window W_2 were now detected at W_3. The number of kicks was very sensitive to the positions of the coils, which therefore usually were readjusted

Fig. 7.

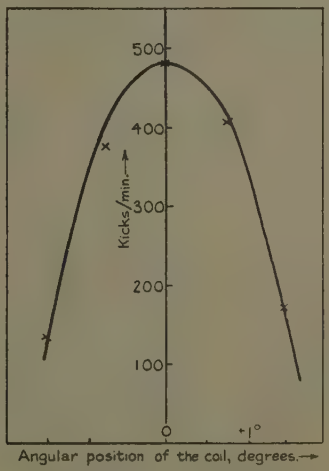

Adjustment of a magnetic lens.

again in this stage. For instance, in fig. 7 the number of kicks per min. in the tube counter (diameter of the counter window = 5 mm.) is plotted against the angular position of the lens L_2. One can see that the optimum position must be adjusted accurately to a fraction of a degree. After this adjustment the whole curve, *i. e.*, the number of kicks/min. in the counter as a function of the Dubois current, was measured. It was a nearly symmetrical curve with a half-width of about 40 milliamps.

* A similar arrangement of magnetic fields was studied originally for deflexion of focussed cathode rays: see O. Klemperer, *Ann. d. Physik*, xv. p. 367 (1932).

Using a 1 mm. wide slit at the tube counter window W_3 this half-width decreased to 30 milliamps. Putting the source behind the cellophane window W_1 inside the spectrograph, and thus avoiding initial straggling effects, the half-width diminished still more, and a very sharp peak was then observed. The curve obtained under these conditions is shown as the solid line in fig. 8. The source had a strength of several hundredths of a millicurie. The natural effect of the counter and a γ-ray effect of

Fig. 8.

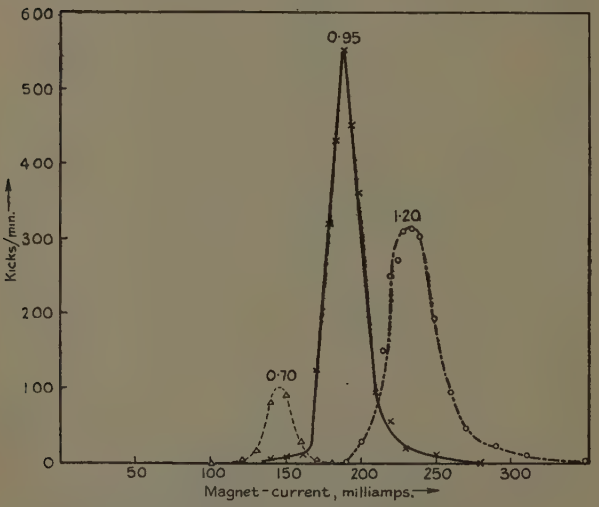

Velocity distributions of focussed β-rays for lens currents of 0·7, 0·95, and 1·2 amps.

25 kicks/min. was allowed for in the values plotted in fig. 8. As a test of how accurately the apparatus worked it may be mentioned that the maximum of the solid curve occurred at $I_{Db}=190$ milliamps., which was 10 milliamps. more than in the first experiment, where the source was outside the tube and the β-rays lost energy in traversing the cellophane window. For the same reason the lens current had to be slightly higher than in the first experiment, namely $I_L=0{\cdot}95$ amps., in order to develop the

maximum fully, but actually the size of the maximum was not too sensitive to the lens current. For instance, a change of I_L of 0·01 amp. could hardly be noticed. Using different lens currents one selects quite different parts of the β-ray spectrum. Measuring the number of kicks per min. as a function of the Dubois magnet current one gets the velocity distribution of the spectral region selected in this way. The broken curves in fig. 8 show such distributions for the lens currents 0·7 and 1·2 amps. respectively. The half-widths of these curves spread over about 20 and 30 milliamps. respectively, showing that in both cases the homogeneity of velocities, produced only by the focussing effect of the lenses, lies within ∓ 7 per cent. of the $H\rho$ value belonging to the intensity maximum. The degree of homogeneity of these focussed β-ray beams is such that one can get a rough estimate of the resolving power of the single lens spectrograph which must be of the order of magnitude

$$\frac{H\rho}{\Delta(H\rho)} = \frac{100}{7} = 14.$$

On the other hand, the resolving power of the two lens spectrograph must be much higher.

It is of interest to calculate approximately the dispersion of the latter instrument. If Ω is the deviation of the central ray and R denotes an effective radius of the magnetic field, that is the radius of a uniform field, zero outside R, which produces the same deflexion as the actual field, then

$$R = \rho \tan \theta/2, \quad . \quad . \quad . \quad . \quad . \quad . \quad (3)$$

where ρ is the radius of curvature of the electron path inside the box. If the slit of the counter is a distance x from the centre of the deflexion box, and δy measures the movement of the focus point for rays of slightly different velocity, then

$$y = x \frac{d\theta}{d(H\rho)} (H\rho). \quad . \quad . \quad . \quad . \quad . \quad (4)$$

From (3) and (4) therefore we obtain the dispersion

$$\frac{dy}{d(H\rho)} = \frac{x \sin \theta}{H\rho} \quad . \quad . \quad . \quad . \quad . \quad . \quad . \quad (5)$$

For the present apparatus $\theta = 60°$ and $x = 110$ cm., yielding for the F-line $H\rho = 1385$, a dispersion of 0·07 cm./$H\rho$.

This is seven times greater than that obtainable with an ordinary semicircular spectrograph working at the usual radius of curvature of about 7 cm. However, the dispersion of an instrument is not an important criterion, and it is the resolving power that one must consider, and this depends on the breadth of a focussed line. We can see at once that the breadth of the F-line shown by the solid curve in fig. 8 cannot have been affected by the width, 1 mm., of the slit over the counter, since this corresponds to less than 0·1 per cent. variation in $H\rho$. The actual width is due partly to imperfections in the focussing and partly to the method of taking the measurements. It must be remembered that the F-line is superimposed on a continuous background of electrons, and that while the lenses are set to focus the F-electrons they will also transmit with gradually decreasing efficiency electrons of slightly higher or lower speeds. As the field of the deflecting magnet is altered such electrons will in turn be brought into the counter slit. It is clear that to obtain more information we must photograph the spectrum formed with constant lens and deflecting fields.

For this purpose the lid P_3 (see fig. 5) was removed from the tube T_2, and instead of it the photographic box Bx was slipped in its place. This box contained the photographic plate Ph, which could be so adjusted that its middle came exactly at the same place which the tube counter window occupied before—that means, for the properly adjusted apparatus, at the point of focus of the F-line. The plane of the plate had to be inclined to the normal plane of the β-beam at an angle of about 78°. Assuming, as was approximately the case, that for each lens object and image were each twice the focal length f from the lens, then for a slightly changed velocity it is easy to see that the focus point moves a distance equal very approximately to $8\dfrac{df}{d(H\rho)}\delta(H\rho)$ along the axis. But the movement perpendicular to the axis due to the deflecting field is $\dfrac{dy}{d(H\rho)}\delta(H\rho)$, so that the inclination of the plate ψ is given by

$$\tan\psi = \frac{8df}{d(H\rho)} \Big/ \frac{dy}{d(H\rho)}. \quad . \quad . \quad . \quad . \quad . \quad (6)$$

Using equation (5) and also $f=\text{const.}\times(H\rho)^2$, one obtains

$$\tan\psi=16\,f/x\,\sin\theta.$$

Giving for $\theta=60°$,

$f=27{\cdot}3$ cm.,

and $x=110$ cm.,

one obtains $\psi\approx 78°$.

Owing to the author's departure from Cambridge it has only proved possible to carry out preliminary experiments by this method, and as yet no sharply focussed line has been obtained. However, using 1/3 millicurie of thorium active deposit on a 0·3 mm. wire definite patches of blackening were obtained on the photographic plate in 3/4 hour exposure. It was possible to estimate that the total blackening in the patch was of the same order as that obtainable in the F-line, using semicircular focussing and the same exposure. It was clear from these experiments that to obtain good photographs all the adjustments would need to be carried out very carefully, and, in particular, the field of the deflecting magnet kept very constant, as, for example, by the use of a permanent magnet.

The author has much pleasure in expressing his thanks to Dr. C. D. Ellis for his kind interest in this work. He also wishes to record his gratitude to the British Academic Assistance Council for a grant, and to thank especially Lord Rutherford for the great hospitality which enabled the author to do this work in the Cavendish Laboratory.

Summary.

The magnetic field distributions of various electron lenses have been measured and their optical qualities are discussed.

Two different types of β-ray spectrographs have been constructed: one in order to obtain high intensity and the other to obtain high resolving power. Practical experience gained with these spectrographs is described.

Cavendish Laboratory, Cambridge.
Feb. 1935.

XL. *The Development of a Spark from a Glow.* *By* Prof. E. L. E. Wheatcroft, *M.A.*, *and* H. Barker, *B.Sc.**

[Plate IV.]

THE existence of the phenomena of spark and glow are both well known, and it is known in general that the spark occurs at higher gas-pressures than the glow. Rogowski and Tamm (*Archiv für Elektrotechnik*, xix. p. 235 (1928)) have shown that a transient glow precedes the spark produced by impulsive voltages, and found that the glow was stable at pressures greater than 7 mm. Hg. No systematic measurements, however, seem to have been made at any time of the distinction between these two forms. The most obvious of these investigations is that of finding the pressure at which the discharge takes the visible form of a spark rather than a glow. It is first, however, necessary to note the visible changes which occur as the pressure is raised, and decide (if necessary, arbitrarily) which shall be taken as marking the point of distinction.

Experimental Arrangement.

All the experiments described here are made in air admitted from a jar containing calcium chloride.

Fig. 1.

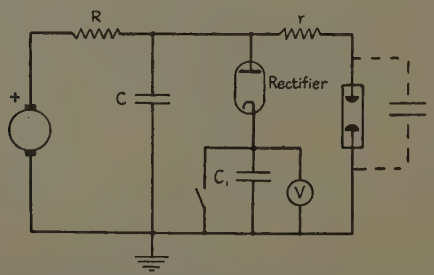

The circuit was connected as shown in fig. 1, and the values of the constants were —

$R = 150$ megohms ;

$C = 5530\ \mu\mu$fd. ;

$C_1 = 0{\cdot}1\ \mu$fd.

* Communicated by the Authors.

The generator charged up the condensers C and C_1 through the charging resistance R until the striking voltage was reached, when the condenser C discharged through the tube. Owing to the rectifying valve, the electrostatic voltmeter V retained the reading of the striking voltage until it was discharged by the key.

The tube, which is shown in fig. 2, was constructed of two bell jars 10 cm. diameter, and made vacuum-tight

Fig. 2.

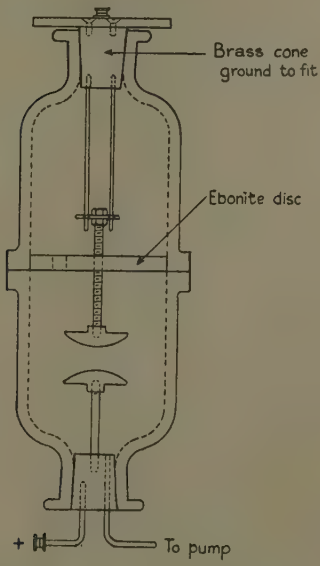

by Apiezon sealing compound. The electrodes were 4 cm. diameter, thus permitting a maximum distance of about $1\frac{1}{2}$ cm. whilst retaining a sensibly uniform field. They were set at a known distance apart by means of a cathetometer, the upper electrode being movable by means of the screw-thread shown.

Visible Forms of Discharge.

The following changes were observed in the discharges as the pressure was varied. It should be remembered that the descriptions refer to intermittent discharges, and

no attempt was made to obtain a continuous discharge. The sparks or glows occurred at intervals of about 15 seconds except where stated otherwise. The nature of the change from glow to spark can be followed by reference to the photographs of fig. 3 (Pl. IV.).

At low pressures the discharge is definitely a glow of the type illustrated in fig. 3 (*a*) (Pl. IV.), with or without the discharge resistance, *r* (fig. 1.). The inclusion of discharge resistance may alter the colour and area of the glow, but it still takes the form shown. The variation of this type of discharge with pressure is in the cross-section area and in the size of the Faraday dark space, which is clearly seen in fig. 3 (*a*) (Pl. IV.). At very low pressures the Faraday dark space occupies the whole of the space between the electrode, and the only indication of the discharge is the negative glow which covers the whole of the cathode. (In the photographs the cathode is the lower electrode.) As the pressure is raised, the cross-sectional area of the discharge is decreased so that it covers only part of the electrodes, and the Faraday dark space decreases in length with the formation of the positive column. The glow has then the appearance of fig. 3 (*a*) (Pl. IV.).

The next stage in the development of the spark is the formation of a bright core. The colour of this core may be bright pinky white, pink, or orange, according to the amount of discharge resistance in the circuit, and its development with rising pressure varies according to the same factor. The core of the glow when it first appears may be short, and it develops rapidly with increasing pressure if there is no discharge resistance, or very slowly if there is a large amount of discharge resistance. It should be understood that when this stage is reached the discharges are not a succession of glows of identical appearance, but may appear haphazardly, as in figs. 3 (*a*) or 3 (*b*) (Pl. IV.) or as some intermediate stage between them. When there is no discharge resistance the core is bright pinky white and develops almost at once to its full length and then begins to shoot through the Faraday dark space. With a discharge resistance of 40 or 100 ohms the core is pink, less bright, and of larger cross-section than that with no resistance. It develops more slowly, and quite a number of the type of fig. 3 (*b*) (Pl. IV.) may be seen. This type is, of course, bordering on a spark, and where

there is no discharge resistance it is only seen intermittently with sparks and coreless glows. The cross-section of the anode column, and also of the cathode glow, is also reduced as the pressure is increased. This is clearly seen from the photographs. The anode column is bright pink when no discharge resistance is used, and becomes more blue as this is increased.

For the purpose of this work it has been decided to distinguish between a spark and a glow by the presence or not of an unbroken dark space. If the central core does not penetrate the Faraday dark space the discharge is referred to as a glow, and if the core penetrates the dark space it is referred to as a spark. Various other differences between sparks and glows have been suggested, such as the formation of bright spots at the cathode, jaggedness of the spark, fluorescence of the walls. These latter, however, are only attendant upon the spark in certain cases, and cannot be regarded as essential to it. The transition from spark to glow is gradual. There is no doubt that the discharge shown in fig. 3 (*a*) (Pl. IV.) is a glow possessing all the accepted features of glows, and there is no doubt that in fig. 3 (*d*) (Pl. IV.) is a spark according to the usual meaning of the word. But between the two we get a gradual change of appearance, of which figs. 3 (*b*) and 3 (*c*) (Pl. IV.) are examples of intermediate states. The spark in fig. 3 (*c*) shows no sign of jaggedness, and in certain cases has no bright spots at anode or cathode. There is certainly no fluorescence of the walls of the discharge-tube if they are far enough away from the electrodes. The only *definite* change which does occur in all cases in the course of the change from glow, as in fig. 3 (*a*) (Pl. IV.), to spark, as in fig. 3 (*d*) (Pl. IV.), is the penetration of the Faraday dark space by the core. This occurs suddenly and distinctly, and so is adopted as the criterion for differentiation.

In fig. 3 (*c*) (Pl. IV.) the core has penetrated the dark space *, and so the discharge is now called a spark. The photographs were taken for a discharge resistance of 100 ohms. When the discharge resistance was zero the change was rather more definite. On shooting through the dark space the core became fine, much brighter and jagged, more as in fig. 3 (*d*) (Pl. IV.), but still retaining

* This is more clearly shown on the original photographs than on Pl. IV.

the anode and cathode glows. The change in the case of 45 ohms discharge resistance was accompanied by the formation of bright white spots at the anode and cathode. These spots were also present, but not so bright, in the case of 100 ohms, as close examination of fig. 3 (*c*) (Pl. IV.) will reveal. With lower current values the penetration of the Faraday dark space was not marked by any changes in colour or shape of the core. With values of discharge resistance of 5000 ohms there appears to be no further change in appearance of the discharge beyond the point where the core penetrates the dark space. The core remains orange, and, apart from appearing more fierce and bright, does not seem to become smaller in cross-section or more jagged as the pressure is raised.

With higher current values the effect of raising the pressure above that in fig. 3 (*c*) (Pl. IV.) results in the disappearance of the anode and cathode and the core becoming brighter and jagged, as in fig. 3 (*d*) (Pl. IV.). This spark becomes more fierce as the pressure is raised, and changes from pink to blue, being bright and jagged, with bright spots at the ends. When no discharge resistance is used the colour of the spark is white, and becomes very intense and bright indeed.

Variation of Proportion of Sparks with Increasing Pressure.

For these experiments the discharge resistance, r, was fixed at 100 ohms. For each spacing and pressure the number of sparks occurring in thirty observations was noted.

The results are embodied in fig. 4, where for the spacings (in millimetres) marked against the curves the number of sparks observed is plotted against pressure.

Change in Method of Observation.

Since the method of obtaining results described above was found to be very lengthy, and only the boundary pressures for sparks and glows are required, the method of making observations was changed.

The second method was as follows. To obtain the boundary pressure for sparks at one electrode spacing, the electrodes were set to this spacing and the pressure

to some value about 1 cm. Hg below the boundary (as determined from previous results). The applied potential was then adjusted so that discharge occurred at the rate of about four per second, and dry air was admitted through a needle-valve at a slow rate. The discharges were observed, and as soon as one spark was seen the pressure was read.

To obtain the boundary pressure for glows the pressure was gradually decreased, and immediately one glow was observed the value of pressure was taken.

Fig. 4.

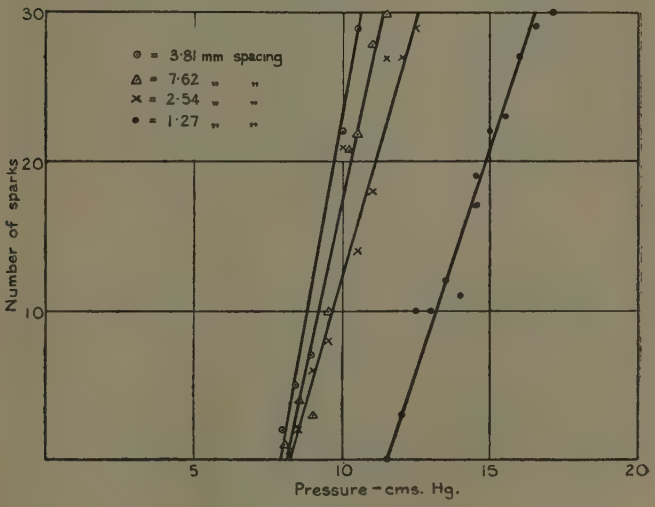

The cathetometer was dispensed with for observing discharges, since when they pass in rapid succession the eye will naturally not wander from the position of the discharge, and will, therefore, not miss some, as happens if there is a long interval between discharges. The eye can focus the core of the discharge more sharply than with a cathetometer, and so can observe with more certainty whether it passes through the Faraday dark space. This method was only used for the variation of boundary pressure with dark current. For other tests still another method was used, as described below.

In this third method of observation the boundary pressures were found by trial and error method, *i. e.*, the discharges were observed with constant spacing and pressure, and when one spark in, say, a hundred glows occurred the pressure was taken to be the boundary for sparks. Similarly, if one glow in a hundred sparks occurred the pressure is taken to be the boundary for glows.

The pressures at which the above occurred we found by trial, and in practice the method was found to take no longer than the previous methods of determining the boundary pressures.

The new method is probably more accurate than the others, since the pressure is not falling or rising whilst the hundred discharges are being observed. For example, suppose the pressure were such that one spark in a hundred discharges occurred. With the old method, if the spark did not occur till the hundredth discharge, the pressure would have risen considerably before it occurred, and so give a high reading of boundary pressure.

Variation of Critical Pressures with Electrode Spacing.

On fig. 5 is plotted the variation of the critical pressures with electrode spacing.

Since the capacity of the electrodes must increase as the electrode spacing decreases, it was decided to investigate whether this was affecting the critical pressure range. To see whether capacity had any effect a condenser of value 1000 $\mu\mu$fd. was shunted across the electrodes, as shown by the dotted lines in fig. 1. No effect could be detected, so that it is clear that the variation of critical pressure with decreased spacing is not due to this cause.

The group of unusually high readings for the upper boundary pressure appeared during a few consecutive days. Subsequent, as well as previous, measurements followed the curve, as shown in the figure.

Variation of Critical Pressure with Current.

The following experiments were carried out to determine the effect of variation of the discharge resistance on the boundary pressures between sparks and glows.

The electrode spacing was held constant at 5 mm. and the capacity was constant at 5530 $\mu\mu$fd. Starting

from a low pressure at which no sparks occurred, the pressure was gradually raised, whilst the discharges were allowed to pass at a rate of about five per second, the applied voltage being adjusted to give this rate of discharging. As soon as one spark was observed the pressure was noted. The above procedure was repeated five times and a mean value was taken. The whole was repeated for different values of discharge resistance.

Fig. 5.

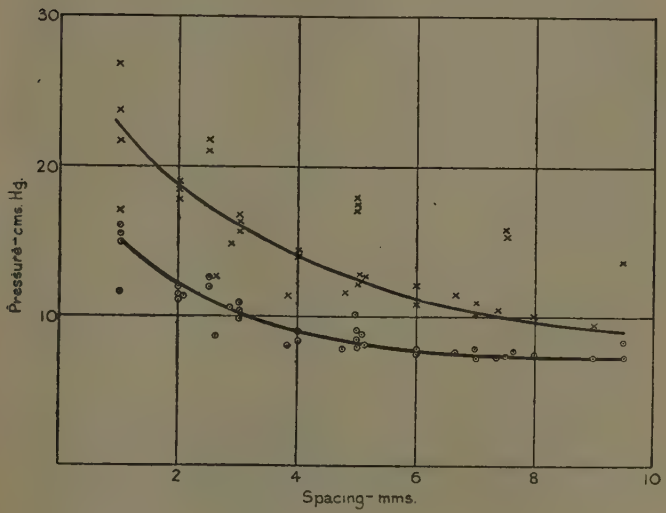

The other boundary pressure, *i. e.*, the maximum pressure at which a glow could occur, was found by starting at a high pressure and gradually lowering it until a glow occurred. This was repeated for different values of discharge resistance.

The results are plotted in fig. 6.

To determine whether the dryness of the air affected the readings, the tube was flushed out with dry air and the readings for 50 ohms repeated, then flushed out with atmospheric air and the readings for 50 ohms repeated. The results were quite consistent.

Notes on taking of Photographs.

To obtain the photographs of fig. 3 (Pl. IV.) double exposures were made. The electrodes were taken separately from the discharges.

Difficulty was experienced in illuminating the electrodes in such a way that the images of the discharges would not be impaired. To obtain a clear image of the discharge a dark background was required, and this meant direct

Fig. 6.

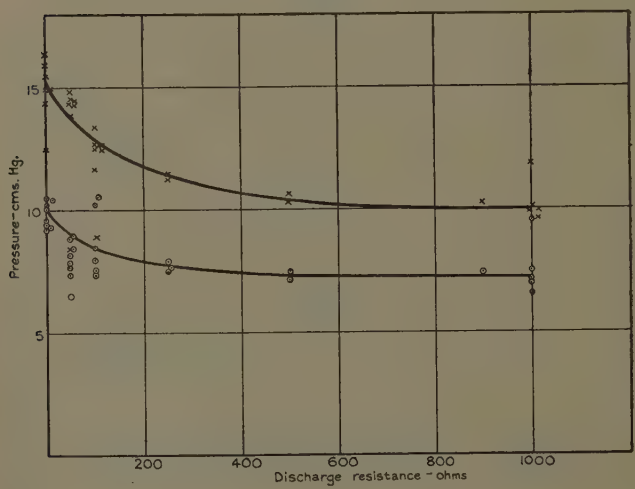

illumination of the electrodes. Owing to the electrodes being spherical and highly polished brass, it was found exceedingly difficult to illuminate the inner surfaces of the electrodes. The illumination was restricted to the sides, since the cylindrical shape of the glass discharge-tube produced reflexions if the illumination was from the front. To avoid reflexions from the back wall of the tube a piece of black felt was placed as background inside the jar.

Illumination was by means of two galvanometer lamps projecting images of their line-filaments on to the electrodes, one on each. It was also found that a satisfactory image

could only be produced if the axis of the camera lens passed midway between the electrodes.

The exposures were made on Ilford Double X-Press plates, and by trial 10 sec. exposure was found to give a good image.

The discharges were photographed in the dark. In the case of fig. 3 (*a*) (Pl. IV.) ten glows were photographed, since it had previously been ascertained that all glows were alike and in the same place.

For figs. 3 (*b*) and 3 (*c*) (Pl. IV.) only five discharges were photographed, since it was not certain that ten consecutive discharges would be alike. However, good results were obtained.

For fig. 3 (*d*) (Pl. IV.) only one discharge was photographed, since sparks have not all the same "jaggedness," and do not all fall in the same place. Moreover, a spark is brighter than a glow, and one discharge will produce a reasonably bright image.

XLI. *Paschen's Law at Low Striking Potentials.* *By* Prof. E. L. E. Wheatcroft, *M.A.*, *and* H. Barker, *B.Sc.**

ACCORDING to Paschen's Law the sparking votlage of a gas as measured between parallel electrodes is a function only of the product of the pressure of the gas and the electrode spacing. If this law holds good, it may be taken as evidence of a certain type of breakdown mechanism—for example, that the ionization processes are dependent on the ratio of electric field strength to pressure †. It is, therefore, important to know to what extent it does hold good over the range where the resultant discharge is sometimes a glow and sometimes a spark. It is, however, just over this region that the results of previous investigators (see below) are inconsistent. For this reason the experiments described herein were undertaken—first, to see if the law holds good over this range; secondly, to establish for air the striking potential curve;

* Communicated by the Authors.
† Townsend, 'Electricity in Gases.'

and, thirdly, to see if there is any distinction between the striking potentials of sparks and glows.

It is concluded that the law does hold good, and the curve found for air is given in the figure.

It is also concluded that the difference between spark and glow is small, the striking potential of the former being some 50 to 100 volts lower.

The experimental circuit and the discharge tube were the same as in the previous paper*, and are not separately described here. The air was dried over calcium chloride.

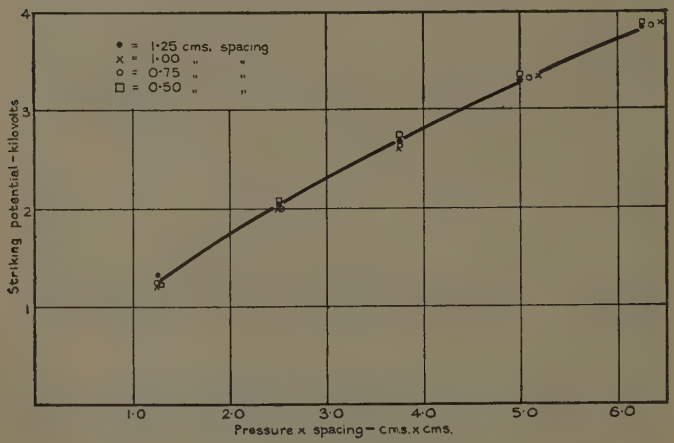

Previous Work.

Whitehead ('Dielectric Phenomena: Electrical Discharge in Gases') has collected the available data on the breakdown of gases in uniform fields. In the region where the sparking voltage is below 5 kv. measurements of sparking voltage were carried out by the following investigators:—Kelvin, Proc. Roy. Soc. A, x. p. 326 (1859–60); Liebig, Phil. Mag. xxiv. p. 106 (1887); De la Rue and Müller, Phil. Trans. clxxi. p. 65 (1880); Baille, *Ann. de Chim. et de Phys.* xxv. p. 488 (1882); xxix. p. 181 (1883); Peace, Proc. Roy. Soc. A, lii. p. 99 (1892); Strutt, Phil. Trans. A, cxciii. p. 377 (1900); Müller, *Ann. der Phys.* xxviii. p. 585 (1909).

* "The Development of a Spark from a Glow," Phil. Mag.

The results of all these experiments, plotted against the product for air, show a wide variation of striking voltage from the minimum value up to about 5 kv.

Paschen * made experiments with air at various pressures and using various sparking distances. His electrodes were spheres 1 cm. radius. The experiments were repeated on different dates, and from mean values of these experiments Paschen constructed a table and formulated his law. His results when plotted against the product undoubtedly lie on a single curve, and he considered the law to be proved, since values of sparking potential found by interpolation agreed fairly closely with actual experimental values.

Carr (Phil. Trans. 1903, p. 403) made very extensive investigations of Paschen's Law. His electrodes were metal plates 3·6 in. in diameter, embedded in ebonite and spaced by ebonite rings made accurate to 0·001 mm. Air was dried by bubbling through sulphuric acid, then with phosphorus pentoxide. The pressure was measured with a MacLeod pressure gauge accurate to 0·001 mm. The potentials were applied to the plates for a considerable time before increasing it in order to see if sparking occurred with a long application of potential. Between each discharge a time was allowed for the gas to become normal. The experiments were repeated using electrodes of different materials, and also using different electrode areas. He concluded that —

(i.) The sparking potential is independent of the material of the electrode.

(ii.) The sparking potential is independent of the area of the electrodes.

(iii.) The minimum sparking potential is a physical constant of the gas.

Carr's results also appear to lie on a single curve.

From the references given above it will be seen that two experimenters only have proved Paschen's Law—Paschen himself and Carr. All other experimenters have either used non-uniform fields or have used one distance only or one pressure only.

Liebig and Kelvin made observations at atmospheric pressure only.

* *Ann. der Phys.* **xxxvii. p. 69** (1889).

De la Rue and Müller and Strutt used fixed electrode distances.

Baille's results do not prove Paschen's Law.

The curve drawn from Carr's results is a straight line between 350 and 1500 volts, and may be taken to prove Paschen's Law, but it must be remembered that Carr restricted the path of the spark and used embedded electrodes.

Paschen's results give a curve approximating to a straight line, and they are fairly consistent. Paschen used spherical electrodes, and his values are taken over a bigger range than Carr's, namely, from 0·7 to 5 kilovolts.

Consistency of Breakdown Voltage with repeated Renewals of Dried Air in Tube.

The following procedure was adopted to find the consistency of different samples of air. The pressure was adjusted as accurately as possible, and the breakdown potential determined. The tube was then evacuated to as high a degree of vacuum as the pump permitted, and fresh dry air was allowed in so as to adjust the pressure to the previous value. The breakdown voltage was again determined. The procedure was repeated a second time. We thus have a value for the breakdown voltage of three samples of dry air under the same conditions of pressure and electrode spacing.

If Paschen's Law holds even approximately at a pressure of 2·5 cm. a variation in pressure of 0·1 mm. would be expected to produce a voltage variation of about 10 volts. The electrode spacing was not disturbed during the three tests, so no variation can be produced by inaccurate spacing. An error of 0·1 mm. in the pressure value is probable, since the manometer could not be read to within this accuracy. The variation in voltage in the three tests is 13 volts, and so the results may be regarded as consistent within the limits of accuracy of the apparatus.

A similar test was made using a pressure of 1·25 cm. In this case the voltage variation is 18 volts. At 1·25 cm., however, an error of 0·1 mm. in pressure would be expected to produce a voltage variation of 20 volts.

These experiments seem to indicate that within the limits of accuracy of the apparatus the sparking potential does not depend on the air in a discharge-tube attaining

a particular physical state, but can be repeated with dry air.

It was found that in checking previous values agreement was in many cases not so good. It was also found that if the scale of the manometer was set on one day to read the same as the barometer when completely evacuated, it would not do so the following day. The scale was re-set each day, and this probably accounts for some

TABLE I.

Striking Potentials in Volts.

D = 1·25 cm. p = 1·0 cm. Hg.		pD = 1·25 cm. × cm.
1st set.	2nd set.	3rd set.
1330	1300	1305
1350	1320	1330
1330	1300	1350
1350	1350	1300
1340	1320	1330
1350	1300	1320
1360	1330	1305
1360	1305	1340
1360	1330	1330
1360	1350	1320
Mean.. 1349	Mean.. 1320	Mean.. 1323

Mean value of all readings.... 1330.

divergence of results. It was decided that the chief variation was in the barometer owing to its being in a closed glass-fronted case, and thus not taking up the correct reading of atmospheric pressure. When the case was left open this error was eliminated, and further readings of sparking potential showed consistency.

Typical sets of results are shown in Table I., the ten readings for any one setting of pressure and distance being taken at approximately 15 seconds interval, and successive sets of ten with fresh samples of air.

The figure shows the striking curve obtained from these results. There is no doubt that the deviation of the individual points from the curve is within the limits of experimental accuracy.

The possible error in reading the pressure would be about $\pm 0{\cdot}02$ cm. This is due to the scale used, zero error, parallax, and the thickness of the lines. The effect of this error is not very great even at low pressures, it being only 2 per cent. at the minimum pressure of 10 mm.

The error in reading the distance between the electrodes is more serious. Although a cathetometer was used, the curvature of the electrodes makes measurements of the distance difficult. It is difficult to focus on a curve-surface, even when viewing the outline of the electrode against the light. Unless the electrodes are set perfectly coaxially the outlines of the two do not focus in the same plane, and it is due to the fact that one electrode is viewed dead in focus and one out of focus that the possible error is estimated at $\pm 0{\cdot}01$ cm. Coupled with the above difficulties is the uncertainty of the position of the spark or glow.

Subsequently a different method of measurement was employed. The electrodes were set at approximately the required distance by the cathetometer. The pressure was then set to a value giving distinct sparks, and the discharges were allowed to take place in rapid succession. The cathetometer was then focussed on the sparks, *i. e.*, on the plane of the discharge, and with the vertical hair-line covering the spark. Keeping the cathetometer focussed in this plane, the electrodes were set to give the required distance. The sparks were again passed to ensure that their position had not been affected by the movement of the electrodes. It was hoped that with this method of measurement the error introduced would be considerably lessened.

It should be noted that in the determination of the figure, although the measurements of distance were made by the inaccurate method described previously, five different electrode spacings were used for each value of pD. This would tend to balance out somewhat the spacing error.

Whilst the cathetometer was focussed on the spark for the purpose of measurement it was observed that the position of the sparks was not stationary, *i. e.*, every spark did not occur in the plane of the hair-line. This

TABLE II.

p (cm. Hg)	8	8·5	9·0	10·0	10·5
pD (cm.× cm.) ..	3·04	3·24	3·43	3·81	4·00
	2230	2320	2470	2580	*2670*
	2230	2370	2380	*2530*	*2640*
	2270	2310	2470	2620	*2640*
	2290	2310	*2370*	*2530*	*2640*
	2240	2340	*2380*	*2530*	*2640*
	2210	2300	*2370*	*2510*	*2640*
	2250	2350	2380	2700	*2660*
	2250	*2280*	2390	2620	*2660*
	2170	*2280*	2400	*2510*	*2640*
	2230	2310	2400	2580	*2670*
	2260	*2280*	2420	*2530*	*2640*
	2260	2340	2400	*2510*	*2640*
	2240	2310	2400	*2510*	*2640*
	2250	2300	2440	*2510*	2770
	2170	2280	2400	*2510*	*2660*
	2250	2350	2430	*2530*	*2640*
	2210	2300	2430	2580	*2640*
	2230	2340	2380	*2530*	2800
	2260	2340	2380	*2510*	*2640*
	2230	2340	*2370*	*2510*	*2640*
	2260	2310	2470	2580	*2640*
	2210	2340	2380	*2530*	*2660*
	2210	2330	2380	2580	*2640*
	2260	2410	2400	*2510*	*2640*
	2250	2370	*2370*	*2530*	*2640*
	2230	2390	2500	*2510*	*2660*
	2250	*2280*	2470	*2510*	*2660*
	2240	2300	*2370*	*2510*	*2670*
	2230	2300	*2370*	*2510*	*2660*
	2250	*2280*	2400	*2530*	*2670*
Mean	2240	2325	2410	2550	2660
No. of sparks ...	2	5	7	22	28

Sparks noted with italicised figures.

may account for variations in the sparking voltage. This is more constant than the breakdown voltage for glows, as will be apparent on reference to the tables of results.

Other Precautions.

In order to avoid stale air causing variations in sparking voltage it was ensured that this was absent by "swilling" out the apparatus with dry air when it had been left standing for more than a few minutes or when atmospheric air had been admitted to the pump. To give a reasonable chance of the discharge occurring at constant time intervals the voltmeter was discharged to the same value every time after the spark or glow.

Difference in Striking Potentials for Spark and Glow.

In Table II. are given typical results of striking voltage tests. The glows are noted with normal and the sparks with italicised figures. The sparking voltage is always lower and more consistent than the glow. Nevertheless, there is so little difference between them that it appears perfectly justifiable to take an average for the purpose of proving Paschen's Law and of finding the striking voltage curve.

XLII. *The Theory of the Glow Discharge.*

By Prof. E. L. E. Wheatcroft, *M.A.**

IT was established by Paschen (*Ann. d. Phys.* 1889, p. 306) and Carr (Proc. Roy. Soc. lxxi. p. 374 (1903)) that the breakdown voltage of a gas between parallel plate electrodes is a function of the product of gas density p and electrode spacing d. This is known as Paschen's Law. Carr, Strutt (Phil. Trans. cxciii. p. 377 (1900)), and others have measured this function—which may for brevity be called the breakdown curve—and found it to have the form given in fig. 1. The curve is divided by a minimum at B into two regions, one, AB, the region of

* Communicated by the Author.

"short breakdown" and the other, BC, the region of "long breakdown"*.

The shape of this curve could, presumably, be calculated on the basis of Townsend's theory of breakdown, given the values of α, the electron-ionization coefficient, and β and γ, the coefficients of ionization or bombardment by positive ions. This has not yet been done because, although measurements of α are not difficult, and have been made by Townsend ('Electricity in Gases') and others (*e. g.*, Paavola, *Arch. f. Elekt.* xxii. p. 443 (1928)), yet there are no independent data on β or γ under the conditions of breakdown. As a result, therefore, we have to deduce the values of these coefficients, as Townsend did,

Fig. 1.

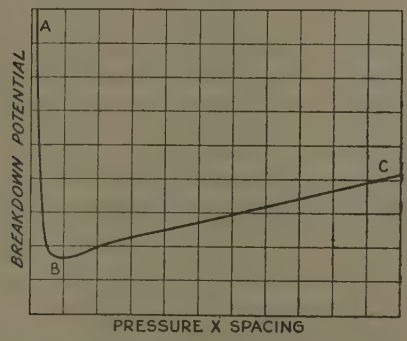

from the experimental conditions of breakdown. Thus, in our present state of knowledge, the breakdown curve affords a summary of the ionization data beyond which it is not, from a quantitative point of view, practicable to go. More especially is this true since the impurity of the gases and the state of the electrodes in a practical discharge-tube present a complication which the most elaborate data are not likely to overcome except in special cases.

If, therefore, the main features of any other form of discharge, such as the glow, can be interpreted quanti-

* This seems to be the best translation of the German words "Nahdurchschlag" and "Weitdurchschlag"—see Rogowski, *loc. cit. infra*. There seem to be few experiments made in the region of the short breakdown since those of Carr, possibly because there is some experimental difficulty in confining the discharge to the shortest distance between the electrodes.

tatively in terms of the breakdown curve for the same gas and the same electrodes, this must be considered at present a satisfactory explanation, and it will show, among other things, that the ionization conditions (α, β, γ) for the one are the same as those of the other, and that no important new process of ionization * is involved.

The main features of the glow which any theory must explain are (1) the normal or minimum cathode fall when the current density has its minimum or normal value ; (2) the abnormal or increasing cathode fall which accompanies a forced rise of current density when the current is increased over a limited cathode area. It is well known also that the regions of the discharge essential to its maintenance are the Crookes dark space and the cathode end of the negative glow, since (*a*) the other visible features are only found in a long tube, and disappear as the tube is shortened, and (*b*) practically the whole of the potential drop of a short tube is concentrated across the region mentioned. It is also known that as the cathode fall increases in the abnormal discharge the visible dark space decreases, and that, therefore, the relation between the maintenance potential and dark space length is similar in shape to the part AB of the breakdown curve. The diagram of fig. 2 illustrates this. Here the ordinates are potentials and the abscissæ distance measured from the cathode. The dotted line (1) represents the potential distribution along the tube for a high value of current density, and the dotted line (2) similarly for a lower current density. The " knees " of the curves lie on the solid line, which we may call for the moment the " cathode fall line," giving as it does the relation between V, the cathode fall, and D, the dark space length.

The potential difference between the electrodes is substantially equal to the cathode fall provided that the interelectrode spacing is not very great. If at any given current density the anode is brought close to the cathode so that the interelectrode spacing is less than the natural value of the dark space length for that particular current density, the " restricted " glow discharge results, and the maintenance potential is forcibly raised even higher †. Thus the cathode fall, and hence the maintenance potential, depend (at a given gas density) on the length of the dark

* Using the word ionization in the widest possible sense.

† Güntherschulze, *Zeits. f. Phys.* lxi. p. 1 (1930).

space, and that length may be limited either, as in the restricted case, by the interelectrode spacing, or, as in the abnormal case, by the current density at the cathode.

The contraction of the dark space due to the rise in current density follows from the positive ion space charge which accompanies the current and which causes the knee in the potential distribution curve. The greater the current the greater the space charge and the sharper the angle at the knee. Since, therefore, the knees lie on the cathode fall line and the latter slopes up to the

Fig. 2.

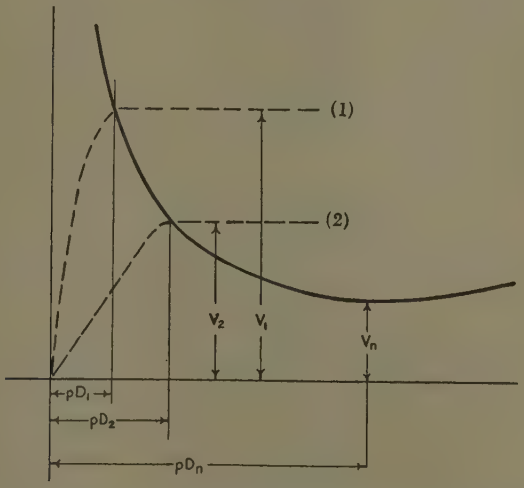

left, the increased current density results in a reduced dark space and a higher cathode fall. The quantitative relations for the angle of the knee have been studied theoretically and experimentally by Aston *, who showed that the law

$$\frac{Ip D^3}{V^2} = \text{constant}$$

was obeyed, where I is the current density and the other symbols have the meanings assigned above.

If Paschen's Law can be taken to apply to the maintenance potentials, gas-density is taken into account by

* Proc. Roy. Soc. lxxix. p. 80 (1907).

making the product pD the abscissa of fig. 2. This has been confirmed for experimental discharge-tubes by the present author * and by Heer †.

In order, therefore, to provide a quantitative explanation of the glow-discharge phenomena it is necessary to know for a given tube and given gas and electrode conditions the cathode-fall curve.

Fig. 3.

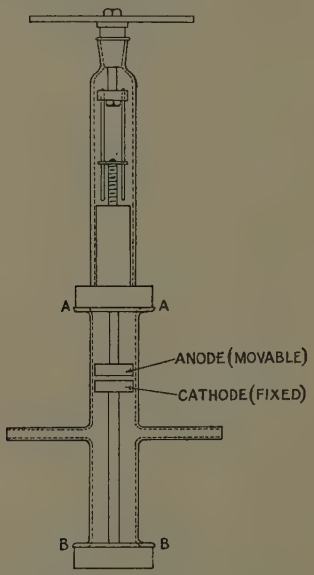

Rogowski ‡ sugggested a similarity between this curve and the breakdown curve as follows :—"Since we have long ago related the lowest point of the breakdown curve with the lowest cathode fall, why should we not connect the higher points of the breakdown curve with the higher cathode falls." This relation had previously been established by the present author §, and the results given below are an extension of those then published. Fig. 3 shows

* Proc. Leeds Phil. Soc. ii. 10, p. 483 (1933).
† *Arch. f. Elekt.* xxvii. p. 196 (1933).
‡ *Arch. f. Elekt.* xxvii. p. 857 (1933).
§ Proc. Leeds Phil. Soc. ii. 10 p. 483 (1933).

the discharge-tube which was used for the experiments. The electrodes were metal disks of 23·5 mm. diameter, enclosed in a glass tube of slightly greater diameter, so that the clearance between the edges of the electrodes and the glass varied with the irregularities of the tube from about $\frac{1}{4}$ to $\frac{1}{2}$ mm. The close-fitting glass is necessary, of course, to limit the cathode area and to force the abnormal current density. It was thought to be better to avoid actual contact between the electrodes and the insulation at the boundary of the discharge, as must be the case with embedded electrodes of the type used by Carr. As a result of the gap there is a slight "edge effect," due to the fringing of the discharge round the sides of the cathode, and at very short spacings (less than 1 mm.) it was necessary to make an empirical correction. It was found that if the effective spacing were taken to be 0·45 mm. greater than the measured distance between the parallel faces, Paschen's Law was accurately obeyed at pressures ranging from 46 to 960 microns of mercury and from 38 down to 0·63 mm. measured spacing. The edge effect is only important at the highest pressure.

The anode, the upper electrode, was movable under vacuum by screw-thread operated from the ground cone at the top of the tube. The tube was demountable at the flat ground surfaces AA and BB to facilitate changing the electrodes. The joints were sealed with Apiezon tap-grease. Since absolute values of cathode fall were not being sought, a high standard of purity of the gas or the electrode surfaces was not necessary. In fact one of the objects of the investigation was to show that, taking the breakdown curve as a datum line, a good quantitative measurement of the cathode fall could be obtained for any state of the gas or for any electrodes. The gas was in contact with P_2O_5 in a side tube, but no liquid air was used. Exhaustion was made with a mercury-vapour pump.

The Abnormal Discharge.

A typical result for air with brass electrodes is given in fig. 4. The points marked o are the striking potentials observed intermittently between the measurements of maintenance potential, which are marked 1, 2, 3, for the corresponding current values. D is the electrode spacing corrected, as stated above, for the edge effect. It would

appear from this result that the cathode-fall curve would lie slightly below the breakdown curve for air.

The Normal Discharge.

The normal cathode fall may be regarded as the limiting case of the abnormal. As the current density is reduced, the knees of the potential distribution curves in fig. 2 pass further to the right until they reach the point corresponding to the minimum of the breakdown curve. Any further

Fig. 4.

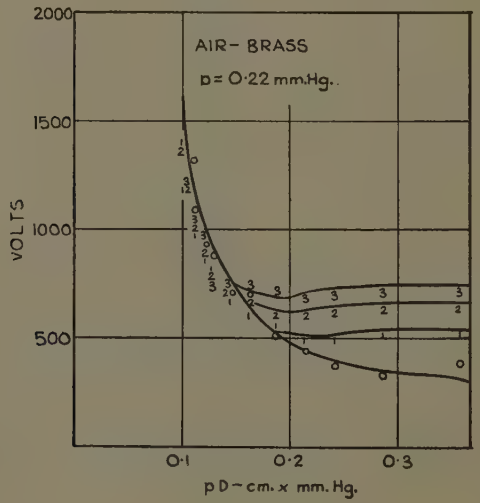

reduction of current density would then call for a higher cathode fall and a higher maintenance potential. The discharge naturally avoids this condition by maintaining the normal current density, since there is no artificial means by which a lower current density can be imposed.

The exact form of the "volt-ampere characteristic" of the tube depends upon the gas and the electrodes. Fig. 5 shows the results obtained with aluminium electrodes in argon at spacings marked against each curve. At 4 mm. spacing the glow is "restricted," and the cathode fall is independent of the current until current

density is so high that the natural dark space length is less than 4 mm., and this occurs at about 1 milliamp. The cathode fall appears to have for this tube two possible values, as indicated by the drop of 15 volts at 0·2 milliamperes. There is at the same time a slight movement of the negative glow. It is probably similar to that found by Güntherschulze *. It would, however, destroy the perspective if the maintenance potentials were plotted on the scale of fig. 5, and 15 volts on the scale of fig. 4 is quite negligible. In the same way Paschen's Law can only be taken to hold true to an accuracy of, say, ± 25 volts, yet it may be considered sufficiently established for our purposes here.

Fig. 5.

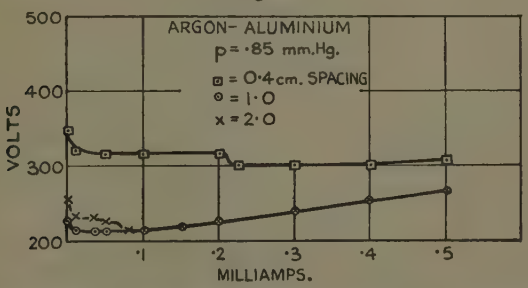

The region of the normal cathode fall is not extensive at the pressures used in these experiments, being masked by a rise of potential (in most cases) at very low values of current. For the purpose of measuring the normal discharge as a limit of the abnormal, the minimum maintenance potential was found by varying I and D at each pressure. These minima were then plotted against pD for comparison with the breakdown curve.

Figs. 6, 7, 8 show typical results, and establish the essential inter-relation of the two curves. With hydrogen the minimum maintenance potential coincided (within 1 or 2 volts) with the striking potential, and there was no marked fall with increasing current such as shown in fig. 5.

It is not to be expected that these results should agree with those of Schaufelberger † or Pike ‡, since in order to

* *Zeits. f. phys.* xxx. p. 175 (1924).
† *Ann. d. Phys.* lxxiii. p. 21 (1923).
‡ See Thomson, 'Conduction of Electricity through Gases,' ch. viii.

obtain absolute results comparable with thermionic work functions extraordinary precautions are necessary. In fact the absolute values of the minimum maintenance potentials do not repeat with fresh electrodes of the same

Fig. 6.

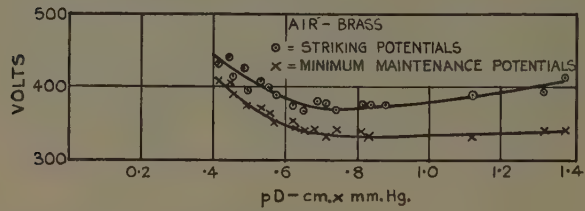

Fig. 7.

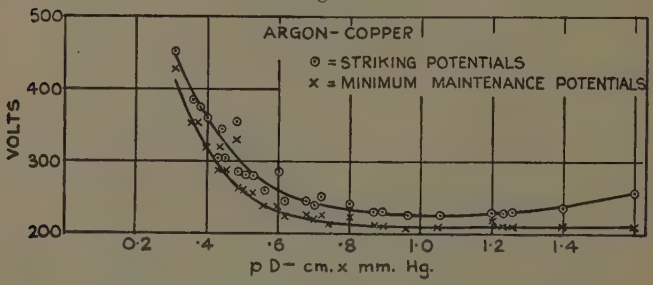

Fig. 8.

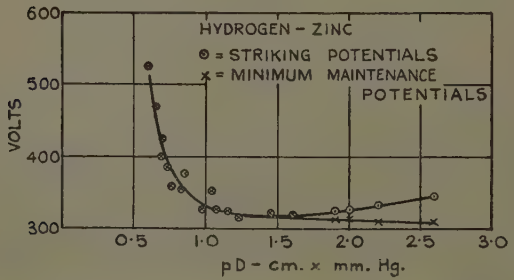

material, and must also depend on small traces of vapour in the gas. They do, however, establish for a variety of cases the essential inter-relation between the breakdown and the cathode fall curves, and show that the theory of fig. 2 is essentially correct.

XLIII. *Constitution of Water in Solutions of Non-Electrolytes.*—I. *Acetone.* *By* C. S. Siva Rao, *M.A., Andhra University, Waltair (India)* *.

1. *Introduction.*

In two previous communications † the author has described the results of his investigations on the constitution of water in solutions of a number of strong electrolytes in it. The investigations were continued with a view to study the constitution of water in solutions of some typical substances of the other characteristic groups, namely, weak electrolytes and non-electrolytes. It is proposed to describe in this paper the results of the author's researches on the latter class of substances, viz., non-electrolytes. These too, besides the weak electrolytes, have not been thus far investigated with a view to study the variations that take place in the structure of the Raman water-band in their aqueous solutions. Not much has been achieved even by the physical chemists in this direction. Jones and his collaborators ‡ studied the solutions of certain non-electrolytes in water with a view to detect the presence of hydrates, if any, and arrived at the conclusion that there was no appreciable formation of hydrates in aqueous solutions of non-electrolytes. As their classification signifies, non-electrolytes do not dissociate into free ions in their aqueous solutions, which are therefore electrically non-conducting. The absence of charged ions perhaps accounts for the absence or smallness of hydration in solutions of these substances in water, although the formation of hydrates does not depend on the presence of charged ions alone, and the water molecules themselves, on account of their highly polar nature, might attract the molecules of the dissolved substance to form what are called "physical hydrates"—a process somewhat different from chemical hydration, in which ions alone are concerned, and which is a closer union between the solvent and the dissolved substance.

* Communicated by Prof. I. R. Rao, M.A., Ph.D., D.Sc. (Lond.).

† 'Current Science,' vol. iii. p. 154 (1934); and Ind. Journ. Phys. vol. ix. p. 195 (1934).

‡ Carnegie Institution of Washington, Publication No. 60 (1907).

2. *Experimental.*

As contrasted with strong electrolytes, a comparatively smaller number of the class of non-electrolytes dissolve in water to high concentrations, and of those that do, most of them, even with the most careful purification, give a large amount of continuous background in their Raman spectra. Most of the filters that are generally employed and found usually very effective have been tried, and yet this continuous spectrum persisted almost as strong as it was without the filter, except for the general weakening of the intensity produced due to partial absorption of the incident light by the filtering solution. The author has tried to work with solutions in water of glycerine and sugar at different concentrations, but not with much success. The presence of the continuous background in the spectra in all cases was very considerable, and the water-band could be hardly detected in any of them. Solutions of acetone in water alone have been thus far successfully tackled, although they too in the beginning gave considerable trouble. The results obtained with this substance alone will therefore be given in the following pages.

The experimental arrangement employed in these investigations is that devised by Wood *. The filtering solution employed in the present case is that of chromium sesquichloride in water, and is contained in a pyrex-glass condenser interposed between the mercury lamp and the experimental tube containing the liquid under study. The lamp is run under low intensity, and is cooled by means of a table-fan, to make the continuous spectrum inherently present in it as small as possible. With this arrangement, about forty-five hours of continuous exposure has been found necessary to obtain the Raman water-band in a 75 per cent. (by volume) solution of acetone in water, and at smaller concentrations correspondingly smaller times of exposure are sufficient.

3. *Results.*

The figure represents the intensity curves of the water-band excited by 3650 λ group in pure water, and solutions of acetone at 75, 50, and 25 per cent. (by volume) concentration in water, all of them having been studied at the

* Phys. Rev. vol. xxxvii. p. 1022 (1931).

laboratory temperature, viz., 31° C. To draw the intensity curve, the value of the intensity corrected for the continuous background at each point on the band is marked against the corresponding frequency. The band being very diffuse it is not possible to measure wave-lengths by means of a micrometer. Hence to determine the Raman frequency corresponding to any desired point on the water-band the dispersion curve for the region of the spectrum between 4047 λ and 4358 λ mercury lines is

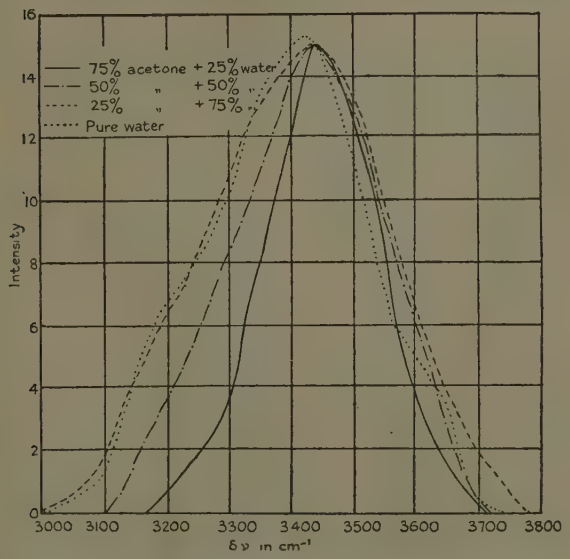

Intensity distribution along the Raman water-band in solutions of acetone at different concentrations and pure water.

drawn. The distance of each point on the microphotometric curve of the band from the 4078 λ line is measured, and the corresponding wave-length of this point is determined from the above dispersion curve. The distribution of intensity with Raman frequency along the band in the four cases is contained in Table I. (p 590).

From a study of the intensity curves the following results are clear, as contrasted with solutions in water of strong and weak electrolytes previously studied :—

(1) There is no shift in the maximum of the band in this case either to smaller or to greater frequency side with increasing concentration of acetone.

(2) The maximum of the band at all the concentrations studied coincides very nearly with that of the band for pure water.

(3) While there is a progressive shift in the smaller frequency portion of the intensity curve to the side of larger frequency with increasing concentration of the

TABLE I.

Intensity Distribution along the Raman Band for Water in the pure solvent and 25, 50, and 75 per cent. solutions of Acetone in Water.

Pure water.		25 per cent. acetone.		50 per cent. acetone.		75 per cent. acetone.	
$\delta\nu$ in cm.$^{-1}$.	Intensity.	$\delta\nu$ in cm.$^{-1}$.	Intensity.	$\delta\nu$ in cm.$^{-1}$.	Intensity.	$\delta\nu$ in cm.$^{-1}$.	Intensity.
3013	0·15	3054	1·30	3128	0·53	3206	0·79
3157	4·59	3124	3·94	3216	4·09	3236	1·61
3233	7·42	3216	8·44	3291	7·79	3281	2·50
3300	9·94	3285	10·95	3349	10·63	3331	6·27
3360	13·65	3335	13·08	3395	13·59	3366	9·56
3403	14·90	3435	15·00	3440	15·00	3416	12·43
3435	15·00	3492	13·86	3489	13·59	3440	15·00
3503	10·97	3594	7·64	3530	10·63	3496	13·03
3568	5·91	3656	4·07	3587	7·01	3546	8·50
3627	3·96	3712	1·89	3639	3·33	3592	3·85
3689	0·53	—	—	3686	0·83	3656	1·14

non-electrolyte, there appears to be no appreciable change in the larger frequency branch of the curve.

Similar to the results obtained with aqueous solutions of strong and weak electrolytes, with solutions of acetone also :

(4) The band gets sharper with increasing concentration.

(5) There is a gradual change in the shape of the smaller frequency branch of the intensity curve from a decisive convexity at the smallest (25 per cent.) concentration studied to a decreased convexity in shape at the next higher concentration (50 per cent.), and further

to a pronounced concavity at the highest concentration studied.

The magnitude of the above changes is as great as that observed in solutions of weak and strong electrolytes, and is perhaps even greater than the variation noticed with the second group of substances, viz., strong electrolytes, paying due regard to the extent of the change in concentration in each of the cases studied.

Table II. contains the positions of the maximum of the water-band in the pure solvent and solutions of acetone at the three concentrations.

TABLE II.

Solution.	Concentration.	Position of maximum.
1. Water	—	3424 cm.$^{-1}$.
2. Acetone in water .	75 per cent. (by volume).	3438 ,,
,, ,,	50 ,, ,, ,,	3438 ,,
,, ,,	25 ,, ,, ,,	3435 ,,

4. *Discussion.*

The influence of dissolved substances on the constitution of water in their aqueous solutions has been found, as seen before from the author's investigations on strong and weak electrolytes described in separate communications, to result in the following changes :—

(i.) There may be a change in the water equilibrium due to variations in the proportions of the single (H_2O), double ($H_2O)_2$, and triple ($H_2O)_3$ molecules assumed to exist in liquid water. It has been invariably found that the effect of the dissolved substance is to reduce the proportion of the triple molecules by dissociation into simpler types, especially single molecules, the proportion of which has always been found to increase with increasing addition of the substance.

(ii.) There may be a change in hydration of the dissolved substance, the extent and complexity of which has been found to decrease with increasing addition of the dissolved substance, owing to dissociation of the more complex hydrates into simpler ones and single water molecules.

The fact that in solutions of acetone in water studied in the present investigation there is no shift with increasing concentration of acetone in the position of the maximum, which more or less coincides with the maximum of the band in pure water, shows that the double molecules of the type $(H_2O)_2$ are exceedingly stable in solutions of acetone and that their proportion greatly preponderates over that of the other two types, especially at the higher concentrations. That this may be so is also supported by the observation of Ramakrishna Rao * that in liquid water at ordinary temperatures double molecules are far more stable than the other types. Further, the results noticed above with increasing concentration of acetone, namely, that there is an increased sharpening of the band at the higher concentrations with no shift in the position of the maximum, and that the smaller frequency portion of the intensity curve becomes more and more concave and shifts to the side of greater frequency, while the larger frequency branch of the curve remains more or less unaltered, all go to indicate that at the higher concentrations the triple water molecules dissociate and recombine amongst themselves or with the single molecules to form largely double water molecules $(H_2O)_2$, while the proportion of the single molecules remains nearly constant.

If, as has been observed by the physical chemists, there is no appreciable hydration in solutions of non-electrolytes in water, then perhaps the effect of acetone on the constitution of water in its aqueous solutions is mainly to bring about a change in the water equilibrium as discussed above.

But as the magnitude of the changes observed in the appearance of the band with increasing concentration of acetone is as great as that of the changes obtained with weak electrolytes, and perhaps even greater than that noticed with strong electrolytes, the author is led to think that at the lower concentrations there are present the so-called physical hydrates, which probably dissociate at higher concentrations into double water molecules and simpler hydrates with two associated molecules of water of hydration, or into free acetone molecules and dihydrol. It may be that both the effects—one due to change in water equilibrium and the other due to change

* Proc. Roy. Soc. vol. cxlv. p. 489 (1934).

in hydration—are present, as is found to be the case with the other groups of substances studied before, and that each of these contributes its own share to produce the observed results.

The fact that there is no appreciable shift in the position of the maximum of the water-band in solutions of acetone, and that it almost coincides with the maximum of the band in the pure solvent, leads to the presumption that the behaviour of water under the influence of dissolved acetone is something analogous to that in solutions of hydrochloric acid and chlorides discussed in a previous paper * ; but the fact that, whereas there is a slight broadening of the band at the higher concentrations as compared with the lower in the latter class of substances, there is observed in the present case a pronounced sharpening of the band at the higher concentrations, differentiates it from hydrochloric acid and chlorides. Although this latter result is similar to that observed with strong and weak electrolytes, the former makes it different from these classes of substances with regard to its influence on the constitution of water. It may be therefore that non-electrolytes behave as a class by themselves as regards this property of their aqueous solutions. But it is too early to come to any definite conclusions on this point from the results obtained with only one substance, and further work with a number of non-electrolytic solutions in water is necessary to make this point clearer.

In conclusion, the author takes this opportunity of expressing his grateful thanks to Dr. I. Ramakrishna Rao for his very keen interest and advice during the progress of the above investigation.

5. *Summary.*

The author has investigated the constitution of water in solutions of acetone at different concentrations by a study of the structure of its Raman water-band as a first step towards such a determination in non-electrolytic solutions.

The main results obtained may be briefly summed up as follows :—

(i.) The Raman band for water gets sharper with increasing concentration of the dissolved substance.

* Ind. Journ. Phys. vol. ix. p. 195 (1934).

(ii.) The intensity maximum of the band, which is in about the same position as for water, does not shift with change of concentration as is the case with strong and weak electrolytes.

(iii.) While the larger frequency portion of the intensity curve of the water-band does not suffer any appreciable change, the smaller frequency branch shifts to the greater frequency side and changes from convex to concave in its shape as the concentration of acetone is increased.

These results are discussed in relation to change in water equilibrium and in "physical hydration," and are shown to indicate the preponderance of double water molecules and double hydrates over the other types, especially at higher concentrations of the dissolved substance.

Andhra University College of
Science and Technology, Waltair.
January 1935.

XLIV. *The Contact Potential Difference between Clean and Oxygenated Tungsten.* *By* A. L. Reimann, *B.Sc., Ph.D., F.Inst.P.* (Communication from the Research Staff of the M.O. Valve Company, Limited, at Wembley *.)

Introduction.

THE contact potential difference V_{12} between two systems 1 and 2 is theoretically related to the corresponding difference of work functions $\chi_2 - \chi_1$ by the simple equation †

$$eV_{12} = \chi_2 - \chi_1, \quad \ldots\ldots (1)$$

e being the electronic charge. In this the work function is defined as the quantity χ in the thermionic equation

$$i = A_0 DT^2 \epsilon^{-\chi/kT}, \quad \ldots\ldots (2)$$

where i represents the electron emission at the absolute temperature T from unit area of emitting surface, A_0

* Communicated by C. C. Paterson, M.I.E.E.

† See, for example, J. A. Becker and W. H. Brattain, Phys. Rev. xlv. p. 694 (1934).

stands for $\frac{4\pi mek^2}{h^3}$ and has the numerical value of 120 amp. cm.$^{-2}$ deg.$^{-2}$, and D is the mean transmission coefficient. Tolerably good experimental verification of equation (1) has been obtained in a few cases where it has been tested, but in the case of clean tungsten and tungsten covered with a film of adsorbed oxygen (" oxygenated tungsten ") there is not even any approach to agreement between the experimental data hitherto obtained for eV_{12} and $\chi_2 - \chi_1$. It was in the hope of clearing up this situation that the experiments here to be described were undertaken. Incidentally some observations were made on the evaporation of oxygen (whether in chemical combination with tungsten or otherwise) from oxygenated tungsten.

Discussion of Earlier Experiments.

Data for the electron emission from oxygenated tungsten were obtained by Kingdon * in 1924. As the adsorbed oxygen was found to evaporate at an appreciable rate at temperatures sufficiently high for the electron emission to be measurable, oxygen was admitted continuously to the experimental vessel at a slow rate and allowed to be consumed by the filament. In this way Kingdon hoped to compensate for the evaporation and keep the filament practically completely covered. The temperature range over which the emission was measured was from 1500° to 1680° K. and the results obtained may be represented by the empirical formula

$$i = AT^2\epsilon^{-\psi/kT} \quad . \quad . \quad . \quad . \quad . \quad . \quad . \quad (3)$$

in which the values of the constants A and ψ are $\frac{5\times10^{11}}{\rho}$ amp. cm.$^{-2}$ deg.$^{-2}$ and 9·22 e.v. respectively, ρ being the ratio of the true effective emitting area to the apparent (macroscopic) area. The quantity ψ was taken by Kingdon to be the work function of oxygenated tungsten, but, as we shall see presently, modern theory demands a different interpretation.

We have no direct means of knowing the precise value of the roughness factor ρ of Kingdon's specimen. It is, nevertheless, possible to arrive at a sufficiently good estimate of its value for our purpose. In the first place

* K. H. Kingdon, Phys. Rev. xxiv. p. 510 (1924).

it should be noted that very large values of ρ are excluded on account of the fact that the field cannot penetrate into deep cuttings or hollows, and areas lying in these will, therefore, not contribute to the thermionic current. It is because of this that the word "effective" has been used in the definition of ρ. On the other hand, there is good reason for believing that ρ is appreciably greater than 1. It has been calculated by Tonks * that for etched tungsten whose crystals are oriented at random (which, however, the crystals in a drawn wire are not) the true exposed surface area must exceed the apparent area by a factor of at least 1·225. In the case of an actual specimen of heat-treated (thermally etched) tungsten wire Taylor and Langmuir † found strong evidence that the true exposed area was about 1·35 times the apparent area. It is possible, however, that not the whole of this was effective in the sense discussed above. If we assume a round 1·3 for the ρ of Kingdon's specimen, we shall probably be within something like 10 per cent. of the truth, and an error of this order will not have any appreciable effect on the conclusions in which it is involved. With ρ equal to 1·3 the A of Kingdon's data would become $3{\cdot}8\times10^{11}$ amp. cm.$^{-2}$ deg.$^{-2}$.

Comparing (3) with (2), we see that, since $\bar{D}$ cannot be greater than unity, the only way in which the high value found for A can be reconciled with thermionic theory is to suppose the χ of Kingdon's specimen to have varied linearly with the temperature. Setting $\bar{D}$ equal to 1—this seems justified in view of the electronegative character of the contamination—it is an easy matter to calculate the value χ must have had at any temperature in the range covered. Thus at the lower end of the range, 1500° K., to account for A being greater than A_0 by a factor of $3{\cdot}2\times10^9$, χ must have been less than ψ by an amount such that

$$\epsilon^{\frac{\psi-\chi}{1500k}}=10^{\frac{5040\,(\psi-\chi)}{1500}}=3{\cdot}2\times10^9,$$

whence χ is found to have had the value 6·39 e.v. Similarly, at 1680° K. (the upper end of Kingdon's range) χ must have been 6·05 e.v.

* L. Tonks, Phys. Rev. xxxviii. p. 1030 (1931).
† J. B. Taylor and I. Langmuir, Phys. Rev. xliv. p. 423 (1933).

It is important to remember that these figures apply only to Kingdon's specimen for whatever dynamic equilibrium condition its surface was in at the two temperatures. A corresponding variation of the work function with temperature is by no means to be taken as characteristic of tungsten with a constant covering of oxygen, for in view of Kingdon's difficulty with evaporation it seems probable that the surface of his specimen became progressively less completely covered as the temperature was raised. There must be some degree of covering—perhaps that corresponding to a complete monatomic film—which makes the work function a maximum. It will be convenient to refer to this as the "most effective" covering. Then, according to the evidence, Kingdon's covering approached more and more closely to the most effective as the temperature fell, down as far as 1500° K. Of course, even at 1500° K. the covering may still have been less than the most effective, and 6·39 e.v. must, therefore, be regarded as a lower limit rather than as the actual value of the work function of a most effectively covered surface at this temperature.

As Becker and Brattain * and the author † have pointed out, there is good reason to believe that for clean tungsten $\overline{D}$ is practically equal to 1, the discrepancy between its A and the theoretical A_0 being due to a slight temperature variation of the work function, brought about mainly by thermal expansion. The work function of clean tungsten at 1500° K., calculated from its known emission at that temperature on the assumption that $\overline{D}$ is equal to 1 and ρ is equal to 1·3, is 4·64 e.v. Subtracting this from 6·39, we find for the theoretical contact potential difference at 1500° K. between clean tungsten and Kingdon's best-covered tungsten 1·75 volts. If, as one would naturally suppose, the rate of variation of the work function with temperature is of the same order for oxygen-covered as for clean tungsten, about 1·75 volts must be the contact potential difference between the two systems at room temperature also. And since the covering of Kingdon's specimen at 1500° K. may have been less than the most effective, we should expect the contact potential difference between clean tungsten and most effectively

* *Loc. cit.*

† A. L. Reimann, 'Nature,' cxxxiii. p. 833 (1934); Phys. Rev. xlv. p. 898 (1934).

oxygenated tungsten to be, if anything, somewhat greater than this.

An attempt to measure directly the contact potential difference at a low temperature between clean tungsten and tungsten oxygenated by exposure, cold, to oxygen was made by Langmuir and Kingdon * in 1929, but a value of only 0·8 volt was obtained. If this result is to be taken as applying to really clean and most effectively oxygenated tungsten, it can be reconciled with Kingdon's thermionic data only by supposing that the work function of oxygenated tungsten increases with temperature at a far greater rate than does that of clean tungsten. However, apart from the question of the relative merits of oxygenating tungsten hot or cold, there would appear to be some doubt whether the surface conditions achieved by Langmuir and Kingdon were really those aimed at. Their experimental tubes, besides having oxygen admitted to them, contained cæsium. This must have contaminated at least the support wires of the test filaments, and it might conceivably have spread from thence over their entire surfaces, despite the liquid-air cooling to which the tubes were subjected during the course of the experiments. In the present investigations none but the wanted contaminant, oxygen, was admitted to the experimental tube.

The Experimental Tube.

This is depicted in fig. 1. Within a glass bulb were mounted coplanarly two U-shaped electrodes A and B, of 0·10 and 0·20 mm. tungsten wire respectively, and similarly oriented, with their tips about 1·5 mm. apart. The lengths of wire in A and B were 3·2 cm. and 12 cm. respectively. Filament A was intended as a constant source of electrons, and B, either clean or oxygenated, as a collector. As in the experiments of Langmuir and Kingdon, the idea was to determine the infra-saturation thermionic current flowing between A and B as a function of the potential difference between them, first with B clean and then with B oxygenated, A being kept hot enough during the measurements to prevent retention of oxygen by its surface. The voltage displacement between the two corresponding current-voltage curves

* I. Langmuir and K. H. Kingdon, Phys. Rev. xxxiv. p. 129 (1929).

should then be a measure of the contact potential difference between clean and oxygenated tungsten.

In Langmuir and Kingdon's tubes the cathode and anode filaments, which were of equal dimensions, were placed side by side, and surrounding them were two auxiliary electrodes of metal sheet, one of which, by being kept at a negative potential with respect to the cathode,

Fig. 1.

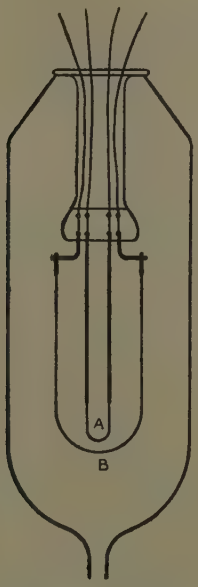

The experimental tube.

served to eliminate effects due to the cold ends of the filaments, where one might expect surface conditions to be somewhat ill-defined. In the present work no such auxiliary electrodes were used, as it was feared that they might act as a source of unwanted contamination, *e. g.*, of oxygen which could condense on B when it was supposed to be clean. It was hoped to render effects due to ends negligible by the geometrical arrangement chosen, in which the filament tips (between which the main thermionic current might be expected to flow) were much nearer to

one another than any other parts. That this hope was realized, at least so far as A was concerned, was shown by the fact that the voltage displacement between current-voltage curves corresponding to different conditions of the surface of B was independent of the temperature of A within a wide range of the latter.

The Experiments.

The tube was attached to a mercury condensation pump system with the filaments hanging vertically downwards. Between the mercury trap, cooled by liquid air, and the pump was a mercury cut-off which could be used, when necessary, to imprison oxygen. The oxygen was obtained by heating small particles of potassium permanganate contained in a horizontal side tube between the cut-off and the mercury trap. After the pump had been set in action the side tube was heated in sections by a flame until this acquired a sodium yellow coloration, the permanganate always having been previously tapped out of the section to be heated. Liquid air was then applied to the mercury trap and the experimental tube baked for about 30 minutes at 400° C. Finally, both filaments were aged for several hours at 2500-2600° K.

The first attempt to obtain the required current-voltage curves was unsuccessful, owing to large and erratic time changes of the thermionic current at any given temperature of filament A and potential difference between A and B. This was remedied by enclosing the whole tube in a metal gauze connected to one terminal of A. After this, relatively small time changes were still observed, but they were no longer erratic, and it seemed that by taking proper account of them current-voltage curves corresponding to at least an approximately clean and the oxygenated condition of filament B might be obtained.

If, after oxygen had been admitted to the tube and pumped away again, filament A was switched on, the electron current from A to B rose asymptotically to a limiting value, the time taken to practically reach the limit being about 20 minutes. For example, in one case where B was maintained at a potential of 5 volts positive with respect to the negative end of A, the initial value of the thermionic current was about 14 μA., and it rose to a final value of 16·8 μA. This rise had nothing to do

with the passage of the space current, as was found by breaking the circuit in which it flowed for definite intervals. It was, however, associated in some way with filament A being alight. If this filament was switched off for a time, and then on again, the space current was now found to be smaller than just before switching off, and, after long enough rests, it recommenced at its original value. It always then again rose towards the same asymptotic limit as before.

The rise might have been due either to a gradual cleaning of the cooler ends of A, which became recontaminated during the rest intervals, or to a distillation of some electropositive material from A to the surface

Fig. 2.

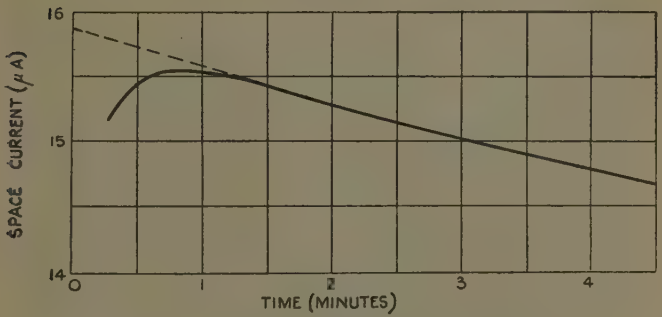

Typical thermionic current-time curve obtained after flashing anode filament.

of B. Since the effect did not diminish after prolonged heating of A at a high temperature, and seemed also approximately independent of the temperature at which this filament was operated, the distillation hypothesis was rejected, and the final values of the thermionic currents were used for plotting the current-voltage curve for B in its oxygenated state.

The kind of time effect that was observed after filament B had been flashed at a high temperature ($\sim$2800° K.) to clean it, filament A having been at its operating temperature for some time previously, is shown by the curve of fig. 2. This curve was obtained with B kept 3·2 volts positive with respect to the negative end of A. The initial rise may be attributed to the combined effects

of change in the distance between the filament tips and change in the work function of B associated with its gradual cooling after flashing. The subsequent approximately linear fall can hardly have been due to anything other than progressively increasing electronegative contamination of B by the condensation on it of residual gas. In support of this conclusion it was found that the rate of fall and the residual gas pressure increased and decreased together. It was assumed that by producing the linear part of one of these time curves backwards to the current axis the space current corresponding to the cold and an at least approximately clean condition of filament B would be obtained, and, accordingly, the intercepts on the current axis were used for plotting the "clean tungsten" current-voltage curve corresponding to any given temperature of A.

In fig. 3 are given current-voltage plots for the two conditions of filament B, obtained in the manner described. The temperature of filament A was in the region of 2600° K. Curve α was obtained when the vacuum was at its best, and corresponds to the clean or nearly clean condition of B, this filament having been flashed at a high temperature and a time curve like that of fig. 2 then taken for each point. The points through which curve β passes were obtained after filament B had been first flashed to clean it and then exposed cold to various pressures of oxygen for various different times, each kind of point corresponding to a different pressure and time of exposure. Curve β was obtained by shifting curve α bodily to the right until it best represented the points for the oxygenated condition of B. It is satisfactory to note that this curve passes through the points everywhere equally well, this indicating that the displacement between the curves α and β represents a true contact potential difference. It should also be observed that there is no tendency for points of one kind to lie more to the right or left of curve β than those of another. This shows that the final condition of filament B was independent of the pressures or times of exposure to oxygen within the limits tried, and, since these limits were wide, the further inference seems justified that the oxygenation was as complete as it could be made by mere exposure of the filament to oxygen at room temperature.

The voltage separation of the two curves corresponds

to a contact potential difference between tungsten in the two conditions of 1·70 volts. This agrees well with the contact potential difference between clean tungsten and Kingdon's oxygenated tungsten at 1500° K. calculated from his thermionic data, viz., 1·75 volts. As we have seen, however, there is reason to believe that the contact potential difference between clean and most effectively

Fig. 3.

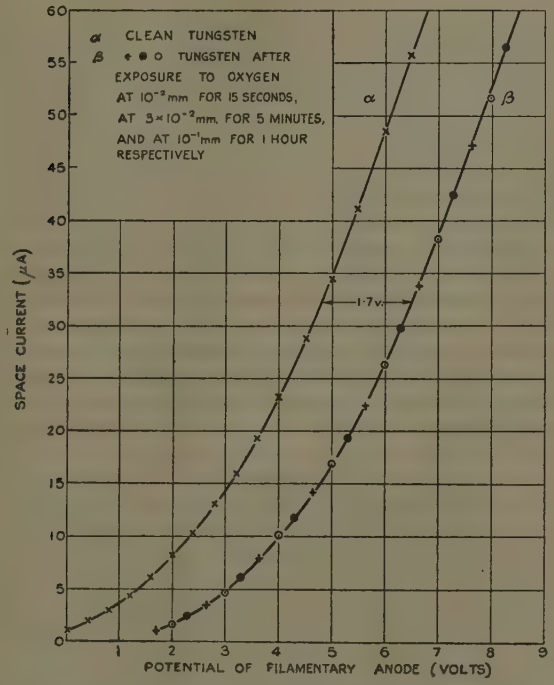

Current-voltage curves for the approximately clean and oxygenated conditions of the anode filament.

oxygenated tungsten may be somewhat greater than this. If this is so, then either curve α does not correspond to perfectly clean tungsten or else the degree of oxygenation corresponding to curve β is not the most effective.

There is evidence pointing to the former of these alternatives in a certain want of constancy of the intercepts

on the current axis of the linear parts of the current-time curves obtained after filament B had been flashed. If, before being flashed, B had been oxygenated, the current intercept for any given applied voltage always at first corresponded to a condition of B about 0·5 volt more electronegative than that ultimately arrived at. Even after a prolonged flashing of B the intercept was still somewhat short of its limiting value. This was generally attained only after a series of short flashes. Thus it appears that, in addition to the contamination acquired by B resulting from the condensation of residual gas on it, some independent dose of contamination was able in some way to spread over its surface while it was cooling, and this can hardly have arrived there otherwise than by surface migration from the relatively cool ends. In a short flash the ends would not have had time to attain as high a temperature as in a long one, and consequently the movement of adsorbed gas along them would have been relatively sluggish. But even the final value of the intercept obtained after a series of short flashes was not always quite the same. It was in general highest when most pains were taken to secure good vacuum conditions. Since there was always some residual gas, and the ends could never have been free of contamination, it is probable that even the highest intercepts did not correspond to a perfectly clean condition of the electron-collecting part of B.

This difficulty could probably be avoided by making filament B much longer and/or thinner, and providing for an independent heating of its ends to render them, as well as the central region of B, as nearly clean as possible. A subsequent flash of B without the auxiliary heating of its ends would then, presumably, clean its central region much more effectively than in the present experiments. With a less rigid anode filament it might, in addition, be necessary to arrange matters so that the experiments could be carried out with the tube and oxygen supply sealed off, to avoid the effects of pump vibration, providing for the burning up of excess oxygen by another filament. However, pending a more elaborate investigation along some such lines as these, the results of the present work at least set a lower limit to the contact potential difference in which we are interested.

There still remains the question of whether or not

the oxygenation resulting from the exposure of flashed tungsten, cold, to oxygen is the most effective possible. To test for this, filament B was heated for some seconds at 1900° K. in oxygen at a pressure of the order of 10^{-2} mm., after which the oxygen pressure was found to have been reduced by an appreciable fraction, owing to consumption by the filament. The filament took several seconds to cool below visible redness after the heating current had been switched off, so if, as we should conclude from Kingdon's results, evaporation is too vigorous at 1900° K. for the filament to have acquired its most effective covering of oxygen at that temperature, it had a chance to do so at a lower temperature. The excess oxygen was now pumped away and the space-charge-limited thermionic current observed for some chosen temperature of filament A and potential difference between A and B. This was found to be the same as the corresponding current obtained after B had been oxygenated by mere cold exposure to oxygen. Filament B was then heated (in a vacuum) to successively higher temperatures, the thermionic current under the chosen standard conditions being observed after the heating of B at each temperature. The first change in this current (brought about, of course, by evaporation) was found to be an increase, showing that the filament was now less effectively covered than before. It is, therefore, to be concluded that the most effective degree of oxygenation possible may be achieved by merely exposing flashed tungsten, cold, to oxygen, and then pumping the excess gas away. It would be surprising if the adsorbed film resulting from this were anything other than a single complete layer of oxygen atoms.

The method of observing the thermionic current under standard conditions after filament B had been heated was used to obtain some rough idea of the dependence of the rate of evaporation of oxygen on temperature. While, owing to the complications of condensation of residual gas and migration of adsorbed gas along the surface of the filament, no great accuracy can be claimed for the results obtained, they are, nevertheless, interesting so far as they go. It will be appreciated that the complications just mentioned render the method not only inaccurate, but also somewhat insensitive. In spite of this, the effects of evaporation could easily be detected after a twelve-minutes' heating of filament B at as low a tempera-

ture as 1300° K. The amounts δV by which this filament was found to have become more electropositive after various total times of heating at temperatures between 1300° and 1700° K. are given in the table. The filament had previously been oxygenated by exposure, cold, to oxygen, but in separate experiments no difference could be detected in rates of evaporation after cold and hot oxygenation.

Table of Values of δV found after Various Times of Heating of the Anode Filament at Different Temperatures.

Temperature (deg. K.).	Time of heating (min.). 1.	4.	12.
1300....	—	—	0·10
1400....	0·08	0·16	0·22
1500....	0·16	0·37	0·50
1600....	0·50	0·60	0·63
1700....	0·62	0·70	0·72

The results support the conjecture already made after the discussion of Kingdon's thermionic data that even at his lowest temperature, 1500° K., his surface was less than most effectively covered.

Summary.

1. The contact potential difference at room temperature between slightly electronegatively contaminated tungsten and tungsten having an oxygen covering such as appeared to be the most effective in raising the work function was found to be 1·70 volts.

2. The contact potential difference at 1500° K. between perfectly clean tungsten and what was probably less than most effectively oxygen-covered tungsten is calculated from published thermionic data to be 1·75 volts.

3. Both these figures are to be regarded as only lower limits to the contact potential difference between perfectly clean and most effectively oxygen-covered tungsten.

4. Loss of electronegativeness of oxygenated tungsten by evaporation of oxygen was first detected with certainty at 1300° K., and beyond this the rate of evaporation was found to increase rapidly with temperature.

5. No difference could be detected between an oxygenated surface formed by exposing previously cleaned tungsten, cold, to oxygen and one formed in oxygen by a hot process, either in regard to electronegativeness or to volatility of the oxygen.

6. It appears that of the various degreees of oxygen covering that are stable in a vacuum the most effective in raising the work function is the most complete possible.

In conclusion, the author wishes to tender his acknowledgments to the General Electric Company and the Marconiphone Company, on whose behalf the work was done which has led to this publication.

XLV. *Rectangular Plates supported on Flexible Beams.* *By* E. H. Bateman, *M.A.**

1. THE theory of flexure of rectangular plates carrying a uniformly distributed transverse load is well established for the case in which the edges rest freely on rigid rectilinear supports, and for the corresponding case of clamped edges. The assumption, common to both these cases, that the edge lines of the plate remain straight, limits the value of the standard results, since in practice the edges of the plate are more often supported on flexible stringers, purlins, or beams. A common application may be noticed in the floor of a building supported on horizontal beams, the ends of which are attached to vertical columns. Here the flexure of the supporting beams will affect the deformation of the floor plate, and will also modify the distribution of reaction on the beams themselves.

If a number of panels of such a floor, of uniform thickness t and flexural rigidity D, all carry a uniformly distributed load p per unit area and are supported on continuous beams, an intermediate panel may be represented as in fig. 1.

Here the lines $x=\pm a$, and $y=\pm b$, define the position of the supporting beams and the four points $x=\pm a$,

* Communicated by the Author.

$y=\pm b$ locate the vertical columns. Owing to the continuity of the plate with adjacent panels,

$$\frac{\partial w}{\partial x}=0, \text{ at } x=\pm a, \quad \text{and} \quad \frac{\partial w}{\partial y}=0, \text{ at } y=\pm b, \quad . \quad (1)$$

where w is the deformation of any point (x, y) normal to the plate.

The deformation must satisfy the equation

$$\nabla^4 w=p/D, \quad . \quad . \quad . \quad . \quad . \quad . \quad . \quad (2)$$

where $D=Et^3/12(1-\sigma^2)$, E is Young's Modulus, σ is Poisson's Ratio, and ∇^4 is the operator

$$\left(\frac{\partial^2}{\partial x^2}+\frac{\partial^2}{\partial y^2}\right)^2.$$

Fig. 1.

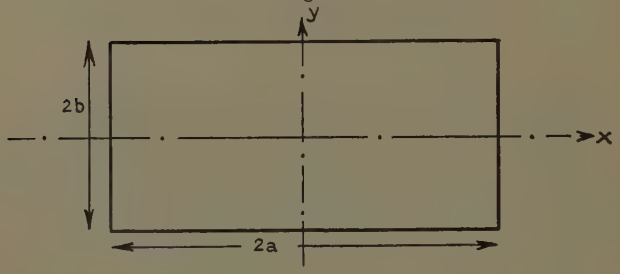

A particular integral in the form

$$w_0=\frac{p}{48D}\{(x^2-a^2)^2+(y^2-b^2)^2\} \quad . \quad . \quad . \quad (3)$$

satisfies the equation (2), and also the boundary conditions defined by (1).

A complementary function in the form

$$w_n=A_n\left\{L_n\cosh\frac{n\pi x}{b}+\frac{x}{a}.\sinh\frac{n\pi x}{b}\right\}.\cos\frac{n\pi y}{b}$$

$$+B_n\left\{M_n\cosh\frac{n\pi y}{a}+\frac{y}{b}.\sinh\frac{n\pi y}{a}\right\}.\cos\frac{n\pi x}{a}+C, \quad (4)$$

where $n=1$, 3, 5, etc., and A, B, L, M are numerical constants, satisfies the equation $\nabla^4 w=0$.

It will also conform to the boundary conditions defined by (1), if

$$\frac{\partial}{\partial x}\left\{ \mathrm{L}_n \cosh\frac{n\pi x}{b} + \frac{x}{a}\sinh\frac{n\pi x}{b} \right\} = 0,$$

when $x = \pm a$, *i.e.*, if

$$\mathrm{L}_n \cdot \frac{n\pi}{b}\sinh\frac{n\pi a}{b} + \left(\frac{1}{a}\cdot\sinh\frac{n\pi a}{b} + \frac{n\pi}{b}\cosh\frac{n\pi a}{b}\right) = 0, \quad (5)$$

etc., and to the condition $w=0$, at the four points $x=\pm a$, $y=\pm b$, if

$$\mathrm{C} = \mathrm{A}_n \cdot \left\{ \mathrm{L}_n \cosh\frac{n\pi a}{b} + \sinh\frac{n\pi a}{b} \right\} + \mathrm{B}_n \cdot \left\{ \mathrm{M}_n \cosh\frac{n\pi b}{a} + \sinh\frac{n\pi b}{a} \right\} . \quad (6)$$

Then the expression (4) for the complementary function will take the abbreviated form

$$w_n = \mathrm{A}_n \left\{ \operatorname{cash}\left(\frac{a}{b}\cdot\frac{n\pi x}{a}\right) \cdot \cos\frac{n\pi y}{b} + \operatorname{cash}\frac{n\pi a}{b} \right\} + \mathrm{B}_n \left\{ \operatorname{cash}\left(\frac{b}{a}\cdot\frac{n\pi y}{b}\right) \cos\frac{n\pi x}{a} + \operatorname{cash}\frac{n\pi b}{a} \right\}, \quad (7)$$

if we may write

$$\operatorname{cash}\left(\frac{a}{b}\cdot\frac{n\pi x}{a}\right) = \mathrm{L}_n \cosh\frac{n\pi x}{b} + \frac{x}{a}\sinh\frac{n\pi x}{b},$$

where L_n is defined by (5), *i.e.*, if

$$\operatorname{cash}\left(\frac{a}{b}\cdot\frac{n\pi x}{a}\right) = -\left(\frac{b}{an\pi} + \coth\frac{n\pi a}{b}\right)\cosh\frac{n\pi x}{b} + \frac{x}{a}\sinh\frac{n\pi x}{b} \quad . \quad . \quad . \quad (8)$$

Then the complete solution will be

$$w = w_0 + w_1 + w_3 + w_5 + \ldots,$$

where the constants A_1, B_1; A_3, B_3; etc., enable the edge deformations to be matched to the deformation curves of the supporting beams.

These constants may be determined either by harmonic analysis* or by balancing the deflexions at different points along the edges.

* *Cf.* C. E. Inglis, "Stresses in Rectangular Plates clamped at their Edges and loaded with a Uniformly Distributed Pressure," Trans. I. N. A. 1925.

2. As an illustration of the accuracy which may be obtained by a first approximation, the method is applied to the case of a square plate clamped at the edges. The first approximation is $w=w_0+w_1$, where

$$w_0=\frac{p}{48D}\{(x^2-a^2)^2+(y^2-a^2)^2\}, \quad . \quad . \quad . \quad (9)$$

$$w_1=A_1\left\{\operatorname{cash}\frac{\pi x}{a}\,.\,\cos\frac{\pi y}{a}+\operatorname{cash}\frac{\pi y}{a}\,.\,\cos\frac{\pi x}{a}+2\operatorname{cash}\pi\right\}, \quad . \quad . \quad . \quad (10)$$

and A_1 is obtained by making $w=0$, at the centre of an edge.

Thus

$$0=\frac{pa^4}{48D}+A_1\{\operatorname{cash}\pi-\operatorname{cash}0+2\operatorname{cash}\pi\} \quad . \quad . \quad (11)$$

and

$$A_1=\frac{pa^4}{48D}\times\frac{1}{10{\cdot}007}.$$

Then the central deflexion is

$$(w)_{0,0}=\frac{p}{48D}\cdot\left\{2a^4+\frac{2a^4}{10{\cdot}007}(\operatorname{cash}0+\operatorname{cash}\pi)\right\}$$
$$=0{\cdot}1636\,pa^4/8D.$$

This compares with the value given by Love*, $0{\cdot}16597\,pa^4/8D$, using three terms of a series, as an approximation to the agreed value, $0{\cdot}162\,pa^4/8D$, given by Hencky, Inglis, and Ritz.

The closeness of the approximation given by using only the first term of the complementary function is due to the similarity between the edge deflexion curves due to w_0 and w_1.

3. The application of the method to the general case will give approximate numerical solutions, and since the deflexion curve of a uniformly loaded continuous beam is identical with the edge deflexion curve of w_0, the first approximation will give sufficient accuracy for design and for checking experimental results.

* A. E. H. Love, "Biharmonic Analysis, especially in a Rectangle, and its Applications to the Theory of Elasticity," Proc. Lond. Math. Soc. xxix. p. 232 (1929).

XLVI. *The Standard Electrode Potential of Lithium in Methyl Alcohol.*

By Angus Macfarlane *and* Sir Harold Hartley, *F.R.S.**

LITHIUM is not among the elements the standard electrode potentials of which have been measured in methyl alcohol by Buckley and Hartley [1], although its value in water has been determined by Lewis and Keyes [2] and in ethyl alcohol by us [3]. Amalgam electrodes show anomalous behaviour in dilute solutions, the probable reasons for which have been reviewed by Philpot, Ross-Kane, and Wolfenden [4]. Hence it is scarcely possible to make a self-contained determination of the electrode potential of an alkali metal, since the measurements cannot be extended into sufficiently dilute solutions to enable an independent evaluation of the activity coefficients of the electrolyte to be made. The activity coefficients of hydrogen chloride determined by Nonhebel and Hartley in their measurements of the e.m.f. of cells of the type

$$H_2, \quad HCl \text{ in MeOH}, \quad AgCl.Ag,$$

have therefore been used, and it has been assumed that the activity of lithium chloride in dilute solution is equal to that of hydrogen chloride in a solution of the same concentration.

The potential that would be exerted by metallic lithium has been calculated from our results obtained with amalgam electrodes in the cell

0·350 per cent. Li amalgam, | LiCl in MeOH, | AgCl.Ag,

by making use of the measurements of Lewis and Keyes of the e.m.f. of the combination

Li metal, | LiCl in propylamine, | 0·350 per cent. Li amalgam.

Experimental Procedure.

The measurements were made in a paraffin thermostat at a temperature of 25° C.$\pm$0·1° C. The potentiometer system and the preparation of the silver-silver chloride reference electrodes have already been described [5].

* Communicated by the Authors.

The design of the cell was a modification of that referred to in the paper on the standard electrode potentials in ethyl alcohol [3]. This was in the form of an H, the two vertical limbs providing a compartment each for the amalgam dropper and the reference electrode. Waste amalgam and solution could be sucked off from the bottom of these, and fresh liquid from the solution reservoir could be introduced through an upright tube sealed into the horizontal limb, the connexion being made by a ground-glass joint.

The amalgam electrode, designed by Mr. Philpot to maintain constant dropping-rates and to prevent films of solution creeping up the inside, consisted of two concentric tubes. From the reservoir amalgam fell through a thin capillary at a rate controlled by a grooved tap and rose into a wider tube fitting around it. The upper end of this external tube was connected to the inner by a piece of rubber tubing; through a side-tube the pressure was maintained equal to or greater than that over the solution in the cell. The lower end was drawn out and bent upwards to provide an overflowing electrode, the diameter of which was narrowest at the orifice, so that an excess pressure of amalgam prevented the entrance of solution. A further constriction some distance from the end served to keep the dropping-rate more constant than would have been possible by manipulation of a tap alone. The electrode was held in the cell by a rubber connexion. All compartments of the amalgam electrode and the cell could be evacuated or filled with pure hydrogen as required.

Lithium amalgam was made from purified and redistilled mercury by electrolysis of lithium chloride solution, using a platinum foil as anode. Its composition was determined by weight titration with standard acid, and adjusted by addition of mercury to that employed by Lewis and Keyes, 0·350 per cent. by weight of lithium. The solutions were freed from oxygen by bubbling purified nitrogen, saturated with methyl alcohol vapour, through them for twenty-four hours. They were made up by weight from conductivity methyl alcohol and from specimens of lithium chloride which had been dried to constant weight at 80° C. in a vacuum oven. The cadmium cell used as the ultimate standard of e.m.f. has been recently calibrated at the N. P. I.

Results.

The concentrations of the lithium chloride solutions used were 0·1 and 0·05 molal. In both experiments the e.m.f. remained independent of the dropping-rate over the extreme range of a half to four drops a second. The e.m.f. slowly sank as the solution around the electrode became more concentrated by dissolution of lithium, but, after changing the solution, was restored to its original value within a few tenths of a millivolt. The measured potential difference was $2{\cdot}295_7$ volts when 0·1 molal solution was used, and $2{\cdot}320_8$ volts when the concentration was 0·05 molal. After adding 0·950 volts, the Lewis and Keyes value for the potential difference between lithium metal and 0·350 per cent. lithium amalgam, E_{0_m}, the e.m.f. of the cell

$$\underset{(a=1)}{\text{Li metal, LiCl in MeOH,}} \quad \text{AgCl.Ag,}$$

may be calculated by insertion of Nonhebel and Hartley's values for the molal activity coefficients of hydrogen chloride, 0·461 at 0·1 molal, 0·541 at 0·05 molal, in the equation

$$E = E_{0_m} - \frac{2RT}{F} \ln m\gamma.$$

In this way E_{0_m} is calculated to be $3{\cdot}087_6$ volts from the first experiment and $3{\cdot}085_3$ volts from the second. After addition of 0·0081 volts the e.m.f. of the cell

$$\underset{}{\text{Ag.AgCl,}} \quad \underset{(a=1)}{\text{HCl in MeOH,}} \quad \underset{(p=1\ \text{atmos.})}{H_2\ \text{gas,}}$$

two values for the difference in the electrode potentials of hydrogen and lithium, namely, $3{\cdot}095_7$ and $3{\cdot}093_4$ volts, are obtained. Hence, to the nearest millivolt, the standard electrode potential of lithium in methyl alcohol may be taken to be $-3{\cdot}095$ volts.

Discussion.

In Table I. are given the standard electrode potentials that have been measured in methyl and ethyl alcohols as well as in water, the values for the latter solvent being taken from Lewis and Randall's 'Thermodynamics.' Two misprints which were overlooked in the table in our earlier paper have been corrected.

Table II. contains the partial molal free energies of transfer of a number of electrolytes between infinitely dilute solutions in these solvents, derived from the corrected electrode potentials by methods already described [6]. The figures under the heading "Calculated"

TABLE I.

Element.	E.P.$_{c.}$			Differences.	
	H_2O.	MeOH.	EtOH.	H_2O./MeOH	H_2O./EtOH
Li	−2·958	−3·095	−3·042	0·137	0·084
Na	−2·7125	−2·728	−2·657	0·015	−0·056
Tl	−0·3363	−0·379	−0·343	0·043	0·007
H	0	0	0	0	0
Ag	0·7995	0·764	0·749	0·036	0·051
I.....	0·5357	0·357	0·305	0·179	0·231
Br	1·0659	0·837	0·777	0·229	0·289
Cl	1·3594	1·116	1·048	0·243	0·311

TABLE II.

Partial Molal Free Energies of Transfer at 25° C. in Calories.

H_2O—MeOH.

	Calculated.			Observed.			
	Cl.	Br.	I.	Cl.	Br.	I.	CNS,
Li	6570	6360	6160	2450	2120	970	540
Na ...	5370	5160	4960	5260	4930	3780	3350
Tl.....	4270	4060	3860	4610	4290	3140	2700
H	...	...	...	5610	5280	4130	3700
Ag ...	5270	5060	4860	4780	4450	3300	2870

H_2O—EtOH.

Li	8970	8690	8410	5230	4730	3390	2900
Na ...	7270	6990	6710	8460	7960	6620	6130
Tl.....	5670	5390	5110	7010	6500	5170	4680
H	...	...	...	7170	6670	5330	4840
Ag ...	7070	6790	6510	6000	5490	4150	3660

are based on the Born equation [7] for the difference in free energy between charging up an ion of valency z and radius r in vacuo and in a solvent of dielectric constant D. The expression takes the form

$$F_i = \frac{z^2\epsilon^2}{2rJ}\left[1-\frac{1}{D}\right]$$

where ϵ is the electronic charge and J is the mechanical equivalent of heat. For a uni-univalent electrolyte, when the radii of the two ions are r_1 and r_2, the partial molal free energy of transfer between solvents of dielectric constants D_1 and D_2 is therefore to be calculated from the equation

$$\Delta\overline{F} = \frac{Nz^2\epsilon^2}{2J}\left[\frac{1}{D_2} - \frac{1}{D_1}\right]\left[\frac{1}{r_1} + \frac{1}{r_2}\right],$$

where N is Avogadro's number. The ionic radii derived from the X-ray study of the crystal lattices have been substituted in this equation to find the calculated free energies.

As Bjerrum [8] has pointed out, this calculation makes no allowance for the difference in the free energies of solution of the uncharged ions in the two solvents. The magnitude of this quantity can be gauged, however, from the measurements of the solubilities of the rare gases made by Lannung [9], and is found to be insufficient to account for the discrepancy between theory and experiment.

The failure of the Born equation to reproduce the observed free energies of transfer is largely due to the assumption that the solvents can be represented as continuous media and that the macroscopic dielectric constant persists at the surface of the ion. The error introduced through ignoring the effect on the dielectric of the electric field due to the ionic charge will increase with the intensity of that field. This is in accordance with the data given in Table II., where it is seen that the difference between the observed and calculated figures is most marked among the salts of lithium, the metallic ion of smallest radius.

The insertion in the Born equation of the ionic radii deduced from measurements of the crystal lattice may also be responsible for the varying degrees of agreement between experiment and theory with different electrolytes. The effective radii of the ions of the alkali metals deduced from the mobilities at infinite dilution by application of Stokes's Law are in the inverse order of their atomic numbers, a result which has been generally explained by assuming that the lighter ions are the more heavily solvated. If such complex formation occurs, it would be expected to be accompanied by a considerable

change in the free energy of the system and, indeed, substitution in the Born equation of the ionic radii calculated from conductivity data leads to figures for the free energy of transfer of electrolytes from water to methyl alcohol that are some thirty times greater than those observed. These uncertainties as to the correct values of the dielectric constant and of the ionic radii are of course related; it is impossible to calculate the magnitude of one of them from a single set of measurements unless the effect of the other is entirely neglected.

Our thanks are due to Mr. O. L. Hughes, who kindly made the resistance measurements in these experiments.

Bibliography.

(1) Buckley and Hartley, Phil. Mag. viii. p. 320 (1929).
(2) Lewis and Keyes, J. A. C. S. xxxv, p. 340 (1913).
(3) Macfarlane and Hartley, Phil. Mag. xiii. p. 425 (1932).
(4) Philpot, Ross Kane, and Wolfenden, Phil. Mag. xiii. p. 425 (1932).
(5) Nonhebel and Hartley, Phil. Mag. l. p. 729 (1925).
(6) Gatty and Macfarlane, Phil. Mag. xiii. p. 283 (1932).
(7) Born, *Z. Physik*, xlv. p. 1 (1920).
(8) Bjerrum, British Association (1931).
(9) Lannung, J. A. C. S. lii. p. 68 (1930).

Balliol College and Trinity College Laboratories,
Oxford.

XLVII. *The Raman Spectrum and Constitution of Fuming Sulphuric Acid.* *By* N. Gopala Pai, *M.A.*, *Research Scholar, Indian Association for the Cultivation of Science, Calcutta* *.

[Plate V.]

1. *Introduction.*

SOME important applications have been made of the Raman effect for studying the progress of chemical and physical changes. As an example we may mention the study of the dimerization of sulphur trioxide,

$$2SO_3 \rightleftarrows S_2O_6,$$

at different temperatures by Bhagavantam †. Examining the Raman scattering of a specimen of the substance

* Communicated by Prof. K. S. Krishnan, D.Sc.
† Ind. Journ. Phys. v. p. 49 (1930).

enclosed in a sealed tube Bhagavantam finds that as the temperature is raised the 535, 1068, and 1403 cm.$^{-1}$ Raman lines increase in intensity, while the 290, 370, 666, 697, 1271, and 1499 cm.$^{-1}$ lines diminish in intensity. The former are characteristic of SO_3 and the latter of S_2O_6 molecules (see table, columns 1 and 2). The transformation of the one to the other can thus be followed easily by observing the change in the relative intensities of the two groups of lines.

Another interesting example of the application of the Raman effect is the study of the electrolytic dissociation of nitric acid at various dilutions by Rao*. The characteristic frequencies of the HNO_3 molecule are different from those of the NO_3^- ion so that a study of the development of intensity of the Raman lines characteristic of NO_3^- with dilution gives a quantitative estimate of the progress of the dissociation.

The same method has also been applied by Rao†, Nisi ‡, and others to the study of the dissociation of sulphuric acid. For this acid, however, a quantitative study of the dissociation is made difficult by the occurrence of a strong continuous spectrum superimposed on the Raman lines, which makes the measurement of the intensities of the Raman lines uncertain §. Qualitative results of importance have, however, been obtained with these solutions. For example, from the observation that some of the Raman lines of 100 per cent. sulphuric acid are almost the same as those of sulphur dioxide Rao concludes that at least part of the H_2SO_4 molecules must have the structure $SO_2{<}^{OH}_{OH}$ (suggested also by chemical considerations). As the acid is diluted with water some new lines appear, which can be identified as due to HSO_4^- and SO_4^- ions, which continually increase in intensity with progressive dilution.

As is well known, concentrated sulphuric acid can take into solution large amounts of SO_3 forming "fuming

* Proc. Roy. Soc. A, cxxvii. p. 279 (1930).
† Ind. Journ. Phys. viii. p. 123 (1933).
‡ Jap. Journ. Phys. v. p. 119 (1929).
§ Recently, however, Medard (*Comptes Rendus*, cxcvii. p. 582 (1934)) has been able to remove most of the continuous spectrum by heating the acid with a trace of $KMnO_4$ to about 150° C.

sulphuric acid." The amounts of SO_3 that can thus go into solution are not stoichiometric, even though the compound having the formula $H_2S_2O_7$ is known from chemical evidence to be one of the products of the solution. Since the Raman frequencies of SO_3 and of H_2SO_4 are definitely identifiable, it would be possible by a study of the Raman effect of fuming sulphuric acid of various concentrations to follow these two constituents separately, and also to decide whether any definite molecular compound like $H_2S_2O_7$ is formed. We can also follow the development of this compound with increase in the concentration of SO_3. Further, the characteristic frequencies of this compound may throw some light on its molecular structure. The present paper gives an account of some investigations in this direction. Fuming sulphuric acid of four different concentrations, containing respectively 21·3, 49·3, 71·5, and 80·4 grms.* of SO_3 per 100 grms. of the fuming acid, were studied for their Raman spectra; the results are discussed specially with a view to obtain information on these various points.

2. *Experimental.*

The specimens of fuming sulphuric acid used in these investigations were all Schering-Kahlbaum's "reagent" variety. Since the liquids as obtained from the makers were very clear and transparent, and particularly free from any suspended impurities, no special precautions were taken to purify them. For the study of the Raman spectrum the original method of Raman and Krishnan was used. The vessel containing the liquid was kept immersed in a water-bath, so as to minimize the reflexion from the surface; the light from the mercury arc was condensed on the liquid with a large aperture lens, and the scattered radiations were studied spectroscopically in the usual manner.

The specimen of the acid containing 49 per cent. SO_3 was a solid at ordinary temperatures, m.p. 37°C. (unlike the acids of other concentrations, which were all liquids).

* The percentages of SO_3 given here are calculated, as usual, on the assumption that the fuming acid is a solution of SO_3 in H_2SO_4. Thus the first concentration corresponds to 21·3 grms. of SO_3 and 78·7 grms. of H_2SO_4 per 100 grms. of the fuming acid. This acid is referred to in the later portions of this paper for convenience as "21·3 per cent. fuming acid." Similar remarks apply to the other concentrations also.

The 49 per cent. acid was therefore kept surrounded by water at about 45°–50° C. during the exposure.

			Fuming sulphuric acid.			
SO_3.	S_2O_6.	H_2SO_4.	Percentage of SO_3 equal to			
			21·3.	49·3.	71·5.	80·4.
			139 1	139 0	149 0	149 1
				228 0	247 1	230 2
	290 6	—	305 2	301 3 *d*	292 2	289 4
			330 3	330 3 *d*	326 3	326 6
	370 8	—	—	—	367 2	365 5
		391 4	384 2			
		433 5	422 2	—	—	435 0
			487 0	477 0 *d*	492 1 *d*	482 2
535 3	—	—	533 0	525 1 *d*	533 3	530 5
		564 8	557 3 *d*	569 1 *d*	558 0 *d*	566 0
	666 2	—	630 0 *d*	630 0	634 0	656 1
	697 2	—	—	682 0	682 2	682 3
			724 3	730 2	717 1	715 0
		742 0				
			776 1	776 0	757 0	757 0
						845 0
		917 10	912 4	905 1	905 0	918 0
			938 0	938 0	944 1	947 2
		974 1	962 2	962 1	985 0	978 0
			1004 1 (?)			
		1043 2				
1068 8	—	—	—	1067 0	1070 5	1070 8
			1108 0	1108 0	1108 0	1105 1 *d*
		1141 8	1140 2	1140 0		
					1176 0	1184 1
	1271 10	—	1258 0	1258 0	1241 4	1263 5
		1370 3	1380 1	1384 3		
1403 3	—	—	1415 0 (?)			
			1460 2	1457 2	1462 2	1463 3
	1489 0	—	—	—	—	1482 0

3. *Results.*

The results of the measurements are collected together in columns 4 to 7 in the table. In general two or three independent exposures were taken for each of the concentrations, and the frequencies given in the table are the

mean frequencies obtained by measurement of these different plates. The numbers appended to the frequencies indicate the relative intensities of the lines. Some typical spectrograms of the Raman spectra for these acids are reproduced in figs. 1 to 4 (Pl. V.).

The continuous spectrum referred to in the introduction as occurring in the scattering of sulphuric acid is also present in the fuming acids; its intensity in the latter case seems, however, to be slightly smaller. In all the cases the number of Raman frequencies appearing in the spectrum is quite large, being as many as twenty-three in the 80 per cent. acid.

4. *The Raman Frequencies of* SO_3, S_2O_6, *and* H_2SO_4 *Molecules.*

Before proceeding to interpret the above results in terms of the chemical constitution of the acids at various degrees of concentration of SO_3 it would be necessary to have definite data regarding the characteristic Raman frequencies of H_2SO_4 and of SO_3 and S_2O_6 molecules. For the latter two molecules there is no difficulty in fixing the frequencies. As mentioned in the introduction, Bhagavantam has sorted out the Raman lines appearing in the scattering of SO_3–S_2O_6 mixture into two groups, one of which increases in intensity with rise of temperature and the other decreases in intensity. The former group is evidently due to SO_3 molecules and the latter to S_2O_6. These frequencies are given in columns 1 and 2 of the table.

The Raman spectrum of sulphuric acid has been studied by a large number of investigators. In trying to deduce from their data the characteristic frequencies of the H_2SO_4 molecule it should be remembered that even small quantities of water present in the acid tend to give extra lines characteristic of SO_4^{--} or HSO_4^- ions, which are not present in the spectrum of H_2SO_4 molecules. Thus the 1043 line obtained by Nisi and by Rao is probably to be attributed to the HSO_4^- ion originating in this manner, because (1) the intensity of this line increases on dilution with water, (2) the line appears in the spectrum of aqueous solutions of $KHSO_4$ as well, and, finally, (3) Woodward and Horner find that with really 100 per cent sulphuric acid this line does not appear.

On the other hand, the weak line at 742 cm.$^{-1}$ obtained by both Nisi and Rao, which, however, is not obtained by Woodward and Horner, seems to be a genuine H_2SO_4 line for the following reasons :—(1) it cannot be due to either SO_4^{--} or HSO_4^- ions, since solutions of neither the sulphates nor the bisulphates give this line ; (2) as we shall see in the next section, the fuming sulphuric acid with 21 per cent. SO_3, which shows all the characteristic lines of the H_2SO_4 molecule, has this line also in appreciable intensity, and it cannot be attributed to any of the other molecules present.

Before closing this section we should mention that the actual values of the frequencies as given by the various investigators slightly differ, evidently due to the diffuse nature of many of the lines. The values adopted in the table are the most probable values.

5. *The Raman Spectra of Fuming Sulphuric Acids and their Composition.*

Considering now the Raman spectra of the fuming acids, we observe the following prominent features :—

(1) All the Raman lines characteristic of H_2SO_4 are present in the 21 per cent. fuming acid also, with their relative intensities nearly the same as in H_2SO_4, but their absolute intensities much feebler. In the acids of higher concentration the feebler lines are absent, though the two strong lines at 564 and 917 persist even in the 80 per cent. acid *.

(2) In the 21 per cent. acid even the strongest line of SO_3, namely 1068, does not appear, suggesting that for this concentration practically all the SO_3 molecules go into combination with H_2SO_4, to form probably the $H_2S_2O_7$ molecules indicated by chemical evidence. In our present investigations the formation of this new compound is evidenced by the appearance of several new lines. Their frequencies are 139 (1), 305 (2), 330 (3), 487 (0), 533 (0), 630 (0), 938 (0), 1004 (1)?, 1108 (0), 1258 (0), 1415 (0)?, and 1460 (2). The numbers enclosed

* We may mention here that in the place of the 742 cm.$^{-1}$ line reported by Nisi and Rao in H_2SO_4 we get in the fuming acids two close lines at about 720 and 760 cm.$^{-1}$ respectively. It is probable that the 742 line in H_2SO_4 is also a doublet.

in brackets indicate the relative intensities of the lines in arbitrary units.

(3) At the higher concentrations, however, in addition to SO_3, which is present in combination as $H_2S_2O_7$, there is an appreciable proportion present in the *free* state, as evidenced by the development of the SO_3 lines in these acids.

(4) Along with the development of the SO_3 lines those characteristic of its dimer, S_2O_6, also make their appearance and increase in intensity with the increase in the concentration of the SO_3 molecules.

We may mention here that the relative intensities of the different SO_3 lines, as also of the S_2O_6 lines, are nearly the same as those given by Bhagavantam, thus confirming their origin. (The 1403 line, however, appears to be weaker and the 666 and 697 lines stronger than reported by Bhagavantam.)

6. *Proportion of* SO_3 *to* S_2O_6 *Molecules present in the Fuming Acids.*

It is possible to make a rough estimate of the relative proportions of the SO_3 and S_2O_6 molecules in the various fuming acids from a comparison of the intensities of the Raman lines of these two molecules. In the ordinary $2SO_3 \rightleftarrows S_2O_6$ mixtures under chemical equilibrium at room temperature (30° C.) Bhagavantam finds that the strongest line of SO_3, viz. 1068, is slightly weaker than the strongest line of S_2O_6, viz. 1271. This is also nearly the case in our 72 per cent. fuming acid, thus showing that in this acid the proportion of SO_3 to S_2O_6 molecules is the same as though only these molecules were present in the enclosure and all the H_2SO_4 and $H_2S_2O_7$ molecules had been removed—*i. e.*, in the 72 per cent. acid the presence of the H_2SO_4 and $H_2S_2O_7$ molecules does not influence the equilibrium of the reaction

$$2SO_3 \rightleftarrows S_2O_6.$$

On the other hand, in the 49 per cent. acid, as judged by the relative intensities of the 1068 and 1271 lines, the proportion of SO_3 molecules is less than that corresponding to the above equilibrium, while in the 80 per cent. acid it is appreciably greater.

7. *Summary.*

The Raman spectra of fuming sulphuric acids of four different concentrations have been studied. The following are the main results obtained:—

(1) At the earlier stages all the SO_3 molecules go into combination, forming $H_2S_2O_7$. The H_2SO_4 lines weaken correspondingly in intensity.

(2) In the higher concentration acids a considerable amount of free SO_3 molecules and of its dimer S_2O_6 are present. In the 71 per cent. acid their relative proportions are nearly the same as in an ordinary SO_3–S_2O_6 mixture in equilibrium.

(3) Even in the 80 per cent. acid, there is a small concentration of free H_2SO_4 molecules.

The author's best thanks are due to Dr. K. S. Krishnan for kind guidance and interest in the work.

XLVIII. *The Branching Ratio of the Actinium Family of Radioactive Elements.*

By Marcus Francis *and* Tcheng Da-Tchang, *Institut du Radium, Paris* *.

Summary.

(1) The branching ratio of the actinium family has been determined for three different minerals, and found to be constant.

(2) The same result is obtained, whether tantalum or zirconium is used to precipitate the protactinium.

(3) The mean of seven determinations of the branching ratio is $4{\cdot}05 \pm 0{\cdot}1$ per cent.

I. Introduction.

THE quantitative relationship existing between the members of the actinium family and the uranium present in unaltered minerals has formed the subject of numerous investigations. Although most workers agree as

* Communicated by the Authors.

to the constancy of the relationship, there is still some uncertainty regarding the numerical value to be assigned to it. The manner of expressing the relationship uniformly adopted is to give the number of atoms of any member of the actinium family which disintegrate in the same interval of time as one hundred atoms of uranium. On the basis of earlier views regarding the common parenthood of the actinium and the radium families this number was called the "branching ratio." We propose to retain this designation as a matter of convention, although the general tendency today is to regard the families as genetically independent *.

The first estimate of the branching ratio, 8 per cent., made by Rutherford † on the basis of Boltwood's analysis of some uranium minerals, was almost certainly too high. On the other hand, the value of 2 per cent. obtained by Antonoff ‡ and by Hahn and Meitner § for the ratio of UY to UX is too low. The authors state clearly that the value is either a minimum (A.) or valid only for the apparatus employed (H. and M.). There remain a number of determinations ranging from 3 to 5 per cent. The higher value was obtained by Piccard and Kessler ‖, who compared the active deposits of radon and actinon. Wildish ¶ obtained a similar value from the Pa content of a Colorado carnotite, though the high value of this author is rendered doubtful by the fact that v. Grosse ** later obtained only 4 per cent. for the same specimen of mineral. In favour of the value of 3 per cent. a number of authors may be cited. Thus Hahn and Meitner †† and Widdowson and Russell ‡‡ obtained 3 and 2·9 per cent. respectively from a comparison of the activities of protactinium and uranium in the same mineral, while Guy and Russell §§ obtained 3·1 per cent. from a comparison of the β radiation of UY and UX. Since the direct

* *Cf.* H. J. Walke, Phil. Mag. (7) xviii. p. 256 (1934).

† E. Rutherford, 'Radiations from Radioactive Substances,' p. 523 (1912); B. B. Boltwood, Sill. J. xxv. p. 269 (1908).

‡ G. Antonoff, Phil. Mag. (6) xxvi. p. 1058 (1913).

§ O. Hahn and L. Meitner, *Phys. Zeits* xv. p. 236 (1914).

‖ A. Piccard and E. Kessler, *Arch. Sci. phys. et nat.* (5) v. p. 491 (1923).

¶ J. E. Wildish, J. Am. C. S. lii. p. 163 (1930). W. obtained results varying from 1·47 to 5·16 per cent. for different minerals.

** A. v. Grosse, Phys. Rev. xlii. p. 565 (1932).

†† O. Hahn and L. Meitner, *Phys. Zeits.* xx. p. 529 (1919).

‡‡ W. B. Widdowson and A. S. Russell, Phil. Mag. xlvi. p. 915 (1923).

§§ W. G. Guy and A. S. Russell, J. C. S. cxxiii. p. 2618 (1923).

method of separating and measuring the protactinum has certain advantages not possessed by the other methods, the value of 3 per cent. was adopted * in 1930 by the International Commission of the Radium Standard, despite the existence of two closely agreeing values in the neighbourhood of 4 per cent. (4·2 per cent., from the ratio UY : UX, due to G. Kirsch †; and 4·1 per cent. by St. Meyer ‡ from the Pa content of the "Rückrückstände" of the Bohemian radium extraction).

This choice appeared to receive confirmation from the results of Gleditsch § and co-workers, 2·7 to 3·3 per cent., based on determinations of the actinium and protactinium content of various Swedish uranium minerals. In the meantime, however, appeared a paper by v. Grosse ‖ giving the value $4{\cdot}0 \pm 0{\cdot}1$ per cent. as the mean of five determinations. Since the method of separation of protactinium adopted by v. Grosse, coprecipitation with zirconium phosphate, differed from the method employed by previous authors, coprecipitation with tantalum oxide, we decided to examine the question anew, paying particular attention to the tantalum separation and to the errors involved in the subsequent measurements.

A redetermination of the branching ratio has been made on a sample of Katanga pitchblende containing 88·7 per cent. of U_3O_8, employing the tantalum method and varying the quantities of mineral and of coprecipitant taken. The result has been checked by examination of a Colorado carnotite containing 49·5 per cent. U_3O_8. Finally, in order to remove all possible doubt we have applied the zirconium separation to the Katanga pitchblende and to a Canadian pitchblende containing only 42·3 per cent. U_3O_8.

Both methods have been found to give identical results, and the value of the branching ratio resulting from our measurements is $4{\cdot}05 \pm 0{\cdot}10$ per cent.

* *Journ. de phys.* vii. p. 273 (1931). The same value was adopted by Meyer and Schweider, 'Radioaktivität,' p. 473, 1927 edition, and by Rutherford, Chadwick, and Ellis, 'Radiations from Radioactive Substances,' 1930 ed., p. 31.

† G. Kirsch, *Wien. Ber.* cxxix. p. 309 (1920).

‡ St. Meyer, *Wien. Ber.* cxxix. p. 483 (1920).

§ E. Gleditsch and E. Foyn, *C. R.* cxciv. p. 1571 (1932); E. Gleditsch and S. Klementson, *C. R.* cxciv. p. 1731 (1932).

‖ A. v. Grosse, *loc. cit.*

Experimental.

(1) *Analysis of the Minerals* (*Uranium Content*).

The powdered ore is attacked by HCl or aqua regia, SiO_2 removed, and other impurities removed from the solution by H_2S, followed by precipitation with AmHS in the presence of Am_2CO_3. After acidifying and boiling the uranium may be precipitated by CO_2-free ammonia and weighed as U_3O_8.

In the case of ores containing phosphates or vanadates it is convenient to precipitate the uranium with ammonium phosphate and weigh as $(UO_2)P_2O_7$.

(2) *Radioactive Purification of Uranium.*

The method of Meyer and Paneth * has been followed, the oxalate precipitation of added thorium (to remove Io and UX) being, however, replaced by an ether extraction † and repeated crystallizations from water. A solution of the purified salt is precipitated hot with H_2O_2, and the dry precipitate ignited at 700° C. ‡ in air.

The conditions of the H_2O_2 precipitation must be chosen to give as fine a product as possible, for the subsequent hand-grinding is relatively inefficient §.

(3) *Separation and Radioactive Purification of Protactinium.*

(a) *With Tantalum Pentoxide.*

After attack by $HNO_3+H_2SO_4$ and removal of the insoluble residue a solution of Ta_2O_5 in H_2SO_4 containing H_2O_2 is added. Heating on the water-bath precipitates the hydrated pentoxide, which carries with it the protactinium. The precipitate is dissolved in HF and taken down to fuming with a little H_2SO_4. The filter-paper ashes and the residue from the initial attack are added, and the whole is well fused with KHSO and a little $BaSO_4$ to fix the radium. The mass is taken up with water and boiled, to precipitate the Ta_2O_5, which is filtered and again dissolved in HF containing a little H_2SO_4. Radioactive impurities are precipitated by adding small

* St. Meyer and F. Paneth, *Wien. Ber.* cxxi. p. 1403 (1912).
† F. Soddy and T. D. Mackenzie, Phil. Mag. xiv. p. 284 (1907).
‡ W. Biltz and H. Müller, *Zeits. anorg. Chem.* clxiii. p. 257 (1927).
§ M. Francis, *Journ. de phys.* vi. p. 303 (1935).

quantities of $Ba(NO_3)_2$, $Th(NO_3)_4$, and SeO_2*, followed by reduction with hydrazine (to remove Po). After filtering and evaporating to fuming water is added, and precipitation of the tantalum completed by the addition of ammonia.

(b) *With Zirconium Phosphate.*

The mineral is taken up with aqua regia, and 20–50 mg. ZrO_2 in the form of oxychloride is added for each gram of uranium present. Excess of phosphoric acid is added, and the precipitated ZrP_2O_7 carries down with it the protactinium. The precipitate is dissolved in HF and freed from radioactive impurities along the lines of (*a*).

(4) *Preparation and Measurement of Deposits.*

A few centigrams of a representative sample are carefully ground with alcohol in an agate mortar. The larger grains are allowed to settle out, and the suspension is drawn up into a camel-hair brush (no. 5 is a suitable size) for transference to the disks of thin sheet nickel (0·05 mm.) which serve as supports. More alcohol is added, and the process repeated until the whole of the sample taken has been transferred to the disks for measurement. By proceeding in this manner we minimize errors due to a non-uniform distribution of Pa throughout the substance of the coprecipitant. In order that they may be more strictly comparable the deposits of uranium oxide are prepared in the same way, although the chemical homogeneity of the oxide renders possible in this case the adoption of methods capable of furnishing deposits of uniformly fine-grained material†.

The manipulation of the thin disks of nickel is facilitated by the use of a form of tweezer, which in the position of rest is closed, but which opens on application of pressure. We prefer to use a camel hair brush rather than wads of cotton-wool ‡, for transferring the suspension to the disks, since in the former case contamination of the deposit, *e. g.*, by a broken bristle, is at once revealed by an

* F. Reymond and Tcheng Da-Tchang, *C. R.* p. 1723 (1931).

† *E. g.*, electrolysis, or pulverization by the action of ultra-sound-waves, followed by elutriation and centrifugation of the suspension directly on to the disks.

‡ As advocated by Wildish, *loc. cit.*

unduly low activity per mg. With cotton-wool smaller, and consequently not so readily detectable, contaminations are possible.

Before weighing and measuring all deposits were dried in the oven at 150° C. for an hour to remove adsorbed alcohol or moisture. Weighings were performed on an aperiodic microbalance with air dampers, and the ionization-current measurements in a monofilar electrometer of the Pohl type. The usual precautions were taken in both cases.

In order to control the fidelity of the electrometer readings for such feeble sources of α-radiation as here employed a number of small, rimmed disks containing U_3O_8 in thick layer (to reduce the statistical fluctuations) were constructed. From measurements made on six different disks over a period of two months the probable error of a single observation (the mean of a group of ten consecutive readings) was found to be $\pm 0{\cdot}33$ per cent. The electrometer was found to have a temperature coefficient of ca. $-0{\cdot}8$ per cent. per °C. rise in temperature.

(5) *Calculation of the Branching Ratio.*

Let W be the weight of mineral taken, containing P per cent. of U_3O_8;
let w be the weight of coprecipitant carrying the protactinium from W of mineral;
let A be the activity (ionization current) per mg. of U_3O_8 in infinitely thin layer and
let a be that of the protactinium preparation.
Then the branching ratio

$$= \frac{\text{the number of } \alpha\text{-particles from } w \times 100}{\text{the number of } \alpha\text{-particles from } \frac{P}{100} \cdot \frac{W}{2} \text{ of } U_3O_8}$$

$$= \frac{20{,}000\ a.w.}{\text{P.A.W.}} \times \frac{\text{ionizing power of } \alpha\text{-particle from U}}{\text{ionizing power of } \alpha\text{-particle from Pa}}$$

$$= \frac{20{,}000\ a.w.}{\text{P.A.W.}\ x}.$$

The factor 2 is necessary because both isotopes of uranium emit an α-particle. The value of x is obtained by comparing the areas under the Bragg curves for Pa

and Ur. These may be constructed from the curve for Po * by displacing the origin of abscissæ through 0·20 and 0·87 cm. respectively. As drawn by us the value of x was calculated to be 1·1643.

(6) *Experimental Results.*

The value of A expressed in arbitrary units was found to be $132{\cdot}3 \pm 0{\cdot}7$ (mean of observations on 70 disks using several different preparations of U_3O_8). The results obtained with the different minerals are summarized in the following table —

No.	Mineral.	P.	W gm.	w gm.	Coppt.	No. of obs.†	a.	Branching ratio. p. c.
1.	Katanga pitchblende.	88·7	50	0·995	Ta_2O_5	41	$131{\cdot}8 \pm 0{\cdot}55$	$3{\cdot}84 \pm {\cdot}025$
2.	Do. do.	,,	20	0·198	,,	19	$270{\cdot}9_6 \pm 1{\cdot}6$	$4{\cdot}02 \pm {\cdot}042$
3.	Do. do.	,,	10	0·200	,,	28	$141{\cdot}5_6 \pm 1{\cdot}3$	$4{\cdot}14_3 \pm {\cdot}032$
4.	Colorado carnotite.	49·5	15	0·200	,,	32	$113{\cdot}5_5 \pm 1{\cdot}0$	$3{\cdot}97 \pm {\cdot}039$
5.	Katanga pitchblende.	88·7	15	0·358	ZrP_2O_7	35	$121{\cdot}9_5 \pm 2{\cdot}2$	$4{\cdot}26 \pm {\cdot}079$
6.	Do. do.	,,	10	0·240	,,	18	$120{\cdot}1 \pm 1{\cdot}0$	$4{\cdot}22 \pm {\cdot}041$
7.‡	Canadian pitchblende.	42·3	10	0·195	,,	23	$83{\cdot}3_6 \pm 1{\cdot}7$	$4{\cdot}05 \pm {\cdot}085$

(7) *Discussion of Results.*

The mean of the seven values in the last column of the table is $4{\cdot}07 \pm 0{\cdot}16$ per cent. Weighting each value proportionately to the inverse square of its probable error we obtain a value of $4{\cdot}01 \pm {\cdot}04$ per cent. for the weighted mean.

The difference between the two means taken in conjunction with their probable errors appears to indicate the influence of sources of error other than the chance errors of the weighing and measuring. Considering

* I. Curie, *C. R.* clxxv. p. 220 (1922).

† Each consisting of 10 consecutive readings.

‡ The separation of the Canadian pitchblende was carried out by Miss Zavizziano after the departure of one of us (T. Da-T.) for China. Miss Zavizziano also carried out a separation of this mineral with tantalum as coprecipitant. Since this tantalum preparation gave the same activity product as the other tantalum preparations (nos. 1–4) in thick layer it was not measured in thin layer.

separately the results obtained by the two methods of extracting the protactinium, we observe that the zirconium method tends to yield systematically higher values than the tantalum method. Assuming that the chemical separations are complete, there are two possible explanations for the difference.

The first explanation depends on the chemical behaviour of the bodies concerned. Our experience indicates that protactinium is more easily hydrolysable than tantalum and less easily precipitable as phosphate than zirconium under the conditions of the separations. In the one case therefore we should expect to find an enrichment of protactinium towards the centre of the grains of precipitate, in the other case an impoverishment.

The second explanation depends on the chemical and physical nature of the deposits. The weight of material distributed on a single disk was sufficiently low (0·2 mg. per cm.^{2}) to render negligible the loss of ionization owing to absorption of α-particles in the material itself, provided the deposits were in the form of thin continuous films. Microscopic examination of the deposits revealed the presence of grains of unsuspected dimensions, and rendered untenable the assumption of negligible absorption losses. Assuming the grains to be spherical we may calculate the loss of ionization as a function of the diameter. The losses * calculated for the substances with which we are here concerned are given in graph form in the figure.

It is evident that only differences in the absorption losses give rise to errors in the branching ratio. The mean of the tantalum results alone is 3·99, that of the zirconium results alone 4·18; the difference between the two is 0·19, *i. e.*, ca. 4·6 per cent. of the value of the branching ratio. Assuming this difference to be entirely due to differences in the stopping powers of the different materials, the

* The following values have been used in calculating the percentage losses :—

Stopping powers relative to air at 15° C. and 760 mm. pressure :
O = 1·05 P = 1·53 Zr = 2·60 Ta = 3·70 U = 4·24.

Densities : $ZrP_2O_7 = 3{\cdot}8$ $Ta_2O_5 = 8{\cdot}3$ $U_3O_8 = 7{\cdot}2$.

Ranges of α-particles in air at 15° C. and 760 mm. Hg :
Pa = 3·67 cm. U = 3·00 cm. (mean of U I and U II).

For details of the calculation see M. Francis, *loc. cit.*

tantalum results will be about 1·5 per cent. too low and those with zirconium about 3·1 per cent. too high. Correcting on this basis the non-weighted mean becomes 4·05±0·1 per cent., the weighted mean being 4·03±·04 per cent. The difference between the two is insignificant, and we may take the former value, considering the latter merely as a check.

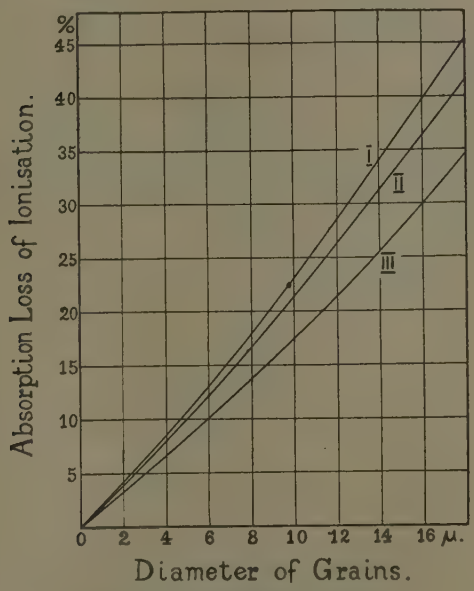

Curve I. Protactinium on Ta_2O_5.
,, II. Uranium oxide.
,, III. Pa on ZrP_2O_7.

The value adopted, 4·05±0·1 per cent.*, is in excellent accord with the value 4·0±0·1 per cent. obtained by v. Grosse.

This investigation was carried out at the suggestion of the late Mme Pierre Curie, to whom we are deeply

* The value of 4·0 per cent. reported by us previously (*C. R.* cxcviii. p. 733 (1934)) was calculated from the tantalum results alone, the zirconium results not being available at the time. Since completion of the experimental work a value of 4·12±·06 per cent. has been published by Gleditsch and Foyn (*C. R.* cxcix. p. 412 (1934)).

indebted for according us the hospitality of her laboratory and the benefit of her long experience in radioactive research work.

Paris.
April 1935.

XLIX. *On the General Solution of a Class of Physical Problems.* *By* B. R. Seth, *M.A., M.Sc., Ph.D.**

1. *Introduction.*

An important class of physical problems requires the solution of Laplace's equation satisfying given boundary conditions. A very general solution of this

Fig. 1.

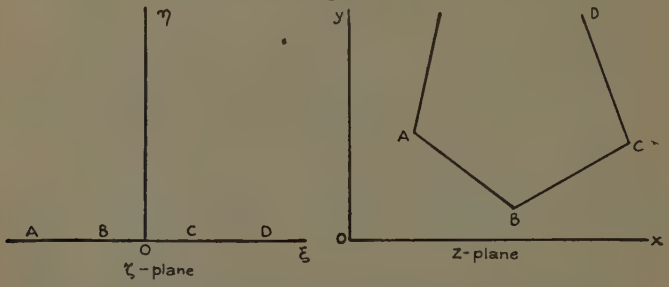

class can be obtained if the problem is a two-dimensional one and the boundary consists only of straight lines.

Let AB, BC, CD, etc. (fig. 1) be the straight lines which constitute the boundary in the plane of a complex variable $z(=x+iy)$. Our method consists in the conformal transformation of the z-area into the upper half of a ζ-plane bounded by the real axis, and thus getting a relation of the form

$$z=F_1(\zeta). \quad . \quad . \quad . \quad . \quad . \quad . \quad . \quad . \quad (1)$$

The boundary condition is now changed into a form such that it can be interpreted as giving rise to another rectilinear area in a Ω-plane. To determine the nature of the singularities of Ω at the points which correspond

* Communicated by the Author.

to the angular points of the z-figure we solve the same physical problem for a circular sector, and then examine the corresponding form of Ω near its vertex. By transforming the Ω-area into the same upper half of the ζ-plane we get another relation of the form

$$\Omega = F_2(\zeta). \quad . \quad . \quad . \quad . \quad . \quad . \quad . \quad (2)$$

If we can eliminate ζ between (1) and (2) we shall get the solution in the form

$$\Omega = f(z). \quad . \quad . \quad . \quad . \quad . \quad . \quad . \quad (3)$$

But in general it is not possible to carry out this elimination, and hence the solution may be said to have been obtained in terms of the parameter ζ.

It may be remarked here that the solution of the problem can be uniquely determined. The problem has been supposed to be physically possible. Hence the function which represents its solution, and which satisfies Laplace's equation, is unique, as it has assigned boundary values that are everywhere finite, uniform, and continuous except at isolated points.

2. *Form of the Boundary Condition.*

Let us assume that χ, which is a solution of

$$\frac{\partial^2 V}{\partial x^2} + \frac{\partial^2 V}{\partial y^2} = 0, \quad . \quad . \quad . \quad . \quad . \quad . \quad (4)$$

satisfies a boundary condition of the type

$$\left[\frac{\partial \chi}{\partial x} - (f_0 + f_1 + f_2 + \ldots f_n)\right] \cos(x\nu) + \left[\frac{\partial \chi}{\partial y} + (\phi_0 + \phi_1 + \phi_2 + \ldots \phi_n)\right] \cos(y\nu) = 0, \quad (5)$$

where f_n and ϕ_n are homogeneous integral polynomials of the nth degree in x and y, and ν denotes the direction of the normal drawn to the boundary. Since the boundary is rectilinear, we can put

$$\cos(x\nu) = \sin \alpha_p, \quad \cos(y\nu) = -\cos \alpha_p,$$

where α_p is the argument of dz when the pth side of the boundary is described in the positive sense (*i. e.*, so as to keep the area included within the boundary on the left) by the point whose affix is z.

Now, if ψ be the function conjugate to χ, and δs an element of the boundary, we can write (5) as

$$\frac{\partial\psi}{\partial s}=(f_0+f_1+f_2+\ldots f_n)\sin\alpha_p$$
$$+(\phi_0+\phi_1+\phi_2+\ldots\phi_n)\cos\alpha_p,\quad (p=1,\,2,\,3,\ldots m),\quad (6)$$

m being the number of different sides present in the boundary.

Differentiating (6) n times in succession with respect to s we get

$$\left.\begin{aligned}\frac{\partial^{n+1}\psi}{\partial s^{n+1}}&=\lfloor\underline{n}[\sin\alpha_p f_n(\cos\alpha_p,\,\sin\alpha_p)\\&\qquad+\cos\alpha_p\phi_n(\cos\alpha_p,\,\sin\alpha_p)]\\&=\left(\cos\alpha_p\frac{\partial}{\partial x}+\sin\alpha_p\frac{\partial}{\partial y}\right)^{n+1}\psi,\\&=\cos(n+1)\alpha_p\frac{\partial^{n+1}\psi}{\partial x^{n+1}}+\sin(n+1)\alpha_p\frac{\partial^{n+1}\psi}{\partial x^n\partial y}.\end{aligned}\right\}\quad (7)$$

If we put

$$X_{n+1}=\frac{\partial^{n+1}\psi}{\partial x^n\partial y},\quad\text{and}\quad Y_{n+1}=\frac{\partial^{n+1}\psi}{\partial x^{n+1}},$$

we see that the boundary condition can be put in the simple form

$$X_{n+1}\sin(n+1)\alpha_p+Y_{n+1}\cos(n+1)\alpha_p$$
$$=\lfloor\underline{n}[\sin\alpha_p f_n(\cos\alpha_p,\,\sin\alpha_p)+\cos\alpha_p\phi_n(\cos\alpha_p,\,\sin\alpha_p)]$$
$$(p=1,\,2,\,3,\ldots m).\quad (8)$$

Again, let

$$\Omega_{n+1}=X_{n+1}+iY_{n+1}=\frac{\partial^{n+1}\psi}{\partial x^n\partial y}+i\frac{\partial^{n+1}\psi}{\partial x^{n+1}}$$
$$=\frac{\partial^{n+1}(\chi+i\psi)}{\partial x^{n+1}}=\frac{d^{n+1}(\chi+i\psi)}{d^{n+1}z},$$

which shows that Ω_{n+1} is a function of z.

3. *Interpretation of the Boundary Condition.*

Since Ω_{n+1} and z are connected by a functional relation the rectilinear area in the z-plane is mapped thereby on an area of the Ω_{n+1}-plane, and the boundary condition (8) shows that this area is also bounded by straight lines. Again, $\chi+i\psi$, and hence Ω_{n+1}, is to have no singularities.

qua function of z, within the z-area. In general it will have singularities at the angular points, whose nature should now be determined.

Again, since the Ω_{n+1}-area can be conformally represented by the upper half of the ζ-plane bounded by the real axis of ξ, the boundary condition (8) can also be interpreted as showing that arg $(d\Omega_{n+1}/d\zeta)$ is constant along each segment of the ξ-axis [except that if $(d\Omega_{n+1}/d\zeta)$ has a zero, there will be a discontinuity of π in arg $(d\Omega_{n+1}/d\zeta)$].

4. *Conformal Transformation of the z-area.*

Let $\xi_1, \xi_2, \ldots \xi_m$ be the points on the ξ-axis in the ζ-plane that correspond to the angular points of the z-figure. If the z-area does not extend to infinity in all directions, and if $\pi a_1, \pi a_2, \ldots \pi a_m$ are the internal angles at these points, we have the relation

$$z = A \int \prod_{r=1}^{m} (\zeta - \xi_r)^{a_r - 1} d\zeta + B, \quad . \quad . \quad . \quad . \quad (9)$$

where A and B are in general complex constants. If the z-area extends to infinity in all directions, and is internally bounded by a polygon, the Schwarz-Christoffel transformation given by (9) should be modified as

$$z = A \int \frac{\prod_{r=1}^{m} (\zeta - \xi_r)^{a_r - 1} d\zeta}{(1+\zeta^2)^2} + B. \quad . \quad . \quad . \quad (10)$$

This result was first given by Kluyver * and again by Bickley †.

5. *Solution of the Problem for a Circular Sector.*

To get an idea of the nature of $(d\Omega_{n+1}/d\zeta)$ near an angular point we proceed to obtain the solution of the similar physical problem when the boundary is a circular sector given by $\theta = \pm \frac{1}{2}\pi a$, $r = c$.

From (5 the boundary condition can be written as

$$\frac{\partial \psi}{\partial s} = (f_0 + f_1 + f_2 + \ldots f_n) \cos(xv) - (\phi_0 + \phi_1 + \ldots \phi_n) \cos(yv). \quad . \quad (11)$$

* *Zeitschrift für Math. and Phys.* xl. pp. 129–50 (1895).
† Phil. Trans. Roy. Soc. (A) ccxxviii. pp. 225–274 (1929).

Along $\theta=\pm\frac{1}{2}\pi a$, (11) gives

$$\frac{\partial\psi}{\partial r}=\sum_{S=0}^{n}(A_s\pm B_s)r^s, \quad \ldots \quad (12)$$

A's and B's being known constants.

We can satisfy (12) if we take *

$$\psi=\sum_{S=0}^{n}\frac{r^{S+1}}{S+1}\left[A_s\frac{\cos(S+1)\theta}{\cos\frac{1}{2}(S+1)\pi a}+B_s\frac{\sin(S+1)\theta}{\sin\frac{1}{2}(S+1)\pi a}\right]+\psi_1, \quad (13)$$

where ψ_1 is such a solution of Laplace's equation that $(\partial\psi_1/\partial r)$ vanishes for $\theta=\pm\frac{1}{2}\pi a$.

Along $r=c$, (11) and (13) give

$$\frac{\partial\psi_1}{\partial\theta}=\sum_{S=0}^{n}c^{S+2}\left[A_s\frac{\sin(S+1)\theta}{\cos\frac{1}{2}(S+1)\pi a}-B_s\frac{\cos(S+1)\theta}{\sin\frac{1}{2}(S+1)\pi a}\right]$$
$$+\text{ a finite known function of }\theta. \quad \ldots \quad (14)$$

Since $-\frac{1}{2}\pi a\leqslant\theta\leqslant\frac{1}{2}\pi a$, the right-hand side of (11) can be expanded in a Fourier's series of the form

$$\sum_{S=0}^{\infty}\left[\frac{2S}{a}F_s\cos\frac{2S\theta}{a}-\frac{2S+1}{a}E_s\sin\frac{(2S+1)\theta}{a}\right],$$

which shows that we can take ψ_1 as

$$\psi_1=\sum_{S=0}^{\infty}\left[F_s\left(\frac{r}{c}\right)^{2S/a}\sin\frac{2S\theta}{a}+E_s\left(\frac{r}{c}\right)^{(2S+1)/a}\cos\frac{(2S+1)\theta}{a}\right]. \quad (15)$$

It obviously satisfies the condition that $(\partial\psi_1/\partial r)=0$, over $\theta=\pm\frac{1}{2}\pi a$.

The corresponding value of $\chi+i\psi$ is now given by

$$\chi+i\psi=\sum_{S=0}^{n}L_{S+1}z^{S+1}+\sum_{S=0}^{\infty}F_sz^{2S/a}+\sum_{S=0}^{\infty}iE_sz^{(2S+1)/a}. \quad (16)$$

6. *Form of* $(d\Omega_{n+1}/d\zeta)$ *near an Angular Point.*

We shall now examine the form of $(d\Omega_{n+1}/d\zeta)$ with the help of (16) near the vertex of the sector, which has been taken as $z=0$. The following three cases arise :—

* If $a=1$, S is odd for A's and even for B's.

(i.) $a=1$.

Since any point on the boundary of the z-figure (except an angular point) is given by $a=1$, this case is important. If the coefficient of z^{n+2} in (16) is not zero (it cannot be infinite since there is no L_{n+2}), we get

$$\Omega_{n+1} \sim C + Dz, \quad \ldots \ldots \quad (17)$$

where C and D are known finite constants *. If now the z-figure is mapped on a ζ-half plane with $z=0$ corresponding to $\zeta=0$, we have

$$z \sim k\zeta^a, \quad \ldots \ldots \quad (18)$$

k being another constant. In the present case $a=1$, and hence we conclude from (17) that $(d\Omega_{n+1}/d\zeta)$ is constant near such an angular point. The internal angle at the corresponding point of the Ω_{n+1}-figure is, therefore, also π. This is what we get from the consideration that an ordinary point on the straight boundary in the z-plane corresponds to an ordinary point of the straight boundary in the Ω_{n+1}-plane.

If D vanishes in (17), $(d\Omega_{n+1}/d\zeta)$ should be of the form $D_1\zeta^{2p}$, where p is a positive integer. This requires the absence of one of the infinite series in (16), according as n is even or odd.

(ii.) No value of L, F, or E becomes infinite for any value of a in (16).

At first let us assume that $E_0 \neq 0$, and $1/a$, when it is an integer, is greater than $(n+1)$. In the neighbourhood of the vertex

$$\Omega_{n+1} \sim C + Dz^{-(n+1)+1/a},$$

and hence

$$\frac{d\Omega_{n+1}}{d\zeta} = \zeta^{-(n+1)a} F(\zeta), \quad \ldots \ldots \quad (19)$$

where $F(\zeta)$ is a power series with, in general, non-vanishing constant term for all values of a except $a=1$.

If $E_0=0$, or $1/a$ is an integer not greater than $(n+1)$, we shall have

$$\Omega_{n+1} \sim C + Dz^{-(n+1)+p/a},$$

where p is a positive integer greater than 1. In this case, too, (19) may be said to hold good, for we can

* These constants are different in all the three cases discussed in this section.

absorb the extra factor ζ^{p-1} in $F(\zeta)$. $F(\zeta)$ now has a zero of the $(p-1)$th order coincident with the angular point $\xi=0$.

(iii.) When an E or F becomes infinite for some value of a.

Let the coefficient of $z^{q/a}$ in one of the infinite series in (16) become infinite for $a=a_0$. $\chi+i\psi$ must still have a definite meaning. Hence one of the L's in (16) must also become infinite for $a=a_0$. This implies that q/a is an integer $\leqslant(n+1)$. The two infinite terms combined together should give the result

$$\lim_{\epsilon\to 0}\left[Az^t.\frac{z^{t\epsilon}-1}{(t\epsilon)^r}\right], \quad . \quad . \quad . \quad . \quad (20)$$

where A is a finite constant, $q/a_0=t$, r a positive integer, and $a=a_0(1-\epsilon)$, ϵ being so small that it vanishes in the limit. The expression in (20) has only a finite limit for $\epsilon\to 0$ if $r=1$. Hence $a=a_0$ can only be a pole of order unity. In the neighbourhood of $z=0$ ($\zeta=0$) we now get

$$\Omega_{n+1}\sim C+D\log z, \quad t=n+1;$$
$$\sim C+Dz^{t-n-1}, \quad t<n+1.$$

Using (18) we see that in both cases we have

$$\frac{d\Omega_{n+1}}{d\zeta}=\zeta^{-(n+1)a_0}F(\zeta),$$

which is of the same form as (19).

Thus we see that (19) holds good near an angular point of the Ω_{n+1}-figure for all values of a, it being understood that $F(\zeta)$ may have a zero of some order coincident with $\xi=0$. Combining the results for the m angular points we get

$$\frac{d\Omega_{n+1}}{d\zeta}=R(\zeta)\prod_{r=1}^{m}(\zeta-\zeta_r)^{-(n+1)a_r}, \quad . \quad . \quad . \quad (21)$$

where $R(\zeta)$ is a function which leaves $(d\Omega_{n+1}/d\zeta)$ without singularities other than $\xi_1, \xi_2, \ldots \xi_m$. In particular, the ζ-point infinity must not be a singularity, and since

$$a_1+a_2+\ldots a_m=m\mp 2,$$

the upper or lower sign being taken according as (9) or (10) is to be used, $R(\zeta)$ is of the $[(n+1)m-2(n+2)]$th degree in the first case, and of the $[(n+1)m+2n]$th degree in the second case.

Now $\arg\left\{\prod_{r=1}^{m}(\zeta-\xi_r)^{-(n+1)a_r}\right\}$

is constant along each segment of the ξ-axis. Hence, from what we have said in Section 3, it follows that arg $\{R(\zeta)\}$ must also be constant [except for discontinuities of $k\pi$ at the real zero, if there are any]. Thus when a complex factor of the form $e^{i\beta}$ (β being a real constant) has been removed, all the coefficients of $R(\zeta)$ are real. We may, therefore, rewrite (21) as

$$\frac{d\Omega_{n+1}}{d\zeta}=e^{i\beta}R(\zeta)\prod_{r=1}^{m}(\zeta-\xi_r)^{-(n+1)a_r}. \quad . \quad . \quad (22)$$

7. *Determination of Constants.*

If we can eliminate ζ between the value of Ω_{n+1} obtained from (22) and (9) or (10), we shall get a relation of the form

$$\Omega_{n+1}=X_{n+1}+iY_{n+1}=f^{n+1}(z)+c_{n+1}. \quad . \quad (23.1)$$

Integrating it in succession with respect to z, we get

$$\Omega_n=X_n+iY_n=f^n(z)+c_{n+1}z+c_n, \quad . \quad . \quad . \quad . \quad . \quad (23.2)$$

$$\Omega_{n-1}=X_{n-1}+iY_{n-1}=f^{n-1}(z)+\tfrac{1}{2}c_{n+1}z^2+c_nz+c_{n-1}, \quad (23.3)$$

$$\Omega_1=X_1+iY_1=f'(z)+\frac{1}{n\,!}c_{n+1}\frac{1}{(n-1)\,!}c\,z^{n-1}+\ldots c_1z, \quad . \quad . \quad . \quad (23.4)$$

$$\chi+i\psi=f(z)+\frac{1}{(n+1)\,!}c_{n+1}z^{n+1}+\frac{1}{n\,!}c_nz^n+\ldots c_1z+c_0. \quad (23.5)$$

By suitably choosing the origin we can make $c_0=0$. In general $c_1, c_2, \ldots c_{n+1}$ are all complex constants. Hence there are $2(n+1)$ unknown real constants of integration. If we have to use (9), $R(\zeta)$ is of the $[(n+1)m-2(n+2)]$th degree. Hence, along with β, it gives rise to $[(n+1)m-2(n+1)]$ unknown real constants. In this case the total number of unknown constants is, therefore, $(n+1)m$.

The boundary condition (8), corresponding to (23.1), gives rise to m equations (one for each side) involving the unknown constants if we equate to zero the constant term after putting the values of X_{n+1} and Y_{n+1} in it. In like manner the boundary conditions

$X_n \sin n\alpha_p+Z_n \cos n\alpha_p=$ a known linear function of x or y.
$X_{n-1} \sin (n-1)\alpha_p+Y_n \cos (n-1)\alpha_p=$ a known quadratic function of x or y,

corresponding to (23.2) and (23.3) respectively, give rise to $2m$ equations. Thus we get $(n+1)m$ different equations to determine the $(n+1)m$ unknown constants.

If, however, (10) is used, the number of unknown constants is easily seen to be $(n+1)(m+4)$. The boundary conditions for the m sides give $(n+1)m$ equations. We can get $2(n+1)$ more equations if we observe that Ω_{n+1}, $\Omega_n, \ldots \Omega_1$ are all zero at the z-point at infinity (which is the same as $\zeta=i$ in the ζ-plane). Again, the z-point at infinity is an ordinary point of $\chi+i\psi$. Hence, when $|z|$ is large

$$\chi+i\psi=(\chi+i\psi)_\infty+\frac{A}{z}+\frac{B}{z^2}+\ldots\ldots \quad (24)$$

(24) shows that the z-point at infinity is a zero of the $(n+2)$th order of Ω. Hence the point $\zeta=i$ is a zero of the same order of Ω, and thus a zero of the $(n+1)$th order of $d\Omega/d\zeta$. This implies $(n+1)$ relations amongst the coefficients of $R(\zeta)$ present in (22). And since the coefficients of all terms in $R(\zeta)$ are all real, $\zeta=-i$ must also be a zero of the $(n+1)$th order of $d\Omega/d\zeta$. This gives rise to $(n+1)$ more relations amongst the coefficients of $R(\zeta)$. Thus we get $(n+1)(m+4)$ equations to determine the $(n+1)(m+4)$ unknown constants.

8. *Applications.*

The above method can be successfully employed to quite a few problems in Hydrodynamics, Elasticity, Electricity, and Magnetism, etc., etc. E. Trefftz * has discussed the torsion problem by a method in which the form of the boundary condition is a particular case of (8), obtained by putting $n=1$. The rest of his analysis does not follow the lines of this paper. But the final result, obtained by a rather unsatisfactory method, is the same as we get from (21) by putting $n=1$. A few applications of this method have been recently made by me†. I propose to deal with a few more in a subsequent paper.

Hindu College,
Delhi, India.

* *Math. Ann.* lxxxii. pp. 97–112 (1921).

† Quart. Journ. of Math. v. pp. 161–171 (1934) ; Proc. Camb. Phil. Soc. xxx. pp. 392–403 (1934). Two forthcoming papers deal with Saint-Venant's flexure problem.

L. *A Theory of Elementary Particles.*—Part II. *Electromagnetic Whirls and Elementary Particles.*

By N. S. Japolsky, *formerly Lecturer, Technological Institute, Leningrad* *.

Contents †.

Page

Part II.—Electromagnetic Whirls and Elementary Particles.

13. General Observations 641
14. The Planck Constant 642
15. The Energy of a System of Whirls 644
16. Transformation of Coordinates in a System of Two Whirls. 648
17. The Mutual Energy of a System of Two Whirls 655
18. The Precessional Motion of the Axes and the Average Mutual Energy (the Potential Energy) in a System of Two Whirls 668
19. Distance Forces in a System of Two Whirls. Planetary Motion and Energy Levels. Gravitation 681
20. Elementary Particles as Whirls 695
21. Conclusion 704
Summary 705

13. *General Observations.*

In Part I. it was shown that Electromagnetic Whirls (or simply "Whirls") possess some of the properties ascribed to elementary particles. This includes the connexion of an elementary particle with the waves, in accordance with the de Broglie theory, with the difference that the Whirls are not "associated" with the waves, but *consist* of them, and, besides, these waves are not mysterious "material" waves, but a certain form of electromagnetic waves satisfying the Maxwell equations.

The Whirls possess inertial masses and angular momenta. The relationships between the mass and the total energy of e.m. field and the other parameters of Whirls satisfy the quantum laws and the de Broglie law, and the Einstein relationship between the mass and the energy and the frequency of oscillations

We have also proved the validity of the Principle of Relativity for Whirls.

This, however, is not sufficient to justify the interpretation of elementary particles as Whirls.

* Communicated by Sir W. H. Bragg, O.M., K.B.E., M.A., F.R.S.

† For Part I., see Phil. Mag., Sept. 1935, p. 417.

First of all, we must be able to establish definitely the connexion between the constant $\hbar_1$, which represents a simple fraction of the angular momentum, $2n\hbar_1$, of a Whirl*, and the universal Planck constant $\hbar = \frac{h}{2\pi}$.

Secondly, we must show that the forces acting between the Whirls are, qualitatively and quantitatively, of the same nature as those which are, directly or indirectly, observed between the elementary particles.

The cause of the forces acting between the elementary particles is usually ascribed, in bulk if not in full, to the so-called "electric charges," or, in other words, singularities in the electromagmetic field. A Whirl, which is a system of e.m. waves *in vacuo*, obviously cannot contain such singularities.

Therefore, if the elementary particles can really be interpreted as Whirls, the electric charge in the usual sense must be excluded from the domain of physical realities, and this conception can be used only as a symbolic fiction.

The forces acting between the Whirls can be due only to the e.m. waves which constitute them. To enable the Whirls to play the part of elementary particles, these forces must, on the average, be such as they would be if the Whirls *were* charged particles. In particular, they must, on the average, follow the inverse square law at sufficiently large distances between the centres of the Whirls. The inverse square law must break down when the distance between the centres is small, and also, with a certain small degree of probability, it must admit exceptions, even when this distance is large. Further, the Whirls playing the part of elementary particles must form two classes, so that the Whirls belonging to the same class should be mutually repelled, while the Whirls belonging to the opposite classes should be mutually attracted, at least on the average.

14. *The Planck Constant.*

It was shown that the angular momentum of a Whirl, $2n\hbar_1$, is an invariant constant for a given Whirl. However, generally speaking, this constant can be different for

* See the end of section 6.

different Whirls, and for this reason the notation h_1 was used instead of h, which is reserved for the universal Planck constant.

We shall now try to explain the universality of this constant.

An elementary particle, being a Whirl, or a combination of such, must be considered as a dymanic unit, *i.e.*, as a more or less self-sufficient system, containing a certain quantity of energy, which possesses an angular momentum. We know that in any set of such mutually interacting dynamic units there is a tendency for equalisation of the angular momenta of all the members of the set. The longer and the more eventful is the history of the set, the more complete will be this equalisation. Since the set of particles forming our physical world has a very long and eventful history, we can put with a fairly good degree of accuracy, that, at least on the average, and subject, perhaps, to a small probability of occasional deviations,

$$n\hbar_1 = \text{const.} \quad . \quad . \quad . \quad . \quad . \quad (14.1)$$

This constancy is independent of the mechanism of the interchange of angular momenta between the elementary particles.

This mechanism is implied in the structure of the Whirls.

As was stated at the end of sections 5 and 8, the e.m. field of Whirls is $2n$ pole in the angular (θ) direction.

It could be shown by a more detailed analysis that such systems interact incomparably less when their numbers of poles $2n$ are different than when they are equal. This property of such systems ensues also in daily engineering experience. We know, for example, that an electric a.c. synchronous motor with a stator and a rotor having different numbers of poles will not work. Although, owing to the much more complicated structure of the Whirls, certain interaction between them can take place, even when their numbers of poles are not equal, it is obvious that in this case the interaction, capable to equalise their angular momenta, will be many times weaker.

For this reason, *until the contrary is proved by experience*, we shall assume that all known elementary particles have the same n. With regard to the value of n, we shall

make a simple assumption that for all known elementary particles

$$n=1, \quad . \quad . \quad . \quad . \quad . \quad . \quad (14.2)$$

again bearing in mind that this can be changed if required by experience.

By (14.1) and (14.2) $\hbar_1$ must be equal for all known particles. This agrees with the standard theory, according to which, by comparison of the formulæ for Whirls (say formulæ (12.5)) with the corresponding standard formulæ, we must put for all known elementary particles

$$\hbar_1=\hbar=\frac{h}{2\pi}=\frac{6{\cdot}545}{2\pi}\times 10^{-27}\ \text{gr. cm. sec.}^{-1}. \quad (14.3)$$

During the following discussion we shall, however, assume the possibility of an arbitrary value of $\hbar_1$ and of an arbitrary integer for n, so long as this will not make our formulæ appreciably more complicated, and shall introduce the values of (14.2) and (14.3) only at the point where further retaining of the arbitrariness of $\hbar_1$ and n would make our analysis unduly heavy.

15. *The Energy of a System of Whirls.*

In Part I. we have found the expressions for the e.m energy of an isolated Whirl.

We shall call this energy "the internal energy" of a Whirl.

We shall now consider a system of a number of Whirls, say N_m, to each of which we can ascribe, when convenient, an identification number N.

Unless the Whirls are concentric and co-axial, and have the same parameter n, and the same frequency Ω_1 (in which case they lose their individuality and form one common Whirl), the connexion between the e.m. fields of different Whirls will be much weaker than the connexion between the electric and the magnetic fields of the same Whirl, for, in a given element of volume, the e.m. fields of different Whirls will have different space and time periodicity, while the electric and magnetic fields of the same Whirl have the same space and time periodicity, and, moreover, both fields complement and support each other.

In other words, the internal connexions of the e.m. field of a Whirl are much stronger than the connexion

between the e.m. fields of different Whirls occupying the same space.

For this reason we can expect that the structures of the e.m. fields of the individual Whirls which form our system will not undergo any material changes as a result of their interaction, and these individual structures we shall still be able to distinguish as components of the structure of the resultant e.m. field.

However, the *energy* of the resultant e.m. field of a system of Whirls will *not* be equal to the sum $\mathbf{E}_i$ of the internal energies $\mathbf{E}_{iN}$ of the members of this system.

We can write, therefore,

$$\mathbf{E}=\mathrm{W}+\mathbf{E}_i=\mathrm{W}+\sum_N \mathbf{E}_{iN}=\mathrm{W}+\sum_N \hbar_{1N}\Omega_{1N}, \quad . \quad (15.1)$$

by (6.6) and (9.4).

We shall call the energy W " the mutual energy " of the system of Whirls. The existence of this mutual energy shows that in the process of formation of a system of Whirls, each of which conserves its individuality, the energy is either absorbed or liberated. This can either take the form of a flow of energy between the given system of Whirls and an external system, or of a partial conversion of the internal energy $\mathbf{E}_i$ of the system into the mutual one W, and *vice versa*.

In a self contained system of Whirls

$$\mathrm{W}+\mathbf{E}_i=\mathrm{W}+\sum_N \hbar_{1N}\Omega_{1N}=\text{const.} \quad . \quad . \quad (15.2)$$

Assume now that, owing to the mutual interaction, the Whirls acquired the same, or nearly the same, angular momentum $\hbar_1$. Denote by Ω_{1N} and Ω_{1N}' resp. the frequencies of the Whirls at a given moment and before they entered into our system. Then we can write (15.2) in the form

$$\mathrm{W}=\hbar_1\sum_N \Omega'_{1N}-\Omega_{1N}. \quad . \quad . \quad . \quad . \quad (15.3)$$

This formula expresses in a general way the quantum relationships in the mutual configuration of Whirls.

If now a part $\triangle\mathrm{W}$ of the energy W will be lost by the system to the outside world (i.e., *radiated*) or acquired from the outside world (*absorbed*), then, owing to the

conservation of the angular momentum $\hbar_1$ of each member of the system, we shall have

$$\triangle W = -\hbar_1 \sum_N \triangle \Omega_{1N}. \quad . \quad . \quad . \quad . \quad (15.4)$$

This expresses the quantum relationships of radiation or absorption. The radiated energy will take the form of a number of " beats " between the waves forming the Whirls before the change of the energy of the system and the waves which form them after this change.

These beat waves will propagate with the speed of light, and their frequencies will be, of course, equal to the difference of the frequencies of these waves before and after the change of the energy.

In the same way, if the liberation of energy from the system of Whirls (radiation) will be on account of the internal energy $\mathsf{E}_i = \hbar_1 \Sigma \Omega_{1N}$, the loss of this internal energy will be

$$\triangle \mathsf{E}_i = \hbar_1 \sum_N \triangle \Omega_{1N}, \quad . \quad . \quad . \quad . \quad (15.5)$$

which will form beat waves of frequencies $\triangle \Omega_{1N}$. And again the quantum relationships will hold.

The loss of energy from a system of Whirls can also take the form of separating from a compound Whirl a small portion of it corresponding to a certain small interval of χ (see sections 7 and 8), which portion will form an *incomplete* Whirl. To keep its original angular momentum, the separated incomplete Whirl must reduce its frequency to the level corresponding to its energy, in other words, it must follow the quantum relationships which were deduced in section 7.

Thus the quantum relationships in the wave structure of individual Whirls result in the quantum relationships in their systems, and in all the possible forms of radiation of energy from the individual Whirls and from their systems.

In a world of Whirls any energy absorbed by a system of Whirls must be obtained somehow from other systems of Whirls, either directly or by means of radiation. Therefore, in such a world any absorbed energy must also follow the quantum laws.

We shall now try to derive a general expression for the mutual energy W.

Let XYZ be an *orthogonal* system of coordinates, rectilinear or curvilinear (say, rectangular, spherical,

cylindrical, and so on). Let $E_{N\mathrm{X}}$ etc. and $B_{N\mathrm{X}}$ etc. be the components of electric and magnetic vectors resp., of the electromagnetic field of the N-th Whirl.

Then the total energy density in the system

$$\frac{d\mathsf{E}}{d\tau} = \frac{1}{8\pi}\left[\left(\sum_N E_{N\mathrm{X}}\right)^2 + \left(\sum_N E_{N\mathrm{Y}}\right)^2 + \left(\sum_N E_{N\mathrm{Z}}\right)^2 + \left(\sum_N B_{N\mathrm{X}}\right)^2 + \left(\sum_N B_{N\mathrm{Y}}\right)^2 + \left(\sum_N B_{N\mathrm{Z}}\right)^2\right]$$

$$= \frac{1}{8\pi}\sum_N\left(E_{N\mathrm{X}}^2 + E_{N\mathrm{Y}}^2 + E_{N\mathrm{Z}}^2 + B_{N\mathrm{X}}^2 + B_{N\mathrm{Y}}^2 + B_{N\mathrm{Z}}^2\right) + \frac{1}{8\pi}\sum_N\sum_{M\neq N}\left(E_{N\mathrm{X}}E_{M\mathrm{X}} + E_{N\mathrm{Y}}E_{M\mathrm{Y}} + E_{N\mathrm{Z}}E_{M\mathrm{Z}} + B_{N\mathrm{X}}B_{M\mathrm{X}} + B_{N\mathrm{Y}}B_{M\mathrm{Y}} + B_{N\mathrm{Z}}B_{M\mathrm{Z}}\right). \quad (15.6)$$

It can easily be seen that the first term of the third member of this formula is nothing else but the internal energy density $\frac{d\mathsf{E}_i}{d\tau}$. Therefore, by (15.1), the second term must be the mutual energy density $\frac{d\mathrm{W}}{d\tau}$. The second term can also be represented in a vectorial form, as the sum of scalar products of electric vectors $\vec{E}_N$ and $\vec{E}_M$ and magnetic vectors $\vec{B}_N$ and $\vec{B}_M$. We shall have then

$$\frac{d\mathrm{W}}{d\tau} = \frac{1}{8\pi}\sum_N\sum_{M\neq N}\left(\vec{E}_N\vec{E}_M + \vec{B}_N\vec{B}_M\right), \quad . \quad . \quad (15.7)$$

whence

$$\mathrm{W} = \frac{1}{8\pi}\sum_N\sum_{M\neq N}\int\left(\vec{E}_N\vec{E}_M + \vec{B}_N\vec{B}_M\right)d\tau, \quad . \quad (15.8)$$

where the integral must be taken over the whole of space.

If z is a generalized coordinate defining the mutual position of Whirls, then the generalized force corresponding to this coordinate will be

$$\mathrm{F}_z = -\frac{\partial \mathrm{W}}{\partial z}. \quad . \quad . \quad . \quad . \quad . \quad (15.9)$$

Owing to the periodic nature of the structure of the

e.m. field of Whirls at any given instant, and also to the periodic nature of the time variation of this field, it must be expected that W will have very frequent oscillations, apart from possible variations of a steadier nature. For the problems with which we shall deal in the subsequent discussions only the latter variations of W will be important. Therefore, we shall have to consider the average value $\overline{W}$ of the mutual energy W, in which these rapid oscillations (" ripples ") will be eliminated. The average generalized force $\overline{F}_z$ corresponding to the co-ordinate z will be

$$\overline{F}_z = -\frac{\partial \overline{W}}{\partial z}. \quad . \quad . \quad . \quad . \quad . \quad (15.10)$$

The formulæ for the e.m. field of an individual Whirl, which we have obtained in Part I., were expressed in cylindrical coordinates, co-axial with the Whirl and having its centre as the origin. To express the resultant e.m. field of a system, we must, obviously, find a convenient common coordinate system, to which the e.m. field of the whole system must be referred.

It can be seen from (15.8) and (15.10) that the average forces between the Whirls are additive, so long as their structure is not appreciably distorted.

We shall limit our subsequent discussion to the systems of two Whirls.

16. *Transformation of Coordinates in a System of Two Whirls.*

It appears to be generally convenient to place the origin of the common coordinates for a system of Whirls in the centre of inertia of the system.

Accordingly, in our case of the system of two Whirls, we shall place the origin 0 of the coordinates on the straight line $0_1 0_2$ passing through the centres 0_1 and 0_2 of Whirls 1 and 2 resp.

Denoting the masses of Whirls 1 and 2 by m_1 and m_2 resp., and the distance between their centres by $D = \overline{0_1 0_2}$, and the distances $\overline{0_1 0}$ and $\overline{0 0_2}$ by D_1 and D_2 resp., we shall then have

$$D = D_1 + D_2, \quad D_1 = \frac{m_2}{m_1 + m_2} D, \quad D_2 = \frac{m_1}{m_1 + m_2} D. \quad (16.1)$$

We shall denote by Ω_{11} and Ω_{12}, q_{01} and q_{02}, β_1 and β_2 the values of Ω_1, q_0, and β for the Whirls 1 and 2 resp. By

$$\Omega'_{11}=\beta_1\Omega'_{01} \text{ and } \Omega'_{12}=\beta_2\Omega'_{02}, \text{ and } q'_{01}=\left|\frac{\Omega'_{01}}{c}\right| \text{ and } q'_{02}=\left|\frac{\Omega'_{02}}{c}\right|,$$

we shall denote the corresponding quantities which will be obtained taking into account the precessional rotation of the axes of symmetry of the Whirls, and the oscillations of their initial phases, as well as the " planetary " motion of the Whirls about the common centre of gravity 0 (see formula (16.6 *d*)).

The q'_{01} and q'_{02} play in the Whirls, which belong to a system of Whirls, the same parts as regards the frequency, relative size, mass, and energy, as the q_0 would play in an isolated Whirl.

Then by (16.1), (12.5), and (14.3)

$$\left.\begin{aligned} \mathrm{D}_1&=\frac{\Omega'_{12}}{\Omega'_{11}+\Omega'_{12}}\mathrm{D}=\frac{\beta_2 q'_{02}}{\beta_1 q'_{01}+\beta_2 q'_{02}}\mathrm{D},\\ \mathrm{D}_2&=\frac{\Omega'_{11}}{\Omega'_{11}+\Omega_{12}}\mathrm{D}=\frac{\beta_1 q'_{01}}{\beta_1 q'_{01}+\beta_2 q'_{02}}\mathrm{D}. \end{aligned}\right\} \quad . \quad . \quad (16.2)$$

We shall calculate β_1 and β_2 with reference to the origin 0 as fixed in space.

We shall use two rectangular coordinate systems, common for both Whirls, both with the origin at 0 : the fixed one $\mathrm{X_0Y_0Z_0}$, and, generally speaking, the rotating one XYZ.

The position of the coordinate system XYZ relatively to $\mathrm{X_0Y_0Z_0}$ will be determined by three Eulerian angles : the angle θ_0 between the axes Z and $\mathrm{Z_0}$, the angle φ_0 between the axis X and the line of intersection of the planes XY and $\mathrm{X_0Y_0}$—which is called the " nodal line "—and the angle ψ_0 between the nodal line and the axis $\mathrm{X_0}$.

In the coordinate system XYZ the direction of the axis Y will coincide with the direction $0_1 0_2$.

According to the well-known laws of Classical Dynamics, the orbits of the centres 0_1 and 0_2 of Whirls 1 and 2, of the motion resulting from the mutual interaction of these Whirls, must lie in a fixed plane passing through their common centre of inertia 0.

We shall so arrange the coordinate system XYZ that the orbits of 0_1 and 0_2 will lie in the plane XY.

It follows from this that, so long as our system of two Whirls is not interferred with from outside,

$$\left.\begin{aligned}\theta_0&=\text{const.}\\ \psi_0&=\text{const.}\end{aligned}\right\}. \quad . \quad . \quad . \quad . \quad . \quad (16.3)$$

Apart from the coordinate systems XYZ and $X_0Y_0Z_0$, common for the whole system of two Whirls, we shall use two pairs of auxiliary rectangular coordinate systems : $X_1Y_1Z_1$ and $X_{01}Y_{01}Z_{01}$, with the common origin at 0_1, for Whirl 1, and $X_2Y_2Z_2$ and $X_{02}Y_{02}Z_{02}$, with the common origin at 0_2, for Whirl 2.

The respective axes of $X_1Y_1Z_1$, $X_2Y_2Z_2$, and XYZ will be parallel. The coordinate systems $X_{01}Y_{01}Z_{01}$ and $X_{02}Y_{02}Z_{02}$ will be rigidly connected with the cylindrical coordinate systems $x_1\, r_1\theta_1$ and $x_2\, r_2\theta_2$ of their respective Whirls 1 and 2. The axes Z_{01} and Z_{02} will coincide with x_1 and x_2 resp., and the axes X_{01} and X_{02} with the directions $\theta_1=0$ and $\theta_2=0$ resp.

The orientation of the coordination systems $X_{01}Y_{01}Z_{01}$ and $X_{02}Y_{02}Z_{02}$ relatively to $X_1Y_1Z_1$ and $X_2Y_2Z_2$ resp. will be defined by the Eulerian angles θ_1, φ_1, ψ_1 and θ_2, φ_2, ψ_2, which correspond to the above specified angles θ_0 φ_0 ψ_0 which define the mutual position of XYZ and $Z_0Y_0X_0$.

To simplify the formulæ for the transformation of our coordinates, we shall substitute $\theta_1+n\psi_1$ and $\theta_2+n\psi_2$ for θ_1 and θ_2 resp. Then the axes X_{01} and X_{02} will coincide with the corresponding nodal lines.

Since we consider here a system of two Whirls only, we can use, for definition of the e.m. field, the rotating common coordinate system XYZ. We must, however, keep in mind that the centres 0_1 and 0_2 of the Whirls move, owing to the rotation of the system XYZ, and, accordingly, the e.m. fields belonging to these Whirls will undergo corresponding to these speeds deformations which, as has been explained above, will satisfy the requirements of the Principle of Relativity.

It would be more consistent with the Principle of Relativity to define the e.m. field with reference to the fixed system $X_0Y_0Z_0$ and not to the rotating system XYZ, but this would mean an extra step in the transformation of coordinates and a considerable complication of the mathematics without any real difference in the result.

The three Relativity coefficients β for each Whirl (β_{11}, β_{12}, and β_{13} for Whirl 1, and β_{21}, β_{22}, and β_{23} for

Whirl 2) will be defined, in accordance with the formula (4.4), as follows :

$$\left.\begin{aligned}
\beta_{11} &= \left(1-\frac{v_{X_{01}}^2}{c^2}\right)^{-\frac{1}{2}} \\
&= \left(1-\frac{(\dot{\varphi}_0 D\cos\varphi_1 - \dot{D}\sin\varphi_1)^2\beta_2^2 q_{02}'^2}{(\beta_1 q_{01}'+\beta_2 q_{02}')^2 c^2}\right)^{-\frac{1}{2}}, \\
\beta_{12} &= \left(1-\frac{v_{Y_{01}}^2}{c^2}\right)^{-\frac{1}{2}} \\
&= \left(1-\frac{\cos^2\theta_1(\dot{\varphi}_0 D\sin\varphi_1 + \dot{D}\cos\varphi_1)^2\beta_2^2 q_{02}'^2}{(\beta_1 q'_1+\beta_2 q_{02}')^2 c^2}\right)^{-\frac{1}{2}}, \\
\beta_{13} &= \left(1-\frac{v_{Z_{01}}^2}{c^2}\right)^{-\frac{1}{2}} \\
&= \left(1-\frac{\sin^2\theta_1(\dot{\varphi}_0 D\sin\varphi_1 - \dot{D}\cos\varphi_1)^2\beta_1^2 q_{02}'^2}{(\beta_1 q_{01}'+\beta_2 q_{03}')^2 c^2}\right)^{-\frac{1}{2}},
\end{aligned}\right\} \quad \ldots \quad (16.3a)$$

and correspondingly for Whirl 2.

Here $v_{X_{01}}$, etc. are the components of the speed of the centre 0_1 of Whirl 1.

Applying, step by step, the well-known formulæ for the transformation of coordinates, and using for Relativity corrections the coefficients β, as expressed in (16.3*a*), in accordance with section 12, we shall obtain

$$\xi_1 = q_{01}' Z_{01}, \quad \rho_1 = q_{01}'\sqrt{X_{01}^2+Y_{01}^2}, \quad \theta_1 = \tan^{-1}\frac{Y_{01}}{X_{01}}, \quad (16.4)$$

where

$$\left.\begin{aligned}
X_{01} &= \beta_{11}(F_{111}X+F_{121}Y+F_{131}Z+F_{141}D), \\
Y_{01} &= \beta_{12}(F_{112}X+F_{122}Y+F_{132}Z+F_{142}D), \\
Z_{01} &= \beta_{13}(F_{113}X+F_{123}Y+F_{133}Z+F_{143}D),
\end{aligned}\right\} \quad (16.5)$$

where

$$\left.\begin{aligned}
F_{111} &= \cos\varphi_1, & F_{121} &= \sin\varphi_1, \\
F_{131} &= 0, & F_{141} &= -\frac{\beta_2 q_{02}'}{\beta_1 q_{01}'+\beta_2 q_{02}'}F_{121}, \\
F_{112} &= -\sin\varphi_1\cos\theta_1, & F_{122} &= \cos\varphi_1\cos\theta_1, \\
F_{132} &= \sin\theta_1, & F_{142} &= -\frac{\beta_2 q_{02}'}{\beta_1 q_{01}'+\beta_2 q_{03}'}F_{122}, \\
F_{113} &= \sin\varphi_1\sin\theta_1, & F_{123} &= -\cos\varphi_1\sin\theta_1, \\
F_{133} &= \cos\theta_1, & F_{143} &= -\frac{\beta_2 q_{02}'}{\beta_1 q_{01}'+\beta_2 q_{02}'}F_{123}.
\end{aligned}\right\} \quad \ldots \quad (16.5a)$$

In the formulæ (16.3*a*)–(16.5*a*) the axis X_{01} *coincided with the nodal line.* Therefore, in the phases ϕ_1 (see section 3) of Whirls 1 and 2, which we shall denote by ϕ_{11} and ϕ_{12} resp., the θ_1 and θ_2 must be replaced by $\theta_1+n_1\psi_1$ and $\theta_2+n_2\psi_2$ resp., whence instead of ϕ_{11} and ϕ_{12} we must use

$$\phi_1'=\phi_{11}+n_1\psi_1 \quad \text{and} \quad \phi_2'=\phi_{12}+n_2\psi_2 \quad . \quad (16.6)$$

(see the text between formulæ (16.3) and (16.3*a*).

Hence by (4.11) and (4.12)

$$\phi_1'=q_{01}\left(c\frac{t}{\beta_1}-v_1\xi_1\right)+n\theta_1+n\psi_1, \quad . \quad (16.6a)$$

where

$$v=\frac{\beta_{13}v_{Z_{01}}}{c}=\sqrt{\beta_{13}^2-1}. \quad . \quad . \quad . \quad (16.6b)$$

In accordance with the definitions preceding formula (16.2) we have

$$\vec{\Omega}_{11}'=\beta_1\left(\vec{\dot{\phi}}_1'+n_1\vec{\dot{\varphi}}_1+n_1\vec{\dot{\varphi}}_0\right), \quad . \quad . \quad (16.6c)$$

where the vectors $\vec{\dot{\phi}}_1'$, $n_1\vec{\dot{\varphi}}_1$, and $n_1\vec{\dot{\varphi}}_0$ are directed along the axes Z_{01}, Z_1, and Z resp. (The last two axes being parallel are equivalent for this case.)

Hence by (16.6*a*)

$$q_{01}'=\left|\frac{\Omega_{01}'}{c}\right|=\left|\frac{\Omega_{11}'}{\beta_1 c}\right|=\left|\vec{q}_{01}+\frac{n_1\vec{\dot{\psi}}_1}{c}+\frac{\vec{v}\vec{\dot{\xi}}}{c}+\frac{n_1\vec{\dot{\varphi}}_1}{c}+\frac{n_1\vec{\dot{\varphi}}_0}{c}\right|, \quad . \quad . \quad . \quad (16.6d)$$

where the first three vectors in $|\ |$ are directed along Z_{01} and the last two along Z. The $|\ |$ show, as before, that only the modulus of the expression inside them (the length of the vector) is taken.

The formulæ for Whirl 2 corresponding to (16.5*a*)–(16.6*d*) will be obtained by interchanging the identification suffixes 1 and 2 of Whirls 1 and 2 resp., *and substituting* + *for* − *before the right-hand members* in the expressions for* F_{141}, F_{142}, and F_{143} in (16.5*a*).

By (10.5) the resultant Relativity coefficients β_1 and β_2 of Whirls 1 and 2 resp. are

$$\beta_1=\beta_{11}\beta_{12}\beta_{13}, \qquad \beta_2=\beta_{21}\beta_{22}\beta_{23}. \quad . \quad . \quad (16.7)$$

* This is because 0_1 and 0_2 are situated on the axis Y on opposite sides of 0.

The resultant speeds v_1 and v_2 of the centres 0_1 and 0_2 of Whirls 1 and 2 resp. are

$$\left.\begin{aligned} v_1 &= c\sqrt{1-\frac{1}{\beta_1^2}}, \\ v_2 &= c\sqrt{1-\frac{1}{\beta_2^2}}. \end{aligned}\right\} \quad . \quad . \quad . \quad (16.7a)$$

We shall now consider the transformation of vectors.

When we refer the vectors to different coordinate systems we must distinguish two different aspects. The first is the coordinate system according to which *the vectors are resolved into components*, and the second is the coordinate system to which belong *the coordinates*, in *terms of which each vector component is expressed.*

Unless otherwise stated we shall assume that the vectors are resolved into components in *the same coordinate system* to which belong the coordinates, in terms of which the vector components are expressed.

To obtain the transformation formulæ of our vectors we can use the standard formulæ for the transformation of coordinates, taking into account the Relativity relationships of section 12, using them, however, in a slightly different way.

Firstly, while in the case of the transformation of coordinates it is convenient to find the expressions of the *old coordinates in terms of the new ones*, in the case of the transformation of vectors the components with respect to the *new* coordinate axes must be expressed in terms of the components with respect to the *old* coordinate axes.

Secondly, the expressions of the vectors do not change as a result of a parallel displacement of the coordinate system.

Thirdly, the Relativity transformations affect, generally speaking, the vectors and the coordinates in a different way. For instance, in the transformation of $(L_r L_\nu L_\theta)$ into $(L_X L_Y L_Z)$, the Relativity relationships will affect the expressions of the vector components in the new coordinate system only indirectly through the coordinates, in terms of which the vector components are expressed, while in the transformation of $(M_r M_\nu M_\theta)$ into $(M_X M_Y M_Z)$ the Relativity relationships, apart from this indirect influence, will manifest themselves through the factors depending on ζ or ζ_1 (see formulæ (5.6)–(5.9), (8.5) and

(8.10)–(8.12)). We shall express the latter influence of the Relativity relationships in the form of factors, which we shall denote by (ζ) with the corresponding suffixes.

Lastly, we must take into account the phases of the components of the electromagnetic vectors, which correspond to L_x etc. Therefore, in accordance with (8.4), we must introduce $-L_z$ for L_z, iL_r for L_r, and so on.

Bearing this in mind we can obtain the transformation formulæ in question for the "compound" Whirls (section 8), which we can write in the following form :—

$$\left.\begin{aligned}
L_{1X} &= -\mathbf{F}_{111}L_{1x} + i\mathbf{F}_{121}L_{1r} + \mathbf{F}_{131}L_{1\theta},\\
L_{1Y} &= -\mathbf{F}_{112}L_{1x} + i\mathbf{F}_{122}L_{1r} + \mathbf{F}_{132}L_{1\theta},\\
L_{1Z} &= -\mathbf{F}_{113}L_{1x} + i\mathbf{F}_{123}L_{1r} + \mathbf{F}_{133}L_{1\theta},\\
M_{1X} &= -i\mathbf{F}_{111}(\zeta)_{1x}M_{1x} - \mathbf{F}_{121}(\zeta)_{1r}M_{1r} + i\mathbf{F}_{131}(\zeta)_{1\theta}M_{1\theta},\\
M_{1Y} &= -i\mathbf{F}_{112}(\zeta)_{1x}M_{1x} - \mathbf{F}_{122}(\zeta)_{1r}M_{1r} + i\mathbf{F}_{132}(\zeta)_{1\theta}M_{1\theta},\\
M_{1Z} &= -i\mathbf{F}_{113}(\zeta)_{1x}M_{1x} - \mathbf{F}_{123}(\zeta)_{1r}M_{1r} + i\mathbf{F}_{133}(\zeta)_{1\theta}M_{1\theta},
\end{aligned}\right\} \quad (16.8)$$

where

$$\left.\begin{aligned}
\mathbf{F}_{111} &= \sin\boldsymbol{\varphi}_1 \sin\boldsymbol{\theta}_1,\\
\mathbf{F}_{121} &= \cos\theta_1 \cos\boldsymbol{\varphi}_1 - \sin\theta_1 \sin\boldsymbol{\varphi}_1 \cos\boldsymbol{\theta}_1,\\
\mathbf{F}_{131} &= -\sin\theta_1 \cos\boldsymbol{\varphi}_1 - \cos\theta_1 \sin\boldsymbol{\varphi}_1 \cos\boldsymbol{\theta}_1,\\
\mathbf{F}_{112} &= -\cos\boldsymbol{\varphi}_1 \sin\boldsymbol{\theta}_1,\\
\mathbf{F}_{122} &= \cos\theta_1 \sin\boldsymbol{\varphi}_1 + \sin\theta_1 \cos\boldsymbol{\varphi}_1 \cos\boldsymbol{\theta}_1,\\
\mathbf{F}_{132} &= -\sin\theta_1 \sin\boldsymbol{\varphi}_1 + \cos\theta_1 \cos\boldsymbol{\varphi}_1 \cos\boldsymbol{\theta}_1,\\
\mathbf{F}_{113} &= \cos\boldsymbol{\theta}_1,\\
\mathbf{F}_{123} &= \sin\theta_1 \sin\boldsymbol{\theta}_1,\\
\mathbf{F}_{133} &= \cos\theta_1 \sin\boldsymbol{\theta}_1.
\end{aligned}\right\} \quad (16.9)$$

Unless the point is too near to the axis we shall have by (8.10)–(8.12)

$$\left.\begin{aligned}
(\zeta)_{1x} &= \frac{\zeta_{11}}{\sqrt{\zeta_{11}^2+1}},\\
(\zeta)_{1r} = (\zeta)_{1\theta} &= \frac{1}{\sqrt{\zeta_{11}^2+1}}.
\end{aligned}\right\} \quad . \quad . \quad . \quad . \quad (16.10)$$

The first suffixes 1 at $\mathbf{F}$ and (ζ) and the second suffix at ζ are the identification suffixes of Whirl 1. The corresponding formulæ for Whirl 2 are identical, only the

identification suffixes of the Whirl must, of course, be changed accordingly.

The expressions for simple Whirls corresponding to (16.8)–(16.10) will be obtained by substituting G, H, and ζ_1 for L, M, and ζ_{11} resp. This can be easily verified (compare sections 5 and 8).

17. *The Mutual Energy of a System of Two Whirls.*

For the calculation of the mutual energy W we shall use the coordinate system XYZ specified in the previous section.

By (15.8) we can write

$$W=\frac{1}{8\pi}\int_{-\infty}^{\infty}\int_{-\infty}^{\infty}\int_{-\infty}^{\infty}2(\vec{E}_1\vec{E}_2+\vec{B}_1\vec{B}_2)dX\,dY\,dZ. \quad (17.1)$$

We shall concentrate in the following discussion on the compound Whirls, and therefore, *unless otherwise stated*, we shall mean in the future by the term "Whirl" a *compound* one.

In the case of contrapolarized Whirls we shall assume, to fix our ideas, that Whirl 1 is electropolarized and Whirl 2 magnetopolarized.

Denote the amplitude constants A (section 8) of Whirls 1 and 2 by A_1 and A_2 resp., and recall the notation of the phases ϕ and coefficients β used in (16.6) and (16.7) resp. Mark by the suffixes + and − the results of calculation for copolarized and contrapolarized Whirls resp.

Then, taking into account that only real parts of the expressions for the vector components must be used in the calculation of the scalar products, we shall obtain by (17.1), (8.3), and (8.4)

$$\left.\begin{aligned} W_+&=\frac{1}{4\pi}\beta_1\beta_2A_1A_2q_{01}'^2q_{02}'^2(\vec{L}_1'\vec{L}_2'+\vec{M}_1'\vec{M}_2'),\\ W_-&=\frac{1}{4\pi}\beta_1\beta_2A_1A_2q_{01}'^2q_{02}'^2(\vec{L}_1'\vec{M}_1'+\vec{M}_1'\vec{L}_2'),\end{aligned}\right\} \quad (17.2)$$

where $\vec{L}_1'$, $\vec{L}_2'$, $\vec{M}_1'$, and $\vec{M}_2'$ are the vectors having the following components:—

$$\left.\begin{matrix}L_{1X}'\\ Y\\ Z\end{matrix}=R\begin{matrix}(L_{1X}\\ Y\\ Z\end{matrix}e^{i\phi_1'})\right\} \text{ etc., . . . } (17.2\,a)$$

where R, as before, is to show that only the real part of the subsequent expression is to be taken.

We shall assume that the distance D between the centres of the Whirls is large enough to enable us to neglect the influence of the regions, near their axes, to which the formulæ (8.10)–(8.12) are not applicable. We can safely do so if D is large, even when the field of one of the Whirls is strong in these regions, since the field due to the other Whirl will be then weak, owing to the considerable distance D, and, consequently, the scalar products of the vectors of these fields will be small.

Introduce into (17.2) the expressions from (16.8), and then substitute for L_{1x}, L_{2x}, etc. their expressions from (8.10) and (8.10*a*).

The result can be written in the following form:—

$$W_{\pm}=\sqrt{q'_{01}q'_{02}}K_1K_2\sum_{l=1}^{5}\iiint \mathbf{N}_{l\pm}\mathbf{W}_{l\pm}dX\,dY\,dZ + o\{q_{01}^{-2}q_{02}^{-2}\rho_1^{-2}\rho_2^{-2}\}, \quad (17.3)$$

where only the upper or only the lower signs in $\pm$ must be used simultaneously.

In this formula

$$\left.\begin{aligned} K_1&=\frac{\sqrt{2}A_1}{\pi\sqrt[4]{\chi+1_{11}^2}}=\frac{\sqrt{2}\sqrt{\frac{c\hbar_{11}}{Q}}}{\pi\sqrt[4]{\chi_{11}^2+1}},\\ K_2&=\frac{\sqrt{2}A_2}{\pi\sqrt[4]{\chi_{12}^2+1}}=\frac{\sqrt{2}\sqrt{\frac{c\hbar_{12}}{Q}}}{\pi\sqrt[4]{\chi_{12}^2+1}}, \text{ by (9.3),} \end{aligned}\right\} \quad (17.3a)$$

where χ_{11} and χ_{12} and $\hbar_{11}$ and $\hbar_{12}$ are the values of $\hbar_1$ and χ_1 for Whirls 1 and 2 resp.

Each term under the Σ corresponds to a product of two vector components of $\vec{L}_1$, $\vec{L}_2$, $\vec{M}_1$, and $\vec{M}_2$ in cylindrical coordinates (*e. g.*, L_{1x}, L_{2x}, etc.). There will be altogether eighteen such terms, but no more than five of them will be significant, since L_r, L_r, and M_θ are of a small order of magnitude (see (8.10) and (8.10*a*)), and therefore all the products into which they enter can be neglected.

We shall combine the factors in each term in the following manner:—in **N**'s we shall collect all those which depend on $|\zeta_1|$ and on the coefficients **F** for the transformation of vectors from a cylindrical into a rectangular

coordinate system, and in W's all the remaining factors with the exception of common factors brought outside the Σ.

We shall have accordingly

$$\mathbf{N}_{1+}=\mathbf{F}_{131}\mathbf{F}_{231}+\mathbf{F}_{132}\mathbf{F}_{232}+\mathbf{F}_{133}\mathbf{F}_{233},$$

$$\mathbf{N}_{2+}=\frac{|\zeta_{11}|\,|\zeta_{12}|}{|\sqrt{\zeta_{11}^2+1}|\,|\sqrt{\zeta_{12}^2+1}|}(\mathbf{F}_{111}\mathbf{F}_{211}+\mathbf{F}_{112}\mathbf{F}_{212}+\mathbf{F}_{113}\mathbf{F}_{213}),$$

$$\mathbf{N}_{3+}=\frac{1}{|\sqrt{\zeta_{11}^2+1}|\,|\sqrt{\zeta_{12}^2+1}|}(\mathbf{F}_{121}\mathbf{F}_{221}+\mathbf{F}_{122}\mathbf{F}_{222}+\mathbf{F}_{123}\mathbf{F}_{223}),$$

$$\mathbf{N}_{4+}=\frac{|\zeta_{11}|}{|\sqrt{\zeta_{11}^2+1}|\,|\sqrt{\zeta_{12}^2+1}|}(\mathbf{F}_{111}\mathbf{F}_{221}+\mathbf{F}_{112}\mathbf{F}_{222}+\mathbf{F}_{113}\mathbf{F}_{223}),$$

$$\mathbf{N}_{5+}=\frac{|\zeta_{12}|}{|\sqrt{\zeta_{11}^2+1}|\,|\sqrt{\zeta_{12}^2+1}|}(\mathbf{F}_{121}\mathbf{F}_{211}+\mathbf{F}_{122}\mathbf{F}_{212}+\mathbf{F}_{123}\mathbf{F}_{213}),$$

$$\mathbf{N}_{1-}=\frac{|\zeta_{12}|}{|\sqrt{\zeta_{12}^2+1}|}(\mathbf{F}_{131}\mathbf{F}_{211}+\mathbf{F}_{132}\mathbf{F}_{212}+\mathbf{F}_{133}\mathbf{F}_{213}),$$

$$\mathbf{N}_{2-}=\frac{1}{|\sqrt{\zeta_{12}^2+1}|}(\mathbf{F}_{131}\mathbf{F}_{221}+\mathbf{F}_{132}\mathbf{F}_{222}+\mathbf{F}_{133}\mathbf{F}_{223}),$$

$$\mathbf{N}_{3-}=\frac{|\zeta_{11}|}{|\sqrt{\zeta_{11}^2+1}|}(\mathbf{F}_{111}\mathbf{F}_{231}+\mathbf{F}_{112}\mathbf{F}_{232}+\mathbf{F}_{113}\mathbf{F}_{233}),$$

$$\mathbf{N}_{4-}=\frac{1}{|\sqrt{\zeta_{11}^2+1}|}(\mathbf{F}_{121}\mathbf{F}_{231}+\mathbf{F}_{122}\mathbf{F}_{232}+\mathbf{F}_{123}\mathbf{F}_{233}),$$

$$\mathbf{N}_{5-}=0. \qquad \ldots \quad (17.4)$$

Hence, by (16.9) after simple transformations,

$$\begin{aligned}\mathbf{N}_{1+}=&(\sin\theta_1\sin\theta_2+\cos\theta_1\cos\theta_2\cos\boldsymbol{\theta}_1\cos\boldsymbol{\theta}_2)\cos(\boldsymbol{\varphi}_1-\boldsymbol{\varphi}_2)\\&-(\sin\theta_1\cos\theta_2\cos\boldsymbol{\theta}_2-\cos\theta_1\sin\theta_2\cos\boldsymbol{\theta}_1)\sin(\boldsymbol{\varphi}_1\\&-\boldsymbol{\varphi}_2)+\cos\theta_1\cos\theta_2\sin\boldsymbol{\theta}_1\sin\boldsymbol{\theta}_2,\end{aligned}$$

$$\begin{aligned}\mathbf{N}_{2+}=&\frac{|\zeta_{11}|\,|\zeta_{12}}{|\sqrt{\zeta_{11}^2+1}|\,|\sqrt{\zeta_{12}^2+1}|}(\cos\boldsymbol{\theta}_1\cos\boldsymbol{\theta}_2\\&-\sin\boldsymbol{\theta}_1\sin\boldsymbol{\theta}_2\cos(\boldsymbol{\varphi}_1-\boldsymbol{\varphi}_2)),\end{aligned}$$

$$\begin{aligned}\mathbf{N}_{3+}=&\frac{1}{|\sqrt{\zeta_{11}^2+1}|\,|\sqrt{\zeta_{12}^2+1}|}[(\cos\theta_1\cos\theta_2\\&+\sin\theta_1\sin\theta_2\cos\boldsymbol{\theta}_1\cos\boldsymbol{\theta}_2)\,.\,\cos(\boldsymbol{\varphi}_1-\boldsymbol{\varphi}_2)\\&+(\cos\theta_1\sin\theta_2\cos\boldsymbol{\theta}_2-\sin\theta_1\cos\theta_2\cos\boldsymbol{\theta}_1)\\&.\sin(\boldsymbol{\varphi}_1-\boldsymbol{\varphi}_2)+\sin\theta_1\sin\theta_2\sin\boldsymbol{\theta}_1\sin\boldsymbol{\theta}_2],\end{aligned}$$

$$\mathbf{N}_{4+}=\frac{|\zeta_{11}|}{|\sqrt{\zeta_{11}^2+1}|\,|\sqrt{\zeta_{12}^2+1}|}(\cos\theta_2\sin\boldsymbol{\theta}_1\sin(\boldsymbol{\varphi}_1-\boldsymbol{\varphi}_2)$$
$$-\sin\theta_2\sin\boldsymbol{\theta}_1\cos\boldsymbol{\theta}_2\cos(\boldsymbol{\varphi}_1-\boldsymbol{\varphi}_2)$$
$$+\sin\theta_2\cos\boldsymbol{\theta}_1\sin\boldsymbol{\theta}_2),$$

$$\mathbf{N}_{5+}=\frac{|\zeta_{12}|}{|\sqrt{\zeta_{11}^2+1}|\,|\sqrt{\zeta_{12}^2+1}|}(-\cos\theta_1\sin\boldsymbol{\theta}_2\sin(\boldsymbol{\varphi}_1-\boldsymbol{\varphi}_2)$$
$$-\sin\theta_1\cos\boldsymbol{\theta}_1\sin\boldsymbol{\theta}_2\cos(\boldsymbol{\varphi}_1-\boldsymbol{\varphi}_2)+\sin\theta_1\sin\boldsymbol{\theta}_1\cos\boldsymbol{\theta}_2),$$

$$\mathbf{N}_{1-}=\frac{|\zeta_{12}|}{|\sqrt{\zeta_{11}^2+1}|}(\sin\theta_1\sin\boldsymbol{\theta}_2\sin(\boldsymbol{\varphi}_1-\boldsymbol{\varphi}_2)$$
$$-\cos\theta_1\cos\boldsymbol{\theta}_1\sin\boldsymbol{\theta}_2\cos(\boldsymbol{\varphi}_1-\boldsymbol{\varphi}_2)$$
$$+\cos\theta_1\sin\boldsymbol{\theta}_1\cos\boldsymbol{\theta}_2),$$

$$\mathbf{N}_{2-}=\frac{1}{|\sqrt{\zeta_{12}^2+1}|}[(\cos\theta_1\sin\theta_2\cos\boldsymbol{\theta}_1\cos\boldsymbol{\theta}_2-\sin\theta_1\cos\boldsymbol{\theta}_2)$$
$$\cdot\cos(\boldsymbol{\varphi}_1-\boldsymbol{\varphi}_2)-(\sin\theta_1\sin\theta_2\cos\boldsymbol{\theta}_2$$
$$+\cos\theta_1\cos\theta_2\cos\boldsymbol{\theta}_1)\cdot\sin(\boldsymbol{\varphi}_1-\boldsymbol{\varphi}_2)$$
$$+\cos\theta_1\sin\theta_2\sin\boldsymbol{\theta}_1\sin\boldsymbol{\theta}_2],$$

$$\mathbf{N}_{3-}=\frac{|\zeta_{11}|}{|\sqrt{\zeta_{12}^2+1}|}(-\sin\theta_2\sin\boldsymbol{\theta}_1\sin(\boldsymbol{\varphi}_1-\boldsymbol{\varphi}_2)$$
$$-\cos\theta_2\sin\boldsymbol{\theta}_1\cos\boldsymbol{\theta}_2\cos(\boldsymbol{\varphi}_1-\boldsymbol{\varphi}_2)$$
$$+\cos\theta_2\cos\boldsymbol{\theta}_1\sin\boldsymbol{\theta}_2),$$

$$\mathbf{N}_{4-}=\frac{1}{|\sqrt{\zeta_{11}^2+1}|}[(\sin\theta_1\cos\theta_2\cos\boldsymbol{\theta}_2\cos\boldsymbol{\theta}_1$$
$$-\cos\theta_1\sin\theta_2)\cos(\boldsymbol{\varphi}_1-\boldsymbol{\varphi}_2)+(\sin\theta_2\sin\theta_1\cos\boldsymbol{\theta}_1$$
$$+\cos\theta_1\cos\theta_2\cos\boldsymbol{\theta}_2)\sin(\boldsymbol{\varphi}_1-\boldsymbol{\varphi}_2)$$
$$+\sin\theta_1\cos\theta_2\sin\boldsymbol{\theta}_1\sin\boldsymbol{\theta}_2],$$
$$\mathbf{N}_{5-}=0. \qquad \ldots \quad (17.4a)$$

In these formulæ (see (8.12))

$$\left.\begin{aligned}|\zeta_{11}|&=\sqrt{\frac{\chi_{11}^2+1}{\beta_{13}^2\chi_{11}^2+\beta_{13}^2-1}},\\ |\sqrt{\zeta_{11}^2+1}|&=\frac{\sqrt{\beta_{13}^2+\chi_{11}^2(\beta_{13}^2-1)}}{\sqrt{\beta_{13}^2\chi_{11}^2+\beta_{13}^2-1}}.\end{aligned}\right\} \quad \ldots \quad (17.4b)$$

For Whirl 2 the identification suffixes 1 (*i. e.*, the first suffixes at β and the second suffixes at χ) must be replaced by 2.

It will be seen from (17.4*b*) that in the case where $\chi_{11}<<1$ and $\chi_{12}<<1$ and when the speeds of translatory motion are small in comparison with the speed of light, *i. e.*, $\beta_{13}^2-1<<1$, we can put

$$\left.\begin{aligned}\frac{1}{|\sqrt{\zeta_{11}^2+1}|}=\frac{1}{|\sqrt{\zeta_{12}^2+1}|}=0,\\ \frac{|\xi_{11}|}{|\sqrt{\zeta_{11}^2+1}|}=\frac{|\xi_{12}|}{|\sqrt{\zeta_{12}^2+1}|}=1.\end{aligned}\right\} \quad . \quad (17.4c)$$

Further, the W's in (17.3) can be written as follows:

$$\mathrm{W}_{l\pm}=u\Lambda\mathrm{S}_{l\pm}, \quad . \quad . \quad . \quad . \quad . \quad (17.5)$$

where only the lower or only the upper signs in the $\pm$ must be taken simultaneously. In this formula

$$u=\frac{\beta_1\beta_2\sqrt{q_{01}^3q_{02}^3}}{[\rho_1\rho_2(\rho_1^2+\xi_1^2)(\kappa_2^2+\xi_2^2)]^{\frac{1}{2}}}$$

$$=\frac{\beta_1\beta_2}{[(\mathrm{X}_{01}^2+\mathrm{Y}_{01}^2)^{\frac{1}{2}}(\mathrm{X}_{02}^2+\mathrm{Y}_{02}^2)^{\frac{1}{2}}(\mathrm{X}_{01}^2+\mathrm{Y}_{01}^2+\mathrm{Z}_{01}^2)(\mathrm{X}_{02}^2+\mathrm{Y}_{02}^2+\mathrm{Z}_{02}^2)]^{\frac{1}{2}}},$$

by (16.4) . . . (17.5*a*)

$$\Lambda=\exp.(-2\phi_{21}-2\phi_{22})=\exp.(-2\chi_{11}q_{01}'|F_{113}\mathrm{X}+F_{123}\mathrm{Y}$$
$$+F_{133}\mathrm{Z}+F_{143}\mathrm{D}|-2\chi_{12}q_{02}'\ F_{213}\mathrm{X}+F_{223}\mathrm{Y}+F_{233}\mathrm{Z}+F_{243}\mathrm{D}|)$$

by (4.11) and (16.4) and (16.5)). . . . (17.5*b*)

Taking into account the formula (8.6*a*), which in our present notation will be written

$$\chi_{11}=\frac{\kappa_{211}}{q_{01}\beta_{13}}, \quad \chi_{12}=\frac{\kappa_{212}}{q_{02}\beta_{23}}, \quad . \quad . \quad (17.5c)$$

where κ_{211} and κ_{212} are the coefficients $\kappa_{21}=\beta_3q_0\chi_1$ for Whirls 1 and 2 resp., we can write (17.5*b*)

$$\Lambda=\exp.(-2\kappa_{211}|F_{113}\mathrm{X}+F_{123}\mathrm{Y}+F_{133}\mathrm{Z}+F_{143}\mathrm{D}|$$
$$-2\kappa_{212}|F_{213}\mathrm{X}+F_{223}\mathrm{Y}+F_{233}\mathrm{Z}+F_{243}\mathrm{D}|). \quad (17.5d)$$

The last factor in the right-hand member of (17.5)

$$S_{l\pm}=\cos(\Psi_1+\Xi_{1l\pm})\cos(\Psi_2 + \Xi_{2l\pm})\cos(\phi_1'+\Upsilon_{1l\pm})\cos(\phi_2'+\Upsilon_{2l\pm}), \quad (17.6)$$

where only the upper or only the lower signs in $\pm$ in the suffixes must be used simultaneously.

In this formula Ψ_1 and Ψ_2 are the Ψ's of (8.11) corresponding to Whirls 1 and 2 resp. The meaning of Ξ and Υ is shown in the following table :—

Second and third suffixes $l\pm$.	$-4/\pi\,\Xi_1$.	$-4/\pi\,\Xi_2$.	Υ_1.	Υ_2.
1+	$2n_1+3$	$2n_2+3$	0	0
2+	$2n_1+1$	$2n_2+1$	$\delta_1-\pi/2$	$\delta_2-\pi/2$
3+	$2n_1+3$	$2n_2+3$	$-\gamma_1+\pi$	$-\gamma_2+\pi$
4+	$2n_1+1$	$2n_2+3$	$\delta_1-\pi/2$	$-\gamma_2+\pi$
5+	$2n_1+3$	$2n_2+1$	$-\gamma_1+\pi$	$\delta_2-\pi/2$
1−	$2n_1+3$	$2n_2+1$	0	$\delta_2-\pi/2$
2−	$2n_1+3$	$2n_2+3$	0	$-\gamma_2+\pi$
3−	$2n_1+1$	$2n_2+3$	$\delta_1-\pi/2$	0
4−	$2n_1+3$	$2n_2+3$	$\gamma_1+\pi$	0

. . . (17.6*a*)

where (see (8.12))

$$\left.\begin{aligned}\delta_1&=-\tan^{-1}\frac{\chi_{11}\sqrt{\beta_{13}^2-1}}{\beta_{13}},\\ \gamma_1&=\tan^{-1}\frac{\chi_{11}\sqrt{\beta_{13}^2-1}}{\beta_{13}}-\tan^{-1}\frac{\beta_{13}\chi_{11}}{\sqrt{\beta_{13}^2-1}},\end{aligned}\right\} \quad (17.6b)$$

n_1 and n_2 are the values of n for Whirls 1 and 2 resp.

When $\theta_1\equiv 0$ the Whirl obviously moves perpendicularly to its axis, *i. e.*, $v_{Z_{01}}\equiv 0$, and hence $\beta_{13}\equiv 1$ (by 16.3*a*). Then

$$\delta_1=0, \quad \gamma_1=-\frac{\pi}{2}. \quad . \quad . \quad . \quad . \quad . \quad (17.6c)$$

If θ_1 does not equal zero *identically*, then, in our applications, we can put $\chi_{11}<<\sqrt{\beta_{13}^2-1}$, for in a system of two Whirls they both move continuously and $\chi_{11}<<1$.

Then we shall have

$$\delta_1=0, \quad \gamma_1=0. \quad . \quad . \quad . \quad . \quad (17.6\,d)$$

Of course, the same is true for Whirl 2.

We shall put now the formula (17.3) into a form which is convenient for further discussion.

Transform, in the right-hand member of (17.6) the first two factors, and the second two factors, separately, according to the trigonometrical formula

$$\cos a \cos b = \tfrac{1}{2}[\cos(a+b)+\cos(a-b)],$$

perform the multiplication of the binomials thus obtained, and then transform each of the four terms of the product according to the same trigonometrical formula, and, lastly, transform each of the eight terms of the result according to the formula

$$\cos(a+b)=\cos a \cos b - \sin a \sin b,$$

putting in the latter formula all Ξ and Υ into a, and all Ψ and ϕ' into b. We shall then obtain the expression for $S_{l\pm}$ which we can write in the following form:

$$S_{l\pm}=\frac{1}{8}\sum_{f=1}^{4}\sum_{g=1}^{4} U_{fg}\, s_{fgl\pm}, \quad . \quad . \quad . \quad . \quad (17.7)$$

where

$$U_{fg}=\sin\left(\Psi_1+\bar{f}\Psi_2+\bar{g}\phi_1'-(-)^g\phi_2'-f\frac{\pi}{2}\right), \quad (17.7\,a)$$

and

$$s_{fgl\pm}=-\sin\left(\Xi_{1l\pm}+\bar{f}\Xi_{2l\pm}+\bar{g}\Upsilon_{1l\pm}-(-)^g\Upsilon_{2l\pm}+f\frac{\pi}{2}\right), \quad . \quad . \quad . \quad (17.7\,b)$$

where

$$\bar{f}=\sqrt{2}\cos\left(\frac{\pi}{4}+f\frac{\pi}{2}\right), \quad \bar{g}=\sqrt{2}\cos\left(\frac{\pi}{4}+g\frac{\pi}{2}\right). \quad (17.7\,c)$$

To f, $g=1$, 2, 3, and 4 will obviously correspond $\bar{f}$, $\bar{g}=1$, -1, -1, and 1 resp.

An explicit expression for s_{fgl} can be easily found by (17.7 *b*) and (17.6 *a*). We shall write down the result for the case where $n_1=n_2=1$ and $\gamma_1=\gamma_2=\delta_1=\delta_2=0$ (*i. e.*, for the case corresponding to formula (17.6 *d*)).

	$s_{3gl+\cdot}$					$s_{3gl-\cdot}$			
g \ l	1	2	3	4	5	1	2	3	4
1.....	1	−1	1	−1	1	−1	−1	1	−1
2.....	1	−1	1	1	−1	1	−1	−1	−1
3.....	1	1	1	1	1	−1	−1	−1	−1
4.....	1	1	1	−1	−1	1	−1	1	−1
$\frac{s_{4gl}}{s_{3gl}}$	1	−1	1	1	−1	−1	1	1	1
$s_{1gl\pm}=s_{2gl\pm}=0.$									

. . . (17.7*d*)

By (17.3), (17.5), and (17.7)

$$W_{\pm}=\tfrac{1}{8}\sqrt{q'_{01}q'_{02}}\mathbf{K}_1\mathbf{K}_2\sum_{f=1}^{4}\sum_{g=1}^{4}\iiint u\Lambda H_{fg\pm}U_{fg}\,dX\,dY\,dZ, \quad (17.8)$$

where
$$H_{fg\pm}=\sum_{l=1}^{5}\mathbf{N}_{l\pm}s_{3gl\pm}. \quad . \quad . \quad . \quad . \quad (17.8a)$$

In the suffixes $\pm$ in these formulæ only upper or only lower signs must be used simultaneously.

We shall now write the expressions of H_{fg} in terms of the parameters defining the position of the axes of Whirls 1 and 2 (*i. e.*, φ_1, θ_1, φ_2, θ_2, and D) for the case when both Whirls are two-pole ones (*i. e.*, $n_1=n_2=1$) and $\chi_{11}<<1$ and $\chi_{12}<<1$.

We shall write them in the form

$$\begin{aligned}H_{fg\pm}=&{}^0H_{fg\pm}+{}^1H_{fg\pm}\sin\theta_1+{}^2H_{fg\pm}\sin\theta_2+{}^3H_{fg\pm}\cos\theta_1\\&+{}^4H_{fg\pm}\cos\theta_2+{}^5H_{fg\pm}\sin\theta_1\sin\theta_2+{}^6H_{fg\pm}\sin\theta_1\cos\theta_2\\&+{}^7H_{fg\pm}\cos\theta_1\sin\theta_2+{}^8H_{fg\pm}\cos\theta_1\cos\theta_2, \quad . \quad (17.8b)\end{aligned}$$

where only the upper or only the lower signs of the suffixes $\pm$ must be used simultaneously.

We shall assume that neither θ_1 nor θ_2 is *identically* equal zero, and that $\beta_1-1<<1$ and $\beta_2-1<<1$.

Then by (17.4*a*), (17.4*c*), (17.6*d*), and (17.7*d*), we shall

have the following expressions for ${}^{m}H_{fg\pm}$ in the right-hand member of (17.8*b*).

m.	Suffix $\pm$ in ${}^{m}H_{fg\pm}$.	Sign before the expression for ${}^{m}H_{fg\pm}$ when $f=3$ (upper sign) and 4 (lower sign), and $g=$ 1	2	3	4	Expression for ${}^{m}H_{fg\pm}$ apart from the sign when $f=3$ or 4.
0	+	$-$ $+$	$-$ $+$	$+$ $-$	$+$ $-$	$\cos\theta_1\cos\theta_2$ $-\sin\theta_1\sin\theta_2\cos(\varphi_1-\varphi_2)$
1	$-$	$-$ $+$	$+$ $-$	$-$ $+$	$+$ $-$	$\sin\theta_2\sin(\varphi_1-\varphi_2)$
2	$-$	$-$ $-$	$+$ $+$	$+$ $+$	$-$ $-$	$\sin\theta_1\sin(\varphi_1-\varphi_2)$
3	$-$	$+$ $-$	$-$ $+$	$+$ $-$	$-$ $+$	$\cos\theta_1\sin\theta_2\cos(\varphi_1-\varphi_2)$ $-\sin\theta_1\cos\theta_2$
4	$-$	$-$ $-$	$+$ $+$	$+$ $+$	$-$ $-$	$\sin\theta_1\cos\theta_2\cos(\varphi_1-\varphi_2)$ $-\cos\theta_1\sin\theta_2$
5	+	$+$ $+$	$+$ $+$	$+$ $+$	$+$ $+$	$\cos(\varphi_1-\varphi_2)$
6	+	$-$ $-$	$-$ $-$	$-$ $-$	$-$ $-$	$\cos\theta_2\sin(\varphi_1-\varphi_2)$
7	+	$+$ $+$	$+$ $+$	$+$ $+$	$+$ $+$	$\cos\theta_1\sin(\varphi_1-\varphi_2)$
8	+	$+$ $+$	$+$ $+$	$+$ $+$	$+$ $+$	$\cos\theta_1\cos\theta_2\cos(\varphi_1-\varphi_2)$ $+\sin\theta_1\sin\theta_2$

$${}^{m}H_{1g\pm}={}^{m}H_{2g\pm}=0.$$

$${}^{0}H_{fg-}={}^{1}H_{fg+}={}^{2}H_{fg+}={}^{3}H_{fg+}={}^{4}H_{fg-}$$
$$={}^{5}H_{fg-}={}^{6}H_{fg-}={}^{7}H_{fg-}={}^{8}H_{fg-}=0.$$

. . . . (17.8*c*)

For further investigation we shall represent the argument of the sin in (17.7*a*) in the following form:

$$\Psi_1+\bar{f}\Psi_2+\bar{g}\phi_1'-(-)^g\phi_2'-f\frac{\pi}{2}=\mathrm{T}_g+\mathrm{P}_{fg}+\mathbf{M}_{fg}-f\frac{\pi}{2}. \quad (17.9)$$

Here in T_g we shall concentrate all the terms explicitly depending on time t and on ψ. The term P_{fg} we shall construct in such a way that sin and cos P_{fg} should be either single harmonic functions of X, Y, and Z, or at least be resolvable into a series of such functions with a sufficient degree of accuracy, while the term $\mathbf{M}_{fg}$ will be

so constructed that sin and cos of $\mathbf{M}_{fg}$ will be aperiodic functions of X, Y, and Z.

As was already stated in the Appendix to Part I., sin and cos $\sqrt{x^2+y^2}$ are resolvable into a series of sin and cos $(x \pm y)$. Therefore we shall include $\rho_1=\sqrt{X_{01}^2+Y_{01}^2}$ and $\rho_2=\sqrt{X_{02}^2+Y_{02}^2}$ in $\mathbf{P}_{fg}$.

Then by (16.6 *a*) and (8.11)

$$\mathrm{T}_g=\left(\bar{g}\frac{q_{01}}{\beta_1}-(-)_g\frac{q_{02}}{\beta_2}\right)ct+\bar{g}n_1\psi_1-(-)^g n_2\psi_2. \quad (17.9\,a)$$

$$\mathrm{P}_{fg}=\rho_1\sqrt{\chi_{11}^2+1}+\bar{f}\,\rho_2\sqrt{\chi_{12}^2+1}-\bar{g}v_1\xi_1+(-)^g v_2\xi_2. \quad (17.9\,b)$$

$$\mathbf{M}_{fg}=\bar{g}n_1\theta_1-(-)^g n_2\theta_2-\tan^{-1}\frac{\rho_1}{\xi_1}-\bar{f}\tan^{-1}\frac{\rho_2}{\xi_2}. \quad (17.9\,c)$$

By (17.8), (17.7 *a*), and (17.8 *b*), taking into account that ${}^mH_{fg\pm}$ are independent of X, Y, and Z, we have

$$\mathrm{W}_{\pm}=\sqrt{q'_{01}\,q'_{02}}\,\mathbf{K}_1\mathbf{K}_2\sum_{m=0}^{8}\sum_{f=1}^{4}\sum_{g=1}^{4}{}^mH_{fg\pm}\,{}^m\mathbf{X}_{fg}, \quad (17.10)$$

where

$${}^m\mathbf{X}_{fg}=\frac{1}{8}\iiint {}^mu\,\Lambda\sin\left(\mathrm{T}_{fg}+\mathrm{P}_{fg}+\mathbf{M}_{fg}-f\frac{\pi}{2}\right)d\mathrm{X}\,d\mathrm{Y}\,d\mathrm{Z}, \quad (17.10\,a)$$

where

$$\left.\begin{array}{lll} {}^0u=u, & {}^1u=u\sin\theta_1, & {}^2u=u\sin\theta_2, \\ {}^3u=u\cos\theta_1, & {}^4u=u\cos\theta_2, & {}^5u=u\sin\theta_1\cos\theta_2, \\ {}^6u=u\sin\theta_1\cos\theta_2, & {}^7u=u\cos\theta_1\sin\theta_2, & {}^8u=u\cos\theta_1\cos\theta_2, \end{array}\right\} \quad (17.10\,b)$$

${}^mu$ is an aperiodic function of X, Y, and Z, tending to zero when any of these independent variables approaches to $\pm\infty$ (see (17.5 *a*), (16.4), and (16.5)); $\mathbf{M}_{fg}$ is also an aperiodic function of X, Y, and Z; Λ is an exponential function of the same variables. We can, therefore, apply to ${}^m\mathbf{X}_{fg}$ a method of approximate integration which is shown in the Appendix to Part I.

For this purpose we shall denote

$$\left.\begin{aligned}
L_{1fg}=&q'_{01}[\sqrt{\chi_{11}^2+1}\,(\beta_{11}F_{111}+\beta_{12}F_{112})-\bar{g}v_1F_{113}]\\
&+q'_{02}[\bar{f}\sqrt{\chi_{12}^2+1}\,(\beta_{21}F_{211}+\beta_{22}F_{212})+(-)^g v_2F_{213}],\\
L_{2fg}=&q'_{01}[\sqrt{\chi_{11}^2+1}\,(\beta_{11}F_{121}+\beta_{12}F_{122})-\bar{g}v_1F_{123}]\\
&+q'_{02}[\bar{f}\sqrt{\chi_{12}^2+1}\,(\beta_{21}F_{221}+\beta_{22}F_{222})+(-)^g v_2F_{223}],\\
L_{3fg}=&q'_{01}[\sqrt{\chi_{11}^2+1}\,(\beta_{11}F_{131}+\beta_{12}F_{132})-\bar{g}v_1F_{133}]\\
&+q'_{02}[\bar{f}\sqrt{\chi_{12}^2+1}\,(\beta_{21}F_{231}+\beta_{22}F_{232})+(-)^g v_2F_{233}],\\
L_{4fg}=&q'_{01}[\sqrt{\chi_{11}^2+1}\,(\beta_{11}F_{141}+\beta_{12}F_{142})-\bar{g}v_2F_{143}]\\
&+q'_{02}[\bar{f}\sqrt{\chi_{12}^2+1}\,(\beta_{21}F_{241}+\beta_{22}F_{242})+(-)^g v_2F_{243}],
\end{aligned}\right\} \quad . \quad . \quad . \quad (17.10c)$$

and (see formula (17.5*d*))

$$\left.\begin{aligned}
H_1&=2(\kappa_{211}F_{113}+\kappa_{212}F_{213}),\\
H_2&=2(\kappa_{211}F_{123}+\kappa_{212}F_{223}),\\
H_3&=2(\kappa_{211}F_{133}+\kappa_{212}F_{233}),
\end{aligned}\right\} \quad . \quad . \quad (17.10d)$$

(compare formulæ (17.10*c*) and (17.10*d*) combined with (17.10*a*) and (17.9*b*)—taking into account (16.4) and (16.5)—with the formulæ (2.2 ap.) of the Appendix to Part I.).

Further, we shall denote the values of ${}^m\mathbf{X}_{fg}$ at different orders of magnitudes of $L_1^2+H_1^2$, $L_2^2+H_2^2$ and $L_3^2+H_3^2$ by ${}^m\mathbf{X}_{fg}$ with triple suffixes at the bottom, consisting of heavy dots (•) and zeros (0), in which a zero in the first, in the second, and in the third place will show that

$$\sqrt{L_{1fg}^2+H_1^2}>>1,\ \sqrt{L_{2fg}^2+H_2^2}>>1,\ \text{and}\ \sqrt{L_{3fg}^2+H_3^2}>>1$$

resp., while a thick point in the same places will show that the same quantities are small in comparison with unity. So that, for instance, ${}^m\mathbf{X}_{fg\bullet 0\bullet}$ will denote the value of ${}^m\mathbf{X}_{fg}$ when

$$\sqrt{L_{1fg}^2+H_1^2}<<1,\ \sqrt{L_{2fg}^2+H_2^2}>>1,\ \text{and}\ \sqrt{L_{3fg}^2+H_3^2}<<1.$$

Correspondingly, we shall denote by ${}^m u$ with similar triple suffixes at the bottom, in which zero on the first, second, and third place will show that X, Y, and Z resp. will be equal either to zero or—when this makes either ρ_1 or ρ_2 so small as to overlap the region near the axes of one of the Whirls, which is excluded from our integration—

to a small quantity, so as to put the corresponding point on the boundary of integration (see formulæ (17.5 *a*), (16.4), and (16.5), and an observation after formula (17.2 *a*.)

The same suffixes with the same meaning we shall use for $\mathbf{M}_{fg}$.

Then, using the method of integration described in the Appendix to Part I., Section 2 ap., we shall obtain

$$ {}^{m}\mathbf{X}_{fg000} = \frac{{}^{m}u_{000}\sin\Phi_{fg000}}{\sqrt{(L_{1fg}^2+\mathrm{H}_1^2)(L_{2fg}^2+\mathrm{H}_2^2)(L_{3fg}^2+\mathrm{H}_3^2)}} + o\{(L_1^2+\mathrm{H}_1^2)^{-1}(L_2^2+\mathrm{H}_2^2)^{-1}(L_3^2+\mathrm{H}_3^2)^{-1}\}, \quad (17.11) $$

$$ {}^{m}\mathbf{X}_{fg00\bullet} = \frac{\int_0 {}^{m}u_{00\bullet}\,\mathrm{d}Z.\sin\Phi_{fg00\bullet}}{\sqrt{(L_2^2+\mathrm{H}_2^2)(L_3^2+\mathrm{H}_3^2)}} + o\{(L_3^2+\mathrm{H}_3^2)^{\frac{1}{2}}(L_1^2+\mathrm{H}_1^2)^{-1}(L_2^2+\mathrm{H}_2^2)^{-1}\}, \quad (17.11\,a) $$

$$ {}^{m}\mathbf{X}_{fg\bullet0\bullet} = \frac{\int_0^\infty\int_0^\infty {}^{m}u_{\bullet0\bullet}\,dX\,dZ.\sin\Phi_{fg\bullet0\bullet}}{\sqrt{L_2^2+\mathrm{H}_2^2}} + o\{(L_1^2+\mathrm{H}_1^2)^{\frac{1}{2}}(L_3^2+\mathrm{H}_3^2)^{\frac{1}{2}}(L_2^2+\mathrm{H}_2^2)^{-1}\}, \quad (17.11\,b) $$

$$ {}^{m}\mathbf{X}_{fg\bullet\bullet\bullet} = \int_0^\infty\int_0^\infty\int_0^\infty {}^{m}u_{\bullet\bullet\bullet}\,dX\,dY\,dZ.\sin\Phi_{fg\bullet\bullet\bullet} + o\{(L_1^2+\mathrm{H}_1^2)^{\frac{1}{2}}(L_2^2+\mathrm{H}_2^2)^{\frac{1}{2}}(L_3^2+\mathrm{H}_3^2)^{\frac{1}{2}}\}, \quad (17.11\,c) $$

where

$$ \left.\begin{aligned} \Phi_{fg000} &= \mathrm{T}_g+\mathbf{M}_{fg000}+|L_{4fg}|\,\mathrm{D}-\tan^{-1}\frac{L_{1fg}}{\mathrm{H}_1} \\ &\qquad -\tan^{-1}\frac{L_{2fg}}{\mathrm{H}_2}-\tan^{-1}\frac{L_{3fg}}{\mathrm{H}_3}-f\frac{\pi}{2}, \\ \Phi_{fg00\bullet} &= \mathrm{T}_g+\mathbf{M}_{fg000}+|L_{4fg}|\,\mathrm{D}-\tan^{-1}\frac{L_{1fg}}{\mathrm{H}_1}-\tan^{-1}\frac{L_{2fg}}{\mathrm{H}_2}-f\frac{\pi}{2}, \\ \Phi_{fg\bullet0\bullet} &= \mathrm{T}_g+\mathbf{M}_{fg000}+|L_{4fg}|\,\mathrm{D}-\tan^{-1}\frac{L_{2fg}}{\mathrm{H}_2}-f\frac{\pi}{2}, \\ \Phi_{fg\bullet\bullet\bullet} &= \mathrm{T}_g+\mathbf{M}_{fg000}+|L_{4fg}|\,\mathrm{D}-f\frac{\pi}{2}. \end{aligned}\right\} \quad . \quad . \quad . \quad (17.11\,d) $$

By (17.9*c*), (16.4), (16.5), and (16.5*a*)

$$\mathbf{M}_{fg000}=gn_1\tan^{-1}\left(\frac{\beta_{12}}{\beta_{11}}\cot\boldsymbol{\varphi}_1\cos\boldsymbol{\theta}_1\right)$$
$$-(-)^g n_2\tan^{-1}\left(\frac{\beta_{22}}{\beta_{21}}\cot\boldsymbol{\varphi}_2\cos\boldsymbol{\theta}_2\right)$$
$$-\tan^{-1}\sqrt{\left(\frac{\beta_{11}}{\beta_{13}}\frac{\tan\boldsymbol{\varphi}_1}{\sin\boldsymbol{\theta}_1}\right)^2+\left(\frac{\beta_{12}}{\beta_{13}}\cot\boldsymbol{\theta}_1\right)^2}$$
$$-\bar{f}\tan^{-1}\sqrt{\left(\frac{\beta_{21}}{\beta_{23}}\frac{\tan\boldsymbol{\varphi}_1}{\sin\boldsymbol{\theta}_2}\right)^2+\left(\frac{\beta_{22}}{\beta_{23}}\cot\boldsymbol{\theta}_2\right)^2}. \quad . \ . \ . \quad (17.11\,e)$$

It will be borne in mind that the regions near to the axes of the Whirls should be in principle excluded from the integration in (17.11 *a*)–(17.11 *c*), but in practical calculations it may happen that there will be no need of such exclusion if these regions will not contribute materially to the result.

The expressions for ${}^m\mathbf{X}_{fg\bullet 0\bullet}$ and ${}^m\mathbf{X}_{fg\bullet 00}$, and for ${}^m\mathbf{X}_{fg 0\bullet\bullet}$ and ${}^m\mathbf{X}_{fg\bullet\bullet 0}$ can be easily obtained in the same way as the expressions (17.11 *a*) and (17.11 *b*) resp. and need not be written here.

We shall write now the expressions for L_{1fg}, L_{2fg}, L_{3fg}, and L_{4fg}, and H_1, H_2, and H_3 in terms of the parameters defining the position of the axes of Whirls, *i.e.*, in terms of $\boldsymbol{\theta}_1$, $\boldsymbol{\theta}_2$, $\boldsymbol{\varphi}_1$, $\boldsymbol{\varphi}_2$, and D.

By (17.10*c*) and (16.5*a*)

$$L_{1fg}=q'_{01}[\sqrt{\chi_{11}^2+1}\,(\beta_{11}\cos\boldsymbol{\varphi}_1-\beta_{12}\sin\boldsymbol{\varphi}_1\cos\boldsymbol{\theta}_1)$$
$$-\bar{g}v_1\sin\boldsymbol{\varphi}_1\sin\boldsymbol{\theta}_1]+q'_{02}[f\sqrt{\chi_{12}^2+1}\,(\beta_{21}\cos\boldsymbol{\varphi}_2$$
$$-\beta_{22}\sin\boldsymbol{\varphi}_2\cos\boldsymbol{\theta}_2)+(-)^g v_2\sin\boldsymbol{\varphi}_2\sin\boldsymbol{\theta}_2],$$

$$L_{2fg}=q'_{01}[\sqrt{\chi_{11}^2+1}\,(\beta_{11}\sin\boldsymbol{\varphi}_1+\beta_{12}\cos\boldsymbol{\varphi}_1\cos\boldsymbol{\theta}_1)$$
$$+gv_1\cos\boldsymbol{\varphi}_1\sin\boldsymbol{\theta}_1]+q'_{02}[f\sqrt{\chi_{12}^2+1}\,(\beta_{21}\sin\boldsymbol{\varphi}_2$$
$$+\beta_{22}\cos\boldsymbol{\varphi}_2\cos\boldsymbol{\theta}_2)-(-)^g v_2\cos\boldsymbol{\varphi}_2\sin\boldsymbol{\theta}_2],$$

$$L_{3fg}=q'_{01}(\sqrt{\chi_{11}^2+1}\,\beta_{12}\sin\boldsymbol{\theta}_1+\bar{g}v_1\cos\boldsymbol{\theta}_1)$$
$$+q'_{02}(f\sqrt{\chi_{12}^2+1}\,\beta_{22}\sin\boldsymbol{\theta}_2+(-)^g v_2\cos\boldsymbol{\theta}_2),$$

$$L_{4fg}=\frac{q'_{01}q'_{02}}{\beta_1 q'_1+\beta_2 q'_{02}}\{\beta_2[\sqrt{\chi_{11}^2+1}\,(\beta_{11}\sin\boldsymbol{\varphi}_1+\beta_{12}\cos\boldsymbol{\varphi}_1\cos\boldsymbol{\theta}_1)$$
$$+g\cos\boldsymbol{\varphi}_1\sin\boldsymbol{\theta}_1]-\beta_1[f\sqrt{\chi_{12}^2+1}\,(\beta_{21}\sin\boldsymbol{\varphi}_2$$
$$+\beta_{22}\cos\boldsymbol{\varphi}_2\cos\boldsymbol{\theta}_2)-(-)^g v_2\cos\boldsymbol{\varphi}_2\sin\boldsymbol{\theta}_2]\}. \quad . \ . \ . \quad (17.12)$$

By (17.10*d*) and (16.5*a*)

$$\left.\begin{aligned} H_1&=2\kappa_{211}\sin\varphi_1\sin\theta_1+2\kappa_{212}\sin\varphi_2\sin\theta_2,\\ H_2&=2\kappa_{211}\cos\varphi_1\sin\theta_1-2\kappa_{212}\cos\varphi_2\sin\theta_2,\\ H_3&=2\kappa_{211}\cos\varphi_1+2\kappa_{212}\cos\theta_2. \end{aligned}\right\} \quad (17.12a)$$

When $\kappa_{211}<<1$ and $\kappa_{212}<<1$ we can take

$$H_3\cong H_2=H_1\cong 0 \quad . \quad . \quad . \quad . \quad (17.12b)$$

and

$$L^2_{1fg}+H_1^2\cong L^2_{1fg} \quad L_{2fg}+H_2^2\cong L^2_{2fg} \quad L^2_{3fg}+H_3^2\cong L^2_{3fg}, \quad (17.12c)$$

and by (17.11*d*)

$$\Phi_{fg}=T_{fg}+M_{fg\,000}+|L_{4fg}D|-(f+a)\frac{\pi}{2}, \quad . \quad (17.12d)$$

where a is the number of zeros in the triple suffix at Φ_{fg}, here omitted.

By means of formulæ (17.10)–(17.12*d*) it is possible to determine the mutual energy W of a system of two Whirls at different positions of their axes, and from this the average value of the mutual energy, $\overline{W}$. We shall see that $\overline{W}$ plays the part of the *potential energy* in relation to steady forces, which in practice are the only observable forces.

We shall call, therefore, the average mutual energy $\overline{W}$, "the potential energy."

18. *The Precessional Motion of the Axes and the Average Mutual Energy (the Potential Energy) in a System of Two Whirls.*

A Whirl, as has been already mentioned (see the end of section 11), is, in a mechanical sense, a gyroscope with an angular momentum $\hbar_1$. A characteristic form of movement of a gyroscope is rotation of its axis round a centre. In the absence of any support this centre of rotation will be the centre of gravity of the gyroscope, which, in our case, will be the centre of the Whirl. This motion of the axis is usually called the "precessional rotation of a gyroscope."

As is well known, there is a simple relationship between the angular velocity of this precessional rotation and the moment of forces (torque) about the axis perpendicular to the plane containing the axis of the gyroscope and the axis of its precessional rotation. Namely this torque is

equal to the product of the angular momentum of the gyroscope and the angular velocity of precessional rotation. The general statement of this law for Whirls was given at the end of section 11 (formula (11.9)). The torque about an axis is equal in magnitude and opposite in sign to the rate of change of the mutual energy per unit of virtual angular displacement about this axis.

Hence

$$\left.\begin{aligned} -\frac{\partial W}{\partial \theta_1} &= 2n_1\hbar_{11}\dot{\varphi}_1, \quad -\frac{\partial W}{\partial \theta_2} = 2n_2\hbar_{12}\dot{\varphi}_2, \\ -\frac{\partial W}{\partial \varphi_1} &= 2n_1\hbar_{11}\dot{\theta}_1, \quad -\frac{\partial W}{\partial \varphi_2} = 2n_2\hbar_{12}\dot{\theta}_2. \end{aligned}\right\} \quad (18.1)$$

We shall call these conditions the "minimum conditions" of the orientation of the axes.

We shall limit ourselves to a case where

$$L_{1fg} \gtrless 1, \quad L_{2fg} \gtrless 1, \quad L_{3fg} \gtrless 1, \quad L_{4fg} \gtrless 1, \quad (18.1a)$$

so that it should be possible to apply the results of integration obtained in (17.11)–(17.11*c*). The conditions (18.1*a*) will be satisfied if $q'_{01} >> 1$ and $q'_{02} >> 1$ (by (17.12)).

Further, we shall only discuss here the case where

$$\left.\begin{aligned} &\hbar_{11}=\hbar_{12}=\hbar_1, && n_1=n_2=1, \\ &\kappa_{211} << 1, && \kappa_{212} << 1, \\ &q_{01} >> 1, && q_{02} >> 1, \end{aligned}\right\} \quad . \quad . \quad (18.1b)$$

whence by (4.12)

$$\chi_{11} << 1, \qquad \chi_{12} << 1, \quad . \quad . \quad . \quad (18.1c)$$

and we shall also assume

$$\beta_1 \cong 1, \qquad \beta_2 \cong 1. \quad . \quad . \quad . \quad . \quad (18.1d)$$

By (18.1*d*) we shall neglect the *squares* of the ratios between the linear velocities of the centres of the Whirls and the speed of light (see formulæ (16.3*a*) and (16.7)). We shall, however, not neglect in general the first powers of these ratios, and, therefore, we shall *not* take generally $v_1=0$ and $v_2=0$ (see 16.6*b*).

We shall assume that the axis of precessional rotation of, at least, one of the Whirls (say, Whirl 1) is perpendicular to the line $0_1 0_2$ passing through the centres of

the Whirls *). Then, denoting by $\bar{\theta}$ the average value of θ, we shall have

$$\bar{\theta}_1 = \text{const.} \quad . \quad . \quad . \quad . \quad . \quad . \quad . \quad (18.2)$$

We shall distinguish two kinds of variations of θ : rapid fluctuations of θ about an average value, $\bar{\theta}$, and comparatively slow changes of $\bar{\theta}$. We shall deal in most cases with average states during time intervals which are, on the one hand, too long to take into account the rapid fluctuations, and, on the other hand, not long enough to take into account the slow variations of $\bar{\theta}$.

In future we shall use generally bars on top of the letters for denoting the average values which do not follow the rapid fluctuations ("ripples") in the configuration of the system. To reduce the printing work we shall make a convention that a derivative with respect to the average value of any quantity should always mean the average value of this derivative—say $\frac{\bar{\partial}}{\partial \bar{\theta}} = \left(\frac{\partial}{\partial \bar{\theta}}\right)^{-}$.

The ripples in the system of Whirls will also include the rapid oscillations of frequencies of the order Ω_{01} and Ω_{02}, as well as the precessional rotation of the axes of the Whirls (*e. g.*, variation of φ_1), and the fluctuations of the initial phases ψ_1 and ψ_2, and of the distance D between the centres of the Whirls.

The angular velocities of the precessional rotation will be of a considerably smaller order than Ω_{01} and Ω_{02}. We shall assume, however, that they are not small enough to be followed by the average values. Therefore, in the expressions of the average values, we can omit all the terms containing as factors sin or cos of φ_1. We cannot always say the same about sin or cos of $q_0 D$ or ψ_1, and ψ_2, or φ_2, for these variables may remain constant or oscillate within an interval smaller than one cycle.

We shall call the whole complex of these rapid fluctuations "the *vibrational state*" of the system.

Although the average values do not follow, by definition, the rapid changes of configuration of the system, implied in the vibrational state, they are, nevertheless, influenced by the general character (general parameters) of the latter.

* In a general case we could resolve the distance $0_1 0_2$ between the centres of the Whirls into two components, the one parallel to Y and the other parallel to Z. This, however, would considerably complicate the mathematical part without yielding any new results essential for this paper.

A system of Whirls, as any dynamic system, will tend to one of the states of minima of its mutual energy. Therefore, we can reasonably assume that $\frac{\partial W}{\partial \bar{\theta}}$ will be most probably near to zero, although not quite equal to zero (for a state of complete equilibrium is in our case most improbable). So we can put

$$\frac{\partial W}{\partial \bar{\theta}_1} = 0. \quad . \quad . \quad . \quad . \quad . \quad . \quad . \quad (18.2\,a)$$

This is confirmed by the well-known experimental fact, that the precessional speeds of gyroscopes are comparatively small.

We shall now try to find the conditions under which the relationship (18.2 *a*) will be approximately satisfied on the average.

By (17.10)

$$\frac{\partial W}{\partial \bar{\theta}_1} = \sqrt{} q'_{01} q'_{02} \kappa_1 \mathbf{K}_2 \sum_{m=0}^{8} \sum_{f=1}^{4} \sum_{g=1}^{4} {}^m H_{fg} \frac{\partial {}^m \mathbf{X}_{fg}}{\partial \bar{\theta}_1} + {}^m \mathbf{X}_{fg} \frac{\partial {}^m H_{fg}}{\partial \bar{\theta}_1}.$$

$$. \quad . \quad . \quad . \quad (18{\cdot}3)$$

We shall first consider the first term under the triple sum.

We can see by (17.5 *a*), (17.5 *b*), and (16.5) that the first factors, in the numerators of (17.11)–(17.11 *c*) depend on θ_1 only through F_{141}, or F_{142}, or F_{143} *.

The latter depend on θ_1 only through $\begin{matrix}\sin \\ \cos\end{matrix} \varphi_1 \quad \begin{matrix}\sin \\ \cos\end{matrix} \theta_1$ (by (16.5 *a*)), and hence $\frac{\partial}{\partial \bar{\theta}_1}$ of the first factors in the numerators of (17.11)–(17.11 *c*) are zero.

The second factors in the numerators of (17.11)–(17.11 *c*) depend on θ_1 through $\mathbf{M}_{fg000}$ and L_4 D (by (17.11 *d*)).

It can be seen from the fourth formula (17.12) that $\frac{\partial L_4}{\partial \bar{\theta}_1} = 0$. Hence, on differentiating (17.11 *a*), taking into account (17.11 *e*), we find that $\frac{\partial \sin \Phi_{fg}}{\partial \bar{\theta}_1} = 0$, if either $\sin \bar{\theta}_1$ or $\cos \bar{\theta}_1$ equals zero.

* For the integrals disappear at the upper limit owing to the presence of the exponential factor Λ in the subintegral expression, and at the lower limit the terms containing X, Y, and Z, of course, equal zero.

Consequently, by (17.11)–(17.11 c), if $\begin{matrix}\sin\\ \cos\end{matrix}\bar{\theta}_1 \cong 0$,

$$\frac{\partial\, {}^m\mathbf{X}_{fg}}{\partial\bar{\theta}_1} \cong 0, \text{ and hence}$$

$$\sum_{m=0}^{8}\sum_{f=1}^{4}\sum_{g=1}^{4} {}^m H_{fg}\frac{\partial\, {}^m\mathbf{X}_{fg}}{\partial\bar{\theta}_1} \cong 0, \quad . \quad . \quad (18.3a)$$

whence by (18.3) and (18.2 a)

$$\sum_{m=0}^{8}\sum_{f=1}^{4}\sum_{g=1}^{4} {}^m\mathbf{X}_{fg}\frac{\partial\, {}^m H_{fg}}{\partial\bar{\theta}_1} \cong 0, \quad . \quad . \quad . \quad (18.4)$$

if $\bar{\theta}_1$ is approximately equal either to zero or to $\pi/2$.

By the same method of reasoning we shall find

$$\sum_{m=0}^{8}\sum_{f=1}^{4}\sum_{g=1}^{4} {}^m H_{fg}\frac{\partial^2\, {}^m\mathbf{X}_{fg}}{\partial\bar{\theta}_1{}^2} \cong 0. \quad . \quad . \quad . \quad (18.4a)$$

From (18.3), (18.3a), and (18.4a)

$$\frac{\partial^2 \mathrm{W}}{\partial\bar{\theta}_1{}^2} \cong \sum_{f=0}^{8}\sum_{f=1}^{4}\sum_{g=1}^{4} {}^m\mathbf{X}_{fg}\frac{\partial^2\, {}^m H_{fg}}{\partial\bar{\theta}_1{}^2}. \quad . \quad . \quad (18.4b)$$

In order that $\bar{\mathrm{W}}$ be a minimum with respect to $\bar{\theta}_1$, we must have

$$\frac{\partial^2 \mathrm{W}}{\partial\bar{\theta}_1{}^2} > 0. \quad . \quad . \quad . \quad . \quad . \quad (18.4c)$$

We can see from (17.8c) that ${}^m H_{fg}$ are sin or cos functions of $\bar{\theta}_1$ and, therefore, $\dfrac{\partial^2\, {}^m H_{fg}}{\partial\bar{\theta}_1{}^2}$ will have an opposite sign to that of ${}^m H_{fg}$. Hence we find from (17.10), (18.4b), and (18.4c) that for any minimum state with respect to $\bar{\theta}_1$

$$\bar{\mathrm{W}} < 0. \quad . \quad . \quad . \quad . \quad . \quad . \quad (18.4d)$$

The negative sign of the $\bar{\mathrm{W}}$ shows that the source of the potential energy is the internal energy of the Whirls (see formulæ (15.2) and (18.7)).

By a glance at (17.8c) we can see that

$$\frac{\partial\, {}^m H_{fg+}}{\partial\bar{\theta}_1} \cong 0,$$

if $$\frac{\partial}{\partial\bar{\theta}_1}(\cos\bar{\theta}_1\cos\bar{\theta}_2) = \frac{\partial}{\partial\bar{\theta}_1}(\sin\bar{\theta}_1\sin\bar{\theta}_2) \cong 0, \quad (18.4e)$$

that is, $$\sin\theta_1\cos\bar{\theta}_2 \cong \cos\theta_1\sin\theta_2 \cong 0,$$

and in the same way

$$\frac{\partial\, {}^{m}H_{fg}}{\partial \bar{\theta}_1} \cong 0, \quad . \quad . \quad . \quad . \quad . \quad (18.4f)$$

if $$\cos\bar{\theta}_1 \cos\bar{\theta}_2 \cong \sin\bar{\theta}_1 \sin\theta_2 \cong 0.$$

Consequently, by (18.3)–(18.4), to satisfy the relationship (18.2*a*) it is necessary and sufficient that either

$$\left.\begin{aligned} &\sin\bar{\theta}_1 \cong \sin\bar{\theta}_2 \cong 0 \\ \text{or} \quad &\cos\theta_1 \cong \cos\bar{\theta}_2 \cong 0, \end{aligned}\right\} \quad . \quad . \quad . \quad . \quad (18.5)$$

in the case of copolarized Whirls, and either

$$\left.\begin{aligned} &\sin\bar{\theta}_1 \cong 0, \quad \sin\bar{\theta}_2 \cong 1, \\ \text{or} \quad &\sin\bar{\theta}_1 \cong 1, \quad \sin\theta_2 \cong 0, \end{aligned}\right\} \quad . \quad . \quad . \quad (18.5a)$$

in the case of contrapolarized Whirls.

When θ_1 is very small, the precessional rotation of a Whirl does not introduce very great disturbances in the structure of its e.m. field. It is nearly equivalent to a change of its frequency Ω (see formula (16.6*d*)),

When, however, $\theta_1 \cong \frac{\pi}{2}$, the precessional rotation would mean a continuous change of the direction of the axis of the Whirl which, of course, would mean a violent disturbance of the e.m. field. Therefore this would be less probable for a stable vibrational state than a small angle θ_1*.

Therefore we shall assume the vibrational state characterized by the *first* equations (18.5) and (18.5*a*), *i. e.*,

$$\sin\theta_1 \cong \sin\theta_2 \cong 0 \quad . \quad . \quad . \quad . \quad . \quad (18.6)$$

in the case of copolarized Whirls, and

$$\sin\theta_1 \cong 0, \quad \sin\theta_2 \cong 1 \quad . \quad . \quad . \quad (18.6a)$$

in the case of contrapolarized Whirls.

It is preferable to omit at this stage the bars on the top of θ_1 and θ_2 (indicating the average values), because in the application of these formulæ to the calculation of W we shall have to substitute the average values for the momentary ones in the corresponding expressions for W.

* This criterion for the relative probabilities of vibrational states is a particular example of the "Minimum Disturbance" principle, which is formulated below (see the text between formulæ (18.7*b*) and (18.8)).

By (17.10) and (17.8*c*), omitting in the latter formulæ all the terms containing $\frac{\sin}{\cos}\,\varphi_1$ and taking into account (18.6), we obtain for the copolarized Whirls

$$\overline{W}_+ = -\sqrt{q'_{01}q'_{02}}K_1K_2\left|-\sum_{g=1}^{4}{}^0X_{3g}-{}^0X_{4g}\right|$$

$$= -\sqrt{q'_{01}q'_{02}}K_1K_2\left|\sum_{f=3}^{4}\sum_{g=1}^{4}f\,{}^0X_{fg}\right| \quad . \quad . \quad . \quad . \quad . \quad (18.7)$$

We have enclosed the last factor in *thick* straight brackets in order to show that the expression therein must be always positive (in contradistinction of ordinary | | showing that the modulus of the expression is taken).

Similarly, taking into account (18.6*a*), instead of (18.6), we obtain for the contrapolarized Whirls

$$\overline{W}_- = -\sqrt{q'_{01}q'_{02}}K_1K_2\left|-\sum_{g=1}^{4}{}^0X_{3g}+{}^0X_{4g}\right| . \quad . \quad (18.7a)$$

As was mentioned above (see the text following formula (18.2)), the average values—and among them the $\overline{W}$'s—are influenced by the parameters of the vibrational state.

To be at all possible, the vibrational state must satisfy the energy equation (15.2), which in the application to the system of two Whirls can be written in the form

$$W+\beta_1\hbar_1\Omega'_{01}+\beta_2\hbar_2\Omega'_{02}=\text{const.} \quad . \quad . \quad (18.7b)$$

and the condition of stability (18.4*d*), and the "minimum" conditions (18.1).

There will be, generally speaking, more than one vibrational state consistent with these conditions. Even the same value of W may correspond to more than one vibrational state.

By (17.11)–(17.11*c*) a necessary condition for $\overline{X}_{fg}\neq 0$ is that $\overline{\sin\Phi_{fg}}\neq 0$, or, in other words, that Φ_{fg} should fluctuate within a small interval about an average value $\bar{\Phi}_{fg}$. It is not difficult to see from (17.11*d*), (17.11*e*), and (17.9*a*), that for any given vibrational state, *i. e.*, for any set of functions $\varphi_1(t)$, $\varphi_2(t)$, $\psi_1(t)$, $\psi_2(t)$, $\theta_1(t)$, $\theta_2(t)$, and $D(t)$, this can happen only at a definite value of g (1, 2, 3, or 4) *if at all.*

From this we can see that only certain vibrational states

out of those which satisfy the conditions (18.1) and (18.7*b*) can be stable, for if $\bar{\mathbf{X}}_{fg}=0$ for every f and g, then $\bar{W}=0$, and the condition (18.4*d*) will not be satisfied, and that for each of these states only one of the four terms of the Σ will be valid.

g

We shall not attempt here to calculate the relative probability of different vibrational states, but it will not be difficult to see that some of them are definitely more probable than others.

For example, we can see from (17.11*d*) that a vibrational state for which the relationship $L_{4fg}=0$ can be maintained, even for one of the f's, is more probable than a vibrational state for which $L_{4fg}\neq 0$ for any f, for in the former case Φ_{fg} will be independent of D, so that any variation of D will not be likely to upset the stability.

Moreover, we can see from (17.11*d*) that, unless D=const. (which is very unlikely), the term for which $L_{4fg}=0$ can be contributory to $\bar{W}$ *only to the exclusion* of those terms for which the condition $L_{4fg}=0$ is not fulfilled, for unless D=const. we cannot have $\sin\Phi_{fg}\neq 0$ for both types of the terms. Therefore if $L_{4fg}=0$ is at all possible, we must take a corresponding vibrational state, and exclude from the expression for $\bar{W}$ all the terms for which this condition is not fulfilled.

In the case where $q'_{01}>>1$ and $q'_{02}>>1$ those terms of the expressions for $\bar{W}$ in which ${}^{m}\mathbf{X}_{fg}$ have a greater number of dots in the triple suffixes will be of much greater order of magnitude than those which have a smaller number (see (17.11)–(17.11*c*) and the text following (18.1*a*)). Therefore in the expressions for $\bar{W}$ we can take only the terms with the ${}^{m}\mathbf{X}_{fg}$'s having a maximum number of dots in the triple suffixes, and neglect the other terms.

Generally speaking, out of the vibrational states satisfying a certain given set of conditions, those will be more stable, and, therefore, more probable, which are associated with a minimum periodic disturbance of the e.m. field of the system. We can call this criterion of relative probabilty the "Minimum Disturbance Principle."

After these observations we shall try to work out the expressions for $\bar{W}$ in a more detailed manner.

First we shall consider $\bar{W}_{+}$, starting from the case where $q_{01}=q_{02}>>1$.

By (18.6) and the third formula (16.3*a*) $v_{z_{01}}=v_{z_{02}}=0$. Hence by (16.6*b*) and (16.6*d*), recalling that $\beta\cong 1$, we can see that

$$q'_{01}=\left|q_{01}+\frac{n\dot{\varphi}_1}{c}\right| \quad \text{and} \quad q'_{02}=\left|q_{02}+\frac{n}{c}\dot{\varphi}_2\right|=\left|q_{01}+\frac{n}{c}\dot{\varphi}_1\right|.$$

Since the Whirls are identical and are symmetrically situated we can deduce from this that $q'_{01}=q'_{02}$.

Hence from (17.12), taking into account (16.3*a*) and (16.6*b*), and (18.1*c*) and (18.1*d*),

$$\begin{aligned}
&L_{1fg}=q'_{01}[(\cos\varphi_1-\cos\theta_1\sin\varphi_1)+\bar{f}(\cos\varphi_2-\cos\theta_2\sin\varphi_2)],\\
&L_{2fg}=q'_{01}[(\sin\varphi_1+\cos\theta_1\cos\varphi_1)+\bar{f}(\sin\varphi_2+\cos\theta_2\cos\varphi_2)],\\
&L_{3fg}=0,\\
&L_{4fg}=\frac{q'_{01}}{2}[(\sin\varphi_1+\cos\theta_1\cos\varphi_1)-\bar{f}(\sin\varphi_2+\cos\theta_2\cos\varphi_2)],
\end{aligned} \quad . \quad . \quad . \quad (18.8)$$

where $\cos\theta_1=\pm 1 \qquad \cos\theta_2=\pm 1.$

We can see from these formulæ that the condition $L_{4fg}=0$ *is* possible : it will be fulfilled if

$$\left.\begin{aligned}
&\sin\varphi_1=\bar{f}\cos\theta_2\cos\varphi_2,\\
&\cos\varphi_1=\bar{f}\cos\theta_1\sin\varphi_2,\\
&\cos\theta_1=\cos\theta_2,
\end{aligned}\right\} \quad . \quad . \quad . \quad (18.8a)$$

or $$\varphi_2=\frac{\pi}{2}-\varphi_1.$$

Since both Whirls are identical in structure, and are, on the average, symmetrically situated, we must expect that the absolute values of the angular velocities of their precessional rotation will be equal ($|\dot{\varphi}_1|=|\dot{\varphi}_2|$). Therefore the conditions (18.8*a*) can be maintained.

Then by (18.8) and (18.8*a*)

$$\left.\begin{aligned}
&L_{1fg}=L_{3fg}=L_{4fg}=0,\\
&L_{2fg}=2q'_{01}(\sin\varphi_1\pm\cos\varphi_1)=2\sqrt{2}\sin\left(\varphi_1\pm\frac{\pi}{4}\right).
\end{aligned}\right\} \quad (18.8b)$$

As was shown above, we must in the present case take, in the expressions for $\overline{W}$, only those terms for which $L_{4fg}=0$, and exclude all the other terms, *i.e.*, we must take either a term with $f=3$ (*i.e.*, $\bar{f}=-1$, by (17.7*c*)) or $f=4$ (*i.e.*, $\bar{f}=1$), depending on the vibrational state.

It will be seen from (17.11 *d*) and (17.11 *e*) that since $L_{4fg}=0$, $\sin \Phi_{fg\bullet 0\bullet}$ at $q_{01}=q_{02}$ (*i. e.*, $\Omega_{01}=\Omega_{02}$) can maintain a constancy of sign only if $\bar{g}=(-)^g$, *i. e.*, if $g=3$ or 4 (by (17·7 *c*)).

Consequently, by (18.7), (18.8 *b*), and (17.11 *b*), taking into account (18.1 *b*), and (17.12 *c*),

$$\left.\begin{aligned}\underset{q_{01}=q_{02}>>1}{\overline{\mathrm{W}}_{+}} &= -q'_{01}\,\mathsf{K}_1\mathsf{K}_2\left|\bar{f}\,{}^{0}\overline{\mathbf{X}}_{fg\bullet 0\bullet}\right| \\ &= -\mathsf{K}_1\mathsf{K}_2\left|\frac{\sin f\Phi_{fg\bullet 0\bullet}}{2\sqrt{2}\left|\sin\left(\varphi_1\pm\frac{\pi}{4}\right)\right|}\int_0^\infty\int_0^\infty {}^{0}u_{\bullet 0\bullet}\,dX\,dZ\right|.\end{aligned}\right\}\quad \begin{matrix} f=3,\ 4 \\ g=3,\ 4 \end{matrix}$$

. . . (18.8 *c*)

When $q_{01}\lessgtr q_{02}$, the precessional speeds $|\dot{\varphi}_1|$ and $|\dot{\varphi}_2|$ cannot be equal, since both Whirls greatly differ in size, and, therefore, no definite ratio between $\frac{\sin}{\cos}\varphi_1$ and $\frac{\sin}{\cos}\varphi_2$ can be maintained, and hence the condition $L_{4fg}=0$ cannot be fulfilled whatever be f or g.

Using in other respects the same method of reasoning we used for $q_{01}=q_{02}$, we shall, then, obtain

$$\left.\begin{aligned}
L_{1fg}&=\sqrt{2}\left[q'_{01}\cos\left(\varphi_1\pm\frac{\pi}{4}\right)+\bar{f}q'_{02}\cos\left(\varphi_2\pm\frac{\pi}{4}\right)\right],\\
L_{2fg}&=\sqrt{2}\left[q'_{01}\sin\left(\varphi_1\pm\frac{\pi}{4}\right)+\bar{f}q'_{02}\sin\left(\varphi_2\pm\frac{\pi}{4}\right)\right],\\
L_{3fg}&=0,\\
L_{4fg}&=\sqrt{2}\,\frac{q'_{01}\,q'_{02}}{q'_{01}+q'_{02}}\left[\sin\left(\varphi_1\pm\frac{\pi}{4}\right)-\bar{f}\sin\left(\varphi_2\pm\frac{\pi}{4}\right)\right].
\end{aligned}\right\}\quad (18.9)$$

It will be recalled that from the very beginning of our discussion we assumed that the axis of Whirl 1 is in a continuous precessional rotation (see the paragraphs preceding formula (18.2)), but we have not bound ourselves in the same way with regard to Whirl 2. When both Whirls are identical ($q_{01}=q_{02}$) we must expect $|\dot{\varphi}_1|=|\dot{\varphi}_2|$, but when $q_{01}\lessgtr q_{02}$ there is no cause for such expectation. Moreover, in the latter case we cannot say in advance whether the axis of Whirl 2 is also likely to

be in a continuous precessional rotation like the axis of Whirl 1, *i. e.*, whether φ_2 will vary unidirectionally, or, on the contrary, φ_2 will oscillate about a certain average value. We shall try to find this out.

Since $L_{1fg} \neq 0$, $L_{2fg} \neq 0$, and $L_{3fg} = 0$ (by (18.9)), we must use formula (17.11 *a*) to find ${}^0\mathbf{X}_{fg}$. Any fluctuations of the denominator in the latter expression, *i. e.*, the fluctuation of $L_1 L_2$ must be associated with violent disturbances of the e.m. field of the system. Hence, in accordance with the Minimum Disturbance Principle—see the text between formulæ (18.7 *b*) and (18.8)—the most probable form of variation of φ_2 will be such at which $L_1 L_2$ will suffer minimum fluctuations.

By (18.9) we find, after simple transformations,

$$L_{1fg}\, L_{2fg} = \pm q_{01}'^2 \cos 2\varphi_1 \pm q_{02}'^2 \cos 2\varphi_2 \pm 2f q_{01}' q_{02}' \cos(\varphi_1 + \varphi_2). \quad . \quad . \quad . \quad (18.9\,a)$$

When $q_{01} \gtrless q_{02}$ this will suffer minimum fluctuations if $q_{02} >> q_{01}$, and

$$\frac{\cos 2\varphi_2}{\cos 2\varphi_1} = \mp \frac{q_{01}'^2}{q_{02}'^2} << 1, \quad . \quad . \quad . \quad (18.9\,b)$$

whence

$$\varphi_2 = \pm \frac{\pi}{4} \pm o\left\{\frac{q_{01}^2}{q_{02}^2}\right\} \cong \pm \frac{\pi}{4}. \quad . \quad . \quad (18.9\,c)$$

It can be seen that the present analysis does not determine any relationship between the sign which must be chosen in the $\pm$ in (18.9 *c*) and the signs taken in the $\pm$'s in (18.9) *.

By (18.9 *a*)–(18.9 *c*) we can write

$$|L_1 L_2| = 2 q_{01}' q_{02}' \left| \sin\left(\varphi_1 \pm \frac{\pi}{4}\right) \right|. \quad . \quad (18.9\,d)$$

We shall see later that only one of the terms of the $\sum_f$ in (18.7) can be contributory to $\overline{\mathrm{W}}_{+\,q_{02} >> q_{01}}$ (as in the case of $\overline{\mathrm{W}}_{+\,q_{01} >> q_{02}}$, although for different reasons).

* It will be recalled that the latter signs depend on the sign in $\cos\theta_1 = \pm 1$ and $\cos\theta_2 = \pm 1$.

Hence by (18.7), (17.11 *a*), (18.9 *a*), and (18.9 *b*) we have

$$\left.\begin{aligned}\overline{\mathrm{W}}_{+\,q_{02}>>q_{01}>>1} &= -\sqrt{q'_{01}\,q'_{02}}\;\mathsf{K}_1\mathsf{K}_2\,|\bar{f}\,{}^0\overline{\mathrm{X}}_{fg00\bullet}| \\ &= -\frac{1}{\sqrt{q'_{01}\,q'_{02}}}\,\mathsf{K}_1\mathsf{K}_2\left|\frac{\sin f\Phi_{fg00\bullet}}{2\left|\sin\left(\varphi_1\pm\frac{\pi}{4}\right)\right|}\int_0^\infty {}^0u_{00\bullet}\,dZ\right|.\end{aligned}\right\}\quad f=3,\,4;\quad g=1,\,2,\,3,\,4$$

. . . (18.10)

Consider now the case of contrapolarized Whirls.

We shall start from $q_{01}=q_{02}$.

Then by (17.12) and (18.6 *a*) taking into account (18.1 *c*) and (18.1 *d*), and (16.3 *a*) and (16.6 *b*) we shall have

$$\left.\begin{aligned}L_{1fg}&=q'_{01}\left[\sqrt{2}\cos\left(\varphi_1\pm\frac{\pi}{4}\right)+\bar{f}\cos\varphi_2+(-)^g v_2\sin\varphi_2\right],\\ L_{2fg}&=q'_{01}\left[\sqrt{2}\sin\left(\varphi_1\pm\frac{\pi}{4}\right)+\bar{f}\sin\varphi_2-(-)^g v_2\cos\varphi_2\right],\\ L_{3fg}&=\bar{f}\,q'_{01},\\ L_{4fg}&=\frac{q'_{01}}{2}\left[\sqrt{2}\sin\left(\varphi_1\pm\frac{\pi}{4}\right)-\bar{f}\sin\varphi_2+(-)^g v_2\cos\varphi_2\right].\end{aligned}\right\}$$

. . . (18.11)

We can easily see that in this case neither of the L's in (18.10) can be very small.

Thus in the case of contrapolarized Whirls with $q_{01}=q_{02}>>1$

$$L_{1fg}>>1,\quad L_{2fg}>>1,\quad L_{3fg}>>1,\quad L_{4fg}>>1. \quad (18.11\,a)$$

Hence, following the previous method, we shall find, by (17.11) and (18.7 *a*),

$$\left.\begin{aligned}\mathrm{W}_{-\,q_{01}=q_{02}>>1} &= -q'_{01}\,\mathsf{K}_1\mathsf{K}_2\left|\frac{-\sin\Phi_{fg00\bullet}}{L_{1fg}\,L_{2fg}\,L_{3fg}}\,{}^4u_{000}\right|.\end{aligned}\right\}\quad f=3,\,4;\quad g=3,\,4 \quad (18.11\,b)$$

In the case of contrapolarized Whirls with $q_{01}\gtrless q_{02}$ the equation (17.12) can be written in the following form

(taking into account (18.1 *c*), (18.1 *d*), (18.6 *a*), (16.3 *a*), and (16.6 *b*)) :

$$\left.\begin{aligned} L_{1fg} &= \sqrt{2}\,q'_{01}\cos\left(\varphi_1 \pm \frac{\pi}{4}\right) + q'_{02}(\bar{f}\cos\varphi_2 + (-)^g v_2 \sin\varphi_2), \\ L_{2fg} &= \sqrt{2}\,q'_{01}\sin\left(\varphi_1 \pm \frac{\pi}{4}\right) + q'_{02}(\bar{f}\sin\varphi_2 - (-)^g v_2 \cos\varphi_2), \\ L_{3fg} &= \bar{f}\,q'_{02}, \\ L_{4fg} &= \frac{q'_{01}\,q'_{02}}{q'_{01}+q'_{02}}\left(\sqrt{2}\sin\left(\varphi_1 \pm \frac{\pi}{4}\right) - \bar{f}\sin\varphi_2 + (-)^g v_2\cos\varphi_2\right). \end{aligned}\right\} \quad . \; . \; . \quad (18.12)$$

We can see that $L_{3fg} \neq 0$ in any case, but L_{1fg} or L_{2fg} can equal zero if $q'_{02} >> q'_{01}$.

Then we can take $v_2 = 0$, for the heavy Whirl will be very near to the centre of gravity of the system (see (16.2), (16.3 *a*), and (16.6 *b*)).

If $L_1 = 0$, $\cos\varphi_2 = o\left\{\frac{q_{01}}{q_{02}}\right\} << 1$, while if $L_2 = 0$, $\sin\varphi_2 = o\left\{\frac{q_{01}}{q_{02}}\right\} >> 1$.

When $L_2 = 0$, and hence $\sin\varphi_2 \sim 0$, the axis of Whirl 2 coincides with the axis Y $\left(\text{since } \theta_2 = \frac{\pi}{2}\right)$, and therefore, in the ${}^4\mathbf{X}_{0\bullet 0}$ corresponding to this case (compare (17.11 *a*)), we shall have $\rho = 0$, and, consequently, by (17.5 *a*), $u_{0\bullet 0}$ in the subintegral expression will become infinity. This will be so because the space near the axis, to which our expressions for the e.m. field and the e.m. energy do not extend, will not only be included, but will completely distort the expression of the total e.m. energy, owing to the position of the axis of one of the Whirls in the centre of the twofold integration with respect to X and Z (see the observation following formula (17.11 *e*)).

For this reason we shall abandon the case $L_2 = 0$ and take $L_1 = 0$. Then $\cos\varphi_2$ will oscillate with the amplitude of $o\left\{\frac{q_{01}}{q_{02}}\right\}$ about the position $\cos\varphi_2 = 0$, and so we shall have from (18.12)

$$\cos\varphi_2 = o\left\{\frac{q_{01}}{q_{02}}\right\},$$

$$\left.\begin{aligned} &L_{1fg}=0,\\ &L_{2fg}=\sqrt{2}\,q'_{01}\sin\left(\varphi_1\pm\frac{\pi}{2}\right)+\bar{f}\,q'_{02}\sin\varphi_2\cong\bar{f}\,q'_{02},\\ &L_3=f\bar{q}'\ ,\\ &L_{01}=\frac{q'_{01}\,q'_{02}}{q'_{01}+q'_{02}}\left(\sqrt{2}\sin\left(\varphi_1\pm\frac{\pi}{4}\right)-\bar{f}\right). \end{aligned}\right\} \quad (18.12\,a)$$

Hence, using exactly the same reasoning as before, we shall find from (18.7 *a*) and (17.11 *a*)

$$\left.\begin{aligned} \overline{W}_{-}{}_{q_{02}>>q_{01}>>1} &= -\sqrt{q'_{01}\,q'_{02}}\,\mathsf{K}_1\mathsf{K}_2\,|-\overline{{}^4\mathbf{X}_{fg\bullet 00}}|\\ &\cong -\mathsf{K}_1\mathsf{K}_2\frac{q'^{\,1/2}_{01}}{q'^{\,3/2}_{02}}\Big|-\sin\Phi_{fg\bullet 00}\overline{\int_0^\infty {}^4u_{\bullet 00}\,d\mathrm{X}}\Big|. \end{aligned}\right\} \quad (18.12\,b)$$

$f=3,\ 4$
$g=1,\ 2,\ \bar{3},\ 4$

19. *Distance Forces in a System of Two Whirls. Planetary Motion and Energy Levels. Gravitation.*

The average distance force $\mathbf{F}_D$*, *i. e.*, the force of attraction or repulsion (if negative) acting between two Whirls, is determined by the formula

$$\mathbf{F}_D=-\frac{\partial\overline{W}}{\partial\mathbf{D}}. \quad . \quad . \quad . \quad . \quad . \quad (19.1)$$

Following our previous notation, we shall denote the distance force in the case of copolarized and contrapolarized Whirls by $\mathbf{F}_{D+}$ and $\mathbf{F}_{D-}$ resp. To determine these forces we shall use the expressions for W_+ and W_- found in the previous section, after having them suitably transformed.

Denote

$$\mathrm{X}'=\frac{\mathrm{X}}{\mathrm{D}},\quad \mathrm{Y}'=\frac{\mathrm{Y}}{\mathrm{D}},\quad \mathrm{Z}'=\frac{\mathrm{Z}}{\mathrm{D}}. \quad . \quad . \quad (19.2)$$

We shall mark X_{01}, Y_{01}, Z_{01}, X_{02}, Y_{02}, and Z_{02} with a suffix $'$ at the top (X'_{01} and so on) when in their expression (16.5), X′, Y′, and Z′ are substituted for X, Y, and Z resp.

* Since we shall deal here only with the average forces $\mathbf{F}_D$ and average distances D, we shall omit the bars on **F** and D denoting the average value.

Then we shall have by (16.5) and (19.2)

$$\left.\begin{aligned}(X_{01}^2+Y_{01}^2)(X_{02}^2+Y_{02}^2)&=\frac{1}{D^4}(X_{01}'^2+Y_{01}'^2)(X_{02}'^2+Y_{02}'^2),\\(X_{01}^2+Y_{01}^2+Z_{01}^2)(X_{02}^2+Y_{02}^2+Z_{02}^2)&=\frac{1}{D^4}(X_{01}'^2+Y_{01}'^2+Z_{01}'^2)\\&\quad\times(X_{02}'^2+Y_{02}'^2+Z_{02}'^2).\end{aligned}\right\}\quad\ldots\quad(19.2a)$$

We shall also use for X_{01}, X_{01}', etc. and their functions the triple suffixes of zero's and heavy dots at the bottom, to indicate which of X, Y and Z equals zero, in accordance with the conventions for these triple suffixes which we used in the previous two sections for u (see the paragraphs following formula (17.10*d*)).

Then, introducing the same data for the θ's which we assumed for $\overline{W}_+$, and putting $q_{01}'=q_{02}'$, we shall have from (19.2*a*), (16.5), and (16.5*a*) (taking into account (18.1*c*), (18.1*d*), and (18.6)),

$$\left.\begin{aligned}[(X_{01}'^2+Y_{01}'^2)(X_{02}'^2+Y_{02}'^2)]_{\bullet 0\bullet}&=(X'^2+\tfrac{1}{4})^2,\\[(X_{01}'^2+Y_{01}'^2+Z_{01}'^2)(X_{02}'^2+Y_{02}'^2+Z_{02}'^2)]_{\bullet 0\bullet}&=[(X'^2+\tfrac{1}{4})+Z'^2]^2.\end{aligned}\right\}\quad\ldots\quad(19.2b)$$

Hence by (17.10*b*), (17.5*a*) (taking into account (18.1*d*)), and by (19.2*a*) and (19.2),

$$\left.\begin{aligned}{}^0u'_{\bullet 0\bullet}&=\frac{1}{(X'^2+\frac{1}{4})^{\frac{1}{2}}[(X'^2+\frac{1}{4})^2+Z'^2]},\\q_{01}&=q_{01},\end{aligned}\right\}\quad\ldots\quad(19.2c)$$

whence

$$\begin{aligned}\int_0^\infty\int_0^\infty {}^0u_{\bullet 0\bullet}\,dX\,dZ&=\frac{1}{D}\int_0^\infty\int_0^\infty {}^0u_{\bullet 0\bullet}\,dX'\,dZ'\\&=\frac{1}{D}\int_0^\infty\int_0^\infty\frac{dX'\,dZ'}{(X'^2+\frac{1}{4})^{3/2}\,[(X'^2+\frac{1}{4})^2+Z'^2]}\\&=\frac{\pi}{2D}\int_0^\infty\frac{dX'}{(X'^2+\frac{1}{4})^{3/2}}=\frac{\pi}{2D}\left[\frac{4X'}{(X'^2+\frac{1}{4})^{1/2}}\right]_0^\infty=\frac{2\pi}{D}.\end{aligned}\quad\ldots\quad(19.2d)$$

Hence by (18.8*c*)

$$\underset{q_{01}=q_{02}>>1}{\overline{W}_+}=-\frac{K_1K_2}{D}\overline{N}_1^2,\qquad\ldots\quad(19.3)$$

where

$$\mathbf{N}_1^2=\frac{\pi \sin f\,\Phi_{fg\bullet 0\bullet}}{\sqrt{2}\left|\sin\left(\varphi_1\pm\frac{\pi}{4}\right)\right|}. \quad . \quad . \quad (19.3a)$$

Since $L_4=0$ (by (18.8*b*)), $\Phi_{fg\bullet 0\bullet}$ in this formula is independent of D ; hence by (19.1) and (19.3)

$$\mathbf{F}_{\substack{\mathrm{D}+\\ q_{01}=q_{02}>>1}}=-\frac{\mathbf{K}_1\mathbf{K}_2}{\mathrm{D}^2}\mathbf{N}_1^2. \quad . \quad . \quad . \quad (19.3\,b)$$

This shows that, on the average, *two copolarized Whirls of equal size and frequency repel each other, in accordance with the inverse square law.*

For the case of copolarized Whirls with $q_{02}>>q_{01}>>1$ we find in the same way

$$\left.\begin{aligned}&[(\mathrm{X}'^2_{01}+\mathrm{Y}'^2_{01})(\mathrm{X}'^2_{02}+\mathrm{Y}'^2_{02})]_{00\bullet}=\frac{q'^2_{01}\,q'^2_{02}}{(q'_{01}+q'_{02})^4},\\ &[(\mathrm{X}'^2_{01}+\mathrm{Y}'^2_{01}+\mathrm{Z}'^2_{01})(\mathrm{X}'^2_{02}+\mathrm{Y}'^2_{02}+\mathrm{Z}'^2_{02})]_{00\bullet}\\ &\quad=\left(\mathrm{Z}'^2+\frac{q'^2_{02}}{(q'_{01}+q'_{02})^2}\right)\left(\mathrm{Z}'^2+\frac{q'_{01}}{(q'_{01}+q'_{02})^2}\right).\end{aligned}\right\} \quad . \quad (19.4)$$

Hence from (17.10*b*), (17.5*a*) (taking into account (18.1*d*)), (19.2), and (19.2*a*)

$${}^0u'_{00\bullet}=\frac{q'_{01}+q'_{02}}{\sqrt{q'_{01}\,q'_{02}}\sqrt{\left(\mathrm{Z}'^2+\frac{q'^2_{02}}{(q'_{01}+q'_{02})^2}\right)\left(\mathrm{Z}'^2+\frac{q'^2_{01}}{(q'_{01}+q'_{02})^2}\right)}}, \quad . \quad . \quad . \quad (19.4a)$$

and

$$\int_0^\infty {}^0u_{00\bullet}\,d\mathrm{Z}=\frac{1}{\mathrm{D}^2}\int_0^\infty {}^0u'_{00\bullet}\,d\mathrm{Z}'=\frac{1}{\mathrm{D}^2}\frac{\left(1+\frac{q'_{01}}{q'_{02}}\right)\mathbf{C}_2(q'_{01}+q'_{02})}{\sqrt{q'_{01}\,q'_{02}}}, \quad . \quad . \quad . \quad (19.4b)$$

where, on substituting

$$\alpha=\tan^{-1}\frac{q'_{01}+q'_{02}}{q'_{01}}\mathrm{Z}',$$

$$\begin{aligned}\mathbf{C}_2&=\int_0^{\frac{\pi}{2}}\frac{d\alpha}{\sqrt{1-\left(1-\frac{q'^2_{01}}{q'^2_{02}}\right)\sin^2\alpha}}\\ &=\log 4\frac{q'_{02}}{q'_{01}}+\frac{1}{4}\frac{q'^2_{01}}{q'^2_{02}}\left(\log\frac{q'_{02}}{q'_{01}}-1\right)+o\left\{\frac{q'^4_{01}}{q'^4_{02}}\right\}, \quad . \quad (19.4c)\end{aligned}$$

by the well-known formula from the Theory of Elliptic Functions *.

By (18.10) and (19.4*b*)

$$\underset{q_{02}>>q_{01}>>1}{\overline{W}_{+}} = -\frac{K_1K_2}{D^2}\frac{q'_{01}+q'_{02}}{q'_{01}q'_{02}}\frac{\left(1+\frac{q'_{01}}{q'_{02}}\right)C_2}{2\sqrt{2}\pi}\overline{N}_2^2, \quad (19.5)$$

where

$$N_2^2 = \frac{\pi\sqrt{2}\sin\bar{f}\Phi_{fg00\bullet}}{\left|\sin\left(\varphi_1 \pm \frac{\pi}{4}\right)\right|}. \quad . \quad . \quad (19.5a)$$

By (19.5*a*), (17.11*d*), and (17.11*e*)

$$\frac{\partial\overline{N}_2^2}{\partial D} = |\overline{L_4{}^{fg}}|\,\overline{N}_2^2 = \frac{\sqrt{2}q'_{01}q'_{02}}{q'_{01}+q'_{02}}\left|\sin\left(\varphi_1 \pm \frac{\pi}{4}\right) - \bar{f}\sin\left(\frac{\pi}{4} \pm \frac{\pi}{4}\right)\right|\overline{N}_2^2$$
$$. \quad . \quad . \quad (19.5b)$$

by (18.9) and (18.9*c*).

By (19.1), (19.5), and (19.5*b*), neglecting the $o\{(q_{02}D)^{-1}\}$,

$$\underset{q_{02}>>q_{01}>>1}{F_{D+}} = \frac{K_1K_2}{D^2}\frac{\left(1+\frac{q_{01}}{q_{02}}\right)C_2}{2\sqrt{2}\pi}$$
$$\times\sqrt{2}\left|\sin\left(\varphi_1 \pm \frac{\pi}{4}\right) - f\sin\left(\frac{\pi}{4} \pm \frac{\pi}{4}\right)\right|\overline{N}_2^2.$$
$$. \quad . \quad . \quad (19.6)$$

We can see from this that, on the average, two copolarized Whirls of widely differing frequencies ($q_{02}>>q_{01}$) *attract each other in accordance with the inverse square law.*

We shall now find the expression for F_{D-} in the case $q_{02}>>q_{01}$.

Taking into account that in this case $\sin\theta_1=0$, $\sin\theta_2=1$, and $\cos\varphi_2=0$, and applying the same method which we

* See, for example, ' Traité de Calcul Différentiel et de Calcul Intégral,' by J. Bertrand, vol. ii. (Calcul Intégral), p. 61 (Paris, Gautier Villars, 1870), and ' Tables of Integrals,' by H. B. Dwight, p. 155 (Macmillan, New York, 1934).

used in deriving the expressions for $\underset{q_{02}>>q_{01}}{\mathbf{F}_{+}}$, we shall obtain

$$^{4}u_{\bullet 00}=\frac{1}{\mathbf{D}^2}\sqrt{\frac{q'_{01}+q'_{02}}{q'_{02}}}\times\int_0^\infty\frac{dX'}{\left(X'^2+\frac{q'^2_{02}}{(q'_{01}+q'_{02})^2}\right)^{3/4}\left(X'^2+\frac{q'^2_{01}}{(q'_{01}+q'_{02})^2}\right)^{1/2}}. \quad . \quad . \quad . \quad (19.7)$$

We have generally, when $a<<b<<1$,

$$\int_0^\infty\frac{dx}{(x^2+b^2)^{3/4}\,(x^2+a^2)^{1/2}}=\int_0^\infty\frac{dy}{\sqrt{[y^4-(b^2-a^2)]\,(y^4-b^2)}}$$

(by substituting $y=(x^2+b^2)^{1/4}$)

$$=\int_{\sqrt{b}}^\infty\frac{dy}{y^4-\left(b^2-\frac{a^2}{2}\right)}\left(1+o\left\{\frac{a^3}{b^3}\right\}\right)\cong b^{-3/2}\int_1^\infty\frac{dz}{z^4-\alpha^4}$$

$$\left(\text{by substituting } z=\frac{y}{\sqrt{b}} \text{ and } \alpha=\left(1-\frac{a^2}{2b^2}\right)^{1/2}\right)$$

$$=\frac{b^{-3/2}}{4\alpha^3}\left(\log\frac{1+\alpha}{1-\alpha}+\pi-2\cot^{-1}\alpha\right)\cong b^{-3/2}\left(\log 2\sqrt{\frac{a}{b}}+\frac{\pi}{8}\right). \quad . \quad . \quad . \quad (19.7\,a)$$

By (18.12 *b*), (19.7), and (19.7 *a*)

$$\underset{2>>q_{01}>>1}{\overline{\mathbf{W}}_{-}}=-\frac{(q'_{01}+q'_{02})^2}{q'^3_{02}}\sqrt{\frac{q'_{01}}{q'_{02}}}\,\mathbf{C}_3\,\bar{\mathbf{N}}_3^2, \quad . \quad (19.8)$$

where $$\mathbf{N}_3^2=\sin\left(-\Phi_{fg\bullet 00}\right) \quad . \quad . \quad . \quad . \quad (19.8\,a)$$

and $$\mathbf{C}_3=\log 2\sqrt{\frac{q'_{02}}{q'_{01}}}+\frac{\pi}{8}. \quad . \quad . \quad . \quad (19.8\,b)$$

Hence, by (19.1), (17.11 *d*), and (17.11 *e*), applying the same method which we used in deriving the formula (19.6), we find

$$\underset{q_{02}>>q_{01}>>1}{\mathbf{F}_{D-}}=\frac{\mathbf{K}_1\mathbf{K}_2}{\mathbf{D}^2}\left(\frac{q'_{01}}{q'_{02}}\right)^{3/2}\left(1+\frac{q'_{01}}{q'_{02}}\right)\times\mathbf{C}_3\,\sqrt{2}\sin\left(\varphi_1\pm\frac{\pi}{4}\right)-\overline{f}\,\bar{\mathbf{N}}_3^2. \quad (19.9)$$

We can see from (19.9) that two contrapolarized Whirls with $q_{02} >> q_{01} >> 1$ *attract each other following the inverse square law*, but the force of this mutual attraction for a given $\mathbf{K_1K_2}$ is approximately only $\left(\frac{q_{01}}{q_{02}}\right)^{3/2}$ part of the corresponding force of mutual attraction of copolarized Whirls.

We shall not consider here in detail the force $\underset{q_{02}=q_{01}>>1}{\mathbf{F}_{D-}}$ between two Whirls of equal magnitude and frequency. As it is not difficult to find from (18.11 *b*), this force is of the order q_{01}D times smaller than $\mathbf{F}_{D+}$, *i. e.*, it varies according to the inverse cube law, and unless q_{01} D is small it belongs to the order of magnitude which we neglected in our calculations.

So we shall simply write

$$\underset{q_{01}=q_{02}}{\mathbf{F}_{D-}} = \frac{\mathbf{K_1K_2}}{q_{01}D^2}\mathbf{N}_4^2. \quad . \quad . \quad . \quad (19.9b)$$

We shall now consider a little closer the coefficients $\mathbf{N}$ representing the average influence of the precessional rotation.

By (17.12 *d*), (17.11 *e*), and (17.9 *a*), taking into account formula (18.6) for the copolarized Whirls, and (18.6 *a*) and the first formula (18.12 *a*) for the contrapolarized ones, and also the conditions (18.1 *b*) and (18.1 *d*), we have

$$\begin{aligned}\Phi_{fg} &= (g q_{01} - (-)^g q_{02})\, ct + \bar{g}\psi_1 - (-)^g\psi_2 - \bar{g}\left(\frac{\pi}{2} - \varphi_1\right) \\ &\quad + (-)^g\left(\frac{\pi}{2} - \varphi_2\right) - (1-\bar{f})\frac{\pi}{2} - (f+a)\frac{\pi}{2} + |L_{4fg}|\,D \\ &= C_4 + (\bar{g} q_{01} - (-)^g q_{02})\, ct + \bar{g}\psi_1' - (-)^g\psi_2' - \bar{g}\varphi_1 \\ &\quad + (-)^g\varphi_2 + |L_{4fg}|\,D, \quad . \quad . \quad . \quad . \quad . \quad . \quad (19.9c)\end{aligned}$$

where C_4 is a constant in which also a constant part of ψ_1 and ψ_2 is included; ψ_1' and ψ_2' are the variable parts of ψ_1 and ψ_2 resp.

Since ψ_1 and ψ_2 are, so far, undetermined, the constant C_4 is, so far, also undetermined, and so are, so far, the variables ψ_1' and ψ_2'. Their limits will be defined by the conditions that $\mathbf{N}^2$ must be always finite, and it must be positive on the average ($\mathbf{N}^2 > 0$) (compare (19·3), (19·5), (19·8), and (18·4 *d*)).

Within these limits the most probable functions of φ_1 for the variables ψ_1' and ψ_2', ($\psi_1'(\varphi_1)$ and $\psi_2'(\varphi_1)$) and the most probable value of C_4 will be those which would make N^2 positive at each given moment (and not only on the average), for this would mean the stability at any given phase of the precessional rotation. Further, subject to these conditions, a given value of C_4 and a given form of $\psi_1'(\varphi_1)$ and $\psi_2'(\varphi_1)$ will be the more probable the greater is the corresponding N^2 (for the second derivative of $\bar{W}$ with respect to any parameter on which $\bar{W}$ depends will, obviously, be in proportion to N^2 owing to the sinusoidal nature of the latter) and the smaller are the associated disturbances of the e.m. field of the system, in accordance with the above discussed Minimum Disturbance Principle *.

In the case of N_1^2 (formula (19.3 *a*)) we shall have $L_{4fg}=0$ (by (18·8 *b*)), and since $q_{01}=q_{02}$, the minimum disturbance will correspond to $g=(-)^g$ (*i. e.*, $g=3$, 4), as has been already mentioned †.

Hence by (18·8 *a*) the formula (19·9 *c*) can be written

$$\Phi_{fg}=C_4+\bar{g}(\psi_1'-\psi_2'-2\varphi_1). \quad . \quad . \quad (19.9\,d)$$

Consequently, by (19.3 *a*) N_1^2 will be always finite and positive if

$$C_4=(\bar{f}-1)\frac{\pi}{2},$$

$$\psi_1'-\psi_2'=2\varphi_1+a\left|\sin\left(\varphi_1\pm\frac{\pi}{4}\right)\right|, \quad . \quad (19.9\,e)$$

where a is a constant. Then by (19.3 *a*), (19.9 *d*), and (19.9 *e*)

$$\mathsf{N}_1^2=\frac{\pi\sin\left|a\sin\left(\varphi_1\pm\frac{\pi}{4}\right)\right|}{\sqrt{2}\left|\sin\left(\varphi_1\pm\frac{\pi}{4}\right)\right|}. \quad . \quad . \quad . \quad (19.9\,f)$$

The average value of N_1^2 depends on the manner in which φ_1 varies with the time t. It would be simplest to assume a uniform precessional rotation, but this would mean a discontinuity in $\frac{d\mathsf{N}_1^2}{dt}$, and hence in the *power*

* See the text between formulæ (18.7 *b*) and (18.8).

† See the text between the formulæ (18.8 *b*) and (18.8 *c*).

$\frac{dW}{dt}$, when $\varphi_1 = \mp\frac{\pi}{4}$, owing to the discontinuity of $\frac{d}{d\varphi_1}\sin\left(\varphi_1 \pm \frac{\pi}{4}\right)$ at this point (due to the | |). Such an abrupt change of the power of the energy transformation from the "internal" to the "mutual" state, or *vice versa*, appears to be very improbable. We must assume, therefore, that the precessional rotation is not uniform. A simple form of a non-uniform precessional rotation not involving any discontinuity in $\frac{dW}{dt}$ can be represented by the formula

$$\left|\sin\left(\varphi_1 + \frac{\pi}{4}\right)\right| = \sin^2 \bar{\varphi}_1 t, \quad . \quad . \quad . \quad (19.9\,g)$$

where $\bar{\varphi}_1$ is the average velocity of the precessional rotation.

By (19·9 *f*) and (19·9 *g*) the average value of N_1^2

$$\bar{\mathsf{N}}_1^2 = \frac{\pi}{\sqrt{2}} \times \frac{2\bar{\dot{\varphi}}_1}{\pi}\int_0^{\frac{\pi}{2\bar{\dot{\varphi}}_1}} \frac{\sin a\,(\sin^2 \bar{\dot{\varphi}}_1 t))}{\sin^2 \dot{\varphi}_1 t}\,dt$$

$$= \sqrt{2}\int_0^{\frac{\pi}{2}} \frac{\sin^2(a\sin^2 x)}{\sin^2 x}\,dx = \sqrt{2}\sum_{m=0}^{\infty}\frac{(-)^m a^{2m+1}}{(2_{m+1})\,!} \times \int_0^{\frac{\pi}{2}} \sin^{4m} x\,dx$$

(by expanding the numerator in Maclaurin Series)

$$= \frac{\pi}{\sqrt{2}}\sum_{m=0}^{\infty}\frac{(-)^m a^{2m+1}\ 1.3.5.\ldots.(4m-1)}{(2_{m+1})\,!\ \ 2^m\,(2m)\,!}\,*. \quad (19.9\,h)$$

The maximum value of $\bar{\mathsf{N}}_1^2$ will correspond to $a = 1{\cdot}65$, when

$$\bar{\mathsf{N}}_1^2 \cong 2{\cdot}52. \quad . \quad . \quad . \quad . \quad . \quad (19.9\,i)$$

In the case of $\bar{\mathsf{N}}_2^2$ (formula (19·5 *a*)) the formula (19.9 *c*)—taking into account the fourth formula (18·9) and formula (18.9 *c*)—can be written as follows:

$$\Phi_{fg} = C_4 + (\bar{g}\,q_{01} - (-)^g q_{02})\,ct - g\varphi_1 + \bar{g}\psi_1{}'$$

$$-(-)^g\psi_2{}' + \frac{\sqrt{2}q_{01}'q_{02}'}{q_{01}'+q_{02}'}\left|\sin\left(\varphi_1 \pm \frac{\pi}{4}\right) - \bar{f}\sin\left(\frac{\pi}{4} \pm \frac{\pi}{4}\right)\right|. \quad . \quad . \quad . \quad (19.10)$$

* See, for example, Table of Integrals by Dwight, *loc. cit.*, art. 854.1.

Here we shall have two different kinds of variations involving two greatly differing frequencies, the one being the angular velocity of the precessional rotation (the "precessional" frequency) and the other, the $(gq_{01}-(-)^g q_{02})c$, which is of much higher order (the "fundamental" frequency). Since the fundamental frequency is many times greater than the precessional one, their influences can be considered independently.

Considering only the precessional frequency, we shall arrive at $\overline{\mathsf{N}}_2^2=2\mathsf{N}_1^2$ by comparing (19.3 *a*) and (19·5 *a*) and using exactly the same reasoning as in the case of N_1^2. The influence of the superimposition of the fundamental frequency will be expressed by means of an additional coefficient, which we shall denote by $\frac{\epsilon'^2}{2}$.

Then we can write

$$\overline{\mathsf{N}}_2^2=\epsilon'^2\,\overline{\mathsf{N}}_1^2. \quad . \quad . \quad . \quad . \quad (19.10\ a)$$

We shall now try to determine $\frac{\epsilon'^2}{2}$.

In order that $\overline{\mathsf{N}}_2^2\neq 0$, the influence of the second term in (19.10)—which involves the fundamental frequency, and which by itself would, of course, give $\mathsf{N}_2^2=0$—must be compensated by a variation of all other terms which would also involve the fundamental frequency. This can be done partly by suitable variations of ψ_1' and ψ_2' and partly by a variation of D. If any of these variations were unidirectional this would be equivalent to the change of $q_{01}\pm q_{02}$ and the continuous variation of D—in other words, to the change in the character of the Whirl in the first case, and to a continuous unidirectional motion which would exclude the possibility of a state of equilibrium (say of the planetary motion) in the second case. Therefore these variations must be *reversive*.

A combination of a unidirectionally varying term of an argument and a reversively and symmetrically varying one, which would give a maximum average value of the sin, can be conceived in the following way.

Let the absolute value of the speed $(|d/dt|$ of the reversive term be always the same as that of the unidirectional one, but let the direction of the former be opposite to the direction of the latter during, say, the

first, third, and any *odd* half-cycle, but coincide with it during the second, fourth, and any *even* half-cycle. Then during the *odd* half-cycles the total argument will remain at its *initial* value, while during the *even* half-cycles it will vary with double speed, completing in the course of a half-cycle the whole period of variation, and thus returning again to the initial value.

Therefore the value of the sin during the *odd* half-cycles will be the initial value, but the *average value* of the sin during the *even* half-cycles will be zero. Hence the *total average value* of the sin will be *half the initial value*. Consequently the *maximum* total average value of the sin will be $\frac{1}{2}$, or, in other words, the maximum value of $\frac{\epsilon'^2}{2}=\frac{1}{2}$, that is $\epsilon'^2=1$.

This, however, corresponds to the abruptly reversive variation, which will really represent an abruptly reversive motion, either circular (variations of ψ_1 and ψ_2) or linear (a variation of D). Such a motion is hardly conceivable in reality. Therefore we must assume that in reality there will be only a limited number of harmonics of this reversive variation. This would involve certain ripples which would slightly alter ϵ'^2. It would not be difficult to show, using the well-known Fourier expansion of reversive uniform motion, that

$$\epsilon'^2=\frac{1}{\pi}\int_{-\pi}^{\pi}\sin\Big(\Phi_0-\frac{\pi}{2}+x+\frac{4}{\pi}\sum_{m=0}^{m_1}\frac{\cos(2m+1)x}{(2m+1)^2}\Big)dx, \quad . \; . \; . \quad (19.10\,b)$$

where Φ_0 is the initial value of Φ_{fg} (at $t=0$). When $\Phi_0=\frac{\pi}{2}$

$$\underset{m_1=0}{\epsilon'^2}\cong 1{\cdot}03 \qquad \underset{m_1=\infty}{\epsilon'^2}=1, \quad . \; . \; . \quad (19.10\,c)$$

where m_1+1 is the number of the harmonics of the reversive component of the argument.

Since $\mathfrak{N}^2$ tends to its possible maximum (see the text preceding formula (19.9 *d*)), Φ_0 must be very near to $\frac{\pi}{2}$. Hence $\epsilon'^2\cong 1$. We must, however, anticipate the possibility of deviation from this maximum value, caused by the ripples represented by the terms of the expression for W, which were left out in our calculation (see section 18).

Referring to $\bar{\mathfrak{N}}_3^2$, we observe that in the expression

for this coefficient (formula (19.8*a*)) there is no denominator which becomes zero at times. Consequently, using exactly the same reasoning as in the case of $\bar{\mathsf{N}}_2^2$, we shall find that

$$\mathsf{N}_3^2=\epsilon'^2. \quad . \quad . \quad . \quad . \quad . \quad (19.10\,d)$$

We shall now average the penultimate factors in (19.6) and (19.9). First of all we shall take the average between the expressions for $\bar{f}=1$ and $f=-1$, and then, recalling (19.9 *g*), we shall take the average for the whole cycle of the precessional rotation, which, of course, will be a Root Mean Square, owing to the quadratic nature of the right-hand member in (19.9 *g*). In this way we shall easily find

$$\left.\begin{aligned}\overline{\left|\sqrt{2}\sin\left(\varphi_1\pm\frac{\pi}{4}\right)-\bar{f}\sin\left(\frac{\pi}{4}\pm\frac{\pi}{4}\right)\right|}&=1,\\ \overline{\left|\sqrt{2}\sin\left(\varphi_1\pm\frac{\pi}{4}\right)-\bar{f}\right|}&=1.\end{aligned}\right\}. \quad (19.10\,e)$$

Assume now that we have four kinds of Whirls, two classes of electropolarized ones with $q_0=q_{0+}$ and $q_0=q_{0-}$, where $q_{0+}>>q_{0-}>>1$, and two classes of magnetopolarized ones *with the same values of* q_0.

Consider the electropolarized and magnetopolarized Whirls as belonging to two different *categories*.

The Whirls with large q_0 can be considered as positive, and those with comparatively small q_0 as *negative*. Accordingly we shall mark with the suffixes + and − the quantities relating to the positive and the negative Whirls resp.

Then the Whirls belonging to the same category will repel each other if their respective signs are the same, and attract each other if the signs are opposite, in both cases according to the inverse square law.

The Whirls belonging to different categories will affect each other very little if their respective signs are identical. If, however, the signs are different, they will attract each other according to the inverse square law, but with a force much smaller than the corresponding force of mutual attraction of the Whirls belonging to the same category.

Further, we shall assume that the force of mutual repulsion between Whirls of the same sign is equal to

that of the mutual attraction of Whirls of opposite signs.

Then we shall be able to represent our distance force $\mathbf{F}_{D+}$ in the form of Coulomb's law, and express the "electric charge" of our Whirls in terms of the parameters of their e.m. fields.

Denoting the "electric charges" of the positive and negative Whirls by $+e$ and $-e$ resp., we shall be thus able to write (19.3 *b*) and (19.6) (taking into account (19.10 *e*)) in the form

$$\underset{(+,+)}{\mathbf{F}_{D+}}=\underset{(-,-)}{\mathbf{F}_{D+}}=-\frac{e^2}{D^2},\quad \underset{(+,-)}{\mathbf{F}_{D+}}=\frac{e^2}{D^2}, \quad . \quad (19.11)$$

where

$$e=\mathsf{K}_+\sqrt{\mathsf{N}_1^2}=\mathsf{K}_-\sqrt{\mathsf{N}_1^2}=\sqrt{\mathsf{K}_+\mathsf{K}_-}\sqrt{\frac{\left(1+\frac{q_{0-}}{q_{0+}}\right)\mathbf{C}_2}{2\sqrt{2}\pi}\mathsf{N}_2^2},$$
$$. \quad . \quad . \quad (19.11\,a)$$

whence by (17.3 *a*), taking into account that $\hbar_{11}=\hbar_{12}=\hbar_1$ (by (18.1 *b*)),

$$\mathsf{K}_+=\mathsf{K}_-, \quad \text{and} \quad A_+=A_-, \quad \chi_{1+}=\chi_{1-}. \quad (19.11\,b)$$

Further, by (19.11 *a*), (19.10 *a*), and (19.10 *c*),

$$\frac{2\sqrt{2}\pi}{\left(1+\frac{q_{0-}}{q_{0+}}\right)\mathbf{C}_2}=\epsilon'^2\cong 1 \quad . \quad . \quad . \quad (19.11\,c)$$

(see the text between the formulæ (19.10 *c*) and (19.10 *d*)).

The "stationary" masses of our Whirls are (formula (12.5))

$$\left.\begin{aligned} m_{0+}&=\frac{\hbar_1\Omega_{0+}}{c^2}=\frac{\hbar_1}{c}q_{0+},\\ m_{0-}&=\frac{\hbar_1\Omega_{0-}}{c^2}=\frac{\hbar_1}{c}q_{0-}. \end{aligned}\right\} \quad . \quad . \quad . \quad (19.11\,d)$$

Hence, by (19.11 *a*) and (17.3 *a*),

$$\frac{e}{m_{0+}}=\frac{\mathrm{C}_e}{q_{0+}},\quad \frac{e}{m_{0-}}=\frac{\mathrm{C}_e}{m_{0-}}, \quad . \quad . \quad (19.11\,e)$$

where

$$\mathrm{C}_e=\frac{1}{\pi}\sqrt{\frac{\Gamma_1^2c^3}{\sqrt{\chi_1^2+1}\,Q\hbar_1}}=\frac{ec}{\hbar_1}. \quad . \quad (19.11\,f)$$

When the two Whirls belong to different categories

and have opposite signs their force of mutual attraction will be found from (19.9), (19.10 *e*), (19.11), (19.11 *a*), (19.11 *c*), and (19.11 *d*).

$$\underset{(+,-)}{\mathbf{F}_{D-}} = \left(\frac{m_{0-}}{m_{0+}}\right)^{3/2}\left(1+\frac{m_{0-}}{m_{0+}}\right)^{2} C_3 \frac{\epsilon'^2}{\mathbf{N}_1^2}\frac{e^2}{D^2}. \quad (19.11\,g)$$

When both Whirls are of the same sign we have, from (19.9 *b*),

$$\left.\begin{aligned}\underset{(+,+)}{\mathbf{F}_{D-}} &= \frac{e^2}{D^2}\times o\{(q_{0+}D)^{-1}\},\\ \underset{(-,-)}{\mathbf{F}_{D-}} &= \frac{e^2}{D^2}\times o\{(q_{0-}D)^{-1}\}.\end{aligned}\right\} \quad . \quad . \quad (19.11\,h)$$

By (19.11) and (17.3 *a*)

$$A = \frac{\pi\sqrt[4]{\chi_1^2+1}\,e}{\sqrt{2}\,\sqrt{\mathbf{N}_1^2}} \cong \frac{\pi e}{\sqrt{2}\,\sqrt{\mathbf{N}_1^2}}, \quad . \quad . \quad (19.11\,i)$$

by (18.1 *c*).

It will be borne in mind that the expressions for the distance forces, which we have derived here, hold only when $q_0 D >> 1$. When D is very small the terms of the order D^{-3}, which were omitted in our expressions, become prominent, and the force may entirely change its characteristics. For example, in the case of co-polarized Whirls with $q_{02} >> q_{01}$ the attraction changes into a repulsion when D is small (see (19.6)); on the other hand, the attraction between contrapolarized Whirls of the same sign, which is negligible when $q_0 D >> 1$, becomes very considerable when $q_0 D$ is small (by (19.9 *b*)). It could be also shown that $\mathbf{F}_D$ can momentarily reverse if the axis of a Whirl takes some of the unstable orientations.

The distance forces between two mutually attracted Whirls determine their relative planetary motion.

In this motion only those trajectories will be stable which are associated with a stable vibrational state. If the precessional motion of the axis of the Whirl is upset by an external agent (e.m. waves or another Whirl), the stability can be upset, and the vibrational state and the trajectory altered in a " trigger-like " manner.

There will be—as a result of the combined influence of the law of conservation of energy and that of angular momentum—a certain relationship between this energy

and all the mean angular velocities (or frequencies) of cyclic motions which take place in the system, and also between the frequencies and the energies which are lost or acquired (radiated or absorbed) by the systems of Whirls.

These relationships are the "quantum relationships," which were discussed in more definite terms in section 15, when the question was considered generally.

Since our Whirls must answer the description of elementary particles, they must possess gravitational properties.

As is well known, the gravitational forces between the particles are extremely small in comparison with the electrostatic ones.

It is, therefore, natural to seek the explanation of the gravitational forces in the vibrational states, assuming that on the average the attractive force $\mathbf{F}_{D+}$ is slightly greater than the repulsive force $\mathbf{F}_{D+}=\mathbf{F}_{D+}$.
$\quad\quad\quad

by the attractive force according to the inverse cube law, which acts *independently of the orientation of the axes* (see formulæ (19.9 *b*) and (18.11*b*)).

Let us take two groups consisting of equal numbers, say N_1 for one of the groups and N_2 for the other, of positive and negative Whirls.

Denote by θ_g the ratio of the number of the free magnetopolarized particles to the total number of the free Whirls, and by γ the gravitational constant.

Then we shall have, by (19.11) and (19.11*g*),

$$\gamma N_1 N_2 (m_{0+} + m_{0-})^2 = 2 \frac{\mathbf{F}_{D-}}{\mathbf{F}_{D+}} \begin{matrix} (+,\,-) \\ (-,\,-) \end{matrix} N_1 N_2 \theta_g (1-\theta_g). \quad (19.12)$$

Whence, neglecting the order $\theta_g{}^2$,

$$\theta_g = \frac{\gamma}{2} \frac{\mathbf{F}_{D-}}{\mathbf{F}_{D+}} \begin{matrix} (+,\,-) \\ (+,\,-) \end{matrix} \left(1 + \frac{m_{0-}}{m_{0+}}\right)^2 \left(\frac{m_{0+}}{e}\right)^2. \quad . \quad (19.12\,a)$$

We shall not discuss in this paper the interaction between the incomplete simple Whirls and between the simple Whirls and the compound ones. This may present some difficulties, chiefly due to the spreading of the incomplete Whirls. However, these difficulties do not appear to be insuperable.

20. *Elementary Particles as Whirls.*

We shall now apply the theory of Whirls to the electromagnetic interpretation of elementary particles.

I suggest that the elementary particles are really different forms of Whirls. The electrons, protons, and other material particles are the compound Whirls, while the photons (light quanta) are incomplete simple Whirls. Material elementary particles do not contain any " electric charges " in the usually accepted sense, *i. e.*, they do not involve any discontinuity in the e.m. field, and the apparent discontinuities of the lines of force which they create are due to the average distance forces between the Whirls which, as we have found, follow the inverse square law.

Thus the " electric charge " should not be considered as a separate entity, but can only be retained as a useful fiction.

Neither is there any need to attribute to the elementary particles any "material mass" in the usually accepted sense. Their inertia is purely an electromagnetic inertia, while their gravitational forces are due to the excess of the electromagnetic forces of attraction over the electromagnetic forces of repulsion, which is caused by the free contrapolarized particles.

Hence the conception of matter, in the usually accepted sense, as something fundamentally different from the e.m. waves need not be retained.

The electromagnetic waves, of which the Whirls consist, satisfy the de Broglie's relationships, and therefore the conception of "material waves" of de Broglie, as distinct from the e.m. waves, need not be retained.

It is, therefore, unnecessary to retain a dualism between the waves and particles, because the particles are only certain systems of e.m. waves.

Since the Whirls follow the Relativity relationships on the basis of the Maxwell equations, these relationships need not be postulated : they are only a corollary.

We know from experience that matter, which, as far as we can see, consists chiefly of electrons and protons, is affected much less by the magnetic field than by the electric of the same energy density. No serious effect on the stability of matter is experienced with magnetic fields of the order of 10^5 gauss and higher (Kapitza), which correspond, by their energy density, to the electric fields of 3×10^7 volts per cm. and more.

It appears that the transversal vectors in the Whirls are more active than the longitudinal ones. We shall assume, therefore, that electrons and protons are the *electropolarized* Whirls. However, along with the electrons and the protons we shall assume the existence of two classes of magnetopolarized Whirls of the same respective masses. We shall call them "magneto-electrons" and "magneto-protons."

We shall now define, on the basis of the known data of elementary particles, the data of the Whirls, which form these particles according to my hypothesis.

We shall mark the data for the proton with the suffix + and for the electron with the suffix —.

We have the following experimental data :—

$$\hbar_{1+}=\hbar_{1-}=\hbar=1{\cdot}023\times10^{-27}\text{ gr. cm.}^2\text{ sec.}^{-1} \quad (20.1)$$

(see formula (14.3)), and also

$$\left.\begin{aligned} e &= 4{\cdot}77\times10^{-10}\ \text{gr.}^{1/2}\ \text{cm.}^{3/2}\ \text{sec.}^{-1}, \\ m_{0+} &= 1{\cdot}66\times10^{-24}\ \text{gr.},\quad m_{0-} = 9\times10^{-28}\ \text{gr.}, \\ \frac{m_{0+}}{m_{0-}} &= 1846. \end{aligned}\right\} \quad . \quad (20.2)$$

Hence, by (19.11 *d*),

$$\left.\begin{aligned} q_{0+} &= \frac{m_{0+}c}{\hbar} = 4{\cdot}85\times10^{13}\ \text{cm.}^{-1}, \\ q_{0-} &= \frac{m_{0-}c}{\hbar} = 2{\cdot}64\times10^{10}\ \text{cm.}^{-1}. \end{aligned}\right\} \quad . \quad . \quad (20.3)$$

Thus our assumption that $q_{02} >> q_{01} >> 1$, which we have made in sections 18 and 19, is quite applicable to the Whirls which answer the descriptions of the electron and the proton.

From (19.11), (19.11 *b*), and (20.2)

$$A_+ = A_- = \frac{\pi e}{\sqrt{2}\sqrt{\mathbf{N}_1^2}} = \frac{\pi}{\sqrt{2}\sqrt{2{\cdot}52}}\, e = 6{\cdot}67 \times 10^{-10}\ \text{gr.}^{1/2}\,\text{cm.}^{3/2}\,\text{sec.}^{-1}. \quad . \quad . \quad (20.4)$$

Hence, by (20.3),

$$\left.\begin{aligned} A_+ q_{0+}^2 &= 1{\cdot}57\times10^{18} \\ A_- q_{0-}^2 &= 4{\cdot}64\times10^{11} \end{aligned}\right\} \text{gr.}^{1/2}\ \text{cm.}^{-1/2}\ \text{sec.}^{-1}. \quad (20.5)$$

From this we can calculate the intensity of the e.m. field of the electron and the proton by using the formulæ (8.10) and (8.10 *a*) for any point not too near to the axis. Then we shall find the intensity of the electric field to be of the order of 10^{20} $\frac{\text{volts}}{\text{cm.}}$ at a distance of the order of 10^{-13} cm. from the axis for the proton, and of the order of 10^{13} $\frac{\text{volts}}{\text{cm.}}$ at a distance of the order 10^{-10} cm. from the axis for the electron.

The result of this calculation is represented on the diagram, which is self-explanatory.

It is usual to talk about the "radius of a particle," as though it were a charged sphere of definite dimensions. It is obvious that no such boundary can exist in a Whirl.

A general idea about the dimensions of the particles can be obtained from the diagram.

We shall now verify our assumption that the elementary particles have very small κ_2, and, *à fortiori*, very small χ_1 (formulæ (18.1 *b*) and (18.1 *c*)).

By (17.3 *a*), (20.1), and (20.4)

$$\mathbf{Q} = \frac{c\hbar}{A^2} \cong 71. \quad . \quad . \quad . \quad . \quad (20.5a)$$

On the other hand, we can obtain from (9.7) *

$$\rho_1\chi_1 \cong 0{\cdot}8\, e^{-\mathbf{Q}_2}, \quad . \quad . \quad . \quad . \quad (20.5b)$$

where $\mathbf{Q}_2$ is the portion of $\mathbf{Q}$ corresponding to the whole space beyond the radius ρ_1, *i. e.*, the space to which the approximate formulæ for the determination of the e.m. field and energy of the Whirl are applicable. Since $\mathbf{Q}_2$ appears to contain the bulk of $\mathbf{Q}$, and ρ_1 is of the order of unity (see sections 8 and 9), we can take for the first approximation $\mathbf{Q}_2 = \mathbf{Q}$ and $\rho_1 = 1$. Then, by (19.11 *b*), (20.5 *a*), and (20.5 *b*)

$$\chi_{1+} = \chi_{1-} = o\{10^{-31}\}. \quad . \quad . \quad . \quad (20.5c)$$

From this and from (18.1 *c*) and (20.5) we can see that our assumption about the smallness of κ_2 and χ_1 is justified.

* From (9.7), on substituting

$$\frac{\pi}{2} - \tan^{-1}\frac{\rho_1}{\xi} = \tan^{-1} y,$$

we obtain

$$\mathbf{Q}_2 = \frac{2}{\pi\sqrt{\chi_1^2+1}} \int_0^\infty \frac{e^{-2\rho_1\chi_1 y}}{y} \tan^{-1} y \, dy.$$

This can be written in the form

$$\begin{aligned} \frac{\pi}{2}\sqrt{\chi_1^2+1}\,\mathbf{Q}_2 = {} & [1-\alpha_1(1-e^{-2\rho_1\chi_1 y_1})] \int_0^{y_1} \frac{\tan^{-1} y}{y}\, dy \\ & + \frac{\pi}{2}\left[1-\alpha_2\left(1-\frac{2}{\pi}\tan^{-1} y_1\right)\right] \int_{y_1}^{y_2} \frac{e^{-2\rho_1\chi_1 y}}{y}\, dy \\ & + \frac{\pi}{2}\left[1-\alpha_3\left(1-\frac{2}{\pi}\tan^{-1} y_2\right)\right] \alpha_4 \frac{e^{-2\rho_1\chi_1 y_2}}{y_2}, \end{aligned}$$

where $0 < \alpha_1 < 1.$

2

3

4

When $\rho_1\chi_1$ is very small—in fact, for the elementary particles, it is of the order less than 10^{-30}—we can so choose y_1 and y_2 that

$$1 << y_1 << \frac{1}{2\rho_1\chi_1}$$

and

$$1 << y_1 << y_2.$$

By (19.11 *c*), (19. 11 *d*), (19. 4*c*), and (20.2) the balance of electrostatic forces requires

$$\epsilon'^2 = \frac{2\sqrt{2\pi}}{\left(1+\frac{m_{0-}}{m_{0+}}\right)C_2} \cong \frac{2\sqrt{2\pi}}{\left(1+\frac{m_{0-}}{m_{0+}}\right)\log 4\frac{m_{0+}}{m_{0-}}} = \cdot 9981. \quad (20.6)$$

This agrees very well with our expectation that $\epsilon'^2 \cong 1$.

It will be noted that this numerical agreement between the theory and the experimental data could not be achieved by adjusting any arbitrary coefficients.

By (19.11 *d*), (19.11 *b*), (19.8 *b*), and (20.2) the force of interaction between the contrapolarized particles of opposite signs (*i. e.*, the electrons with the magneto-protons or the protons with the magneto-electrons)

$$\underset{(+,\,-)}{F_{D-}} = \left(\frac{m_{0-}}{m_{0+}}\right)^{3/2}\left(1+\frac{m_{0-}}{m_{0+}}\right)^2\left(\log 2\sqrt{\frac{m_{0+}}{m_{0-}}}+\frac{\pi}{8}\right) \times \frac{\xi'^2}{N_1^2}\frac{e^2}{D^2} \cong 8{\cdot}75\times 10^{-11}\frac{e^2}{D^2}. \quad . \quad . \quad (20.7)$$

The forces between the distant contrapolarized particles of the same sign are negligible, but they are likely to be bound very strongly when in close proximity (by 19.11 *h*).

The forces of attraction between the distant contrapolarized particles of opposite signs create gravitation.

Taking into account that the gravitational constant

$$\gamma = 6{\cdot}68\times 10^{-8}\ \text{gr.}^{-1}\ \text{cm.}^3\ \text{sec.}^2,$$

Then, taking into account that

$$\int_0^{y_1}\frac{\tan^{-1}y}{y}\,dy = \frac{\pi}{2}\log y_1 + \sum_{m=0}^{\infty}\frac{(-)^m y_1^{-2m-1}}{m^2},$$

$$\int_{y_1}^{y_2}\frac{e^{-2\rho_1\chi_1 y}}{y}\,dy = \frac{\pi}{2}\log\frac{y_2}{y_1} + \sum_{m=1}^{\infty}\frac{(-)^m a^m}{m\,m!}\left(1-\frac{y_1^m}{y_2^m}\right),$$

where $a = 2\rho_1\chi_1 y_2$ (see, for example, Dwight, *loc. cit.*, Art. 526.1 and 568.1), we shall have

$$Q_2 = \log\frac{a}{2\rho_1\chi_1} + \frac{2}{\pi}\sum_{m=1}^{\infty}\frac{(-)^m a^m}{m\,m!} + a_4\frac{e^{-a}}{a} + o\left\{\sqrt{\frac{2\rho_1\chi_1}{a}}\right\}.$$

When ρ, χ, is very small, and with a suitable value of a, this formula can give very great accuracy. In the applications to the Whirls representing the elementary particles the last term is quite negligible, and the error will be practically represented by the penultimate term.

Taking $a=3$ we shall obtain

$$\rho_1\chi_1 \cong \frac{3}{2}e^{-Q_2-0{\cdot}63} \cong 0{\cdot}8e^{-Q_2},$$

where the error is less than 1 per cent.

we can find by (19.12 *a*), (20.7), and (20.2) the ratio θ_y between the number of free magnetopolarized particles

Diagram showing the distribution of electric field in elementary particle.

SCALES.

Length: "a" represents $\begin{cases} 5{\cdot}15\times10^{-14}\text{cm. for the proton.} \\ 9{\cdot}5\times10^{-11}\text{cm. for the electron.} \end{cases}$

Intensity of the electric field:

The thickness "a" of the circular lines represents the field intensity:

$3{\cdot}33\times10^{20}\,\frac{\text{volt}}{\text{cm.}}$ for the proton.

$1{\cdot}0\times10^{12}\,\frac{\text{volt}}{\text{cm.}}$ for the electron.

(*i. e.*, magneto-protons and magneto-electrons) and the electropolarized ones.

$$\theta_g=\frac{\gamma}{2}\frac{\mathbf{F}_{D+}}{\underset{(+,\,-)}{\mathbf{F}_{D-}}}\left(1+\frac{m_{0-}}{m_{0+}}\right)^2\left(\frac{e}{m_{0+}}\right)^2\cong 2{\cdot}91\times10^{-28}. \quad . \quad (20.8)$$

The θ_g may be unequal in different parts of the Universe, and so may be the gravitation.

Apart from being the possible cause of gravitation, the magnetopolarized particles may also "act as a cement" in the atomic nuclei, owing to their close adhesion to the electropolarized particles in their immediate proximity.

It appears to be very probable that the positrons of Cosmic Rays are really the magneto-electrons. They are so penetrating not because their speed is very great, but because their force of interaction with the protons is comparatively small. For the same reason the positrons are influenced so little by the magnetic field, for the magnetic field is nothing else but a resultant of the magnetic fields of those particles of which matter consists, *i. e.*, chiefly of the protons and the electrons.

It is possible that the Cosmic Rays, a considerable part of which consist of positrons (*i. e.*, magneto-electrons), mostly come from the parts of the Universe where θ_g, and hence the gravitational constant, is higher than in our part. The expansion of the Universe may be due to the reduction of θ_g in the remote regions where this expansion is observed, or possibly to the reduction of θ_g everywhere, due to the gradual neutralizing of magneto-polarized particles throughout the Universe.

On the other hand, the electrons can occasionally behave for a very short time like positrons if their axes take an unstable orientation at which the distance forces may reverse.

Magneto-protons and positrons can form combinations similar to hydrogen atoms, only magnetopolarized. It is possible that the neutron may be such a combination.

The general way in which radiation from the systems of Whirls can be produced was discussed in section 15, where it was shown that the radiation can be either in the form of "beats" propagating in the e.m. field of the Whirls and superimposed on it, or in the form of the ejection of incomplete Whirls which break away from the structure of a compound Whirl, as a result of which the coefficient χ_1 of the remaining part of the Whirl becomes larger, and this remaining part becomes more stable.

In both cases of radiation the relationship between

the frequency and the amount of energy will follow quantum laws, which will also govern the absorption.

The energy levels, which determine the frequencies according to the quantum laws, will depend on the trajectories of the members of the atomic systems and on the vibrational states of these systems.

To upset the stability of a vibrational state it may be sufficient to alter the orientation of the axis of a particle, which may require very little energy. Hence the " trigger-like " action of the disturbing factors, which may be " beat waves," or the e.m. fields of the other particles.

The incomplete Whirls, which break away from the structure of elementary particles in the process of radiation, are the light quanta (or the " photons "). They spread all the time, tending to become simple Whirls (section 7). On the other hand, the elementary particle, being a compound Whirl, consists of an infinite number of infinitesimal simple Whirls (section 8). *Therefore matter can be considered as " condensed light."*

When these photons break away from a magneto-polarized elementary particle they represent magneto-polarized incomplete Whirls, and therefore their interaction with electropolarized particles (*i. e.*, electrons and protons), of which matter chiefly consists, is much weaker. These incomplete Whirls together with positrons, constitute penetrating " cosmic " rays. Only in a very rare case, when a positron comes very near to a proton, they interact violently (for in this case the force is inversely proportional to the cube of the distance), and this causes a violent disturbance of the e.m. field, which in its turn produces a partial disintegration of the surrounding atoms (ionization) with an energy which makes an impression of a very high velocity of the particles which constitute the cosmic rays.

If a system consists of pairs of " oppositely charged " particles it becomes neutral, because the force acting on a distant particle by the " oppositely charged " members of the system are equal and opposite, or, more precisely, because the e.m. waves, of which " oppositely charged " particles consist, are of different wave-lengths and frequencies, and this prevents the forcing of the outside particle into a stable phase of relationship with one of the members of the system.

For these reasons such systems as nuclei of atoms, where different particles are intermingled so closely, can interact with outside particles only as a result of a very rare coincidence of phases.

For the same reason an external " ring of electrons " practically protects the internal electrons from the influence of neighbouring elementary particles. Only when the momentum of an " invading " elementary particle is very large the disturbance can penetrate deeply enough. A change of wave-length with the speed (de Broglie relationship) provides a sort of additional defence for a stable system, for this change of wave-length creates a confusion of phases which counterbalance the large momenta in the cases where the velocities of the invaders are high.

All this contributes to the stability of the atomic systems.

We have assumed that the electrons and the protons are two pole Whirls ($n=1$) *. It follows from this assumption that there can be only one definite stable angular position of a proton or a nucleus relatively to an electron for any given distance between the centres of the former and the latter. Therefore the electrons cannot, so to speak, follow each other along the same trajectory. It appears to be possible to explain in this way the Pauli exclusion principle.

The phenomena for the explanation of which the indeterminacy principle has been brought forward can be explained by the vibrational state of the system of elementary particles. This vibrational state is associated with considerable energy, but it includes the fluctuations of the e.m. field, which are too rapid to be followed by observation (see sections 18 and 19).

We have discussed in this paper only " elliptically " polarized particles (electropolarized or magnetopolarized), but the possibility is not excluded that, apart from this kind of particle, combinations of coaxial and concentric contrapolarized particles, or, in other words, elementary particles with " ellipsoidally " polarized fields (see section 2) can exist.

There will not be included in the scope of this paper any detailed consideration of the question of how the macroscopic electric or magnetic fields are formed as a resultant of the corresponding fields of many particles.

* See sections 1 and 15.

It will be only noted that one of the necessary consequences of the present theory must be the impossibility of the existence of the electric or magnetic field which is literally permanent or uniform. The so-called "uniform" or "permanent" fields are all wave-like and oscillating with high frequencies, and they can occur only as a result of a certain coorientation of the axes and coordination of the motion of the great number of particles which create this field. When a free particle is placed in such a field it is synchronized by the force of interaction between this oscillating field and the particle *, in the same way as a frictionless rotor of a polyphase a.c. motor will sooner or later come into synchronism with a rotating magnetic field created by the stator. This appears to be the essence of the "electrization" and the "magnetization."

21. *Conclusion.*

Perhaps there is no need to emphasize that the electrodynamic theory of elementary particles, which is brought forward in this paper, does not come into conflict with modern Wave Mechanics or with the Theory of Relativity.

The preceding discussion has shown that the postulates which form the foundations of these great scientific disciplines can be explained on the basis of the Maxwell electromagnetic theory.

The main value of the Theory of Relativity and of Wave Mechanics is not in their postulates, but in their methods, and obviously the value of these methods can be only increased after having established their fundamental postulates on the basis of Classical Theory, even if the new method of approach would lead to a certain revision of details.

It follows from the present theory of elementary particles that all our present physical experience is determined by the Maxwell equations and by four independent fundamental constants: c, $\hbar$, e, and m_{0-} (since $\frac{m_{0+}}{m_{0-}}$ is determined by the balance of attractive and repulsive electrostatic forces). This is equivalent to four independent scales of the four-dimensional

* An analogous position arises when an elementary particle moves on a rotating magnetic field created by polyphase currents. See N. Japolsky, Royal College of Science, Phys. and Math., Society Scientific Journal, 1931.

continuum which may represent our Universe. In this respect the present theory, in spite of being strictly classical, can provide an additional argument in favour of the Relativistic methods.

It may be noted, however, that the scope of the theory of elementary particles, which was here discussed, is not necessarily limited by present-day experience.

As has been mentioned above (section 15), the force of interaction between the Whirls with different numbers of poles ($2n$) must be very small. Thus it would not be, for instance, beyond the scope of this theory if alongside the world of elementary particles which we can directly observe another world of particles of different n existed at the same time and occupied the same space, which manifested itself to us only by its accidental interactions with the former world.

These indirectly discoverable particles could be still attributed to the same fundamental cause, the electromagnetic oscillations. In the same way as the two-pole elementary particles of our directly observable world can be considered as a condensation of a plurality of two-pole photons, the $2n$-pole particles could be considered as a condensation of $2n$-pole photons.

The Universe would still remain 'The Universe of Light' *.

Summary.

It is suggested that the elementary particles like electrons, protons, positrons, light quanta, and so on can be considered as certain systems of Maxwell electromagnetic Waves, which are called "Electromagnetic Whirls" (or simply "Whirls").

In this way the Quantum and Relativity Relationships, including de Broglie formula and gravitation, can be explained on the basis of Classical Electrodynamics.

The interaction between the particles of such a nature follows, on the average, the Inverse Square Law, which, however, breaks down when the distances between their centres are small, and, moreover, it admits occasional exceptions with a certain small probability.

Being the forms of the Maxwell waves these particles do not imply any discontinuity of electric lines of force—

* The title of the book by Sir William Bragg.

in other words, they do not contain any " charge " in the usually accepted sense.

It follows from this Theory that the balance of the attractive and repulsive electrostatic forces between the particles requires a definite numerical ratio between the masses of the proton and the electron. This happens to agree with the experimental data.

I am greatly indebted to Sir William H. Bragg, O.M., F.R.S., for his kind and encouraging interest in this paper.

I wish to thank Miss A. C. Lewis, B.Sc., for checking the bulk of the mathematical part of the paper and reading the proofs.

I take this opportunity of acknowledging my gratitude to the Managers of the Royal Institution for giving me, at the Davy Faraday Laboratory, the facilities for the experimental work in connexion with which this paper was written.

Royal Institution.
1st April, 1935.

LI. *Studies on the Oxidation of Metals.*—Part II. *Copper, Brass, Aluminium-Brass, Aluminium-Bronze, Magnesium, and some Magnesium Alloys. By* G. D. Preston, *M.A., and* L. L. Bircumshaw, *M.A., D.Sc.** (*From the National Physical Laboratory.*)

Introduction.

THIS paper contains an account of the results of a number of experiments carried out during the year 1934 on alloys of copper and of magnesium oxidized at temperatures up to 400° C. The investigations described have been of an exploratory nature with a view to ascertaining the nature of the oxide film formed at low temperatures. A considerable volume of work on the subject of oxidation of metals at higher temperatures than those here employed has been done by other investigators, and the nature of the film has been determined by chemical analysis. In the case

* Communicated by Sir J. E. Petavel, K.B.E., D.Sc., F.R.S.

of the thin films found at lower temperatures the composition of the film cannot, as a rule, be determined by chemical analysis; but electron diffraction supplies a method of ascertaining the crystal structure of the film, and so, by comparison with the X-ray results, of identifying the oxide or oxides present. The method also supplies information as to the fine grainedness of the oxide film and shows up any tendency to preferred orientation, both of which are factors which probably influence the rate of oxidation of the metal, by altering the ease with which oxygen can diffuse through the oxide film. In the case of alloys the process of oxidation is further complicated by the possibility of the formation of more than one oxide, or of a mixed oxide. To obtain information on this latter point was one of the chief objects of the present investigation.

Copper.

Experiments were carried out on electrolytic copper and on remelted electrolytic copper, at room temperatures. The surface of the specimens to be examined was polished as if for microscopical investigation. In all cases a spectrum was obtained from the polished surface which has been ascribed to Cu_2O crystals. A series of typical results is included in Table I., where the observed spacings can be compared with the X-ray results of Neuburger [1] up to the line (400) where his published list of reflexions stops. The spacings observed in the electron diffraction photographs agree with the structure of Cu_2O. The spectrum of the surface as polished consists of rather broad lines, especially the line (200). The quality of the photograph quoted in the last column is very much better than either of the other two. Whether this is due to some difference in the polishing or to the drying is not certain. The same specimen polished as before, but finished on dry "selvet," yielded a totally different spectrum, the spacings of which are given in Table II. The absence of any ring of spacing 1·50 Å. (the (220) reflexion) indicates that the film is not Cu_2O, nor does the spectrum appear to agree with that of monoclinic CuO. Similar results were obtained from the remelted electrolytic copper, all the specimens yielding spectra of Cu_2O. An attempt was made to examine the surface as soon after polishing as possible. It was placed in the

TABLE I.

hkl.	Cu_2O X-rays.		Polished electrolytic Cu.		After 15 hours in air in apparatus.		Repolished 6 hours in dry air in desiccator.	
	d.	I.	*d.*	I.	*d.*	I.	*d.*	I.
110	3·01	w	3·16	w	...	...	...	...
111	2·45	s	2·40	w	2·43	m	2·40	s
200	2·12	vw	2·0 ±0·1	m	2 09	m	2·09	s
211	1·735	w	1·71	m	..	...	...	...
220	1·50	s	1·47	m	1·50	m	1·49	s
310	1·415	w	...	...	...	...	...	...
311	1·28	s	...	...	1·28	w	...	...
222	1·225	vw	1·20	vw	...	...	1·21	m
312	1·135	w	..	...	...	...	...	...
400	1·06	s	...	...	...	..	1·05	w
420	...	...	0·92	vw	0·95	w	0·93	m
422	...	...	...	...	...	...	0·858	m
440	...	...	...	...	...	...	0·735	w
600 }	...	...	....	...	...	...	0·693	w
442 }								
	$a=4·25$.		$4·16 \pm 0·05$		$4·23 \pm 0·04$		$4·18 \pm 0·03$	

apparatus, which was immediately exhausted and swept out with a stream of hydrogen (from a cylinder) dried by passing over calcium chloride. Even with this treatment good photographs of Cu_2O were obtained. In many cases the rings of indices (111) and (222) showed a marked thickening and intensification in the plane containing the incident beam and the normal to the

TABLE II.

Electrolytic Copper polished and finished on Dry "Selvet."

I.	*d.*	I.	*d.*
w	3·34	s	1·72
m	3·05	w	1·39
m	2·43	m	1·29
vs	2·02	w	1·12
vs	1·92	w	1·00

TABLE III.

Remelted Electrolytic Copper heated for 1 hour in Air at 100° C.

I.	*d.*	Σh^2.	*a.*	I.	*d.*	Σh^2.	*a.*
vs	2·57	3	4·45	w	1·03	...	...
vs	2·17	4	4·34	s	0·973	20	4·35
vw	1·85	...	...	s	0·892	24	4·37
m	1·63	...	...	vw	0·767	32	4·33
vs	1·54	8	4·35	w	0·720	36	4·32
s	1·36	...	...	vw	0·680	40	4·30
s	1·24	12	4·30				$4·35 \pm 0·05$

surface suggesting the existence of some preferred orientation with the (111) plane parallel to the polished surface.

The effect of heating the specimens in a steam oven for one hour was next tried. The results from the electrolytic copper were variable, and the rings were too broad for even approximate measurement. The remelted copper gave quite good diffraction photographs, measurement of which showed that the film, which was now visible as a uniform brown coating, consisted of a mixture of Cu_2O and some new phase, possibly CuO. The analysis of a photograph is given in Table III. The

value of the parameter is about 2 per cent. higher than the X-ray value, the error being due no doubt to faulty measurement of the voltage of the electron beam.

Further heat treatment of the "remelted" copper was carried out at 183° C. in a bath of aniline boiling at atmospheric pressure. The specimen was heated up in the bath in an atmosphere of pure dry hydrogen (electrolytic) and maintained at 183° C. in a stream of hydrogen for ten minutes. A stream of oxygen (from a cylinder) was then introduced, and the heating continued for a further ten minutes. This treatment produced a very uniform slate grey film, which gave good diffraction patterns. The spacings deduced from the measurement of the ring radii again agreed closely with those to be expected from Cu_2O, but the intensities and breadths of the lines were markedly different from those observed in the specimens oxidized at room temperature. At this higher temperature the rings (111) and (220) are both very intense and very broad, (200) is quite sharp and less intense than either of these, while (222) is sharp and consists of a comparatively short arc. At the lower temperature the rings are equally sharp, but (200) is generally as intense as or more intense than either (111) or (220).

The effect of "activating" the polished surface by eight successive reductions and oxidations at 183° was next investigated. The spectra consist of a number of broad rings, the spacings of which agree, within the accuracy to which they can be measured, with those of Cu_2O. All the rings are now broad, unlike the once oxidized surface, which gave a narrow (200), and the (222) rings show no signs of any "arcing." This suggests that the effect of repeated reduction and oxidation is to produce a surface consisting of a number of very small crystals with random orientation.

The results of experiments on freshly polished copper described above have an interesting bearing on Beilby's work on similar surfaces. Beilby [2], [3] found that small pits on the surface of copper after polishing were covered with a thin transparent film, which under high magnification had a uniform blue coloration by reflected light. Some of the blue films contained red patches, which he showed were due to light which, after passing

through the film, had been reflected from the surface of the cavity and then transmitted through the film again into the microscope objective. The films were assumed to be formed of metal which had flowed over the cavities in the process of polishing. The colours of thin films of metals are very variable, but copper films are not generally red [4], while cuprite (Cu_2O) is crimson-red by transmitted light. It seems quite possible, therefore, that Beilby's film on copper was really composed of crystals of Cu_2O and not of vitreous metal, a view which would be in accordance with the experiments described above.

The thickness of the film which Beilby observed was estimated at of the order of 100 to 200×10^{-8} cm. Pilling and Bedworth [5], in an extensive investigation of the rate of oxidation of copper, found that between 400° and 800° C. their results could be represented by

$$W^2 = AT^n t,$$

where

W is the weight in grammes of oxygen absorbed per sq. cm. of surface ;

t is the time in hours ;

T is one-thousandth of the absolute temperature $\left(= \frac{\theta}{1000}\right)$,

and $n = 16.3$;

$A = 10^{-5}$.

Extrapolating to the temperatures used in the present investigation, and converting the weight of oxygen into cubic centimetres of Cu_2O (density = 6·1 g./c.c.), we find

at 27° C.	after 1 hour	a thickness	25×10^{-8} cm.	Cu_2O.
100° C.	,, 1 hour	,,	150×10^{-8} ,,	,,
183° C.	,, 10 minutes	,,	300×10^{-8} ,,	,,

The first of these figures is very much smaller than Beilby's estimate of the film thickness ; it would appear that either Pilling and Bedworth's formula cannot be extrapolated to such a low temperature, or that the process of polishing produced a much thicker film than would be formed by oxidation in air for 1 hour at room temperatures. The film found at 100° C., as mentioned above, was just visible as a faint brown discoloration

of the polished surface, while ten minutes at 183° C. produced a grey film. It seems unlikely that a film of Cu_2O of only 150 Å. should be visible by reflected light on the surface of copper or that one of 300 Å. should be grey. Pilling and Bedworth have analysed the oxide film prepared at the higher temperatures they used, and found that there was about 2 per cent. of CuO present in the Cu_2O. The densities of the two oxides are almost equal, so that if it were assumed that the colour of the film formed at 183° C. was due to CuO superimposed on Cu_2O, it would be caused by a film of only 6 Å. thickness. This seems highly improbable, and it is much more likely that the results of Pilling and Bedworth experiments cannot be extrapolated to the lower temperatures employed in the present work. The films are probably at least ten times the thickness deduced from the formula applicable at the higher temperatures.

Dunn [6], using an optical method, determined the equivalent air thickness of the oxide film on normal and on activated copper at different temperatures. His figures are of the order of 2000 Å. in four minutes at 184° C. for activated copper, and for normal copper the same thickness is produced in the same time at 444° C. He suggests that certain anomalies in the oxidation rate at 200°–230° C. is due to the annealing of a structureless oxide film or a polymorphic change in the oxide. The present investigation shows that the first alternative is untenable because the oxide film formed at lower temperatures is crystalline.

The absence of any definite evidence of the presence of a film of CuO on the surface of the specimens is of some interest. The photographs of the film formed at room temperature do not show any rings other than those to be expected from Cu_2O. At 100° C. and 183° C. extra lines are occasionally observed and intensity variations occur, which may indicate the presence of CuO, but this cannot be detected with certainty. The lowest oxide would naturally be expected to be found in contact with the metal, but on the surface of this there should be a film of the higher oxide, since the oxygen pressure is greatly in excess of the dissociation pressure of CuO [11]. There is a considerable mass of evidence which shows that Cu_2O does not oxidize appreciably at temperatures up to about 100° C. For

instance, Neuburger prepared the material for X-ray examination by precipitation of Cu_2O, which was then dried for 30 hours at 110° C. and showed by analysis a copper content of 88·65 per cent. compared with the theoretical 88·2 per cent. for Cu_2O, representing a purity of 99·81 per cent. Cu_2O. The same treatment is common practice in the estimation of sugars, so that it must be assumed that the film of CuO is too thin to affect the weight of the product.

One further point deserves mention. Finch, Quarrell, and Roebuck have described an experiment in which they were unable to get any diffraction effect from the surface of polished copper. We have been unable to repeat this experiment, but the conditions of polishing may not have been severe enough to produce the layer of highly cold worked metal which these investigators show to have been present on their specimens.

Brass.

The experiments on brass were carried out on material kindly supplied by the British Non-ferrous Metals Research Association. The samples were short lengths of condenser tubing of the following compositions :—

Brass No.	Cu.	Zn.	Al.	Fe.	As.
1	76·1	21·6	2·0	0·06	0·003
2	76·0	21·8	1·96	0·03	0·02
3	69·6	30·28	..	0·196	nil
4	70·3	29·4	..	0·03	0·02

For the present purpose it will be noted that nos. 1 and 2 contain 2 per cent. aluminium and that 2 and 4 are arsenical. The results obtained from specimens cut from the samples are summarized in Table IV. They have been examined after heating in air at 100° C. and in oxygen at 183° C. and 400° C. The presence of arsenic does not appear to have any effect on the results, but it is to be observed that the aluminium brasses yield very poor results at the lower temperatures. The brasses without aluminium show the presence of Cu_2O after treatment at 100° C., and in the case of no. 4 immediately after polishing. The aluminium brasses show the presence of Cu_2O when heated in oxygen at

183° C., and all the specimens yielded a spectrum resembling that of ZnO at 400° C. This film may be due to the condensation of ZnO formed by the oxidation of zinc which has volatilized from the brass at the higher temperature. Condensed films of ZnO give good diffraction photographs, and a film of this nature might mask the

TABLE IV.

Brass No.	Condition of surface.	Structure.
1 ... (2% Al)	Filed.	Face-centred cube $a=3{\cdot}68$ Brass.
	Filed heated 100° C.	No diffraction effect.
	Filed heated 400° C. until colour just changed.	Hexagonal $a=3{\cdot}23$, $c=1{\cdot}61$ ZnO.
	Polished.	? cubic $a=5{\cdot}5$.
	Polished heated 183° C. (10 min.).	Cubic $a=4{\cdot}39$ Cu_2O.
	Polished heated 400° C. (3 min.).	Hexagonal $a=3{\cdot}22$, $c=1{\cdot}61$ ZnO, other lines not identified.
2 ... (2% Al)	Polished.	Very faint broad bands, not measurable.
	Polished heated 183° C. (10 min.).	Cubic $a=4{\cdot}40$ Cu_2O.
	Polished heated 400° C. (3 min.).	Hexagonal $a=3{\cdot}27$, $c=1{\cdot}61$ ZnO, and other lines.
3 ...	Polished.	Faint lines, not identified.
	Polished 100° C. (30 min.).	Cubic $a=4{\cdot}50$ Cu_2O.
	Polished 183° C. (10 min.).	Cubic $a=4{\cdot}50$ Cu_2O.
	Polished 400° C. (3 min.).	Hexagonal $a=3{\cdot}25$, $c=1{\cdot}61$ ZnO, and other lines.
4 ...	Polished.	Cubic $a=4{\cdot}20$ Cu_2O. Oriented (111) parallel surface.
	Polished 100° C. (60 min.).	Cubic $a=4{\cdot}30$ Cu_2O. Oriented (111) parallel surface.
	Polished 183° C. (30 min.).	Cubic $a=4{\cdot}30$ Cu_2O rings broad.
	Polished 400° C. (3 min.).	Hexagonal $a=3{\cdot}21$, $c=1{\cdot}61$ ZnO.

underlying film of copper oxide. The experiments show clearly that the effect of the aluminium is to inhibit the formation of a Cu_2O film on the surface at the lower temperature, but no light is thrown on the mechanism of this protective action. This is quite in accordance with results obtained from the surface of aluminium oxidized in the solid state. Our results, which we hope to publish shortly, show that the protective film on aluminium is almost amorphous, yielding diffraction patterns of the type obtained from glasses and vitreous

silica by X-rays. Liquid aluminium is covered with a layer of γ-Al_2O_3, the cubic modification of the oxide. The absence, therefore, of any diffraction effects which could be ascribed to a film of Al_2O_3 on the surface of the aluminium brasses does not prove that no such film exists. The inference to be drawn from the experiments is that the film if present is amorphous or in such a condition as not to produce diffraction effects of the type characteristic of a crystalline substance. The enhanced corrosion resisting properties produced by the addition of 2 per cent. of aluminium is evidence that the Al_2O_3 film, although not observed in this investigation, is present and inhibits the formation of the oxides of copper and of zinc.

The presence of ZnO in the films formed on brasses has been noticed by Dunn [7]. Using oxidation temperatures between 600° C. and 880° C., he found by chemical analysis that the film on a brass containing 29 per cent. zinc was almost pure ZnO at the higher temperatures, the copper content rising to 11·5 per cent. at the lowest temperature (580° C.). Two other brasses, containing approximately 10 and 5 per cent. zinc, yielded films in which the zinc : copper ratio was essentially identical with that prevailing in the alloy. He suggests that the cuprous oxide and zinc oxide are apparently in solid solution. The present investigation shows that these two oxides exist as separate phases (at any rate at the lower temperatures here employed) with the usual structures of ZnO and Cu_2O.

Aluminium Bronze.

The analysis of the material showed it to contain 89 per cent. copper, 7 per cent. aluminium, and 4 per cent. manganese by weight. The polished surface, examined as polished and after exposure to air at 100° C. for half an hour, yielded spectra which have not yet been assigned to their proper origin. They do not correspond with the spectra of Cu_2O, CuO, MnO, or MnO_2. It is possible that they may arise from $Mn(OH)_2$, but this cannot be stated with certainty, as the agreement is by no means good. Treated in dry oxygen at 183° C. for 10 mins. the surface became covered with a very uniform brown film, which yielded a spectrum with rather broad lines but identified with Cu_2O. At 400° C.

after a few minutes the film showed strong purple interference colours and gave an electron diffraction photograph, the lines of which correspond with tetragonal MnO_2 ($a=4{\cdot}40$ Å., $c=0{\cdot}66$). A freshly filed surface of the metal gave the lines of a face-centred cube of side 3·65 Å., about the value to be expected from the metal. The same surface after treatment at 183° C. for ten minutes showed the presence of Cu_2O, and at 400° C. a new set of lines, rather faint, but probably MnO_2. None of the spectra could be ascribed to γAl_2O_3.

Alloys of Magnesium.

Magnesium and a number of its alloys, whose resistance to corrosion is known to differ from that of magnesium, were examined after oxidation at 100° C. in air and at 400° C. in oxygen. In most cases at the lower temperature some lines of the spectrum of MgO (cubic NaCl type) are observed. At the higher temperature MgO is always present, and in one case (a zinc manganese alloy) a few lines of another phase are present. The results are summarized below :—

Magnesium.—As polished. Four rather faint lines accompanied by a large amount of background scattering. These lines correspond with the reflexions (200), (220), and (222) of cubic MgO. The ring (222) shows distinct signs of being "arced," indicating some preferred orientation with a (111) parallel to the polished surface. After heating the specimen at 100° C. for an hour in air the photographs became so blackened by background scattering that the lines of the diffraction pattern could not be accurately measured. Treatment at 400° C. in oxygen yielded a very good photograph of MgO. The (222) reflexion was thickened in the plane containing the incident ray and the normal to the polished surface.

Magnesium, 1·2 per cent. Manganese (by weight).—The surface was filed and yielded a spectrum, the lines of which could all be assigned to either MgO or Mg. Heating in air at 100° C. spoiled the quality of the photographs, and no conclusions can be drawn as to the nature of the change produced in the surface. Treatment at 400° C. in oxygen produced cubic MgO.

Magnesium, 4 per cent. Zinc, 1 per cent. Manganese.—The surface was filed and gave a photograph on which

lines due to MgO were present. Three other reflexions, two of which were dots, probably arise from ZnO. After heating at 100° C. in air the lines of MgO could still be identified. Treatment at 400° C. in oxygen gave a very good photograph of MgO and two extra lines as before ascribable to the presence of ZnO.

Magnesium, 15 per cent. Cadmium.—The filed surface gave a photograph with five lines, two of which were too broad for accurate measurement. The lines may be due to cubic MgO, or possibly the β-modification of MgO described by Finch and Quarrell. The photographs of the specimen after heating at 100° C. showed little change. Heating at 400° C. produced good photographs of MgO.

0·5 per cent. Magnesium, 4 per cent. Copper, 95·5 per cent. Aluminium.—Although this alloy contains so small a quantity of magnesium, the filed surface after treatment in oxygen at 400° C. gave a photograph on which two lines appeared faintly. The spacings calculated from these rings correspond with those of the most intense rings in the MgO spectrum (220) and (222). Darbyshire [8] found that the oxide film removed from molten antimony containing 1 per cent. magnesium consisted almost entirely of MgO, with traces of metallic antimony. It appears, therefore, that even at very low concentrations there is a preferential oxidation of magnesium.

The Orientation of the Films.

Many of the films described above show signs of preferred orientation. In the case of the films of Cu_2O on polished copper and brass there is a tendency for a (111) plane to lie parallel to the surface. There is a certain amount of variability in the results—some specimens showed orientation after polishing, in others the orientation developed during treatment at 100° C. Increased amounts of oxidation at the higher temperatures tended to reduce the amount of orientation, as judged by the absence of arcs on the diffraction rings. It seems, therefore, that the oriented film is a stage in the growth of the oxide layer on the polished metal, the thinnest films being largely oriented and the orientation disappearing as the film grows at higher temperatures. The lack of orientation in some of the films on polished copper may

be due to variations in the conditions of polishing which have produced a rougher surface than that on which oriented films have been found after polishing.

The type of orientation observed in the Cu_2O films is of particular interest, because in this structure the (111) planes are those in which the copper atoms have the highest density per unit area. The structure consists of a face-centred cube of copper atoms intermeshed with a body centred cube of oxygen atoms, the origin of the latter structure dividing a cube diagonal of the copper lattice in the ratio 1 : 3. The (111) planes of the structure are, therefore, planes of copper atoms dividing the cube diagonal into three equal parts. These planes of copper atoms are interleaved with planes of oxygen atoms, which are separated by one-sixth of the length of the cube diagonal. Two such planes of oxygen atoms lie between every pair of copper planes. The density of packing is one copper atom in $a^2\sqrt{3}/4$ square Ångstrom units and one oxygen atom in $a^2\sqrt{3}$ square Ångstrom units. The copper planes are thus four times as densely populated as the oxygen planes. If the orientation of the crystals is connected with the density of packing in the (111) planes we must suppose that it is the high density of the copper atoms and not the low density of oxygen atoms that is operative, because there are many planes (all those for which the sum of the squares of the indices exceeds twelve) in which the density of oxygen is less than in the (111) planes of the Cu_2O structure. The (111) planes of copper atoms are the most closely packed planes of metal atoms in the crystal. It seems possible, therefore, that the orientation is connected with density of packing on these planes.

In the case of MgO films there is some indication of a tendency to orientation with a (111) plane parallel to the surface. The " arcing " of the reflexion (222) is not so pronounced as in the copper oxide films, and sometimes amounts rather to a broadening of the ring in the plane containing the incident beam and the normal to the surface. This broadening may be due to grain size, and if so indicates that those crystals which have a (111) plane parallel to the surface of the specimen are very thin, or that the electron beam does not penetrate to a sufficient depth for the volume diffraction effect

to be completely effective. Neglecting this broadening there is still in the earlier stages of oxidation some orientation with (111) parallel to the surface. In MgO the (111) planes are the most densely packed per unit area of those planes, which are alternately all magnesium or all oxygen. In the (100) and (110) planes the density of packing is greater than in (111), but these planes all contain equal numbers of magnesium and oxygen. We cannot tell from the fact that the film presents a (111) face to the surface whether this is due to density of packing of metal or oxygen ions, because the density is the same per unit area for both sorts of ion. The idea, derived from a study of the copper films, that it is the most densely packed plane of metal atoms which determines the orientation is quite consistent with the type of orientation observed in MgO films. Some support for this hypothesis can be derived from the observations of other investigators. Finch and Quarrell [9] and Jenkins [10] have shown that the film of ZnO on molten zinc is oriented with a (0001) plane parallel to the surface. This is the most densely packed plane of atoms in the hexagonal structure. Jenkins has also shown that the film of SnO on liquid tin has a (001) plane parallel to the surface. In this case the tin atoms are arranged on a tetragonal lattice of side $a=3{\cdot}80$ Å. and axial ratio $c=1{\cdot}26$, the coordinates of the two tin atoms in the cell being (000) and $(\frac{1}{2}\frac{1}{2}\,u)$, where u is undetermined, but, according to Jenkins is not $\frac{1}{2}$. Actually the most densely packed planes are (110) with one atom in an area $a^2c/\sqrt{2}(=0{\cdot}89a^2)$, while in the (001) planes the area per atom is a^2. If, however, u is small the second atom will be nearly in the (001) plane and the density (with $u=0$) would be $a^2/2$.

Summary.

(1) *Copper.*—The oxide film on copper formed at room temperature and 100° C. in air and at 183° C. in oxygen at atmospheric pressure consists of Cu_2O with the usual cubic structure of this oxide. No definite indication of the presence of CuO could be found. The oxide is oriented with a (111) plane parallel to the polished surface of the metal.

(2) *Brass.*—A brass containing 30 per cent. zinc, 70 per cent. copper oxidized at temperatures up to

183° C., is covered with a film of Cu_2O. At 400° C. the oxide film is ZnO.

Aluminium brasses (22 per cent. zinc, 2 per cent. aluminium) show the presence of Cu_2O after oxidation at 183° C. for 10 minutes. At 400° C. ZnO is present with another phase not identified. The oxide film formed at room temperatures does not give sufficiently good photographs for interpretation. The absence of any trace of Al_2O_3 is ascribed to the amorphous nature of this film.

(3) *Magnesium and Magnesium Alloys.*—In all cases the metal oxidized at 400° C. is covered with film of cubic MgO. At lower temperatures the photographs are difficult to interpret, but the presence of cubic MgO is probable.

(4) The films of oxide on polished surfaces are generally oriented. The nature of the orientation is discussed. It is suggested that the plane in the oxide having the highest density of metal atoms per unit area tends to lie on the polished surface.

Acknowledgments.

We have great pleasure in thanking Dr. C. H. Desch, Superintendent of the Department of Metallurgy and Metallurgical Chemistry, for his interest in and encouragement of the research. We are indebted to Mr. J. Trotter for considerable assistance in the experimental work.

References.

(1) Neuburger, *Zeit. f. Phys.* lxvii. p. 845 (1931).
(2) Beilby, Proc. Roy. Soc. A, lxxxix. p. 593 (1914).
(3) Beilby, Aggregation and Flow of Solids, London, p. 88 (1921).
(4) Turner, Proc. Roy. Soc. A, lxxxi. p, 301 (1908).
(5) Pilling and Bedworth, Journ. Inst. Metals, xxix. p. 529 (1923).
(6) Dunn, Proc. Roy. Soc. A, cxi. p. 210 (1926).
(7) Dunn, Proc. Roy. Soc. A, cxi. p. 203 (1926).
(8) Darbyshire, Trans. Faraday Soc. xxx. p. 1038 (1934).
(9) Finch and Quarrell, Proc. Phys. Soc. xlvi. p. 148 (1933).
(10) Jenkins, Proc. Phys. Soc. xlvii. p. 109 (1935).
(11) Smyth and Roberts, J. Am. Chem. Soc. xlii. p. 2582 (1920).
(12) Finch, Quarrell, and Roebuck, Proc. Roy. Soc. A, cxlv. p. 676 (1934).

LII. *The Circular and Hyperbolic Functions, argument* $x/\sqrt{2}$. By J. R. Airey, *M.A., D.Sc., Sc.D.**

THE circular and hyperbolic functions, $\sin x$, $\cos x$, $\sinh x$, $\cosh x$ have been extensively tabulated in the Memoirs [1] of the National Academy of Science, Washington, and in the Reports [2] of the Mathematical Tables Committee of the British Association for the Advancement of Science.

In the calculation of ber x and bei x, the argument z of the Bessel function of zero order $J_0(z)$ is taken along the "semi-imaginary" axis $z=xe^{-\frac{i\pi}{4}}$: in this case, the circular and hyperbolic sines and cosines of $x/\sqrt{2}$ appear in the asymptotic expansion of $J_0(z)$. Other examples occur in the sine and cosine integrals, $\mathrm{Si}(x\sqrt{i})$ and $\mathrm{Ci}(x\sqrt{i})$.

The calculations of sin, cos, sinh, and cosh $x/\sqrt{2}$ for $x=2$ to 20 were based on values of these functions when $x=1$ to twenty or more places of decimals, viz. :—

$$\begin{aligned}
\sin 1/\sqrt{2} &= 0{\cdot}64963\ 69390\ 80062\ 44413\\
\cos 1/\sqrt{2} &= 0{\cdot}76024\ 45970\ 75630\ 15125\\
\sinh 1/\sqrt{2} &= 0{\cdot}76752\ 31451\ 26116\ 33163\\
\cosh 1/\sqrt{2} &= 1{\cdot}26059\ 18365\ 21356\ 11948
\end{aligned}$$

The accuracy of each calculation, say $\sin(x+h)$, was checked by comparison with $\sin(x-h)$. The same procedure was adopted in finding intermediate values for intervals 0·1.

$$\begin{aligned}
\sin 0{\cdot}1/\sqrt{2} &= 0{\cdot}07065\ 17672\ 83193\ 533\\
\cos 0{\cdot}1/\sqrt{2} &= 0{\cdot}99750\ 10414\ 93071\ 056\\
\sinh 0{\cdot}1/\sqrt{2} &= 0{\cdot}07076\ 96184\ 16898\ 765\\
\cosh 0{\cdot}1/\sqrt{2} &= 1{\cdot}00250\ 10418\ 40293\ 280
\end{aligned}$$

In the early stages of this work, use was made of tables of the first hundred multiples of sin, cos, sinh, cosh $0{\cdot}1/\sqrt{2}$: later, Dr. Comrie kindly provided the first thousand multiples of these values, which facilitated the computations considerably.

* Communicated by the Author.

From the relations between the circular and Bessel functions,

$$\sin x/\sqrt{2}=\sqrt{2}[J_1(x)+J_3(x)-J_5(x)-J_7(x)+J_9(x)+\ldots.]$$

and

$$\cos x/\sqrt{2}=J_0(x)-2[J_4(x)-J_8(x)+J_{12}(x)-J_{16}(x)+\ldots.],$$

the values of $\sin x/\sqrt{2}$ and $\cos x/\sqrt{2}$, $x=1$ to 20, were compared with Meissel's eighteen place tables of $J_n(x)$. This comparison[3] led to the discovery of four errors :

$J_4(5)$	$=+0\cdot391232$	360458	648178
$J_{23}(6)$	$=+0\cdot$	2	495677
$J_{20}(14)$	$=+0\cdot$	16775	399534
$J_{21}(16)$	$=+0\cdot$	152594	322163

x.	$\sin x/\sqrt{2}$.	$\cos x/\sqrt{2}$.
0·0....	+0·00000 00000 00	+1·00000 00000 00
·1....	·07095 17672 83	0·99750 10414 93
·2....	·14095 04228 97	·99001 66555 60
·3....	·21054 46199 93	·97758 42485 39
·4....	·27908 65325 52	·96026 59565 71
0·5....	+0·34623 35937 81	+0·93814 83350 40
·6....	·41165 02082 40	·91134 19259 84
·7....	·47500 94291 21	·87998 07056 10
·8....	·53599 45922 93	·84422 14146 97
·9....	·59430 08989 74	·80424 27752 11
1·0....	+0·64963 69390 80	+0·76024 45970 76
·1....	·70172 61476 76	·71244 67795 34
·2....	·75030 81872 19	·66108 82121 11
·3....	·79514 02487 07	·60642 55806 66
·4....	·83599 82652 18	·54873 20844 93
1·5....	+0·87267 80317 76	+0·48829 60708 99
·6....	·90499 62259 51	·42541 95940 65
·7....	·93279 13240 91	·36041 69054 03
·8....	·95592 44086 02	·29361 28829 58
·9....	·97427 98622 47	·22534 14076 89
2·0....	+0·98776 59459 93	+0·15594 36947 65
·1....	·99631 52575 11	·08576 65881 96
·2....	·99988 50680 53	+0·01516 08273 37
·3....	·99845 75360 01	−0·05552 07060 80
·4....	·99203 97960 42	·12592 47516 15
2·5....	+0·98066 39235 08	−0·19569 94356 91
·6....	·96438 67740 66	·26449 60302 28
·7....	·94328 96995 58	·33197 06955 56
·8....	·91747 81414 12	·39778 61988 96
·9....	·88708 11036 52	·46161 35998 24

x.	$\sin x/\sqrt{2}$.	$\cos x/\sqrt{2}$.
3·0....	+0·85225 05081 52	−0·52313 38942 89
·1....	·81316 04353 38	·58203 96089 62
·2....	·77000 62541 48	·63803 63379 72
·3....	·72300 36456 01	·69084 42143 12
·4....	·67238 75248 31	·74019 93085 99
3·5....	+0·61841 08670 12	−0·78585 49481 69
·6....	·56134 34429 99	·82758 29499 22
·7....	·50147 04710 41	·86517 47607 70
·8....	·43909 11912 84	·89844 24999 61
·9....	·37451 73701 92	·92721 97980 96
4·0....	+0·30807 17423 63	−0·95136 31281 26
·1....	·24008 63975 32	·97075 15241 92
·2....	·17090 11208 09	·98528 81846 98
·3....	·10086 16944 67	·99490 04566 23
·4....	+0·03031 81697 46	·99954 02986 29
4·5....	−0·04037 68826 71	−0·99918 45211 70
·6....	·11087 01347 79	·99383 49023 93
·7....	·18080 92671 54	·98351 81792 48
·8....	·24984 47298 17	·96828 59138 62
·9....	·31763 14892 54	·94821 42358 32
5·0....	−0·38383 07528 66	−0·92340 34617 40
·1....	·44811 16622 28	·89397 75937 77
·2....	·51015 29466 90	·86008 36999 87
·3....	·56964 45290 60	·82189 11792 40
·4....	·62628 90753 45	·77959 09145 85
5·5....	−0·67980 34808 06	−0·73339 43192 33
·6....	·72992 02848 84	·68353 22799 36
·7....	·77638 90079 51	·63025 40030 28
·8....	·81897 74031 86	·57382 57689 14
·9....	·85747 26173 24	·51452 96012 27
6·0....	−0·89168 22544 79	−0·45266 18572 92
·1....	·92143 53377 23	·38853 17469 59
·2....	·94658 31636 16	·32245 97871 98
·3....	·96700 00454 10	·25477 62001 79
·4....	·98258 39412 24	·18581 92628 55
6·5....	−0·99325 69640 42	−0·11593 36162 76
·6....	·99896 57709 79	−0·04546 85431 04
·7....	·99968 18298 94	+0·02522 37780 74
·8....	·99540 15619 82	·09579 00329 02
·9....	·98614 63596 68	·16587 75370 95
7·0....	−0·97196 24796 86	+0·23513 59991 23
·1....	·95292 08118 89	·30321 92709 40
·2....	·92911 65249 53	·36978 70780 05
·3....	·90066 85907 30	·43450 67199 40
·4....	·86771 91896 33	·49705 47333 48

x.	$\sin x/\sqrt{2}$.	$\cos x/\sqrt{2}$.
7·5....	−0·83043 30000 35	+0·55711 85084 46
·6....	·78899 63752 17	·61439 78514 73
·7....	·74361 64119 91	·66860 64850 25
·8....	·69451 99156 49	·71947 34788 49
·9....	·64195 22664 03	·76674 46039 33
8·0....	−0·58617 61930 03	+0·81018 36031 15
·1....	·52747 04596 35	·84957 33718 83
·2....	·46612 84726 83	·88471 70434 41
·3....	·40245 68143 06	·91543 89726 35
·4....	·33677 37101 70	·94158 56138 12
8·5....	−0·26940 74389 78	+0·96302 62882 31
·6....	·20069 46917 63	·97865 38371 78
·7....	·13097 88891 33	·99138 51575 46
·8....	−0·06060 84648 85	·99816 16171 66
·9....	+0·01006 48754 41	·99994 93478 58
9·0....	+0·08068 79123 55	+0·99673 94146 92
·1....	·15090 76777 79	·98854 78606 46
·2....	·22037 32191 52	·97541 56264 28
·3....	·28873 73534 65	·95740 83458 56
·4....	·35565 84024 45	·93461 60178 22
9·5....	+0·42080 19002 45	+0·90715 25564 92
·6....	·48384 22650 68	·87515 52219 65
·7....	·54446 44264 03	·83878 39342 65
·8....	·60236 53997 18	·79822 04740 69
·9....	·65725 58007 52	·75366 75741 85
10·0....	+0·70886 12918 38	+0·70534 79063 08
·1....	·75692 39530 13	·65350 29681 31
·2....	·80120 35710 85	·59839 18763 50
·3....	·84147 88401 97	·54029 00716 29
·4....	·87754 84678 97	·47948 79419 67
10·5....	+0·90923 21811 79	+0·41628 93713 62
·6....	·93637 16274 73	·35101 02210 25
·7....	·95883 11660 78	·28397 67507 32
·8....	·97649 85460 86	·21552 39882 06
·9....	·98928 54673 96	·14599 40546 72
11·0....	+0·99712 80220 37	+0·07573 44549 68
·1....	·99998 70135 71	+0·00509 63407 43
·2....	·99784 81529 97	−0·06556 72445 70
·3....	·99072 21301 62	·13590 31302 36
·4....	·97864 45603 36	·20555 97833 35
11·5....	+0·96167 58062 12	−0·27418 90656 96
·6....	·93990 06762 14	·34144 79738 60
·7....	·91342 80006 35	·40700 03533 86
·8....	·88239 00877 10	·47051 85789 22
·9....	·84694 20623 54	·53168 51916 46

x.	$\sin x/\sqrt{2}$.	$\cos x/\sqrt{2}$.
12·0....	+0·80726 10908 54	−0·59019 44859 05
·1....	·76354 54954 14	·64575 40371 02
·2....	·71601 37629 51	·69808 61632 09
·3....	·66490 34531 20	·74692 93126 05
·4....	·61047 00110 09	·79203 93712 81
12·5....	+0·55298 54904 43	−0·83319 08829 07
·6....	·49273 71942 86	·87017 81756 44
·7....	·43002 62385 22	·90281 63900 72
·8....	·36516 60473 04	·93094 24031 04
·9....	·29848 07864 85	·95441 56432 60
13·0....	+0·23030 37434 66	−0·97311 87932 34
·1....	·16097 56614 48	·98695 83762 35
·2....	·09084 30364 34	·99586 52231 76
·3....	+0·02025 63854 62	·99979 48183 74
·4....	−0·05043 15052 44	·99872 75220 39
13·5....	−0·12086 73434 71	−0·99266 86684 30
·6....	·19069 90967 46	·98164 85391 93
·7....	·25957 77517 61	·96572 22120 21
·8....	·32715 90587 14	·94496 92853 75
·9....	·39310 52518 41	·91949 34806 59
14·0....	−0·45708 67375 42	−0·88942 21238 33
·1....	·51878 37416 60	·85490 55090 41
·2....	·57788 79076 90	·81611 61474 61
·3....	·63410 38379 13	·77324 79051 02
·4....	·68715 05697 77	·72651 50338 81
14·5....	−0·73676 29801 16	−0·67615 11008 13
·6....	·78269 31102 22	·62240 78206 53
·7....	·82471 14051 16	·56555 37978 58
·8....	·86260 78608 47	·50587 31841 13
·9....	·89619 30740 74	·44366 42581 75
15·0....	−0·92529 91886 88	−0·37923 79350 93
·1....	·94978 07347 44	·31291 62122 82
·2....	·96951 53555 07	·24503 05602 10
·3....	·98440 44189 79	·17592 02657 33
·4....	·99437 35108 56	·10593 07363 66
15·5....	−0·99937 28064 46	−0·03541 17739 71
·6....	·99937 73196 84	+0·03528 41735 34
·7....	·99438 70280 12	·10580 37736 67
·8....	·98442 68724 94	·17579 45753 20
·9....	·96954 66331 61	·24490 67702 73
16·0....	−0·94982 06802 15	+0·31279 49415 12
·1....	·92534 76023 31	·37911 97895 91
·2....	·89624 97139 22	·44354 98284 24
·3....	·86267 24438 19	·50576 30420 23
·4....	·82478 36354 31	·56544 84939 09

x.	$\sin x/\sqrt{2}$.	$\cos x/\sqrt{2}$.
16·5....	−0·78277 25730 14	+0·62230 78811 46
·6....	·73684 93052 36	·67605 70252 37
·7....	·68724 33257 80	·72642 72924 19
·8....	·63420 25612 12	·77316 69362 77
·9....	·57799 21048 74	·81604 23559 49
17·0....	−0·51889 28919 61	+0·85483 92636 47
·1....	·45720 02954 34	·88936 37556 45
·2....	·39322 26497 73	·91944 32813 97
·3....	·32727 97099 40	·94492 75059 29
·4....	·25970 10532 76	·96568 90612 03
17·5....	−0·19082 44323 00	+0·98162 41826 88
·6....	·12099 40866 46	·99265 32279 69
·7....	−0·05055 90225 89	·99872 10747 93
·8....	+0·02012 87312 68	·99979 73965 65
·9....	·09071 58833 96	·99587 68139 18
18·0....	+0·16084 96450 67	+0·98697 89216 00
·1....	·23017 94935 61	·97314 81905 36
·2....	·29835 89240 47	·95445 37455 75
·3....	·36504 71813 90	·93098 90199 99
·4....	·42991 09632 15	·90287 12885 61
18·5....	+0·49262 60857 23	+0·87024 10813 48
·6....	·55287 91039 35	·83326 14814 29
·7....	·61036 88782 66	·79211 73097 74
·8....	·66480 80795 97	·74701 42015 40
·9....	·71592 46253 15	·69817 75783 19
19·0....	+0·76346 30391 68	+0·64585 15215 00
·1....	·80718 57281 08	·59029 75523 74
·2....	·84687 41697 65	·53179 33250 67
·3....	·88233 00045 99	·47063 12388 53
·4....	·91337 60272 92	·40711 69767 63
19·5....	+0·93985 70723 98	+0·34156 79778 08
·6....	·96164 07898 51	·27431 18504 46
·7....	·97861 83064 39	·20568 47352 19
·8....	·99070 47699 44	·13602 96247 55
·9....	·99783 97732 23	+0·06569 46495 14
20·0....	+0·99998 76561 22	−0·00496 86621 33

x.	$\sinh x/\sqrt{2}$.	$\cosh x/\sqrt{2}$.
0·0....	0·00000 00000 00	1·00000 00000 00
·1....	0·07076 96184 17	1·00250 10418 40
·2....	0·14189 32323 87	1·01001 66777 82
·3....	0·21372 66081 80	1·02258 45016 64
·4....	0·28662 90623 51	1·04026 73787 95

x.	$\sinh x/\sqrt{2}$.	$\cosh x/\sqrt{2}$.
0·5....	0·36096 52590 77	1·06315 37604 04
·6....	0·43710 70342 35	1·09135 81260 88
·7....	0·51543 52553 56	1·12502 15564 44
·8....	0·59634 17267 56	1·16431 24387 68
·9....	0·68023 11493 75	1·20942 73093 41
1·0....	0·76752 31451 26	1·26059 18365 21
·1....	0·85865 43558 76	1·31806 19495 55
·2....	0·95408 06275 66	1·38212 51187 56
·3....	1·05427 92903 93	1·45310 17934 58
·4....	1·15975 15464 54	1·53134 70049 28
1·5....	1·27102 49767 98	1·61725 21422 60
·6....	1·38865 61804 37	1·71124 69101 41
·7....	1·51323 35584 94	1·81380 14782 64
·8....	1·64538 02574 38	1·92542 88331 61
·9....	1·78575 72861 17	2·04668 73442 03
2·0....	1·93506 68221 74	2·17818 35566 09
·1....	2·09405 57244 04	2·32057 52254 36
·2....	2·26351 92685 98	2·47457 46057 28
·3....	2·44430 51255 87	2·64095 20152 72
·4....	2·63731 76013 54	2·82053 96877 93
2·5....	2·84352 21604 56	3·01423 59358 56
·6....	3·06395 02553 52	3·22300 96443 04
·7....	3·29970 44858 19	3·44790 51166 95
·8....	3·55196 41142 45	3·69004 72990 03
·9....	3·82199 09644 00	3·95064 74066 86
3·0....	4·11113 57331 87	4·23100 89832 90
·1....	4·42084 47469 32	4·53253 44208 82
·2....	4·75266 71960 41	4·85673 19749 32
·3....	5·10826 28841 70	5·20522 33087 35
·4....	5·48941 05307 09	5·57975 16051 04
3·5....	5·89801 66680 79	5·98219 02859 18
·6....	6·33612 51783 72	6·41455 23831 37
·7....	6·80592 75170 19	6·87900 06081 49
·8....	7·30977 36746 29	7·37785 81698 42
·9....	7·85018 39318 46	7·91362 03954 83
4·0....	8·42986 14659 98	8·48896 72125 60
·1....	9·05170 58726 19	9·10677 65539 95
·2....	9·71882 76694 66	9·77013 87538 14
·3....	10·43456 38555 94	10·48237 20052 51
·4....	11·20249 46032 98	11·24703 89586 29
4·5....	12·02646 11664 38	12·06796 45420 36
·6....	12·91058 50947 15	12·94925 50939 38
·7....	13·85928 88500 00	13·89531 89034 20
·8....	14·87731 79278 67	14·91088 82608 26
·9....	15·96976 45949 52	16·00104 31290 64

x.	$\sinh x/\sqrt{2}$.	$\cosh x/\sqrt{2}$.
5·0....	17·14209 33608 99	17·17123 65540 11
·1....	18·40016 83122 99	18·42732 19411 00
·2....	19·75028 24453 33	19·77558 23345 47
·3....	21·19918 91438 75	21·22276 18456 64
·4....	22·75413 59604 74	22·77609 93874 66
5·5....	24·42290 08692 27	24·44336 48843 22
·6....	26·21383 11718 51	26·23289 81377 64
·7....	28·13588 52515 85	28·15365 05428 76
·8....	30·19867 73837 75	30·21522 98639 17
·9....	32·41252 58272 82	32·42794 82931 65
6·0....	34·78850 44372 76	34·80287 40333 66
·1....	37·33849 80575 87	37·35188 66618 07
·2....	40·07526 19696 90	40·08773 65529 57
·3....	43·01248 56956 87	43·02410 86569 11
·4....	46·16486 14744 44	46·17569 09526 49
6·5....	49·54815 77533 98	49·55824 79185 42
·6....	53·17929 80636 54	53·18869 93875 86
·7....	57·07644 56729 00	57·08520 51818 28
·8....	61·25909 44395 91	61·26725 59493 14
·9....	65·74816 63228 66	65·75577 06579 38
7·0....	70·56611 60359 34	70·57320 12338 74
·1....	75·73704 33664 27	75·74364 48679 89
·2....	81·28681 37255 59	81·29296 45520 06
·3....	87·24318 75290 75	87·24891 84473 56
·4....	93·63595 90571 72	93·64129 87338 19
7·5....	100·49710 54879 85	100·50208 06325 09
·6....	107·86094 68501 06	107·86558 23485 95
·7....	115·76431 76942 39	115·76863 67338 43
·8....	124·24675 13427 04	124·25077 55276 22
·9....	133·35067 76384 26	133·35442 70979 68
8·0....	143·12163 51825 58	143·12512 86718 35
·1....	153·60849 91223 76	153·61175 41161 13
·2....	164·86372 56288 54	164·86675 84088 01
·3....	176·94361 42868 20	176·94644 00231 97
·4....	189·90858 97101 94	189·91122 25375 71
8·5....	203·82350 37909 61	203·82595 68789 61
·6....	218·75796 00937 61	218·76024 57129 35
·7....	234·78666 20187 44	234·78879 16019 50
·8....	251·98978 64742 31	251·99177 06738 23
·9....	270·45338 49283 14	270·45523 36694 25
9·0....	290·26981 38455 07	290·27153 63756 93
·1....	311·53819 66615 04	311·53980 15970 06
·2....	334·36491 96069 00	334·36641 49757 40
·3....	358·86416 38600 23	358·86555 71421 61
·4....	385·15847 66907 37	385·15977 48554 87

x.	$\sinh x/\sqrt{2}$.	$\cosh x/\sqrt{2}$.
9·5....	413·37938 44521 46	413·38059 39930 36
·6....	443·66805 04864 14	443·66917 74536 69
·7....	476·17598 12356 17	476·17703 12664 22
·8....	511·06578 40896 46	511·06676 24363 42
·9....	548·51198 07619 77	548·51289 23183 36
10·0....	588·70188 02618 83	588·70272 95875 87
·1....	631·83651 58297 77	631·83730 71732 25
·2....	678·13165 05223 03	678·13238 78418 60
·3....	727·81885 64771 95	727·81954 34609 95
·4....	781·14667 32564 95	781·14731 33408 89
10·5....	838·38185 10622 35	838·38244 74489 79
·6....	899·81068 50432 75	899·81124 07155 44
·7....	965·74044 73675 86	965·74096 51049 01
·8....	1036·50092 42233 57	1036·50140 66154 83
·9....	1112·44606 54370 99	1112·44651 48970 01
11·0....	1193·95575 49602 97	1193·95617 37362 10
·1....	1281·43771 10807 23	1281·43810 12674 02
·2....	1375·32952 58634 35	1375·32988 94126 24
·3....	1476·10085 40228 97	1476·10119 27531 01
·4....	1584·25576 21751 67	1584·25607 77807 42
11·5....	1700·33525 02212 89	1700·33554 42809 20
·6....	1824·91995 74740 68	1824·92023 14586 67
·7....	1958·63306 70645 06	1958·63332 23445 66
·8....	2102·14342 31559 64	2102·14366 10084 18
·9....	2256·16887 65586 42	2256·16909 81732 48
12·0....	2421·47987 54794 02	2421·48008 19646 94
·1....	2598·90331 93681 67	2598·90351 17570 02
·2....	2789·32669 51381 65	2789·32687 43928 88
·3....	2993·70251 64497 38	2993·70268 34669 96
·4....	3213·05308 82633 75	3213·05324 38786 03
12·5....	3448·47562 04946 73	3448·47576 54862 70
·6....	3701·14771 63501 48	3701·14785 14433 75
·7....	3972·33326 27970 18	3972·33338 86676 23
·8....	4263·38875 26315 76	4263·38886 99091 74
·9....	4575·77006 97696 69	4575·77017 90408 92
13·0....	4911·03977 16998 73	4911·03987 35113 05
·1....	5270·87490 55268 08	5270·87500 03877 19
·2....	5657·07539 67010 93	5657·07548 50859 84
·3....	6071·57305 23970 64	6071·57313 47480 44
·4....	6516·44122 45739 19	6516·44130 13029 15
13·5....	6993·90518 10557 17	6993·90525 25465 34
·6....	7506·35323 65072 43	7506·35330 31174 84
·7....	8056·34869 89838 21	8056·34876 10466 75
·8....	8646·64269 18127 00	8646·64274 96386 12
·9....	9280·18791 49421 58	9280·18796 88203 78

x.	$\sinh x/\sqrt{2}$.	$\cosh x/\sqrt{2}$.
14·0....	9960·15341 45937 26	9960·15346 47937 56
·1....	10689·94043 50965 71	10689·94048 18695 16
·2....	11473·19943 21962 55	11473·19947 57760 78
·3....	12313·84833 29398 43	12313·84837 35445 33
·4....	13216·09213 34748 47	13216·09217 13075 13
14·5....	14184·44393 27918 34	14184·44396 80417 18
·6....	15223·74750 76232 34	15223·74754 04666 59
·7....	16339·20154 14198 87	16339·20157 20211 38
·8....	17536·38562 86006 91	17536·38565 71128 38
·9....	18821·28818 41507 91	18821·28821 07164 54
15·0....	20200·33639 81744 49	20200·33642 29265 12
·1....	21680·42838 52377 73	21680·42840 83000 48
·2....	23268·96768 93150 21	23268·96771 08028 68
·3....	24973·90031 69350 88	24973·90033 69559 90
·4....	26803·75448 37710 91	26803·75450 24251 94
15·5....	28767·68327 34888 14	28767·68329 08694 28
·6....	30875·51042 22371 39	30875·51043 84312 03
·7....	33137·77945 77983 16	33137·77947 28868 35
·8....	35565·80643 91962 23	35565·80645 32546 70
·9....	38171·73656 05705 34	38171·73657 36692 30
16·0....	40968·60490 24541 23	40968·60491 46585 91
·1....	43970·40163 43366 77	43970·40164 57079 63
·2....	47192·14199 46631 83	47192·14200 52581 68
·3....	50649·94139 83131 18	50649·94140 81847 97
·4....	54361·09604 72542 20	54361·09605 64519 74
16·5....	58344·16944 75920 91	58344·16945 61619 27
·6....	62619·08526 57811 39	62619·08527 37659 25
·7....	67207·22698 84714 09	67207·22699 59110 85
·8....	72131·54488 44981 89	72131·54489 14299 69
·9....	77416·67080 40472 14	77416·67081 05057 71
17·0....	83089·04138 92305 05	83089·04139 52481 46
·1....	89177·03031 23824 48	89177·03031 79892 73
·2....	95711·09020 35431 32	95711·09020 87671 87
·3....	102723·90497 70621 07	102723·90498 19295 23
·4....	110250·55331 92729 68	110250·55332 38080 93
17·5....	118328·68415 50178 04	118328·68415 92433 22
·6....	126998·70497 07197 35	126998·70497 46567 83
·7....	136303·98393 60113 31	136303·98393 96796 02
·8....	146291·06683 49481 81	146291·06683 83660 25
·9....	157009·90989 19157 23	157009·90989 51002 36
18·0....	168514·12965 68439 84	168514·12965 98110 94
·1....	180861·27119 96769 91	180861·27120 24415 40
·2....	194113·09595 56280 42	194113·09595 82038 60
·3....	208335·89066 10468 73	208335·89066 34468 43
·4....	223600·79892 52217 92	223600·79892 74579 20

x.	$\sinh x/\sqrt{2}$.	$\cosh x/\sqrt{2}$.
18·5....	239984·17709 66666 80	239984·17709 87501 51
·6....	257567·97620 39657 99	257567·97620 59070 34
·7....	276440·15188 16764 83	276440·15188 34851 92
·8....	296695·10433 17733 70	296695·10433 34586 02
·9....	318434·15052 13581 48	318434·15052 29283 31
19·0....	341766·03097 86072 55	341766·03098 00702 44
·1....	366807·45372 19932 94	366807·45372 33564 07
·2....	393683·67804 35596 25	393683·67804 48296 80
·3....	422529·14106 63809 39	422529 14106 75642 89
·4....	453488·13021 03026 53	453488·13021 14052 17
19·5....	486715 50492 96890 34	486715·50493 07163 28
·6....	522377·47133 33726 61	522377·47133 43298 23
·7....	560652·41356 15190 23	560652·41356 24108 41
·8....	601731·78607 80229 27	601731·78607 88538 62
·9....	645821·07134 17579 12	645821·07134 25321 20
20·0....	693140·80764 70304 32	693140·80764 77517 86

References.

(1) "Tables of the Exponential Function and of the Circular sine and cosine to Radian Argument by C. E. Van Orstrand. National Academy of Science, Washington, 1921.—Vol. xiv. Fifth Memoir.

(2) Reports of the Mathematical Tables Committee, British Association. J. R. Airey, "Circular Functions, sin x and cos x," 1916, 1921, 1924, 1928; "Hyperbolic Functions, sinh x, cosh x," 1926. Also 'Mathematical Tables.'—Vol. i., "Circular, Hyperbolic and other Functions," British Association, Burlington House, W. 3, 1931.

(3) J. R. Airey, Report of the Mathematical Tables Committee, 1926.

LIII. *The Circular Sine and Cosine Functions, argument* $\log_e x$. *By* J. R. Airey, *M.A., D.Sc., Sc.D.**

BESSEL, Neumann, Struve, and other related functions of imaginary order $i\nu$, in ascending powers of the real variable x, include the factor $x^{i\nu}$, *e.g.*,

$$J_{i\nu}(x) = \left(\frac{x}{2}\right)^{i\nu} \sum_{p=0}^{\infty} \frac{(-1)^p}{\Gamma(\nu+p+1)\Gamma(p+1)} \left(\frac{x}{2}\right)^{2p}.$$

* Communicated by the Author.

In the construction of tables of these functions of imaginary order, it is necessary, in the first instance, to tabulate $x^{i\nu}$ or $\cos(\nu \log_e x)$ and $\sin(\nu \log_e x)$. The following tables were based upon those of $\sin\alpha$ and $\cos\alpha$, to thirteen places of decimals, calculated some years ago for the range $\alpha=0{\cdot}0000$ to $\alpha=0{\cdot}8000$ by $0{\cdot}0001$ radian intervals, the first and second differences only being needed for twelve places of decimals. The differential coefficients take a simple form, consisting of one or two terms: by Taylor's theorem interpolated values, when the argument is larger than $2{\cdot}5$, may be computed without difficulty from the expressions

$$\sin\log_e(1+\rho)$$
$$=\rho-\frac{\rho^2}{2!}+\frac{\rho^3}{3!}\qquad-\frac{10\rho^5}{5!}+\frac{90\rho^6}{6!}\quad-\frac{730\rho^7}{7!}+\ldots$$
$$\cos\log_e(1+\rho)$$
$$=1-\frac{\rho^2}{2!}+\frac{3\rho^3}{3!}-\frac{10\rho^4}{4!}+\frac{40\rho^5}{5!}-\frac{190\rho^6}{6!}+\frac{1050\rho^7}{7!}+\ldots$$
$$\rho=\frac{h}{x}\quad\text{and}\quad\log_e(x+h)=\log_e(x)+\log_e(1+\rho).$$

ρ.	$\sin\log_e(1+\rho)$.	$\cos\log_e(1+\rho)$.
·000.....	0·00000 00000	1·00000 00000
1.....	099 95001;	0·99999 95005
2.....	199 80013:	9 80040
3.....	299 55045	9 55134:
4.....	399 20106:	9 20319
·005.....	0·00498 75208:	0·99998 75622:
6.....	598 20360	8 21074:
7.....	697 55571:	7 56705
8.....	796 80853:	6 82543
9.....	895 96215	5 98618
·010.....	0·00995 01666:	0·99995 04958:
1.....	1093 97218	4 01594:
2.....	1192 82880	2 88554:
3.....	1291 58661:	1 65867
4.....	1390 24573	0 33561:
·015.....	0·01488 80624:	0·99988 91666:
6.....	1587 26826	7 40210:
7.....	1685 63187	5 79221:
8.....	1783 89718:	4 08729
9.....	1882 06429:	2 28760
·020.....	0·01980 13331	0·99980 39344

ρ.	$-\sin \log_e(1-\rho)$.	$\cos \log_e(1-\rho)$.
·000.....	0·00000 00000	1·00000 00000
1.....	100 05001 :	0·99999 94995
2.....	200 20013 :	9 79960
3.....	300 45045	9 54864 :
4.....	400 80106 :	9 16979
·005.....	0·00503 25208 :	0·09998 74372 :
6.....	601 80360	8 18914 :
7.....	702 45571 :	7 53275
8.....	803 20853 :	6 77423
9.....	904 06215	5 91327 :
·010.....	0·01005 01666 :	0·99994 94958
1.....	106 07218	3 88283 :
2.....	207 22880	2 71273
3.....	308 48661 :	1 43895
4.....	409 84573	0 06118
·015.....	0·01511 30624 :	0·99988 57911 :
6.....	612 86826	6 99243 :
7.....	714 53187	5 30082
8.....	816 29718 :	3 50396
9.....	918 16429 :	1 60153 :
·020.....	0·02020 13330 :	0·99979 59322 :

Central difference interpolation is also effective in this case. To extend the tables, in both directions, multiples and sub-multiples of the argument, values of sine and cosine $\log_e x$, when $x=2$, 5, 10, 100, 1000, and π are given to thirteen or fourteen places of decimals.

x.	$\sin \log_e x$.	$\cos \log_e x$.
2....	+0·63896 12763 13635	+0·76923 89013 63972
5....	+0·99925 35068 2348	−0·03863 19699 3393 :
10....	−0·66820 15101 9031 :	+0·74398 03369 5749 :
100....	−0·99425 75694 1379	−0·10701 34835 5877
1000....	+0·58474 84818 434	+0·81121 46528 397
π....	+0·41329 21161 016	+0·91059 84992 126

Since

$$\sinh \log_e x = \frac{x-\frac{1}{x}}{2} \quad \text{and} \quad \cosh \log_e x = \frac{x+\frac{1}{x}}{2},$$

it is not necessary to tabulate these functions.

The colon : is approximately equivalent to a half unit in the last place of decimals.

x.	$\sin \log_e x$.	$\cos \log_e x$.
0·1.....	−0·74398 03369:	−0·66820 15102
2.....	0·99925 35068	−0·03863 19699:
3.....	0·93347 13034	+0·35865 20957:
4.....	0·79334 90026	0·60876 70819:
0·5.....	−0·63869 12763	+0·76923 89013:
·6.....	0·48889 76390	0·87234 11595
·7.....	0·34916 03822:	0·93706 29794:
·8.....	0·22129 63235	0·97520 66126
·9.....	0·10516 56921:	0·99445 47135
1·0.....	+0·00000 00000	+1·00000 00000
·1.....	0·09516 59452:	0·99546 14221
·2.....	0·18131 31379:	0·98342 54145:
·3.....	0·25936 46327:	0·96577 94713:
·4.....	0·33015 92085	0·94392 52603
1·5.....	+0·39444 61997	+0·91891 90364:
·6.....	0·45288 95211	0·89156 66445:
·7.....	0·50607 53008:	0·86248 92984
·8.....	0·55452 05115	0·83217 00561:
·9.....	0·59868 14085	0·80098 72478
2·0.....	+0·63896 12763	+0·76923 89013:
·1.....	0·67571 73135	0·73716 08455:
·2.....	0·70926 66479:	0·70494 02968:
·3.....	0·73989 15423:	0·67272 61743
·4.....	0·76784 38771	0·64063 70114:
2·5.....	+0·79334 90026	+0·60876 70819:
·6.....	0·81660 90488	0·57719 11827:
·7.....	0·83780 57702:	0·54596 83977:
·8.....	0·85710 29959	0·51514 50809:
·9.....	0·87464 87424	0·48475 72355:
3·0.....	+0·89057 70416:	+0·45483 24228:
·1.....	0·90500 95249	0·42539 13020:
·2.....	0·91805 67987:	0·39644 88797
·3.....	0·92981 96459	0·36801 55243
·4.....	0·94039 00714	0·34009 78000
3·5.....	+0·94985 22218	+0·31269 91473:
·6.....	0·95828 31903	0·28582 04458
·7.....	0·96575 37265:	0·25946 04780
·8.....	0·97232 88631	0·23361 63136
·9.....	0·97806 84688	0·20828 36295:
4·0.....	+0·98302 77404	+0·18345 69747:
·1.....	0·98725 76389:	0·15912 99919
·2.....	0·99080 52786	0·13529 56019
·3.....	0·99371 42736	0·11194 61584:
·4.....	0·99602 50488:	0·08907 35768:

x.	sin $\log_e x$.	cos $\log_e x$.
4·5.....	+0·99777 51177	+0·06666 94421
·6.....	0·99899 93321	0·04472 50990
·7.....	0·99973 01070	0·02323 17278:
·8.....	0·99999 76229	+0·00218 04071:
·9.....	0·99983 00087	−0·01843 78335
5·0.....	+0·99925 35068	−0·03863 19699:
·1.....	0·99829 26230:	0·05841 09470:
·2.....	0·99697 02623:	0·07778 36488
·3.....	0·99530 78520:	0·09675 88735
·4.....	0·99332 54545	0·11534 53138
5·5.....	+0·99104 18690	−0·13355 15402:
·6.....	0·98847 47253:	0·15138 59881
·7.....	0·98564 05691	0·16885 69471
·8.....	0·98255 49396	0·18597 25535
·9.....	0·97923 24416	0·20274 07836:
6·0.....	+0·97568 68105	−0·21916 94499:
·1.....	0·97193 09730	0·23526 61977
·2.....	0·96797 71020	0·25103 85030:
·3.....	0·96383 66679	0·26649 36726:
·4.....	0·95952 04854:	0·28163 88432
6·5.....	+0·95503 87568:	−0·29648 09823
·6.....	0·95040 11120:	0·31102 68899
·7.....	0·94561 66453	0·32528 31998:
·8.....	0·94069 39498:	0·33925 63820:
·9.....	0·93564 11490	0·35295 27452
7·0.....	+0·93046 59259	−0·36637 84392
·1.....	0·92517 55506:	0·37953 94584
·2.....	0·91977 69054	0·39244 16444:
·3.....	0·91427 65080	0·40509 06897:
·4.....	0·90868 05338	0·41749 21406:
7·5.....	+0·90299 48359	−0·42965 14009
·6.....	0·89722 49643:	0·44157 37349:
·7.....	0·89137 61833:	0·45326 42714:
·8.....	0·88545 34881:	0·46472 80068
·9.....	0·87946 16202:	0·47596 98083:
8·0.....	+0·87340 50817:	−0·48699 44179:
·1.....	0·86728 81488:	0·49780 64552:
·2.....	0·86111 48842:	0·50841 04209
·3.....	0·85488 91492:	0·51881 07000:
·4.....	0·84861 46144:	0·52901 15652
8·5.....	+0·84229 47702	−0·53901 71797:
·6.....	0·83593 29364	0·54883 16006
·7.....	0·82953 22714	0·55845 87816
8.....	0·82309 57806:	0·56790 25760:
9.....	0·81662 63248	0·57716 67399

x.	$\sin \log_e x$.	$\cos \log_e x$.
9·0.....	+0·81012 66271:	−0·58625 49343
·1.....	0·80359 92807	0·59517 07285
·2.....	0·79704 67550	0·60391 76022:
·3.....	0·79047 14023:	0·61249 89486:
·4.....	0·78387 54636	0·62091 80763:
9·5.....	+0·77726 10741	−0·62917 82122
·6.....	0·77063 02685:	0·63728 25034:
·7.....	0·76398 49863	0·64523 40201:
·8.....	0·75732 70758	0·65303 57572:
·9.....	0·75065 82993:	0·66069 06368:
10·0.....	+0·74398 03369:	−0·66820 15102
·1.....	0·73729 47904:	0·67557 11598
·2.....	0·73060 31873:	0·68280 23013
·3.....	0·72390 69841	0·68989 75854:
·4.....	0·71720 75698	0·69685 95998
10·5.....	+0·71050 62691	−0·70369 08707:
·6.....	0·70380 43453:	0·71039 38650:
·7.....	0·69710 30034	0·71697 09915
·8.....	0·69040 33924	0·72342 46027
·9.....	0·68370 66082	0·72975 69965
11·0.....	+0·67701 36959	0·73597 04175:
·1.....	0·67032 56522:	0·74206 70589:
·2.....	0·66364 34276	0·74804 90632:
·3.....	0·65696 79281:	0·75391 85243:
·4.....	0·65030 00180:	0·75967 74885
11·5.....	+0·64364 05209:	−0·76532 79557
·6.....	0·63699 02221:	0·77087 18810
·7.....	0·63034 98699:	0·77631 11756:
·8.....	0·62372 01776:	0·78164 77083:
·9.....	0·61710 18248	0·78688 33063:
12·0.....	+0·61049 54587	−0·79201 97566:
·1.....	0·60390 16960:	0·79705 88068
·2.....	0·59732 11239	0·80200 21664
·3.....	0·59075 43013	0·80685 15077
·4.....	0·58420 17601:	0·81160 84668:
12·5.....	+0·57766 40067	−0·81627 46446
·6.....	0·57114 15223	0·82085 16074:
·7.....	0·56463 47648:	0·82534 08885:
·8.....	0·55814 41693:	0·82974 39883:
·9.....	0·55167 01493	0·83406 23756
13·0.....	+0·54521 30972:	−0·83829 74881:
·1.....	0·53877 33858:	0·84245 07337
·2.....	0·53235 13687:	0·84652 34906:
·3.....	0·52594 73811:	0·85051 71087:
·4.....	0·51956 17408:	0·85443 29098:

x.	$\sin \log_e x$.	$\cos \log_e x$.
13·5.....	+0·51319 47487	−0·85827 21887
·6.....	0·50684 66896	0·86203 62134
·7.....	0·50051 78328:	0·86572 62263:
·8.....	0·49420 84330	0·86934 34446:
·9.....	0·48791 87303	0·87288 90609
14·0.....	+0·48164 89515	−0·87636 42436:
·1.....	0·47539 93102	0·87977 01381
·2.....	0·46917 00074	0·88310 78666:
·3.....	0·46296 12322:	0·88637 85294
·4.....	0·45677 31622	0·88958 32048
14·5.....	+0·45060 59636:	−0·89272 29500:
·6.....	0·44448 21450	0·89578 77108
·7.....	0·43833 47940:	0·89881 17758
·8.....	0·43223 11044:	0·90176 28692:
·9.....	0·42614 88499:	0·90465 30593
15·0.....	+0·42008 81480:	−0·90748 33044:
·1.....	0·41404 91074	0·91025 45450
·2.....	0·40803 18286	0·91296 77031
·3.....	0·40203 64040	0·91562 36835:
·4.....	0·39606 29186	0·91822 33740
15·5.....	+0·39011 14498	−0·92076 76453:
·6.....	0·38418 20681	0·92325 73523
·7.....	0·37827 48372	0·92569 33334
·8.....	0·37238 98143:	0·92807 64118
·9.....	0·36652 70505	0·93040 73953
16·0.....	+0·36068 65907	−0·93268 70768:
·1.....	0·35486 84742	0·93491 62347:
·2.....	0·34907 27348	0·93709 56332:
·3.....	0·34329 94009:	0·93922 60225
·4.....	0·33754 84961	0·94130 81391:
16·5.....	+0·33182 00388	−0·94334 27065
·6.....	0·32611 40429	0·94533 04348:
·7.....	0·32043 05179	0·94727 20217:
·8.....	0·31476 94688	0·94916 81524
·9.....	0·30913 08967	0·95101 94996:
17·0.....	+0·30351 47985:	−0·95282 67246
·1.....	0·29792 11676:	0·95459 04765
·2.....	0·29234 99936	0·95631 13934:
·3.....	0·28680 12625:	0·95799 01021:
·4.....	0·28127 49572:	0·95962 72184:
17·5.....	+0·27577 10573	−0·96122 33476
·6.....	0·27028 95392	0·96277 90842
·7.....	0·26483 03766	0·96429 50127:
·8.....	0·25939 35401:	0·96577 17076:
·9.....	0·25397 89980	0·96720 97335

x.	sin $\log_e x$.	sos $\log_e x$.
18·0.....	+0·24858 67156	−0·96860 96452:
·1.....	0·24321 66559	0·96997 19884
·2.....	0·23786 87795:	0·97129 72993:
·3.....	0·23254 30449:	0·97258 61053
·4.....	0·22723 94082:	0·97383 89247:
18·5.....	+0·22195 78236	−0·97505 62673:
·6.....	0·21669 82431:	0·97623 86344:
·7.....	0·21146 06171	0·97738 65189:
·8.....	0·20624 48939	0·97850 04056
·9.....	0·20105 10202:	0·97958 07711:
19·0.....	+0·19587 89421:	−0·98062 80846:
·1.....	0·19072 86002:	0·98164 28072:
·2.....	0·18559 99393:	0·98262 53927:
·3.....	0·18049 28990:	0·98357 62875:
·4.....	0·17540 74185	0·98449 59307
19·5.....	+0·17034 34355:	−0·98538 47543
·6.....	0·16530 08868:	0·98624 31834
·7.....	0·16027 97079	0·98707 16363:
·8.....	0·15527 98329:	0·98787 05246:
·9.....	0·15030 11953	0·98864 02534
20·0.....	+0·14534 37272:	−0·98938 12212:

LIV. *Note on the Nuclear Evolution of Iron, Cobalt, and Nickel.* *By* H. J. Walke, *M.Sc., A.Inst.P., Demonstrator in Physics, Washington Singer Laboratories, University College, Exeter* *.

In previous papers † a theory of nuclear synthesis by neutron capture with the β-radioactivity of missing isotopes has been proposed. The isotopic configurations of the iron group of elements were such as to indicate that additional iron and cobalt isotopes probably exist, and it was, therefore, suggested that Fe_{26}^{58} might be stable, the missing Fe_{26}^{57} giving rise to an unobserved cobalt

* Communicated by Prof. F. H. Newman, D.Sc.

† Walke, Phil. Mag. xviii. p. 795 (1934); xix. p. 33 (1935); xix. p. 365) 1935).

isotope Co_{27}^{57}. Synthesis to nickel was thus due to the β-radioactivity of the missing Co_{27}^{58} and Co_{27}^{60}, viz.,

$$Co_{27}^{58} \rightarrow \beta \rightarrow Ni_{28}^{58};$$

$$Co_{27}^{60} \rightarrow \beta \rightarrow Ni_{28}^{60}.$$

Aston* has recently reinvestigated the isotopic constitution of iron and has shown that Fe_{26}^{57} exists as a stable isotope, whereas Fe_{26}^{58} is most probably missing. This suggests that cobalt is a single element of mass number 59. Accepting these results it is, however, still possible to explain the evolution of cobalt and nickel as below.

Fe_{26}^{58} is missing, whereas Ni_{28}^{58} exists as a stable isotope. In addition, as cobalt is a single element Co_{27}^{59}, synthesis resulting from the β-radioactivity of the missing Co_{27}^{60} gives rise to Ni_{28}^{60}. It thus appears probable that Ni_{28}^{58} is directly evolved as a result of β-ray emission from the missing Fe_{26}^{58}, viz.,

$$Fe_{26}^{58} \rightarrow \beta \rightarrow Co_{27}^{58} \rightarrow \beta \rightarrow Ni_{28}^{58}.$$

In order to explain the synthesis of cobalt from iron it is necessary to assume that Fe_{26}^{58} is of sufficiently long life to allow the formation of the missing Fe_{26}^{59} by neutron capture during the stellar evolution of the elements; Co_{27}^{59} was then produced as a result of the β-radioactivity of the isotope thus:

$$Fe_{26}^{59} \rightarrow \beta \rightarrow Co_{27}^{59}.$$

The synthesis of the lighter isotopes Fe_{26}^{54} and Cr_{24}^{54} proceeds as originally suggested† as a result of the formation of Ni_{28}^{58} in a state of excess energy, viz.,

$$Fe_{26}^{58} \rightarrow \beta \rightarrow Co_{27}^{58} \rightarrow \beta \rightarrow \overset{*}{Ni}{}_{28}^{58}; \quad \overset{*}{Ni}{}_{28}^{58} \rightarrow Ni_{28}^{58} + \gamma;$$

$$\overset{*}{Ni}{}_{28}^{58} \rightarrow \alpha \rightarrow \overset{*}{Fe}{}_{26}^{54}; \quad \overset{*}{Fe}{}_{26}^{54} \rightarrow Fe_{26}^{54} + \gamma;$$

$$\overset{*}{Fe}{}_{26}^{54} \rightarrow \alpha \rightarrow Cr_{24}^{50}.$$

* Aston, Proc. Roy. Soc. A, cxlix. p. 396 (1935).
† Walke, Phil. Mag. xix. p. 33 (1935).

LV. *On the Theory of the Combination Coefficients for Large Ions: a Correction.* *By* W. R. HARPER, *Ph.D., Research Associate, Wills Physical Laboratory, University of Bristol* *.

THE author's theory of the combination coefficients for large ions † requires modification owing to a numerical mistake ‡ having occurred in a previous paper § on which the theory was based. The changes in the final formulæ are as follows :—

Equation (2.1) becomes

$$\nu'(\sigma)=3\pi n'n''\sigma(D'+D'')[1-\exp\{-U\sigma/3(D'+D'')\}],$$

and the abscissæ of fig. 1 should range from 0 to 9. Equation (3.1) remains unchanged, except that σ_0 has a value three times smaller. Equation (4.1) becomes

$$\eta_{10}=\frac{6\pi P a_0 k_1}{eN(\theta)}\{1-\exp(-a_0/2\lambda_1)\},$$

with a corresponding change in the expressions which follow. In (4.3) and (4.4) only the logarithm is affected. Its argument should be multiplied by 3. Finally, (4.5) may be corrected by substituting 3P for P in both places where it occurs.

The numerical values plotted in figs. 2 to 4 require revision, though the general form of the curves remains unchanged. For atmospheric ions the theoretical value of η_{12} becomes $5{\cdot}7.10^{-6}$ instead of $7{\cdot}2.10^{-6}$, in exact agreement with the value found by P. J. Nolan and O'Brolchain. The attraction factor is reduced from 8·7 to 3·4, a value now in excellent agreement with experiment.

A re-discussion of the application of the theory to coagulation phenomena has already appeared ‖.

* Communicated by the Author.
† Phil. Mag. xviii. p. 97 (1934).
‡ For details see a forthcoming issue of the Proc. Camb. Phil. Soc.
§ Proc. Camb. Phil. Soc. xxviii. p. 219 (1932).
‖ Trans. Faraday Soc. xxxi. p. 774 (1935).

LVI. *Notices respecting New Books.*

Colloid Chemistry. By A. W. Thomas. (London: McGraw-Hill Publishing Co., Ltd., 1934.)

In this volume the author has made an attempt to treat colloidal dispersions from the point of view of crystalloidal chemistry. This gives the book a special value for students of physics and of physical chemistry. A certain amount of previous knowledge is necessary if the book is to be fully appreciated, but it may confidently be recommended to the intelligent student.

The book opens with a discussion of optical matters and a discussion of the ultra-microscope. A chapter on liquid dispersed systems follows. After a useful discussion of dialysis and ultra-filtration and the preparation of colloidal solutions, the author devotes a long chapter to the nature of micelles. Other chapters are concerned with electro-kinetics, surface phenomena, adsorption. There is also a useful account of proteins and of carbohydrate colloids. The volume concludes with an account of gels and jellies.

On looking through the subject-matter treated in this book, one cannot but be struck by the extent to which it is of critical importance not only to physics and chemistry but also to biology. To workers in all these various fields the book should be of value.

The Physical Basis of Things. By J. H. Eldridge. (London: McGraw-Hill Publishing Co., Ltd., 1934.)

This is an interesting book, which gives an account of modern views in atomic physics. It is addressed not to the specialist, but to the student having a wide interest in physics as a whole. It opens with relativity, then goes on to a discussion of the kinetic theory. After a useful and clear account of the quantum theory, the author devotes several chapters to the discussion of X-rays. There are also sections on infra-red spectra and on the nucleus.

In view of the growing interest in modern physics evinced not only by the student of the A sciences, but also by workers in the biological field, a book such as this should be of great value. It deals with subject-matter, which is of by no means a simple nature, well and thoroughly, and maintains always the style of exposition which will encourage the non-specialist reader to get at least some measure of insight into the fundamental advances of our times.

Introduction to Mechanics and Heat. By M. H. Frank. (London ; McGraw-Hill Publishing Co., Ltd., 1934.)

This is a useful book in that it gives a clear and connected account of a number of branches of mathematical physics. Too often in this country, at least, the Honours student studies in water-tight compartments, such subjects as Mechanics, Hydromechanics, Elasticity, Acoustics, Thermodynamics. In this volume, however, an attempt has been made to build into one whole a preliminary account of all these fields. The first few chapters are concerned with the dynamics of a particle. We then pass on to rigid bodies. A chapter on hydrostatics is followed by an account of the elements of hydrodynamics. Elasticity and acoustics then follow on. The concluding chapters on thermodynamics and heat conduction are especially well written. We would like to bring this book to the attention of University students and their teachers.

The Structure of Spectral Terms. By W. M. Hicks. [Pp. xi+210-] (London : Methuen, 1935. Price 10*s.* 6*d.*)

The general character of Hicks's extensive and detailed studies in the analysis of spectra is well known. In this book the earlier work (which was presented in his 'Analysis of Spectra' in 1922) is summarized and greatly extended. The author died before the manuscript was printed, and the thanks of spectroscopists are due to J. R. Clarke for the care and patience he has so clearly brought to bear on the final revision and the checking of the proofs.

Essentially an objective study is made of the numerical characteristics of spectral lines and terms and of the relations between them. Most physicists are so accustomed to think of a term series as being given very closely by a formula of the type $R/(m+\mu)^2$ that they will learn with some surprise of the difficulty of representing a series accurately (within observational error) even by more general formulæ. This is discussed in the first chapter, and provides, perhaps, the simplest example of how much more complicated spectroscopic relations are than the usual theoretical approach to them would suggest. Subsequent chapters are concerned with satelloids, multiple terms, collaterals, linkages, summation lines, and the variations in the mantissa values for sequences of terms of different types. In a final chapter comments are made on the present position of the theory.

The discussion is illustrated by a wealth of numerical data on spectral lines and terms, whose value is to a large extent independent of whether the various empirical relations found by Hicks have a theoretical significance. For a large number of multiplets and displaced lines Hicks finds that the separations, expressed as mantissa differences, are equal to integral

multiples of a quantity equal to a constant times the square of the atomic weight. This quantity Hicks calls the "oun." The agreement found is extensive and striking; but against this must be set the fact that the integral multiples are often large (of the order of 100 or even 1000), and that there are no obvious regularities in them.

This is not the place for a criticism of the oun hypothesis; and, in any case, a completely misleading impression would be given of the value of the book if it were implied that it depended on whether or not the particular relations involving the oun were significant.

Hicks's book shows clearly how much further work remains to be done, on the theoretical side, in the analysis and interpretation of spectra; and it contains an enormous amount of critically correlated data. For these reasons it must be strongly commended to the attention of spectroscopists, and, indeed, to all those physicists who are interested in spectra and who do not object to seeing the subject presented from a point of view different from the usual one.

Comment may finally be made on the cheapness of the book, well produced and containing, as it does, a great amount of tabular material admirably set out.

An Introduction to Atomic Physics. By JOHN THOMSON. [Pp. ix+228.] (London: Methuen & Co., 1935. Price 10*s.* 6*d.*)

So many books on various aspects of atomic physics have now appeared that any new book of a not too specialized character must necessarily traverse ground that has been covered many times before. The value of any new book, for particular readers, depends on the choice made from the abundant material, and the manner of presentation of the various topics dealt with. The present book is divided into three parts. In the first, a very clear and logical account is given, without excessive detail, of the fundamental experiments—on the electronic charge, the composition of elements, the nucleus, the quantization of energy, critical potentials—and the conclusions drawn from them. This part of the book could be read with advantage and comparative ease by any student of physics. In the second part the theory is developed—first the Bohr theory, and then wave-mechanics, following closely the methods of Schrödinger. This part will make considerably greater demands on the mathematical equipment of the reader; but, if a student is really to understand recent theories, there is no short cut through the mathematics. The account here is admirable. A wide range is not covered, but in that range adequate detail is given (as in the treatment of the hydrogen atom); the student could

have no better introduction to the subject, and if he works through this part of the book he will gain a clear understanding of the methods by which precise quantitative results can be derived from the theory. In the third part of the book, atomic optical spectra, molecular structure and radiations, X-rays and radioactivity are considered in the light of the theory developed. Clearly these subjects cannot be covered in any detail in some sixty pages; but the brevity, coupled as it is with soundness, has its advantages; for there is a definite need of good short books, of not too elementary a character, which can be recommended to students, who are liable to be overwhelmed by the massive compilations with which they are confronted as soon as they embark seriously on the subject of atomic physics.

If a criticism of the book is to be made it is that it is rather too self-contained. An introduction should point beyond itself; it should open up a prospect, giving an incentive and, perhaps, some guide towards further exploration—and this is not done merely by a rather perfunctory list of suggestions for further reading. It may be remarked too that sufficient basis is hardly provided in the body of the book for the quasi-critical remarks on the wave-particle problem, and more particularly those on statistical methods which are given at the end. On the whole, however, this book may be strongly recommended as a well-proportioned introduction to atomic physics, which will be particularly useful to honours students. It may be added that it is well produced, and that it contains four excellent plates showing electron diffraction photographs, α-, β-, and X-ray tracks, and typical spectra.

Mathematical Tables.—Vol. III. *Minimum Decompositions into Fifth Powers.* (Prepared by L. E. Dickson and published under the auspices of the British Association.)

This volume is the first outcome of a bequest to the British Association from Lt.-Col. A. J. C. Cunningham to assist in the publication of tables in connexion with the theory of numbers. The present table extends to 150,000 and gives a decomposition in the following manner :—

$$44462 \quad 0\ 0\ 3\ 0\ 1\ 2,$$

indicating $44462 = 3\cdot4^5 + 1\cdot6^5 + 2\cdot7^5$. Gaps in the table indicate that the minimum decompositions for the omitted numbers may be obtained by adding on the appropriate multiples of 1. The tables have been reproduced from photographs of type-scripts made by Professor Dickson himself, and one may be sure that no printers' errors have entered.

[*The Editors do not hold themselves responsible for the views expressed by their correspondents.*]

FIG. 3 (*a*).

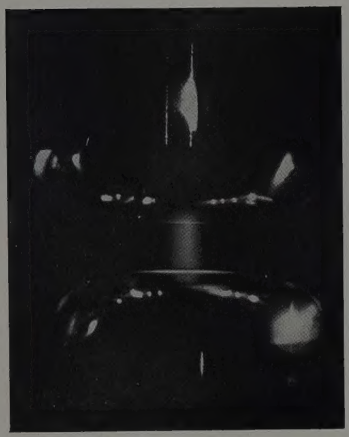

FIG. 3 (*b*).

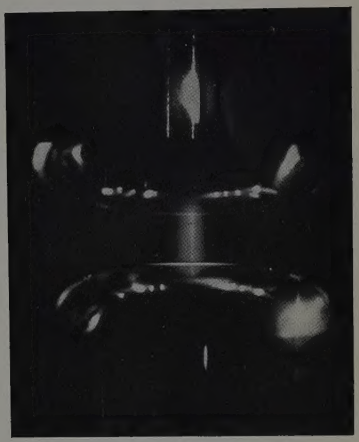

FIG. 3 (*c*).

FIG. 3 (*d*).

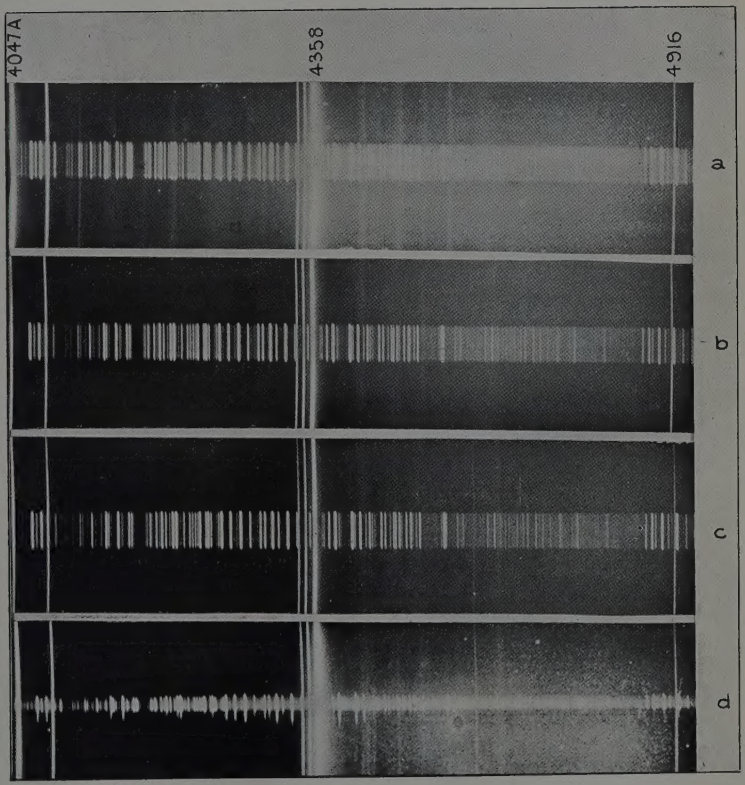

Raman spectra of fuming sulphuric acid containing (*a*) 21·3 per cent., (*b*) 49·3 per cent., (*c*) 71·5 per cent., (*d*) 80·4 per cent. of SO_3.